

**Nitrate uptake, root exudation, and litter quality - crop
plant effects on denitrification and its product
stoichiometry**

Dissertation

to attain the doctoral degree (Dr. rer. nat.)

of the Faculty of Agricultural Sciences

Georg-August-Universität Göttingen

Submitted by

Pauline Sophie Rummel

born in Fürstenfeldbruck, Germany

Göttingen, May 2020

1. Referee: Prof. Dr. Klaus Dittert

2. Referee: Prof. Dr. Johanna Pausch

3. Referee: Prof. Søren O. Petersen, PhD

Date of oral examination: 13.07.2020

*The summit pokes out
Of meaningless clouds
Each step takes me higher and higher
I know I can reach
The impossible goal
The vanishing point of desire*

Diorama – The Summit

Table of Contents

List of abbreviations	4
Introduction.....	6
Chapter 1 - Nitrate uptake and carbon exudation – do plant roots stimulate or inhibit denitrification?	11
Abstract	12
Introduction	12
Material and methods.....	13
Results	18
Discussion.....	22
Conclusions.....	26
Supplementary	29
Chapter 2 - Maize root and shoot litter quality controls short-term CO ₂ and N ₂ O emissions and bacterial community structure of arable soil....	31
Abstract	32
Introduction	33
Material and methods.....	34
Results	37
Discussion.....	41
Conclusions.....	45
Supplement	50
Chapter 3 - Carbon Availability and Nitrogen Mineralization Control Denitrification Rates and Product Stoichiometry during Initial Maize Litter Decomposition.....	66
Abstract	67
Introduction	67
Materials and Methods	68
Results	72
Discussion	81

Conclusions	83
Supplementary	88
Discussion	99
Summary	105
Zusammenfassung	107
References	109
Acknowledgements	114
Curriculum Vitae	115

List of abbreviations:

ADFom	acid detergent fiber
ADL	acid detergent lignin
AIC	Akaike's information criterion
aNDFom	ash-free neutral detergent fiber
ANOVA	analysis of variance
ASV	amplicon sequence variant
CLD	chemoluminescence detector
C _{org}	organic carbon
DAO	days after onset of experiment
DNA	deoxyribonucleic acid
ECD	electron capture detector
FM	fresh matter
GC	gas chromatograph
HSD	honestly significant difference
lme	linear mixed-effect model
MGLM	multivariate generalized linear model
ML	maximum likelihood
N _{min}	mineral Nitrogen
PCR	polymerase chain reaction
PD	phylogenetic diversity
PDD	pulsed discharge detector
PVC	polyvinylchloride
RD	rhizodeposition

REML	restricted maximum likelihood
RNA	ribonucleic acid
rRNA	ribosomal ribonucleic acid
SOM	soil organic matter
TCD	thermal conductivity detector
VWC	volumetric water content
WEOC	water-extractable organic carbon
WFPS	water-filled pore space
WHC	water holding capacity

INTRODUCTION

Nitrous oxide (N_2O) is a potent greenhouse gas contributing to climate change through global warming and stratospheric ozone depletion (Ciais et al., 2013; Ravishankara et al., 2009). Soils under agricultural and natural vegetation are the largest anthropogenic and natural N_2O sources, respectively, and the two main processes contributing to N_2O formation in soils are denitrification and nitrification (Ciais et al., 2013; Reay et al., 2012). Plants strongly affect N cycling and N transformation processes in soils (Knops et al., 2002; Moreau et al., 2019) and may thus have a strong impact on denitrification and N_2O emissions in particular.

Denitrification is the sequential reduction of nitrate (NO_3^-) to nitrite (NO_2^-), nitric oxide (NO), nitrous oxide (N_2O), and dinitrogen (N_2) by bacteria, archaea, and fungi (Zumft, 1997). The prerequisites for denitrification are low O_2 partial pressure ($p\text{O}_2$) and availability of NO_3^- and a degradable organic C source, soil $\text{pH} > 4$, and temperatures above 0°C (Focht and Verstrate, 1977; Knowles, 1982; Payne and Grant, 1981). When $p\text{O}_2$ in soil decreases, denitrifying microorganisms use NO_3^- as an alternative electron acceptor in their respiratory chain to break down organic compounds (Zumft, 1997).

Actively growing plants take up mineral N from soil competing with soil microorganisms for inorganic N (Kuzyakov and Xu, 2013). Although competition for N is highest in direct vicinity of the roots, the rhizosphere is densely colonized by microorganisms due to its higher C availability from rhizodeposition, dying roots and root hairs (Nguyen, 2003). At the same time, plants roots influence distribution of water and $p\text{O}_2$ in soil (Rudolph-Mohr et al., 2017). Thus, growing plants affect the main controlling factors for denitrification, substrate availability (i.e. NO_3^- and C_{org}) and $p\text{O}_2$ (von Rheinbaben and Trolldenier, 1984). After harvest of crops, large amounts of roots remain on the field. Furthermore, aboveground residues (leaves, stalks, straw) and catch crops, which are grown after harvest to prevent nutrient loss through leaching and erosion, are often incorporated into the soil to increase soil fertility. However, plant residues provide

substrates for decomposing and denitrifying microorganisms and lead to increased CO₂ and N₂O emissions (i.e. Chen et al., 2013; Novoa and Tejeda, 2006). Addition of easily degradable C increases microbial respiration and limits O₂ availability, which may lead to the formation of plant-litter-associated hotspots for denitrification (Chen et al., 2013; Kravchenko et al., 2017; Miller et al., 2008). The effects of plant residue addition on N₂O production depend on C and N input and litter quality (Chen et al., 2013; Millar and Baggs, 2004; Novoa and Tejeda, 2006). In detail, litter C:N ratio controls whether N is mineralized or immobilized during litter degradation and may thus restrict N availability for denitrification. Though plants and plant litter modify soil conditions in numerous ways, their effect on NO₃⁻ and C_{org} availability is considered the strongest driver of denitrification in planted soils (von Rheinbaben and Trolldenier, 1984). Furthermore, the ratio of available C to available N controls the ratio of the gaseous end products of denitrification N₂O/(N₂O+N₂) (Firestone, 1982; Morley et al., 2014; Qin et al., 2017).

In addition to denitrification, soil-emitted N₂O can originate from different abiotic and biotic processes taking place under various environmental conditions. Abiotic N₂O formation processes include chemodenitrification, the decomposition of NH₄NO₃, and the chemical decomposition of hydroxylamine (NH₂OH). The importance of the first two processes in natural or agricultural ecosystems is limited (Butterbach-Bahl et al., 2013). Hydroxylamine reduction is a side process of nitrification with NO as a precursor of N₂O (Hooper and Terry, 1979). N₂O production via hydroxylamine reduction (i.e. nitrification) may be enhanced by high NH₃, low NO₂⁻, and high N oxidation rates (Wunderlin et al., 2012).

Biotic N₂O formation processes include heterotrophic and autotrophic denitrification, nitrifier denitrification, coupled nitrification-denitrification, co-denitrification, and dissimilatory nitrate reduction to ammonium (DNRA) (Fig. 1) (Baggs, 2011; Butterbach-Bahl et al., 2013; van Groenigen et al., 2015). Denitrification mainly contributes to N₂O formation when soil moisture increases over 60% WFPS, with a shift to N₂ in soils over 80 % WFPS (Davidson, 1991; Linn and Doran, 1984). In addition to bacteria, fungi are

also capable to denitrify (Laughlin and Stevens, 2002; Maeda et al., 2015), but often lack the N_2O reductase (*Nos*), thus, the end product of fungal denitrification is mostly N_2O (Takaya, 2009). In general, fungi are seen as major contributors to denitrification under oxic and weakly anoxic conditions, while bacterial denitrification predominates under strongly anoxic conditions (Hayatsu et al., 2008; Lavrent'ev et al., 2008). Furthermore, denitrifying archaea and aerobic denitrifying bacteria have been reported but their contribution to denitrification in soils is not fully known yet (Cabello et al., 2004; Ji et al., 2015; Philippot, 2002; Takaya et al., 2003).

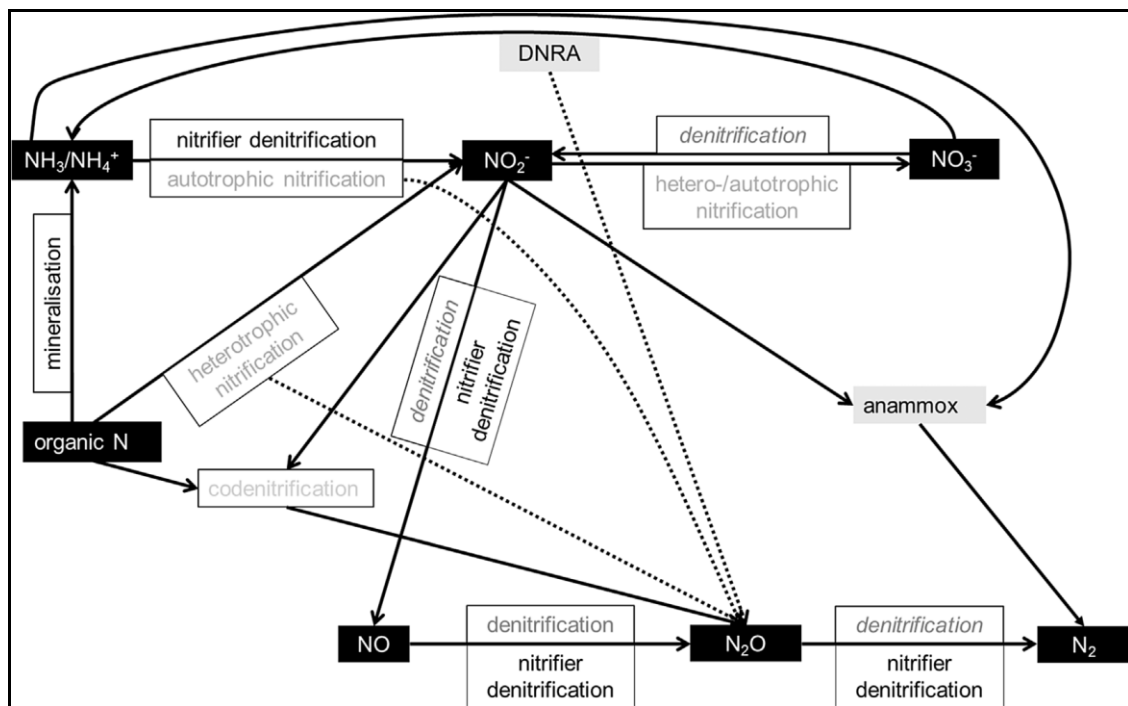


Fig. 1. N pools (black boxes) and microbial transformation processes (white boxes) in soil (Wrage-Mönnig et al., 2018). Solid arrows represent pathways, dotted lines the production of possible by-products (DNRA: dissimilatory nitrate reduction to ammonia).

Nitrifier denitrification, i.e. the reduction of nitrite by ammonia-oxidizing bacteria, is a pathway of autotrophic nitrification and has been reported mostly under high NO_2^- , NH_3 , or urea concentrations and low organic C availability (Wrage-Mönnig et al., 2018; Wrage et al., 2001). In contrast, coupled nitrification-denitrification are two separate processes by distinct microorganisms. NO_2^- and NO_3^- are produced by nitrifiers in oxic habitats and subsequently denitrified by denitrifiers in close-by anoxic habitats

(Butterbach-Bahl et al., 2013; Wrage et al., 2001). Nitrification requires oxygen and only takes place under oxic conditions, while nitrifier denitrification and coupled nitrification-denitrification are often found at oxic/anoxic interfaces.

To quantify total denitrification rates, all gaseous end products, i.e. NO, N₂O, and N₂ need to be measured. However, as atmospheric N₂ concentration is ~78 %, small amounts of soil-emitted N₂ can only be quantified in artificial N₂-free atmospheres or by using ¹⁵N labeling. In artificial atmospheres, N₂ is commonly replaced by He (Köster et al., 2013; Scholefield et al., 1997; Senbayram et al., 2018; Wang et al., 2011), although studies in Ar-O₂ atmosphere have been conducted (Stefanson, 1970). Elsewise, high enrichment ¹⁵N labeled NO₃⁻ can be added to soils to directly quantify N₂O and N₂ produced from the labelled NO₃⁻ pool (Hauck and Melsted, 1956). If ¹⁵N enrichment in the active NO₃⁻ pool undergoing denitrification is 40-60 at%, ²⁹N₂ makes up 48-50 % of N₂ produced from this pool and ³⁰N₂ 16-36 % (Siegel et al., 1982), and can be quantified using an isotope ratio mass spectrometer (Lewicka-Szczebak et al., 2013).

To further differentiate between N₂O-emitting processes, stable isotope methods can be used. Process-oriented studies often use position-specific labeling (i.e. ¹⁵NH₄NO₃ and NH₄¹⁵NO₃) to separate N₂O production from nitrification and denitrification (Müller et al., 2014). In natural abundance studies, the isotopic signatures of N₂O can be determined including bulk nitrogen (δ¹⁵N_{bulk}), the intramolecular distribution of ¹⁵N within the linear N₂O molecule (nitrogen site preference, δ¹⁵N_{SP}), and oxygen (δ¹⁸O) (Brenninkmeijer and Röckmann, 1999; Toyoda and Yoshida, 1999). N₂O isotopomers can be used to separate bacterial denitrification/nitrifier denitrification from nitrification and fungal denitrification (Rohe et al., 2014; Sutka et al., 2008, 2006; Toyoda et al., 2005; Yu et al., 2020). In addition, N₂O reduction to N₂ can be estimated from the isotopic signature of the residual unreduced N₂O fraction (Lewicka-Szczebak et al., 2017).

Although denitrification in soils has been studied for many decades and advanced methods to quantify total denitrification rates have been available for several years,

studies that directly quantify N_2 emissions in the presence of plants are still the exception. Thus, the overarching aims of this thesis were (i) to investigate how growing plants and plant litter affect substrate availability (NO_3^- and C_{org}) for denitrification, (ii) how the interaction between C and N availability controls denitrification product stoichiometry, and (iii) to estimate which processes contribute to N_2O formation depending on C and N availability. The first chapter addresses the period of active plant growth and investigates how growing plants control denitrification through NO_3^- uptake and rhizodeposition. In the presented experiment, the ^{15}N gas flux method with high enrichment $^{15}NO_3^-$ labeling was applied to estimate plant N uptake, total N_2O and denitrification-derived N_2O+N_2 emissions. Simultaneous $^{13}CO_2$ pulse labeling enabled estimation of C translocation from shoots to roots and its release by roots into the soil. The second part of this thesis addresses the post-harvest period. Litter quality and available mineral N control mineralization of organic C and N compounds and thus C_{org} and NO_3^- availability for denitrifying microorganisms. Chapter two concentrates on the dynamic of mineralization from litter and soil organic matter, and subsequent CO_2 and N_2O emissions. Further, the soil-inhabiting bacterial community structure was analyzed using 16S rRNA gene sequencing. Chapter three is a sequel to chapter two, focusing on N_2O -emitting processes and the separation of litter and soil organic matter derived CO_2 . Here, incubation in He- O_2 atmosphere was combined with the isotopocule mapping approach to determine NO, N_2O , and N_2 fluxes, as well as the contribution of N_2O -emitting processes. All studies were conducted in the laboratory to enable working under controlled conditions and maize (*Zea mays* L.) was used as model plant to compare results over all experiments.

Chapter 1

Nitrate uptake and carbon exudation – do plant roots stimulate or inhibit denitrification?

Pauline Sophie Rummel^{1*}, Reinhard Well², Birgit Pfeiffer^{1,3}, Klaus Dittert¹, Sebastian Floßmann⁴, and Johanna Pausch⁴

¹ Division of Plant Nutrition and Crop Physiology, Department of Crop Science, University of Göttingen, Germany

² Thünen Institute of Climate-Smart Agriculture, Federal Research Institute for Rural Areas, Forestry and Fisheries, Braunschweig, Germany

³ Institute of Microbiology and Genetics, Department of Genomic and Applied Microbiology, University of Göttingen, Germany

⁴ Agroecology, Faculty for Biology, Chemistry, and Earth Sciences, University of Bayreuth, Germany

* corresponding author: pauline.rummel@uni-goettingen.de; Phone: ++49 551 39 4471, Fax: ++49 551 39 25570

Published in: Plant and Soil, 459, 217–233, 2021; <https://doi.org/10.1007/s11104-020-04750-7>

Author contributions:

PSR, JP, RW, BP, and KD designed the experiment and PSR and SF carried them out. PSR, and RW analyzed the data. PSR prepared the manuscript and all co-authors provided critical feedback.



Nitrate uptake and carbon exudation – do plant roots stimulate or inhibit denitrification?

Pauline Sophie Rummel · Reinhard Well · Birgit Pfeiffer · Klaus Dittert · Sebastian Floßmann · Johanna Pausch

Received: 12 May 2020 / Revised: 25 September 2020 / Accepted: 20 October 2020
© The Author(s) 2020

Abstract

Background and aims Plant growth affects soil moisture, mineral N and organic C availability in soil, all of which influence denitrification. With increasing plant growth, root exudation may stimulate denitrification, while N uptake restricts nitrate availability.

Methods We conducted a double labeling pot experiment with either maize (*Zea mays* L.) or cup plant (*Silphium perfoliatum* L.) of the same age but differing in size of their shoot and root systems. The ^{15}N gas flux method was applied to directly quantify N_2O and N_2 fluxes in situ. To link denitrification with available C in

the rhizosphere, $^{13}\text{CO}_2$ pulse labeling was used to trace C translocation from shoots to roots and its release by roots into the soil.

Results Plant water and N uptake were the main factors controlling daily $\text{N}_2\text{O} + \text{N}_2$ fluxes, cumulative N emissions, and N_2O production pathways. Accordingly, pool-derived $\text{N}_2\text{O} + \text{N}_2$ emissions were 30–40 times higher in the treatment with highest soil NO_3^- content and highest soil moisture. CO_2 efflux from soil was positively correlated with root dry matter, but we could not detect any relationship between root-derived C and $\text{N}_2\text{O} + \text{N}_2$ emissions.

Conclusions Root-derived C may stimulate denitrification under small plants, while N and water uptake become the controlling factors with increasing plant and root growth.

Responsible Editor: Jorge Durán.

Supplementary Information The online version contains supplementary material available at <https://doi.org/10.1007/s11104-020-04750-7>.

P. S. Rummel (✉) · B. Pfeiffer · K. Dittert
Division of Plant Nutrition and Crop Physiology, Department of Crop Science, University of Göttingen, Göttingen, Germany
e-mail: pauline.rummel@uni-goettingen.de

R. Well
Thünen Institute of Climate-Smart Agriculture, Federal Research Institute for Rural Areas, Forestry and Fisheries, Braunschweig, Germany

B. Pfeiffer
Institute of Microbiology and Genetics, Department of Genomic and Applied Microbiology, University of Göttingen, Göttingen, Germany

S. Floßmann · J. Pausch
Agroecology, Faculty for Biology, Chemistry, and Earth Sciences, University of Bayreuth, Bayreuth, Germany

Keywords Nitrous oxide · Dinitrogen · Nitrogen mineralization · Rhizodeposition · ^{15}N ^{13}C labeling · Carbon cycling

Introduction

Soil conditions for denitrification have frequently been studied with the main prerequisites being availability of nitrate (NO_3^-) and easily decomposable organic substances, and oxygen deficiency (Burford and Bremner 1975; Firestone et al. 1979). Growing plants modify all these parameters, particularly the availability of the main substrates (NO_3^- and C_{org}) and soil moisture, and

may thus play an important role in regulating denitrification in situ (von Rheinbaben and Trolldenier 1984).

Plant N uptake largely controls concentration and distribution of mineral N in soils. Amounts and rates of plant N uptake depend on plant species, age, physiological status, root size, and nutritional status. N uptake rates of maize and cereals remain low during the first two months of growth, then increase linearly with increasing biomass reaching a maximum around the time of flowering (Novák and Vidovič 2003, Malhi et al. 2011).

Plant roots contribute to organic C input to the soil through rhizodeposition and decaying roots and root hairs. Thus, total and available concentration of C_{org} is higher in the rhizosphere compared to bulk soil (Cheng et al. 1993). The amount of rhizodeposited C and its quality depend on plant species, age, and development (Gransee and Wittenmayer 2000; Vancura 1964; Vancura and Hovadik 1965), and plant nutrient status (Carvalhais et al. 2011). In general, younger plants translocate a higher share of assimilated C belowground than mature plants (Kuzyakov and Domanski 2000; Nguyen 2003), and perennial plants translocate a higher share of assimilated C belowground than annual plants (Husáková et al. 2018; Pausch and Kuzyakov 2018).

C and N availability are closely interrelated in the rhizosphere: Under low mineral N concentrations, root morphology is altered, and exudation related to root mass is increased (Paterson and Sim 1999). In addition, the composition of maize root exudates is altered under N deficiency (Carvalhais et al. 2011). On the other side, N fertilization decreases the portion of below-ground translocated C (Kuzyakov and Domanski 2000).

Several studies have tried to disentangle the effects of N and C availability on denitrification with contradictory results. Higher denitrification rates were measured from planted compared to bare soil (Senbayram et al. 2020; Vinther 1984). Some studies showed a strong influence of roots (Philippot et al. 2009), increasing denitrification rates with increasing root biomass (Klemedtsson et al. 1987), and higher potential denitrification activity in rhizosphere soil compared to bulk soil (Hamonts et al. 2013; Malique et al. 2019). Higher denitrification rates in planted soils have been associated with higher C_{org} availability in the rhizosphere (Bakken 1988; Philippot et al. 2009). In addition, denitrification rates correlated with soil NO_3^- content (Philippot et al. 2009; von Rheinbaben and Trolldenier 1984). In contrast, other studies found no differences between planted and

unplanted soil (Haider et al. 1985). Denitrification was increased only with poorly growing plants (von Rheinbaben and Trolldenier 1984) or when root biomass started to decrease (Haider et al. 1987), and NO_3^- availability did not affect denitrification (Haider et al. 1987; Hamonts et al. 2013). The majority of these studies measured potential denitrification applying the acetylene inhibition method (Yoshinari and Knowles 1976), which is considered outdated due to a number of drawbacks such as inhibiting nitrification (Groffman et al. 2006).

Accordingly, it is still unclear whether growing plants stimulate denitrification through root exudation or restrict it through NO_3^- uptake. Reliable measurements of N_2 fluxes and $N_2O/(N_2O + N_2)$ ratios in the presence of plants are scarce. Direct measurement of N_2 fluxes is only possible in either artificial N_2 -free atmosphere (Scholefield et al. 1997, Senbayram et al. 2020) or by applying highly enriched ^{15}N labeled NO_3^- (Hauck and Melsted 1956). The latter is used in the ^{15}N gas flux technique which enables direct quantification of N_2O and N_2 produced from the labelled NO_3^- pool and estimation of processes contributing to N_2O and N_2 formation including denitrification, co-denitrification, or nitrification and nitrifier denitrification (Buchen et al. 2016, Laughlin and Stevens 2002).

This study aimed to directly quantify N_2O and N_2 fluxes from soil with plants of the same age but different size of shoot and root systems and to relate denitrification to C availability from root exudation. As plant water uptake may also affect denitrification (von Rheinbaben and Trolldenier 1984), we aimed to keep soil moisture constant by continuous irrigation. We hypothesized that (I) plant N uptake governs NO_3^- availability for denitrification. When plant N uptake is low due to smaller root system or root senescence, N_2O and N_2 emissions are increased. (II) Denitrification is stimulated by higher C_{org} availability from root exudation or decaying roots increasing total gaseous N emissions and decreasing their $N_2O/(N_2O + N_2)$ ratios.

Materials and methods

Experimental concept

The experiment consisted of a pre-cultivation phase followed by the experimental phase. A schematic overview of both phases is presented in Fig. 1. In the pre-

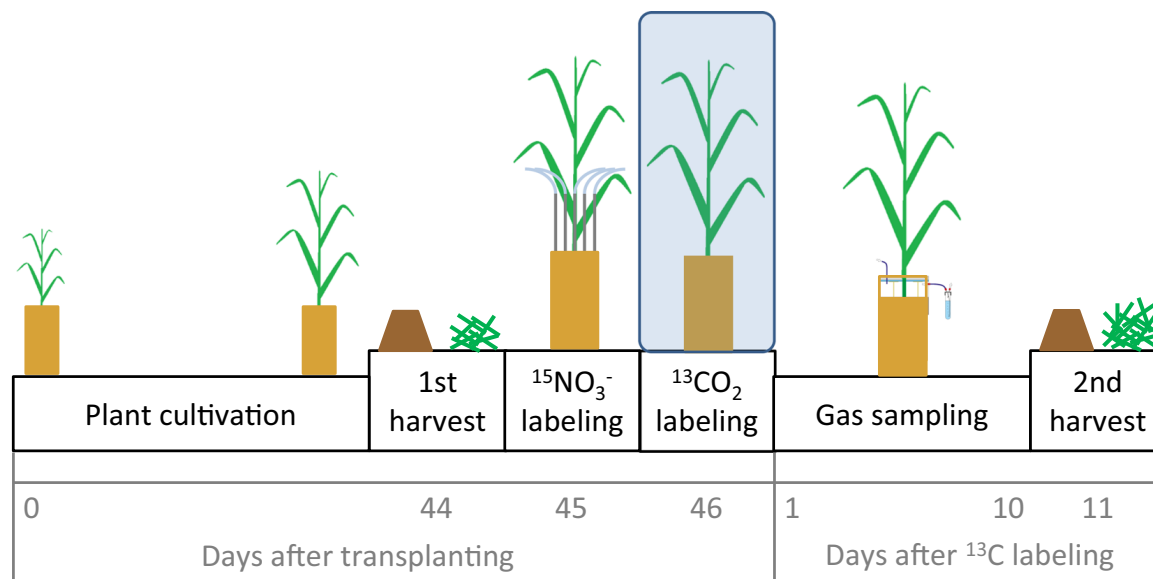


Fig. 1 Timeline of the experiment: pre-cultivation phase from day 0–46 and experimental phase from day 47–57 after transplanting

cultivation phase, plants were raised under controlled conditions. Maize plants (*Zea mays* L. cv. Ronaldinio) were grown under different N fertilization to obtain plants with different root and shoot biomass. As a second species, cup plant (*Silphium perfoliatum* L.) was included, a bioenergy plant that can produce similar aboveground biomass as maize (Gansberger et al. 2015) but has a higher root:shoot ratio. As cup plant is a perennial plant, it likely transfers more C belowground and exudes more organic substances than maize (Husáková et al. 2018; Pausch and Kuzyakov 2018). In all treatments, the N supply was scheduled to assure that at the end of the pre-cultivation phase, the soils were equally depleted in plant available N. With respect to background N supply, this permitted nearly equal starting conditions for the subsequent stable isotope labeling experiment.

To account for all necessary measurements, each treatment was replicated 19 times (Table 1). At the end of the pre-cultivation phase, the first set of replicates (1–

6) was harvested to determine shoot and root biomass, N and C content, and ¹⁵N and ¹³C background concentrations. The second set of replicates (7–12) was labeled with ¹⁵NO₃⁻ and ¹³CO₂, and gases evolving from soil were measured for the following 10 days. At the end of the experiment, replicates 7–12 were harvested. Replicate 13 was used to determine ¹³C uptake during ¹³CO₂ pulse labeling and replicates 14–19 were used to determine ¹³C background values in soil-emitted CO₂.

Pre-experimental plant cultivation

The soil for the experiment was collected from a long-term experimental field site of the Höhere Landbauschule Rotthalmünster, Germany (latitude N48°21', longitude E13°11', elevation 360 m above sea level) in summer 2016. It was sieved to 10 mm, air dried, and stored at 4 °C until setup of the experiment. The soil was classified as a Haplic Luvisol with a silty loam texture (19% clay, 71% silt, 10% sand). Soil

Table 1 Overview of replicates in the experiment

Replicate	Labeling	Sampling of plants and soil	Details
1–6	-	1st harvest (44 days)	Determination of dry matter, C and N background values
7–12	¹⁵ NO ₃ ⁻ and ¹³ CO ₂	Final harvest (57 days)	Measurement of N ₂ O, N ₂ , and CO ₂ , determination of dry matter, total C and N, ¹³ C and ¹⁵ N content
13	¹³ CO ₂	Plants sampled directly after ¹³ CO ₂ labeling	Determination of total ¹³ CO ₂ uptake during labeling
14–19	Treated similar to 7–12, but not labeled	No sampling of plants and soil	Determination of ¹³ C background in CO ₂

properties were: total C 1.23%, total N 0.14%, C:N 8.76, pH (CaCl₂) 6.74.

Seven kg dry soil was mixed with fertilizers (0.14 g P kg⁻¹ as Ca(H₂PO₄)₂, 0.2 g K kg⁻¹ as K₂SO₄ and 0.04 g Mg kg⁻¹ as MgSO₄ * 7 H₂O including 0.135 g S kg⁻¹) and filled in pots of 15 cm diameter and 35 cm height to a bulk density of 1.3 g cm⁻³. Soil moisture was adjusted to 60% water holding capacity (WHC, 21.9% gravimetric water content) and watered regularly. TDR soil moisture sensors (Decagon Devices, Pullman, USA) were used to monitor soil water content during plant growth.

Maize seeds (*Zea mays* L. cv. Ronaldinio) were germinated on wet paper for 4 days. Cup plant (*Silphium perfoliatum* L.) had been pre-cultivated for 2 years in 5 cm-pots and had 2–4 leaves. Per pot, either one germinated maize seed or one cup plant seedling was transplanted. Plants were cultivated in a climate chamber (Weiss, Loughborough, UK) with a diurnal cycle of 16 h day (light intensity 300 μmol m⁻² s⁻¹, air temperature 25 °C, relative humidity 50%) and 8 h night (18 °C, 60%). Daytime included 4 h sunrise and 4 h sunset when light intensity, temperature, and relative humidity were gradually adjusted. All pots were fully randomized weekly to avoid microclimatic effects.

Maize N fertilization differed between treatments to achieve plants of different size: Maize S (no N fertilization, small plants), Maize M (0.05 g N kg⁻¹ (0.35 g N pot⁻¹, as NH₄NO₃ split in 7 doses), medium sized plants), and Maize L (0.086 g N kg⁻¹ (0.6 g N pot⁻¹, as NH₄NO₃ split in 7 doses), large plants). Cup plants were fertilized like Maize M (0.05 g N kg⁻¹ (0.35 g N pot⁻¹, as NH₄NO₃ split in 7 doses)).

Experimental ¹⁵NO₃⁻ and ¹³CO₂ pulse labeling

Replicates 7–12 of each treatment received 0.1 g N kg⁻¹ ¹⁵N-labeled Ca(NO₃)₂ (~60 at% ¹⁵N₂, Campro Scientific GmbH, Berlin, Germany) 45 days after transplanting. The tracer was dissolved in H₂O_{dest} and applied by injection with stainless steel needles as described by Buchen et al. (2016). Briefly, ¹⁵N fertilizer solution was injected via 12 needles to 6 depths (2.5, 7.5, 12.5, 17.5, 22.5 and 27.5 cm) aiming for optimal three-dimensional homogenous label distribution (Wu et al. 2011). Per injection point, 10 ml tracer solution were injected via a peristaltic pump (Ismatec, Wertheim, Germany) to simultaneously increase soil water content

to 75% water-filled pore space (WFPS, equivalent to 80% WHC).

After injection of ¹⁵N tracer solution, all pots were closed with acrylic glass lids with a hole for the plant shoot, leaving a small headspace (2–3 cm) between soil surface and lid. Pots were then sealed with silicone paste (Tacosil 171, Thauer & Co. KG, Dresden, Germany). Plants were labeled with ¹³C in four separate chambers made from translucent greenhouse film (one for each treatment Maize S, Maize M, Maize L, and Cup plant). In each chamber, ¹⁵N labeled replicates 7–12 and the non-labeled replicate 13 were labeled with ¹³C. To enrich the chamber atmosphere with ¹³CO₂, 60 ml of 5 M H₂SO₄ were added to 5 g Na₂¹³CO₃ (99 at%) dissolved in H₂O_{dest} in each chamber. For internal chamber ventilation, two fans were installed. The plants were pulse labeled in the ¹³CO₂ enriched atmosphere for 5 h. Before opening each chamber, an air sample was analyzed for CO₂ concentration to ensure that maximum amounts of CO₂ had been taken up by plants. Chambers were opened and CO₂ evolving from the soil was trapped. Replicate 13 was harvested directly after chamber opening to estimate the amount of ¹³C assimilated during labeling.

To determine natural abundance background of ¹³C in CO₂, replicates 14–19 were used. 0.1 g N kg⁻¹ was injected using Ca(NO₃)₂*6 H₂O dissolved in H₂O_{bidest}, and pots were sealed using the same methods as described above.

Irrigation

After pots had been sealed with silicon paste, plants were irrigated by injecting water through a valve on the bottom of the pots. To irrigate pots without applying too much pressure, peristaltic pumps (Watson-Marlow, Zollikon, Switzerland) with a pumping rate of 1.5 ml min⁻¹ were used. Target soil moisture was 75% water-filled pore space (WFPS, equivalent to 80% WHC) during the gas sampling phase. To estimate irrigation demand, TDR soil moisture sensors (Decagon Devices, Pullman, USA) were used to monitor soil water content during the experiment in one replicate for each treatment. In addition, all pots were weighed one, three, and five days after ¹³C labeling to compare whether irrigation demand differed between pots. As pot weights were comparable within treatments, sensor data were used to compare soil moisture.

Gas sampling

One additional pot was filled with dry quartz sand, sealed with silicone paste as described before, and used as a reference to determine background gas concentrations. To flush the headspace of all pots with CO₂-free air, pressurized air was first run through a glass column filled with soda lime (pellets made of NaOH and Ca(OH)₂ mixture) to remove CO₂. For trapping CO₂ emitted from soils, the outlet tubes of the pots' headspaces were connected to glass tubes containing 15 ml of 1 M NaOH solution. Starting one day after labeling, NaOH solution was changed in intervals of 6, 12, or 24 hours. To determine ¹³C background in CO₂, replicates 14–19 were treated similarly: the headspaces were flushed for 6 hours and CO₂ was trapped in glass tubes containing 15 ml of 1 M NaOH solution. To estimate the total CO₂ efflux, the C concentration of the NaOH solutions was determined with a TIC-analyzer (multi N/C 2100S, Analytik Jena, Jena, Germany). For ¹³C measurements, CO₂ trapped in NaOH was precipitated as SrCO₃ with an excess of 1 M SrCl₂ solution. The precipitants were centrifuged, washed with deionized water until the pH was neutral, the precipitate was frozen, and then freeze-dried with a rotation vacuum concentrator (RVC 2–25 CDplus, Martin Christ, Osterode am Harz, Germany) and a cooling trap (CT 02–50, Martin Christ, Osterode am Harz, Germany), both connected to a vacuum pump.

¹³C enrichment in precipitated SrCO₃ was analyzed: Natural abundance samples were measured on an elemental analyzer NA 11,100 (CE Instruments, Milano, Italy) linked to a Delta Plus gas-isotope ratio mass spectrometer (Finnigan MAT, Bremen, Germany) via a ConFlo III interface (Finnigan MAT, Bremen, Germany). For enriched samples, depending on capacity, one of the following combinations was used: (i) elemental analyzer Flash 2000 (Thermo Fisher Scientific, Cambridge, UK) linked to a Delta V Advantage gas-isotope ratio mass spectrometer (Thermo Electron, Bremen, Germany) via a ConFlo III interface (Thermo Electron, Bremen, Germany), or (ii) elemental analyzer NA1108 (Fisons-Instruments, Milan, Italy) linked to a Delta C gas-isotope ratio mass spectrometer (Finnigan MAT, Bremen, Germany) via a ConFlo III interface (Thermo Electron Cooperation, Bremen, Germany).

For N₂O and N₂ sampling, the airflow through the pots' headspace was interrupted to accumulate gases in the headspace. After 1 h, duplicate samples were taken

using a syringe and filled in pre-evacuated 12-ml Exetainer® glass vials (Labco, High Wycombe, UK). Samples were analyzed for N₂O concentration using a gas chromatograph (GC 7890A, Agilent, Santa Clara, USA). The analytical precision of the GC was determined by repeated measurements of standard gases (300 ppb N₂O) and was consistently < 3%. The second duplicate was analyzed for *m/z* 28 (¹⁴N¹⁴N), 29 (¹⁴N¹⁵N) and 30 (¹⁵N¹⁵N) of N₂ using a modified GasBench II preparation system coupled to an isotope ratio mass spectrometer (MAT 253, Thermo Fisher Scientific, Bremen, Germany) according to Lewicka-Szczebak et al. (2013). This system allows a simultaneous determination of mass ratios ²⁹R (29/28) and ³⁰R (30/28) of three separated gas species (N₂, N₂ + N₂O, and N₂O), all measured as N₂ gas after N₂O reduction in a Cu oven. Typical repeatability of ²⁹R and ³⁰R (1 σ of 3 replicate measurements) was 5 × 10^{−7} for both values. For each of the analyzed gas species, the fraction originating from the ¹⁵N-labeled pool with respect to total N in the gas sample (*F_p*) as well as the ¹⁵N enrichment of the active ¹⁵N-labeled N pool (*a_p*) producing N₂O (*a_{p,N2O}*) or N₂ + N₂O (*a_{p,N2+N2O}*) were calculated after Spott et al. (2006) as described in Lewicka-Szczebak et al. (2017).

Harvest and analyses of plant and soil material

Before labeling (44 days after transplanting), replicates 1–6 were harvested. Eleven days after ¹³C labeling (57 days after transplanting), all labeled plants (replicates 7–12) were harvested. At both harvests, plants were separated into shoots and roots including maize crown roots. As all pots were densely rooted, a separation of rhizosphere and bulk soil was not possible. Roots were shaken gently to separate them from soil and washed. From replicates 7–12, a subsample of root washing water was analyzed for water-extractable organic C (WEOC) and the amount of ¹³C lost during root washing was determined. To estimate their amount in soil, fine roots were picked by hand from a subsample of soil (~ 400 g soil) for a defined time. All plant material and a soil subsample were dried at 60 °C, milled in a ball mill and analyzed for total C, ¹³C, total N, and ¹⁵N content using an elemental analyzer coupled to a gas-isotope ratio mass spectrometer as described earlier. For determination of water-extractable organic C (WEOC) content, a subsample of fresh soil was analyzed according to Chantigny et al. (2007). Briefly, fresh soil was

homogenized with deionized water (1:2 w/v). Samples were centrifuged and filtered with 0.45 µm polyether sulfone filters (Labsolute, Renningen, Germany), split in two subsamples and stored at -20 °C. The extracts were analyzed for total C, organic C, and total N content using a multi N/C® Analyzer (Analytik Jena, Jena, Germany).

For determination of soil mineral N content, a subsample of 50 g was frozen at -20 °C. Frozen samples were extracted with a 2 M KCl solution (1:5 w/v) for 60 min on an overhead shaker (85 rpm). The extracts were filtered with 615 ¼ filter paper (Macherey – Nagel GmbH & Co. KG, Düren, Germany), split in two subsamples, and stored at -20 °C. The extracts were analyzed colorimetrically for the concentrations of NO_3^- and NH_4^+ using a San⁺⁺ continuous flow Analyzer (Skalar Analytical B.V., Breda, The Netherlands). ^{15}N concentration in NH_4^+ and NO_3^- was analyzed using an automated sample preparation unit for inorganic nitrogen coupled to a membrane inlet quadrupole mass spectrometer (QMS, GAM 200, InProcess, Bremen, Germany) as described in detail by Eschenbach et al. (2017, 2018). In parallel subsamples, soil water content was determined by oven drying at 105 °C.

Calculations and statistics

Plant N uptake was calculated by multiplying dry mass with the respective tissue N content (root, shoot).

Cumulative CO_2 emissions were calculated from CO_2 trapped in NaOH, CO_2 fluxes were calculated by dividing cumulative CO_2 through the respective trapping time (6, 12, or 24 h). ^{13}C recovery in CO_2 ($^{13}\text{C}_{\text{recovery}; \text{CO}_2}$, mg) was calculated as the excess (above background) ^{13}C concentration multiplied with the total CO_2 trapped (CO_2 , mg $\text{CO}_2\text{-C}$):

$$^{13}\text{C}_{\text{recovery}; \text{CO}_2} = (^{13}\text{C}_{\text{CO}_2} - ^{13}\text{C}_{\text{NA}; \text{CO}_2}) * \text{CO}_2 \quad (1)$$

where $^{13}\text{C}_{\text{CO}_2}$ is the ^{13}C enrichment of CO_2 (at%) trapped after labeling and $^{13}\text{C}_{\text{NA}; \text{CO}_2}$ is the natural ^{13}C background (at%) from unlabeled plants (replicates 14–19). ^{13}C recovery in soil ($^{13}\text{C}_{\text{recovery}; \text{soil}}$, mg) was calculated as follows:

$$^{13}\text{C}_{\text{recovery}; \text{soil}} = (^{13}\text{C}_{\text{soil}} - ^{13}\text{C}_{\text{NA}; \text{soil}}) * C_{\text{soil}} * \text{mass}_{\text{soil}} \quad (2)$$

where $^{13}\text{C}_{\text{soil}}$ is the enrichment of ^{13}C (at%) of the soil C

pool after labeling, $^{13}\text{C}_{\text{NA}}$; soil is the natural abundance of ^{13}C in soil before labeling (at%), C_{soil} is the total content of C in soil (mg g^{-1}), and $\text{mass}_{\text{soil}}$ is the mass of soil per pot (g). *Relative* $^{13}\text{C}_{\text{recovery}}$ (% of recovered ^{13}C) of a particular pool (CO_2 , soil) was calculated by dividing the amount of ^{13}C recovered in that pool ($^{13}\text{C}_{\text{recovery}; \text{pool}}$) by the sum of the amount of ^{13}C recovered in all pools (CO_2 , shoot, root, soil, root washing water).

$$\text{Relative } ^{13}\text{C}_{\text{recovery}} = \frac{^{13}\text{C}_{\text{recovery}; \text{pool}}}{\sum ^{13}\text{C}_{\text{recovery}; \text{pool}}} * 100 \quad (3)$$

Total N_2O fluxes (f_{tot} , $\mu\text{g N kg}^{-1} \text{h}^{-1}$) were calculated from GC measurements:

$$f_{\text{tot}} = \frac{(C_H - C_B)}{t} * \frac{V}{m} \quad (4)$$

where C_H is the mass concentration in the headspace and C_B is the background concentration in the reference pot ($\mu\text{g N m}^{-3}$) corrected by the chamber temperature according to the ideal gas law, t is the accumulation time (h), V is the volume of the headspace (m^3), and m is the dry mass of soil per pot (kg).

We calculated the ^{15}N enrichment of the active NO_3^- pool undergoing denitrification ($ap_N_2\text{O}$, $ap_N_2\text{O} + N_2$) from the non-random distribution of N_2 and/or N_2O isotopologues using calculations by Spott et al. (2006) as described by Buchen et al. (2016) and Lewicka-Szczebak et al. (2017):

$$a_p = \frac{^{30}X_m - a_{bgd} * a_m}{a_m - a_{bgd}} \quad (5)$$

where a_p is the ^{15}N abundance of the ^{15}N labeled NO_3^- pool undergoing denitrification, a_{bgd} is the measured ^{15}N abundance of atmospheric background N_2 , a_m is the measured ^{15}N abundance of N_2 or N_2O

$$a_m = \frac{^{29}R + 2 * ^{30}R}{2(1 + ^{29}R + ^{30}R)} \quad (6)$$

and $^{30}x_m$ is the measured fraction of m/z 30 in N_2 and converted N_2O :

$$^{30}x_m = \frac{^{30}R}{1 + ^{29}R + ^{30}R} \quad (7)$$

The fraction of N derived from the active NO_3^- pool (F_p) was calculated using Eq. (8) if ^{30}R was significant and otherwise Eq. (9) was used. In the latter case, $ap_N_2\text{O}$ was assumed to be identical with ap_N_2 and $ap_N_2\text{O} + N_2$ and was thus used when calculating

Fp_{N_2} and $Fp_{N_2O + N_2}$ from Eq. 9. If ap_{N_2O} of a sampling date was not available, the mean value from the other replicates from the same sampling date was used as best estimate. Fp calculated from Eq. (9) with a given ^{29}R is relatively insensitive to changes in ap between 0.4 and 0.6 since the nominator yields values between 0.48 and 0.5. Hence, uncertainty in the estimation of ap within that range causes minor uncertainty in calculated Fp (Well and Myrold 1999). Because ap values in our study were typically between 0.4 and 0.6, we assume that uncertainty in Fp calculation from the missing of individual ap values was small.

$$Fp = \frac{a_m - a_{bgd}}{a_p - a_{bgd}} \quad (8)$$

$$Fp = (^{29}R_{sa} - ^{29}R_{bgd}) / (2a_p(1 - a_p)) \quad (9)$$

where lower case *sa* and *bgd* denote sample and background (ambient air), respectively.

Fp values were multiplied with respective total sample N concentration (N_2O , N_2) to obtain pool-derived gas concentrations (in ppm). Then, pool-derived fluxes (fp) were calculated from concentrations similar to Eq. (4). The same calculations were used for N_2O , N_2 , and $N_2O + N_2$, resulting in respective values for fractions of pool-derived N and for the respective ^{15}N abundances of the active N pools (ap_{N_2O} , ap_{N_2} , $ap_{N_2O + N_2}$). Non-pool derived N_2O fluxes were calculated by subtracting pool-derived N_2O fluxes from total N_2O fluxes.

The ratio of denitrification end products was calculated from pool-derived N_2O (fp_{N_2O}) and $N_2O + N_2$ ($fp_{N_2O + N_2}$):

$$Product\ ratio = \frac{fp_{N_2O}}{fp_{N_2O + N_2}} \quad (10)$$

Cumulative N_2O , N_2 , and $N_2O + N_2$ emissions were calculated by linear interpolation of fluxes. The % of $N_2 + N_2O$ emitted with respect to added N was estimated by dividing cumulative pool-derived $N_2O + N_2$ emission by the amount of N added with $^{15}NO_3^-$ labeling.

All statistical analyses were performed using the statistical software R version 3.6.0 (R Core Team 2019). Means and standard deviations were calculated over all replicates. For harvest data, cumulative CO_2 , and ^{13}C recovery a one-way ANOVA was calculated followed by Tukey's HSD post-hoc test at $p \leq 0.05$ to

separate treatment effects. As cumulative N emissions were not normally distributed, the Kruskal-Wallis rank sum test was used followed by LSD post-hoc test at $p \leq 0.05$ to separate treatment effects. To compare soil and plant samples between harvests, and to test whether soil $^{15}a_{NO_3^-}$ contents at final harvest and ap_{N_2O} or $ap_{N_2O + N_2}$ at last sampling date differed, a t-test was used at $p \leq 0.05$. Simple linear regression models were tested to analyze the effects of soil and plant parameters on CO_2 and N fluxes and cumulative emissions.

Results

Plant growth after labeling

Shoot dry matter increased significantly in all treatments between the first and the second harvest, but differences between treatments did not change (Table 2, results of 1st harvest are displayed in supplementary table S1). Root dry matter significantly decreased in Maize S and M until the end of the experiment. Increases in root dry matter in Maize L and Cup plant were not significant. Root:shoot ratio decreased in all treatments but remained twice as high in cup plant compared to maize, which is typical for perennial plants compared to annual plants (Husáková et al. 2018). Nitrogen content increased in previously unfertilized Maize S plants and was similar in all maize treatments at the final harvest. Nitrogen content in cup plant shoots and roots was significantly greater than in all maize treatments and total N uptake corresponded with N fertilization Maize L > Maize M = Cup plant > Maize S. Soil NO_3^- content analyzed at the end of experiment was on average still twice as high in Maize S compared to all other treatments.

Total N_2O and pool-derived $N_2O + N_2$ fluxes and cumulative emissions

Total and pool-derived N fluxes were highest in Maize S but followed a similar pattern in all treatments (Fig. 2a + c). Total N_2O fluxes strongly increased in Maize S reaching highest values on day 3 ($11.3 \mu g N_2O-N kg^{-1} h^{-1}$, Fig. 2a) and a second smaller peak on day 6 ($5.9 \mu g N_2O-N kg^{-1} h^{-1}$). Pool-derived $N_2O + N_2$ fluxes followed a similar general pattern as total N_2O fluxes (Fig. 2c) and peaks were detected at similar times as N_2O peaks, in Maize S on day 3 ($48 \mu g N_2-N kg^{-1} h^{-1}$) and larger

Table 2 Harvest data of final harvest at the end of the experiment (replicates 7–12, 57 days after transplanting/ 11 days after $^{13}\text{CO}_2$ labeling)

	Maize S			Maize M			Maize L			Cup Plant		
Shoot dry matter (g pot^{-1})	63.5 ± 2.7	c	***	89.8 ± 4.0	b	***	115.3 ± 10.8	a	***	34.9 ± 5.4	d	***
Root dry matter (g pot^{-1})	10.1 ± 1.6	c	***	14.5 ± 0.8	b	***	21.5 ± 4.2	a	***	19.7 ± 1.8	a	
Root : Shoot ratio	0.16 ± 0.02	b	***	0.16 ± 0.01	b	***	0.19 ± 0.02	b	***	0.58 ± 0.09	a	
Shoot N content (%)	1.19 ± 0.04	b	***	1.14 ± 0.08	b	***	1.05 ± 0.14	b	***	2.47 ± 0.28	a	
Root N content (%)	1.06 ± 0.10	b	***	0.97 ± 0.08	b		0.95 ± 0.08	b		1.59 ± 0.19	a	
NO_3^- content (mg kg^{-1})	3.39 ± 2.01	a		1.54 ± 1.02	ab		1.04 ± 0.43	b		1.61 ± 0.83	ab	
NH_4^+ content (mg kg^{-1})	1.46 ± 0.19	ab	***	1.94 ± 0.36	a	***	1.64 ± 0.25	ab	***	1.41 ± 0.39	b	***
WEOC content (mg kg^{-1})	6.65 ± 0.95	a	***	7.35 ± 0.66	a	***	7.56 ± 2.69	a	***	8.10 ± 1.24	a	***
N uptake (shoot + root) (g pot^{-1})	0.86 ± 0.35	c		1.16 ± 0.087	b		1.41 ± 0.054	a		1.17 ± 0.044	b	

Shoot dry matter includes cob dry matter

Different letters in one row indicate a significant difference ($p < 0.05$) between treatments

***indicates a significant difference ($p < 0.05$) to first harvest

peaks on day 6.5 ($67 \mu\text{g N}_2\text{-N kg}^{-1} \text{h}^{-1}$) and day 9.5 ($61 \mu\text{g N}_2\text{-N kg}^{-1} \text{h}^{-1}$). Total N_2O and pool-derived $\text{N}_2\text{O} + \text{N}_2$ fluxes in all other treatments followed a similar pattern but on a lower scale. The product ratio ($\text{N}_2\text{O}/(\text{N}_2\text{O} + \text{N}_2)$, Fig. 2d) of pool-derived fluxes followed a similar pattern in all treatments. The product ratio decreased for the first days after onset of incubation reaching values between 0.2 and 0.5 as N_2 became the dominant end product of denitrification. It shortly increased and peaked on day 3.5, then decreased again until

day 6 to values between 0 and 0.2. After day 6.5, the product ratio ranged between 0 and 0.5 until the end.

Total and pool-derived cumulative N emissions were 20–43 times higher in Maize S compared to all other treatments (Table 3). No significant differences were detected between the other treatments. Similarly, recovery of added NO_3^- in $\text{N}_2\text{O} + \text{N}_2$ was highest in Maize S and not significantly different in the other treatments. The mean $\text{N}_2\text{O}/(\text{N}_2\text{O} + \text{N}_2)$ ratio ranged from 0.14 to 0.16 in maize treatments and was 0.24 in cup plant.

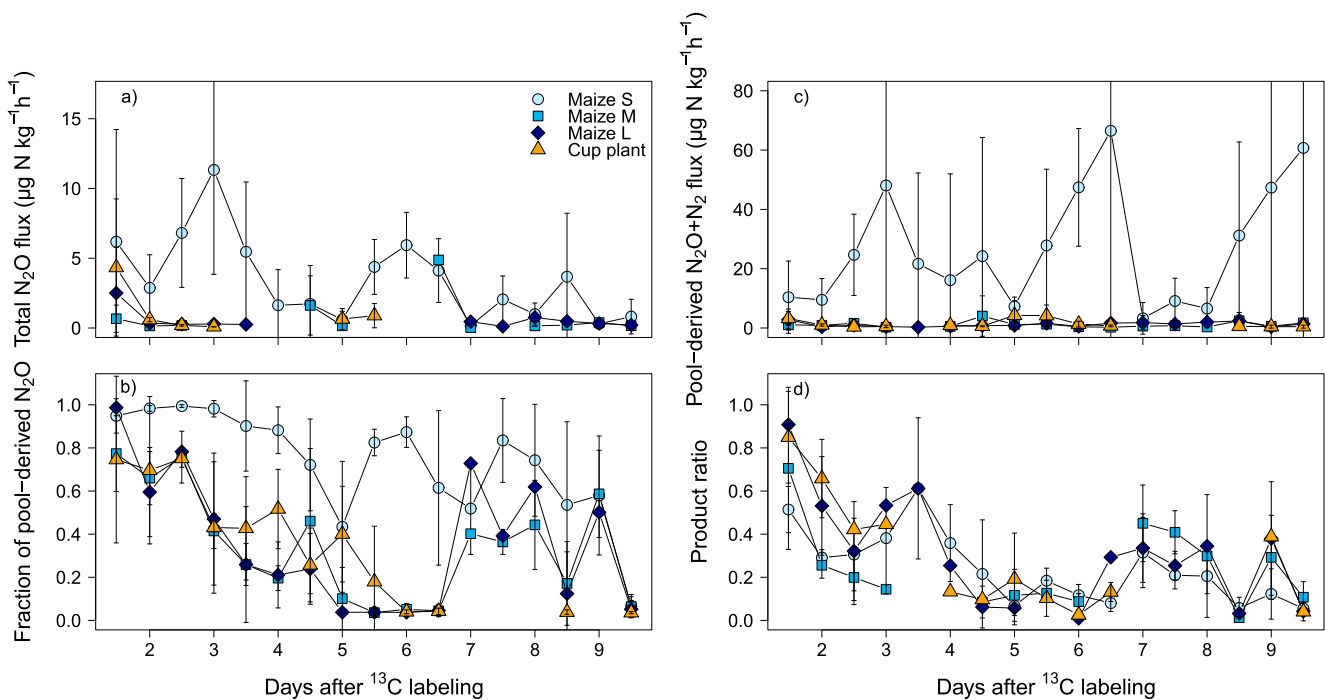


Fig. 2 Total N_2O fluxes (a), fraction of pool-derived N_2O ($F_{p_N_2O}$) (b), pool-derived $\text{N}_2\text{O} + \text{N}_2$ fluxes (c), and product ratio $\text{N}_2\text{O}/(\text{N}_2\text{O} + \text{N}_2)$ of pool-derived fluxes (d). Means and standard deviation for $n = 1-6$

Table 3 Total cumulative N₂O, pool-derived cumulative N₂ and N₂O + N₂ emissions, and product ratio of pool-derived fluxes

	Total cumulative N ₂ O		Pool-derived cumulative N ₂		Pool-derived cumulative N ₂ O + N ₂		N ₂ O/(N ₂ O + N ₂) ratio of cumulative pool-derived emissions		¹⁵ N recovered in N ₂ O + N ₂	
	(μg N kg ⁻¹)		(μg N kg ⁻¹)		(μg N kg ⁻¹)				% of added ¹⁵ N	
Maize S	643.3 ± 310.1	a	4219.0 ± 3963.6	a	4830.4 ± 4235.1	a	0.16 ± 0.06	n.s.	0.690 ± 0.605	a
Maize M	25.3 ± 40.0	b	132.9 ± 110.9	b	159.2 ± 132.9	b	0.15 ± 0.07	n.s.	0.023 ± 0.019	b
Maize L	15.4 ± 25.4	b	97.7 ± 96.4	b	120.7 ± 114.8	b	0.14 ± 0.14	n.s.	0.017 ± 0.016	b
Cup Plant	31.6 ± 39.5	b	105.5 ± 101.0	b	128.7 ± 122.0	b	0.24 ± 0.21	n.s.	0.018 ± 0.017	b

Means and standard deviation for n = 6. Different letters in one column indicate a significant difference, n.s. indicates no significant difference ($p < 0.05$) between treatments

¹⁵N enrichment of N pools and pool-derived fraction of N₂O

Treatments did not exhibit continuous patterns of ap and Fp values throughout the experiment. The fraction of N₂O derived from the active labeled NO₃⁻ pool (Fp_N₂O) decreased during the experiment showing that the contribution of N₂O from sources other than the labeled NO₃⁻ pool increased with time (Fig. 2b). Fp_N₂O was close to 1.0 in Maize S for three days after labeling, then decreased to 0.4 on day 5, and ranged between 0.5 and 0.8 until the end of the experiment. For the other treatments, Fp_N₂O continuously decreased until day 5/6. After day 6.5, Fp_N₂O increased in Maize M and L, fluctuating between 0.1 and 0.6. At the last day, Fp_N₂O was < 0.07 in all treatments.

The time course of ¹⁵N enrichment of the active NO₃⁻ pool producing N₂O and N₂ (ap_N₂O, ap_N₂O + N₂) was different in Maize S than in the other treatments. During the first days after labeling, ¹⁵N enrichment of the active NO₃⁻ pool producing N₂O and N₂ (ap_N₂O, ap_N₂O + N₂) was close to 60 at% in all treatments (Fig. 3). In Maize S, ap_N₂O and ap_N₂O + N₂ were higher than 50 at% during the whole experiment and only decreased on the last day. In all other treatments, ap_N₂O and ap_N₂O + N₂ continuously decreased until day 6.5. On day 7, ap-values were higher than 50 at% and decreased again until the end of the experiment. ¹⁵N enrichment of the total soil NO₃⁻ pool (¹⁵a_NO₃⁻) was measured at final harvest and was mostly significantly lower ($p < 0.05$) than ¹⁵N enrichment of the active NO₃⁻ pool producing N₂O and N₂ (ap_N₂O and ap_N₂O + N₂) from the last gas measurement (Fig. 3, Supplementary table S2).

Soil moisture and its effect on N fluxes

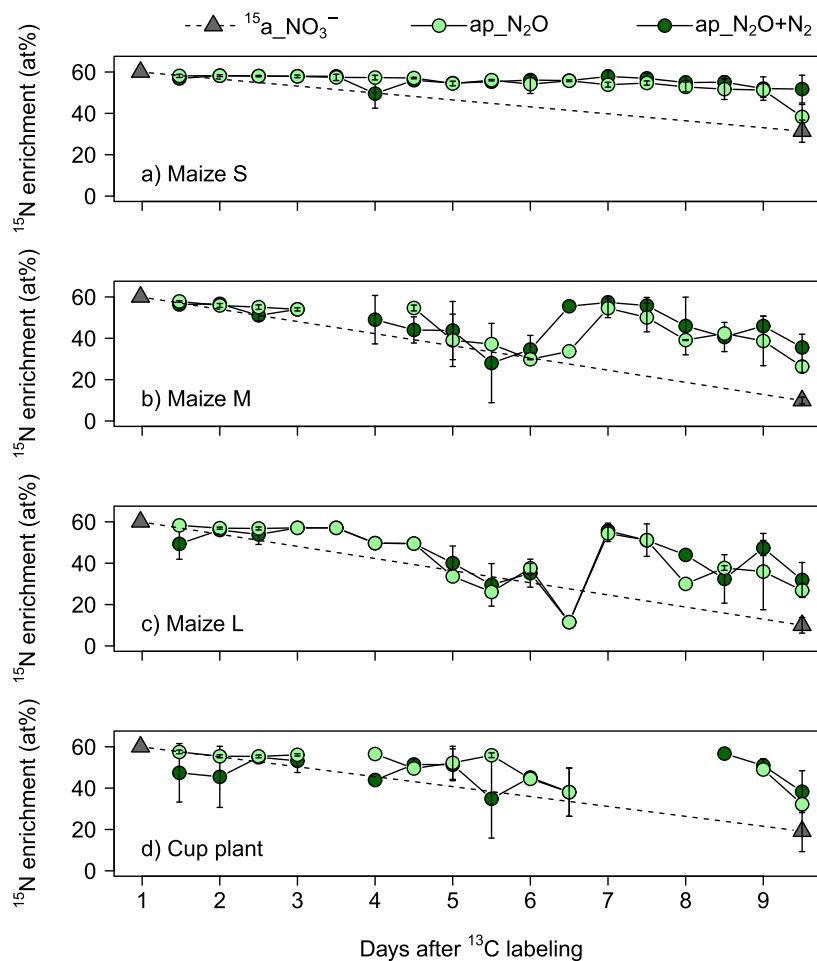
Data from soil moisture sensors showed that soil moisture content was higher in Maize S than all other treatments for the first days after labeling (Fig. 4). However, it was lower than the targeted value of 75%WFPS. As all plants respired large amounts of water, it took a few days to adjust irrigation amounts to plant water demand, and soil moisture could not be kept constant throughout the experiment.

In Maize S and Cup plant, soil moisture increased with irrigation three days after labeling reaching values around 70%WFPS. In Maize M and L, soil moisture increased five days after labeling reaching values around 55%WFPS. In Cup plant, soil moisture stayed on a similar level around 70%WFPS with fluctuations due to water uptake and irrigation. Although soil moisture was in a similar range in Maize S and Cup plant from day 4 to 6 and in all maize treatments after day 7, total N₂O and pool-derived N₂O + N₂ fluxes were always highest in Maize S. Thus, we did not find significant relationships between N fluxes and soil moisture during the experiment indicating that soil moisture was not the only factor controlling gaseous N losses (Table 5, supplementary table S3, supplementary figure S1). However, the N₂O/(N₂O + N₂) ratio of pool-derived fluxes decreased with increasing soil moisture (%WFPS, adj. R²=0.14, $p < 0.05$) indicating that increasing soil moisture stimulated N₂O reduction.

CO₂ and ¹³CO₂ efflux

The time course of cumulative CO₂ efflux and ¹³C enrichment in CO₂ was similar in all treatments (Fig. 5a + b). CO₂ efflux was similar in Maize M and Maize L where it increased almost linearly during the

Fig. 3 ^{15}N enrichment of the active N pool undergoing denitrification (ap N_2O , ap $\text{N}_2\text{O}+\text{N}_2$) and ^{15}N enrichment of total soil NO_3^- pool ($^{15}\text{a_NO}_3^-$). Means and standard deviation for $n=6$. When not visible, error bars are smaller than the symbols



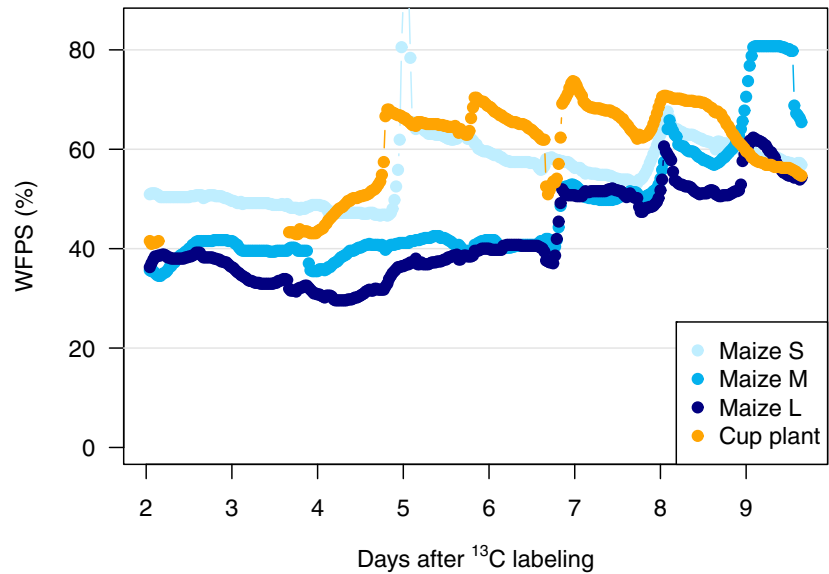
whole experiment, and total cumulative CO_2 was only slightly higher in Maize L than in Maize M (Table 4). Lowest cumulative CO_2 efflux was measured under Maize S plants where efflux decreased considerably after 1.5 days. Cumulative CO_2 efflux under cup plants was significantly lower than from Maize L and not statistically different from the other two maize treatments (Table 4). Overall, cumulative CO_2 efflux was positively correlated with root dry matter at final harvest (adj. $R^2=0.36$, $p < 0.01$, Table 5).

^{13}C enrichment in CO_2 strongly decreased in all treatments two days after labeling until the end of CO_2 sampling (Fig. 5b). Highest ^{13}C enrichment of soil emitted CO_2 was measured under Cup plant and lowest in Maize L. It strongly decreased two days after labeling until the end of CO_2 sampling. No statistically significant differences ($p < 0.05$) were found in relative ^{13}C recovery in CO_2 , soil, or soil + CO_2 (Table 4), but overall, mean relative ^{13}C recovery in soil increased with root dry matter, indicating that root-derived C recovered in soil increased with root biomass.

Interactions between N emissions, soil NO_3^- content, and C_{org} availability

Simple linear regression models were tested to identify effects of plant growth, N uptake, and C_{org} availability on cumulative N_2O and N_2 emissions (Table 5, supplementary table S3). Total cumulative N_2O and pool-derived cumulative $\text{N}_2\text{O} + \text{N}_2$ emissions were significantly ($p < 0.01$) negatively correlated with root dry matter (adj. $R^2=0.41$ and adj. $R^2=0.32$, respectively) and plant N uptake (adj. $R^2=0.49$ and adj. $R^2=0.33$, respectively) indicating that gaseous N losses were highest under plants with small root system and low N uptake. In addition, total cumulative N_2O emissions and soil NO_3^- content at final harvest were positively correlated (adj. $R^2=0.10$, $p < 0.05$). As cumulative CO_2 emissions were positively correlated with root dry matter and cumulative N emissions negatively, total cumulative N_2O and pool-derived cumulative $\text{N}_2\text{O} + \text{N}_2$ emissions were negatively correlated with cumulative CO_2 efflux (adj. $R^2=0.36$, $p < 0.01$). No correlations were found

Fig. 4 Soil moisture as % water filled pore space measured with soil moisture sensors ($n = 1$)



between total or pool-derived cumulative N emissions or $\text{N}_2\text{O}/(\text{N}_2\text{O} + \text{N}_2)$ ratio and ^{13}C recovery in soil and/or CO_2 . However, we identified a weak but significant positive relationship between $\text{N}_2\text{O}/(\text{N}_2\text{O} + \text{N}_2)$ of pool-derived fluxes and CO_2 efflux (adj. $R^2=0.11$, $p < 0.01$).

Discussion

Effect of soil moisture and plant N uptake on N_2O and N_2 emissions

Cumulative N emissions were 20–40 times higher in Maize S compared to all other treatments. Plant transpiration strongly affected soil moisture which was highest in Maize S during the first 4 days after ^{13}C labeling. Soil moisture is an important control of denitrification as it regulates O_2 concentration and diffusion in soil (Schlüter et al. 2018, Rohe et al. 2020). Plant roots constantly alter soil moisture and its distribution in soil by root water uptake. Accordingly, previous studies reported that plant growth controlled soil moisture and denitrification rates (Bakken 1988; von Rheinbaben and Trolldenier 1984). In our study, when soil moisture increased with irrigation, N_2O and, especially, N_2 fluxes increased shortly thereafter. Furthermore, the $\text{N}_2\text{O}/(\text{N}_2\text{O} + \text{N}_2)$ ratio of pool-derived fluxes decreased with increasing soil moisture which is consistent with N_2 being the dominant end product of denitrification under high WFPS (Davidson 1991). Although soil moisture was highest in Cup plant from day 4 to 8, and similar in Maize treatments from day 6 to 9, N fluxes were highest

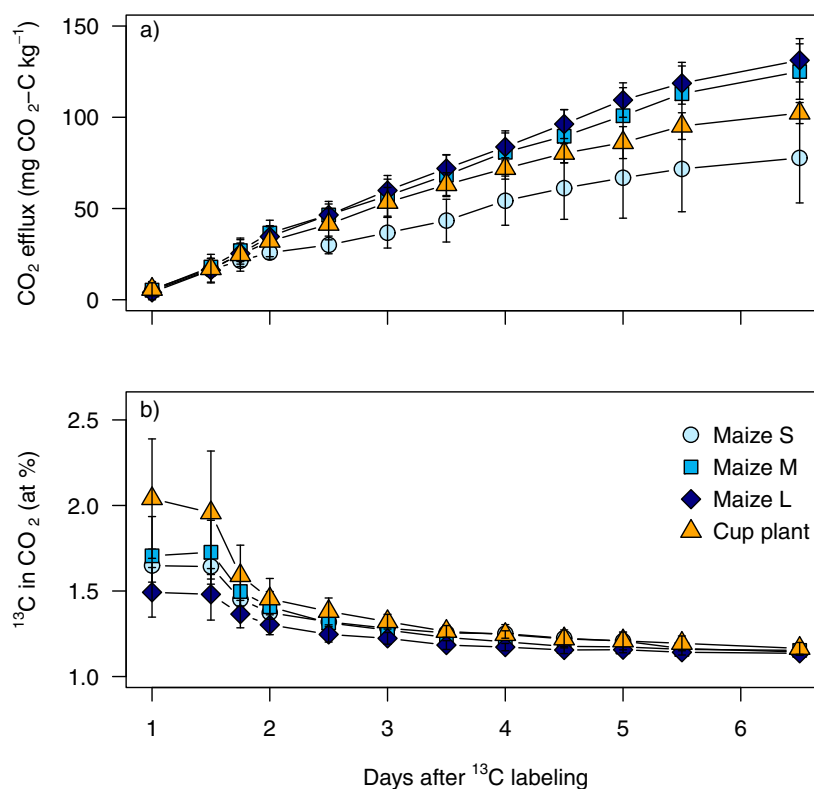
in Maize S throughout the experiment. Thus, differences in soil moisture alone cannot explain the vast differences in N fluxes between Maize S and the other treatments in our study.

Maize S plants were characterized by lowest root dry matter of all treatments and lower shoot dry matter compared to the other maize treatments. Furthermore, soil NO_3^- content at final harvest was more than twice as high in Maize S compared to all other treatments. The relationship between soil NO_3^- content at the end of the experiment and cumulative N_2O emissions was weak (0.10 , $p < 0.05$). However, N uptake was negatively correlated with total cumulative N_2O emissions and pool-derived cumulative $\text{N}_2\text{O} + \text{N}_2$ emissions (adj. $R^2=0.49$, $p < 0.001$ and adj. $R^2 = 0.33$, $p < 0.01$, respectively) indicating that NO_3^- availability played an important role in regulating denitrification. Our results show clearly that an increase in soil moisture led to increasing $\text{N}_2\text{O} + \text{N}_2$ fluxes, but N fluxes remained on a low level when NO_3^- availability was low due to rapid plant N uptake. Only when both N and water uptake were low, high NO_3^- availability and high soil moisture led to strongly increased N losses.

Effect of nitrate availability and soil moisture on pools and processes contributing to N_2O formation

Different NO_3^- pools and N turnover processes contributed to N_2O formation throughout the experiment. The ^{15}N enrichment of the total soil NO_3^- pool ($^{15}\text{a-NO}_3^-$) decreased from 60 at% after labeling to 10–30 at% until the end of the experiment as unlabeled organic N was

Fig. 5 Cumulative CO₂ efflux from soil (a) and ¹³C enrichment of CO₂ flux from soil (b). Means and standard deviation for n = 6. When not visible, error bars are smaller than the symbols



mineralized and diluted the labeled NO₃⁻ pool (Buchen et al. 2016; Deppe et al. 2017). Thus, denitrification of unlabeled NO₃⁻, as well as nitrification, nitrifier denitrification, and coupled nitrification-denitrification may have contributed to N₂O formation (van Groenigen et al. 2015; Wrage-Mönnig et al. 2018; Wrage et al. 2001).

In Maize S, ¹⁵a_NO₃⁻ at final harvest was significantly higher than in all other treatments, indicating that nitrification was less relevant in this treatment. Accordingly, the fraction of N₂O derived from the active labeled NO₃⁻ pool (Fp_N₂O) was >0.5 throughout the experiment indicating that most N₂O was lost through denitrification from labeled NO₃⁻. The ¹⁵N enrichment of the active NO₃⁻ pool producing N₂O and N₂O + N₂

(ap_N₂O and ap_N₂O + N₂) stayed close to its initial value of 60 at% highlighting that N₂O and N₂ were mainly lost from anoxic microsites where labeled NO₃⁻ had not been diluted by nitrification (Buchen et al. 2016).

In the other treatments, ap_N₂O, ap_N₂, and Fp_N₂O did not exhibit continuous trends. While values first decreased due to dilution with NO₃⁻ from nitrification, values increased after day 6.5 (Fig. 3), presumably due to the slight increase in WFPS after irrigation on day 6.5 (Fig. 4). Increasing soil moisture increased denitrification rates in anoxic hotspots, which corresponds with increasing N₂O and especially N₂ fluxes in Maize M and L. At the same time, it restricted nitrification and thus decreased the share of nitrification-dependent processes

Table 4 Cumulative CO₂ emissions, relative ¹³C recovery in soil and CO₂

	Cumulative CO ₂		relative ¹³ C recovery in CO ₂		relative ¹³ C recovery in soil		relative ¹³ C recovery in soil + CO ₂	
	(mg C kg ⁻¹)		(% of recovered ¹³ C)		(% of recovered ¹³ C)		(% of recovered ¹³ C)	
Maize S	77.7 ± 24.6	c	4.24 ± 1.16	n.s.	0.57 ± 3.11	n.s.	4.81 ± 3.72	n.s.
Maize M	125.0 ± 15.2	ab	5.83 ± 3.34	n.s.	1.11 ± 5.71	n.s.	6.94 ± 3.73	n.s.
Maize L	131.2 ± 11.9	a	3.73 ± 1.38	n.s.	3.37 ± 1.62	n.s.	7.10 ± 1.62	n.s.
Cup Plant	102.3 ± 5.8	bc	4.57 ± 1.83	n.s.	2.13 ± 1.37	n.s.	6.70 ± 1.87	n.s.

Mean and standard deviation for n = 6. Different letters in one column indicate a significant difference, n.s. indicates no significant difference (*p* < 0.05) between treatments

Table 5 Results of simple linear regressions between parameters

response	predictor	adjusted R ²	p-value	n
total N ₂ O flux	CO ₂ flux	-0.0136	0.8788	74
pool-derived N ₂ O + N ₂ flux	CO ₂ flux	0.0157	0.1458	74
mean total N ₂ O flux	% water-filled pore space	-0.0252	0.9179	35
mean pool-derived N ₂ O + N ₂ flux	% water-filled pore space	-0.0158	0.5111	35
N₂O/(N₂O + N₂) ratio (pool-derived)	% water-filled pore space	0.1365	0.01402	35
Cumulative CO₂	DM Root 2nd harvest	0.3574	0.00121	24
Total cumulative N₂O	DM Root 2nd harvest	0.4090	0.00046	24
Pool-derived cumulative N₂O + N₂	DM Root 2nd harvest	0.3210	0.00231	24
Total cumulative N₂O	Plant N uptake	0.4894	8.5 × 10⁻⁰⁵	24
Pool-derived cumulative N₂O + N₂	Plant N uptake	0.3300	0.00197	24
Total cumulative N₂O	Soil NO₃⁻ content 2nd harvest	0.0983	0.0477	24
Pool-derived cumulative N ₂ O + N ₂	Soil NO ₃ ⁻ content 2nd harvest	0.0131	0.2656	24
Total cumulative N₂O	cumulative CO₂	0.3573	0.00121	24
Pool-derived cumulative N₂O + N₂	cumulative CO₂	0.3641	0.00107	24
Total cumulative N ₂ O	recovered ¹³ C in soil + CO ₂	-0.0068	0.3683	24
Pool-derived cumulative N ₂ O + N ₂	recovered ¹³ C in soil + CO ₂	0.0051	0.302	24
N ₂ O/(N ₂ O + N ₂) ratio (pool-derived)	recovered ¹³ C in soil + CO ₂	-0.0389	0.7138	24

Significant regressions ($p \leq 0.05$) are marked in bold

contributing to N₂O formation (reflected in increasing Fp_N₂O). Simultaneously increasing ap_N₂O and ap_N₂O + N₂ in Maize M and L on Day 7 indicate that ¹⁵N enrichment of the active labeled NO₃⁻ pool was still close to 60 at% in microsites where denitrification took place. The rise of actual ap-values back towards initial values is in line with a change in the anaerobic volume where denitrification occurs (Bergstermann et al. 2011). A recent study conducted with the same soil but without plants showed that O₂ concentration in repacked soil cores was highly variable and average O₂ saturation decreased with increasing soil moisture while the anaerobic soil volume fraction increased with increasing soil moisture and soil depth (Rohe et al. 2020). After day 6.5, N₂O + N₂ were predominately lost from domains that had been continuously anoxic or were most distant from oxic domains and thus were less diluted with unlabeled NO₃⁻. We anticipate that in these microsites O₂ concentrations had been low enough to prevent nitrification during the first days so that the labeled pool was not diluted by unlabeled NO₃⁻ from nitrification.

While fungal co-denitrification has been reported as the dominant N₂O source in a planted soil with high NO₃⁻ content (Laughlin and Stevens 2002), our data provide no indications for co-denitrification, because ap_N₂O and ap_N₂O + N₂ were always higher than

¹⁵a_NO₃⁻, but co-denitrification would lead to a lower than ¹⁵a_NO₃⁻ due to hybrid formation of N₂O or N₂ (Spott and Stange 2007).

Thus, in our study, N₂O and N₂ fluxes mainly derived from denitrification of labeled ¹⁵NO₃⁻ in anoxic microsites, while nitrification simultaneously occurred in more oxic parts of the soil, potentially contributing to formation of unlabeled N₂O.

Effect of root-derived C on N emissions

One of the core hypotheses of this study was that availability of root-derived C is a key driver of denitrification in planted soils. It was based on a number of studies reporting higher denitrification activity in rhizosphere compared to bulk soil which was explained by higher soil C (Hamonts et al. 2013; Klemetsson et al. 1987; Malique et al. 2019; Smith and Tiedje 1979). Detectable rhizodeposition and C flow into belowground respiration result from C translocation from shoots to roots (Remus and Augustin 2016). Thus, we used ¹³CO₂ pulse labeling to trace C translocation from shoots to roots, its release by roots into the soil, and ¹³CO₂ emitted from soil.

We found a positive correlation between root dry matter at final harvest and cumulative CO₂ efflux

(adj. $R^2=0.36$, $p<0.01$) and, on average, relative ^{13}C recovery in soil increased with increasing root dry matter indicating that root exudation increased with root dry matter. However, we could not detect any relationship between total or pool-derived N fluxes and total CO_2 efflux or root-derived C and cumulative N emissions or the ratio of gaseous products.

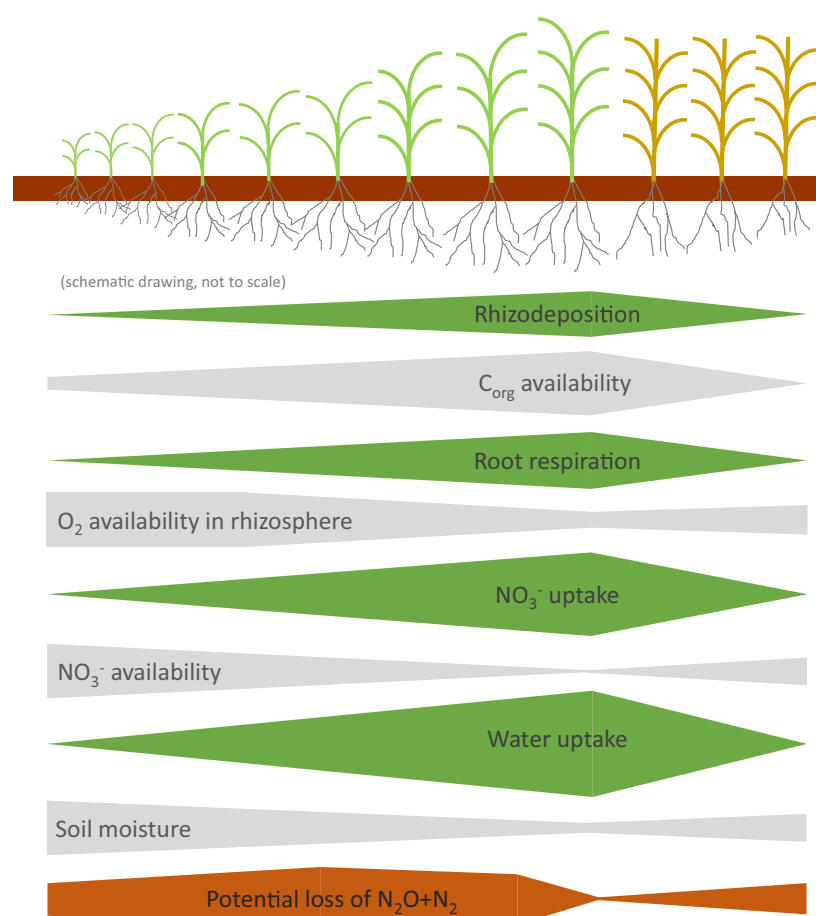
Most previous studies investigating plant effects on denitrification did not measure N_2O and N_2 emissions under growing plants, but either potential denitrification (Klemetsson et al. 1987; Malique et al. 2019; Smith and Tiedje 1979) or denitrification capacity (Hamonts et al. 2013) from soil samples taken from rhizosphere and/or bulk soil. In those studies, conducted under anoxic conditions with unlimited NO_3^- supply, higher C availability in rhizosphere soil samples led to higher emissions of N_2O and N_2 . However, when separation of bulk soil and rhizosphere was not well-defined due to densely rooted soil in pots, no differences in potential denitrification were found (Malique et al. 2019). In the few studies with growing plants, higher denitrification rates were measured

during the first weeks after emergence (Senbayram et al. 2020), with poorly growing plants (von Rheinbaben and Trollenier 1984), or when root biomass was decreasing (Haider et al. 1987). No stimulation of denitrification was found when actively growing maize plants were compared to unplanted soil (Haider et al. 1985). Accordingly, root-derived C may stimulate denitrification when soil NO_3^- is not limited. We were not able to estimate the effect of C availability on denitrification as NO_3^- limitation and O_2 inhibition were the factors controlling denitrification in our study.

Plant root effects on denitrification

The activity of denitrifying microorganisms in soil is primarily controlled by availability of O_2 , NO_3^- , and C_{org} (proximal factors, Groffman et al. 1988). Plant roots affect these through rhizodeposition, root respiration, N and water uptake (distal factors, Groffman et al. 1988). Figure 6 shows how proximal and distal factors change during plant and root growth and how these

Fig. 6 Conceptual drawing of plant root effects (distal factors, green/grey) on drivers of denitrification (proximal factors, light grey) and potential $\text{N}_2\text{O} + \text{N}_2$ losses (orange/dark grey). Based on two assumptions: (i) NO_3^- -based fertilizer is only added before plant growth and (ii) root water uptake is the main regulator of soil moisture



affect denitrification in planted soil. The presented conceptual drawing is based on two assumptions: (i) NO_3^- -based fertilizer is only added before plant growth and (ii) root water uptake is the main regulator of soil moisture.

In most agricultural soils, available C_{org} is low. With increasing root growth, rhizodeposition and root turnover increase C_{org} availability. At the same time, root respiration and microbial activity increase, decreasing O_2 concentrations in the rhizosphere. This offers favorable conditions for denitrifying microorganisms as long as sufficient NO_3^- is available (Klemetsson et al., 1987; Senbayram et al., 2020; Stefanson, 1972). As N uptake increases with plant and root growth, NO_3^- becomes limited for denitrifiers (Haider et al., 1985). Furthermore, increasing water uptake decreases soil moisture and restricts formation of anoxic microsites for denitrification (Bakken 1988, von Rheinbaben and Trollenier, 1984). Accordingly, our study showed that with increasing plant and root growth, plant water and N uptake became the most important controls of denitrification. Similarly, soil moisture can vary strongly under field conditions depending on precipitation and plant water uptake. When NO_3^- is available (i.e. after fertilization), increasing soil moisture after rainfall can lead to strongly increased $\text{N}_2\text{O} + \text{N}_2$ emissions (Buchen et al. 2017, Ruser et al. 2017).

Overall, plants continuously change boundary conditions and substrate availability for denitrification in soil, and it requires high technical input and equipment to keep experimental conditions stable and controlled. However, as plants do control these conditions so strongly, it is very exciting and very important to further investigate these processes to understand and predict N cycling, denitrification, and gaseous N losses on the field scale. Further research is thus indispensable.

Conclusions

We aimed to investigate how plants control the main substrates for denitrification (NO_3^- and C_{org}) through N uptake and root exudation. To our knowledge, this is the first study combining in situ measurements of $\text{N}_2\text{O} + \text{N}_2$ fluxes with estimations of root-derived C availability.

Plant water uptake was a main factor controlling soil moisture and, thus, daily $\text{N}_2\text{O} + \text{N}_2$ fluxes, cumulative N emissions, and N_2O production pathways. However, N fluxes remained on a low level when NO_3^- availability

was low due to rapid plant N uptake. Only when both N and water uptake were low, high NO_3^- availability and high soil moisture led to strongly increased N losses. Our study provides evidence that most N losses originated from denitrification in small anoxic hotspots where NO_3^- was not diluted by nitrification. Simultaneously occurring nitrification in oxic parts of the soil potentially contributed to formation of unlabeled N_2O .

Total CO_2 efflux was positively correlated with root dry matter, but there was no indication of any relationship between recovered ^{13}C from root exudation and cumulative N emissions. We anticipate that higher C_{org} availability in pots with large root systems did not lead to higher denitrification rates, as NO_3^- was limiting denitrification due to plant N uptake. Overall, we conclude that root-derived C stimulates denitrification only when soil NO_3^- is not limited and low O_2 concentrations enable denitrification.

Acknowledgements The authors thank Simone Urstadt, Finn Malinowski, Bridith Angulo Schipper, Ilse Thaufelder, and Jakob Streuber for help during experimental and laboratory work. We are thankful to Tomor Krasniqi for weighing endless numbers of C:N samples and to the Centre for Stable Isotope Research and Analysis of the University of Göttingen for analysis of C and N isotopes of soil and plant samples. Further, we thank Dr. Daniel Ziehe and Kerstin Gilke for GC analyses, Dr. Anette Giesemann and Martina Heuer for IRMS analyses of gas samples, and Dr. Wolfram Eschenbach for analysis of ^{15}N in NO_3^- and NH_4^+ . We thank Prof. Dr. Jürgen Böttcher for soil classification and Prof. Kenneth Albrecht and Dr. Pedro Gerstberger for supplying cup plant seedlings. We thank Dr. Bernd Steingrobe for his feedback on the manuscript. Furthermore, we acknowledge two anonymous reviewers for their advice to improve the quality of the manuscript.

Funding Open Access funding enabled and organized by Projekt DEAL. This study was funded by the Deutsche Forschungsgemeinschaft (DFG, German Research Foundation) through the research unit DFG-FOR 2337 (DI 546/4–1, We 1904/10–2): Denitrification in Agricultural Soils: Integrated Control and Modelling at Various Scales (DASIM).

Open Access This article is licensed under a Creative Commons Attribution 4.0 International License, which permits use, sharing, adaptation, distribution and reproduction in any medium or format, as long as you give appropriate credit to the original author(s) and the source, provide a link to the Creative Commons licence, and indicate if changes were made. The images or other third party material in this article are included in the article's Creative Commons licence, unless indicated otherwise in a credit line to the material. If material is not included in the article's Creative Commons licence and your intended use is not permitted by statutory regulation or exceeds the permitted use, you will need to obtain permission directly from the copyright holder. To view a copy of this licence, visit <http://creativecommons.org/licenses/by/4.0/>.

References

- Bakken LR (1988) Denitrification under different cultivated plants: effects of soil moisture tension, nitrate concentration, and photosynthetic activity. *Biol Fertil Soils* 6:271–278
- Bergstermann A, Cárdenas L, Bol R, Gilliam L, Goulding K, Meijide A, Scholefield D, Vellejo A, Well R (2011) Effect of antecedent soil moisture conditions on emissions and isotopologue distribution of N_2O during denitrification. *Soil Biol Biochem* 43:240–250. <https://doi.org/10.1016/j.soilbio.2010.10.003>
- Buchen C, Lewicka-Szczepak D, Fuß R, Helrich M, Flessa H, Well R (2016) Fluxes of N_2 and N_2O and contributing processes in summer after grassland renewal and grassland conversion to maize cropping on a Plaggic Anthrosol and a Histic Gleysol. *Soil Biol Biochem* 101:6–19. <https://doi.org/10.1016/j.soilbio.2016.06.028>
- Buchen C, Well R, Helfrich M, Fuß R, Kayser M, Gensior A, Benke M, Flessa H (2017) Soil mineral N dynamics and N_2O emissions following grassland renewal. *Agric Ecosyst Environ* 246:325–342. <https://doi.org/10.1016/j.agee.2017.06.013>
- Burford JR, Bremner JM (1975) Relationships between the denitrification capacities of soils and total, water-soluble and readily decomposable soil organic matter. *Soil Biol Biochem* 7:389–394. [https://doi.org/10.1016/0038-0717\(75\)90055-3](https://doi.org/10.1016/0038-0717(75)90055-3)
- Carvalho LC, Dennis PG, Fedoseyenko D, Hajirezaei MR, Borriss R, von Wirén N (2011) Root exudation of sugars, amino acids, and organic acids by maize as affected by nitrogen, phosphorus, potassium, and iron deficiency. *J Plant Nutr Soil Sci* 174:3–11. <https://doi.org/10.1002/jpln.201000085>
- Chantigny MH, Angers DA, Kaiser K, Kalbitz K (2007) Extraction and characterization of dissolved organic matter. In: Carter MR, Gregorich DG (ed) *Soil sampling and methods of analysis*, 2nd edn, Taylor & Francis Group, Abingdon
- Cheng W, Coleman DC, Carroll CR, Hoffman CA (1993) In situ measurement of root respiration and soluble C concentrations in the rhizosphere. *Soil Biol Biochem* 25:1189–1196. [https://doi.org/10.1016/0038-0717\(93\)90214-V](https://doi.org/10.1016/0038-0717(93)90214-V)
- Davidson EA (1991) Fluxes of nitrous oxide and nitric oxide from terrestrial ecosystems. In: Rogers JE, Whitman WB (eds) *Microbial production and consumption of greenhouse gases: methane, nitrogen oxides and halomethanes*. American Society for Microbiology, Washington (DC), pp 219–235
- Deppe M, Well R, Giesemann A, Spott O, Flessa H (2017) Soil N_2O fluxes and related processes in laboratory incubations simulating ammonium fertilizer depots. *Soil Biol Biochem* 104:68–80. <https://doi.org/10.1016/j.soilbio.2016.10.005>
- Eschenbach W, Lewicka-Szczepak D, Stange CF, Dyckmans J, Well R (2017) Measuring ^{15}N abundance and concentration of aqueous nitrate, nitrite, and ammonium by membrane inlet quadrupole mass spectrometry. *Anal Chem* 89:6076–6081. <https://doi.org/10.1021/acs.analchem.7b00724>
- Eschenbach W, Well R, Dyckmans J (2018) NO reduction to N_2O improves nitrate ^{15}N abundance analysis by membrane inlet quadrupole mass spectrometry. *Anal Chem* 90:11216–11218. <https://doi.org/10.1021/acs.analchem.8b02956>
- Firestone MK, Smith MS, Firestone RB, Tiedje JM (1979) The influence of nitrate, nitrite, and oxygen on the composition of the gaseous products of denitrification in soil. *Soil Sci Soc Am J* 43:1140–1144
- Gansberger P, Montgomery LFR, Liebhard P (2015) Botanical characteristics, crop management and potential of *Silphium perfoliatum* L. as a renewable resource for biogas production: A review. *Ind Crop Prod* 63:362–372
- Gransee A, Wittenmayer L (2000) Qualitative and quantitative analysis of water-soluble root exudates in relation to plant species and development. *J Plant Nutr Soil Sci* 163:381–385
- Groffman PM, Tiedje JM, Robertson GP, Christensen S (1988) Denitrification at different temporal and geographical scales: proximal and distal controls. In: Wilson JR (ed) *Advances in nitrogen cycling in agricultural ecosystems*. CAB International, Wallingford, pp 174–192
- Groffman PM, Altabet MA, Böhlke JK, Butterbach-Bahl K, David MB, Firestone MK, Giblin AE, Kana TM, Nielsen LP, Voytek MA (2006) Methods for measuring denitrification: Diverse approaches to a difficult problem. *Ecol Appl* 16:2091–2122. [https://doi.org/10.1890/1051-0761\(2006\)016\[2091:MFMDDA\]2.0.CO;2](https://doi.org/10.1890/1051-0761(2006)016[2091:MFMDDA]2.0.CO;2)
- Haider K, Mosier A, Heinemeyer O (1985) Phytotron experiments to evaluate the effect of growing plants on denitrification. *Soil Sci Soc Am J* 49:636–641
- Haider K, Mosier A, Heinemeyer O (1987) The effect of growing plants on denitrification at high soil nitrate concentrations. *Soil Sci Soc Am J* 51:97–102
- Hamonts K, Clough TJ, Stewart A, Clinton PW, Richardson AE, Wakelin AE, O'Callaghan M, Condron LM (2013) Effect of nitrogen and waterlogging on denitrifier gene abundance, community structure and activity in the rhizosphere of wheat. *FEMS Microbiol Ecol* 83:568–584. <https://doi.org/10.1111/1574-6941.12015>
- Hauck RD, Melsted SW (1956) Some aspects of the problem of evaluating denitrification in soils. *Soil Sci Soc Am J* 20:361–364. <https://doi.org/10.2136/sssaj1956.03615995002000030017x>
- Husáková I, Weiner J, Münzbergová Z (2018) Species traits and shoot-root biomass allocation in 20 dry-grassland species. *J Plant Ecol* 11:273–285. <https://doi.org/10.1093/jpe/rtw143>
- Klemetsson L, Svensson BH, Rosswall T (1987) Dinitrogen and nitrous oxide produced by denitrification and nitrification in soil with and without barley plants. *Plant Soil* 99:303–319. <https://doi.org/10.1007/BF02370877>
- Kuzyakov Y, Domanski G (2000) Carbon input by plants into the soil. Review. *J Plant Nutr Soil Sci* 163:421–431. [https://doi.org/10.1002/1522-2624\(200008\)163:4<421::AID-JPLN421>3.0.CO;2-R](https://doi.org/10.1002/1522-2624(200008)163:4<421::AID-JPLN421>3.0.CO;2-R)
- Laughlin RJ, Stevens RJ (2002) Evidence for fungal dominance of denitrification and codenitrification in a grassland soil. *Soil Sci Soc Am J* 66:1540–1548. <https://doi.org/10.2136/sssaj2002.1540>
- Lewicka-Szczepak D, Well R, Giesemann A, Rohe L, Wolf U (2013) An enhanced technique for automated determination of ^{15}N signatures of N_2 , ($N_2 + N_2O$) and N_2O in gas samples. *Rapid Commun Mass Spectrom* 27:1548–1558. <https://doi.org/10.1002/rcm.6605>
- Lewicka-Szczepak D, Augustin J, Giesemann A, Well R (2017) Quantifying N_2O reduction to N_2 based on N_2O isotopocules-validation with independent methods (helium

- incubation and ^{15}N gas flux method). *Biogeosciences* 14: 711–732. <https://doi.org/10.5194/bg-14-711-2017>
- Malhi SS, Johnston AM, Schoenau JJ, Wang ZH, Vera CL (2011) Seasonal biomass accumulation and nutrient uptake of wheat, barley and oat on a Black Chernozem Soil in Saskatchewan. *Can J Plant Sci* 86:1005–1014. <https://doi.org/10.4141/p05-116>
- Malique F, Ke P, Böttcher J, Dannenman M, Butterbach-Bahl K (2019) Interactive plant and soil effects on denitrification potential in agricultural soils. *Plant Soil* 20:6603
- Nguyen C (2003) Rhizodeposition of organic C by plants: mechanisms and controls. *Agronomie* 23:375–396. <https://doi.org/10.1051/agro:2003011>
- Novák V, Vidovič J (2003) Transpiration and nutrient uptake dynamics in maize (*Zea mays* L.). *Ecol Modell* 166:99–107. [https://doi.org/10.1016/S0304-3800\(03\)00102-9](https://doi.org/10.1016/S0304-3800(03)00102-9)
- Paterson E, Sim A (1999) Rhizodeposition and C-partitioning of *Lolium perenne* in axenic culture affected by nitrogen supply and defoliation. *Plant Soil* 216:155–164. <https://doi.org/10.1023/A:1004789407065>
- Pausch J, Kuzyakov Y (2018) Carbon input by roots into the soil: Quantification of rhizodeposition from root to ecosystem scale. *Glob Chang Biol* 24:1–12. <https://doi.org/10.1111/gcb.13850>
- Philippot L, Hallin S, Börjesson G, Baggs EM (2009) Biochemical cycling in the rhizosphere having an impact on global change. *Plant Soil* 321:61–81. <https://doi.org/10.1007/s11104-008-9796-9>
- R Core Team (2019) R: A Language and Environment for Statistical Computing
- Remus R, Augustin J (2016) Dynamic linking of ^{14}C partitioning with shoot growth allows a precise determination of plant-derived C input to soil. *Plant Soil* 408:493–513. <https://doi.org/10.1007/s11104-016-3006-y>
- Rohe L, Apelt B, Vogel HJ, Well R, Wu GM, Schlüter S (2020) Denitrification in soil as a function of oxygen supply and demand at the microscale. *Biogeosci Discuss*. <https://doi.org/10.5194/bg-2020-221> (in review)
- Ruser R, Fuß R, Andres M, Hegewald H, Kesenheimer K, Köbke S, Rübiger T, Quinones TS, Augustin J, Christen O, Dittert K, Kage H, Lewandowski I, Prochnow A, Stichnothe H, Flessa H (2017) Nitrous oxide emissions from winter oilseed rape cultivation. *Agric Ecosyst Environ* 249:57–69. <https://doi.org/10.1016/j.agee.2017.07.039>
- Schlüter S, Henjes S, Zawallich J, Bergaust L, Horn M, Ippisch O, Vogel HJ, Dörsch P (2018) Denitrification in soil aggregate analogues-effect of aggregate size and oxygen diffusion. *Front Environ Sci* 6:1–10. <https://doi.org/10.3389/fenvs.2018.00017>
- Scholefield D, Hawkins JMBB, Jackson SM (1997) Development of a helium atmosphere soil incubation technique for direct measurement of nitrous oxide and dinitrogen fluxes during denitrification. *Soil Biol Biochem* 29:1345–1352. [https://doi.org/10.1016/S0038-0717\(97\)00021-7](https://doi.org/10.1016/S0038-0717(97)00021-7)
- Senbayram M, Well R, Shan J, Bol R, Burkart S, Jones DL, Wu D (2020) Rhizosphere processes in nitrate-rich barley soil tripled both N_2O and N_2 losses due to enhanced bacterial and fungal denitrification. *Plant Soil*. <https://doi.org/10.1007/s11104-020-04457-9>
- Smith MS, Tiedje JM (1979) The effect of roots on soil denitrification. *Soil Sci Soc Am J* 43:951–955
- Spott O, Stange CF (2007) A new mathematical approach for calculation the contribution of anammox, denitrification and atmosphere to an N_2 mixture based on a ^{15}N tracer technique. *Rapid Commun Mass Spectrom* 21:2398–2406. <https://doi.org/10.1002/rcm>
- Spott O, Russow R, Apelt B, Stange CF (2006) A ^{15}N -aided artificial atmosphere gas flow technique for online determination of soil N_2 release using the zeolite Köstrolith SX6. *Rapid Commun Mass Spectrom* 20:3267–3274. <https://doi.org/10.1002/rcm>
- Stefanson RC (1972) Soil denitrification in sealed soil-plant systems I. Effect of plants, soil water content and soil organic matter content. *Plant Soil* 127:113–127
- van Groenigen JW, Huygens D, Boeckx P, Kuypers ThW, Lubbers IM, Rütting T, Groffman PM (2015) The soil N cycle: New insights and key challenges. *Soil* 1:235–256. <https://doi.org/10.5194/soil-1-235-2015>
- Vancura V (1964) Root exudates of plants I. Analysis of root exudates of barley and wheat in their initial phases of growth. *Plant Soil* 21:231–248. <https://doi.org/10.1007/BF02139643>
- Vancura V, Hovadik A (1965) Root exudates of plants II. Composition of root exudates of some vegetables. *Plant Soil* 22:21–32
- Vinther FP (1984) Total denitrification and the ratio between N_2O and N_2 during the growth of spring barley. *Plant Soil* 76:227–232. <https://doi.org/10.1007/BF02205582>
- von Rheinbaben W, Trolldenier G (1984) Influence of plant growth on denitrification in relation to soil moisture and potassium nutrition. *Zeitschrift für Pflanzenernährung Bodenkd* 147:730–738. <https://doi.org/10.1002/jpln.19841470610>
- Well R, Myrold DD (1999) Laboratory evaluation of a new method for in situ measurement of denitrification in water-saturated soils. *Soil Biol Biochem* 31:1109–1119. [https://doi.org/10.1016/S0038-0717\(99\)00029-2](https://doi.org/10.1016/S0038-0717(99)00029-2)
- Wrage N, Velthof GL, van Beusichem ML, Oenema O (2001) The role of nitrifier denitrification in the production of nitrous oxide. *Soil Biol Biochem* 33:1723–1732. [https://doi.org/10.1016/S0038-0717\(01\)00096-7](https://doi.org/10.1016/S0038-0717(01)00096-7)
- Wrage-Mönnig N, Horn MA, Well R, Müller C, Velthof G, Oenema O (2018) The role of nitrifier denitrification in the production of nitrous oxide revisited. *Soil Biol Biochem* 123: A3–A16. <https://doi.org/10.1016/j.soilbio.2018.03.020>
- Wu H, Dannenmann M, Fanselow N, Wolf B, Yao Z, Wu X, Brüggemann N, Zheng X, Han X, Dittert K, Butterbach-Bahl K (2011) Feedback of grazing on gross rates of N mineralization and inorganic N partitioning in steppe soils of Inner Mongolia. *Plant Soil* 340:127–139. <https://doi.org/10.1007/s11104-010-0575-z>
- Yoshinari T, Knowles R (1976) Acetylene inhibition of nitrous oxide reduction by denitrifying bacteria. *Biochem Biophys Res Commun* 69:705–710. [https://doi.org/10.1016/0006-291X\(76\)90932-3](https://doi.org/10.1016/0006-291X(76)90932-3)

Supplementary to

Nitrate uptake and C exudation – do plant roots stimulate or inhibit denitrification?

Pauline Sophie Rummel^{1*}, Reinhard Well², Birgit Pfeiffer^{1,3}, Klaus Dittert¹, Sebastian Floßmann⁴, and Johanna Pausch⁴

¹ Division of Plant Nutrition and Crop Physiology, Department of Crop Science, University of Göttingen, Germany

² Thünen Institute of Climate-Smart Agriculture, Federal Research Institute for Rural Areas, Forestry and Fisheries, Braunschweig, Germany

³ Institute of Microbiology and Genetics, Department of Genomic and Applied Microbiology, University of Göttingen, Germany

⁴ Agroecology, Faculty for Biology, Chemistry, and Earth Sciences, University of Bayreuth, Germany

* corresponding author: pauline.rummel@uni-goettingen.de; Phone: ++49 551 39 4471, Fax: ++49 551 39 25570

Pre-experimental plant growth and results from first harvest

N fertilization during pre-experimental plant cultivation strongly affected plant growth as shown by significant differences between aboveground dry matter in all maize treatments at first harvest (L>M>S, Supplementary Table 1). Root dry matter was significantly higher in Maize L and M than Maize S. Cup plant produced less shoot dry matter than maize, while root dry matter was similar to maize treatments. Root:shoot ratio was more than twice as high in cup plant compared to maize treatments. While all replicates from each maize treatment showed similar growth, variance in cup plant was much higher. Maize S plants showed clear symptoms of N deficiency such as reduced growth, yellowish leave color, and low shoot N concentration. Tissue N concentration in cup plants was much higher compared to all maize plants.

Table S1: Harvest data of intermediate harvest (replicates 1-6, 44 days after transplanting, before labeling).

	Maize S		Maize M		Maize L		Cup Plant	
Shoot dry matter (g pot ⁻¹)	38.0 ± 3.8	c	56.0 ± 2.0	b	67.8 ± 2.2	a	22.1 ± 3.6	d
Root dry matter (g pot ⁻¹)	13.1 ± 1.4	b	18.1 ± 1.1	a	18.1 ± 2.6	a	16.1 ± 4.0	ab
Root : shoot ratio	0.34 ± 0.03	b	0.32 ± 0.02	b	0.27 ± 0.04	b	0.75 ± 0.23	a
Shoot N content (%)	0.67 ± 0.09	c	0.82 ± 0.05	c	1.15 ± 0.10	b	2.27 ± 0.31	a
Root N content (%)	0.62 ± 0.06	c	0.89 ± 0.18	b	0.88 ± 0.09	b	1.51 ± 0.23	a
NO ₃ ⁻ content (mg kg ⁻¹)	1.47 ± 0.39	a	0.97 ± 0.16	a	2.07 ± 2.62	a	2.79 ± 3.95	a
NH ₄ ⁺ content (mg kg ⁻¹)	0.60 ± 0.206	b	0.74 ± 0.165	ab	1.10 ± 0.417	a	0.85 ± 0.314	ab
WEOC content (mg kg ⁻¹)	9.74 ± 2.057	b	17.05 ± 2.652	a	16.21 ± 5.287	a	11.98 ± 1.665	ab

Different letters in one row indicate a significant difference (p<0.05) between treatments.

Additional simple linear regressions

Table 2 shows the results of additional simple linear regressions tested to identify the effect of plant growth, N uptake, C availability, and soil moisture on total N₂O and pool-derived N₂O+N₂ fluxes and cumulative emissions. All regressions presented here are not statistically significant at p<0.05.

Table S2: Additional results of simple linear regressions between parameters.

response	predictor	adjusted R ²	p-value	n
non-pool-derived N ₂ O flux	CO ₂ flux	-0.005124	0.4308	35
mean ap_N ₂ O+N ₂	% water-filled pore space	0.01558	0.2185	35
mean Fp_N ₂ O	% water-filled pore space	0.01333	0.2309	35
mean non-pool-derived N ₂ O flux	% water-filled pore space	-0.02633	0.7839	35
recovered ¹³ C in soil	DM Root 2 nd harvest	0.004083	0.3069	24
recovered ¹³ C in CO ₂	DM Root 2 nd harvest	-0.04061	0.7519	24
recovered ¹³ C in soil+CO ₂	DM Root 2 nd harvest	-0.00155	0.3358	24
Total cumulative N ₂ O	recovered ¹³ C in soil	-0.03283	0.60093	24
Total cumulative N ₂ O	recovered ¹³ C in CO ₂	-0.0377	0.689	24
Pool-derived cumulative N ₂ O+N ₂	recovered ¹³ C in soil	-0.03754	0.686	24
Pool-derived cumulative N ₂ O+N ₂	recovered ¹³ C in CO ₂	-0.01867	0.455	24
N ₂ O/(N ₂ O+N ₂) ratio (pool-derived)	recovered ¹³ C in soil	-0.03074	0.5809	24
N ₂ O/(N ₂ O+N ₂) ratio (pool-derived)	recovered ¹³ C in CO ₂	0.04615	0.1602	24
N ₂ O/(N ₂ O+N ₂) ratio (pool-derived)	cumulative CO ₂	-0.04464	0.8968	24
N ₂ O/(N ₂ O+N ₂) ratio (pool-derived)	Plant N uptake	-0.04002	0.7377	24
cumulative N ₂ O (non-pool)	cumulative CO ₂	0.07363	0.1068	24
cumulative N ₂ O (non-pool)	Plant N uptake	0.08866	0.0857	24
cumulative N ₂ O (non-pool)	recovered ¹³ C in soil+CO ₂	0.08067	0.09632	24
cumulative N ₂ O (non-pool)	recovered ¹³ C in soil	0.07642	0.1025	24
cumulative N ₂ O (non-pool)	recovered ¹³ C in CO ₂	-0.04009	0.7394	24
cumulative N ₂ O (non-pool)	Soil NO ₃ ⁻ content 2 nd harvest	0.1334	0.04453	24

Chapter 2

Maize root and shoot litter quality controls short-term CO₂ and N₂O emissions and bacterial community structure of arable soil

Pauline Sophie Rummel^{1*}, Birgit Pfeiffer^{1,2}, Johanna Pausch³, Reinhard Well⁴, Dominik Schneider², and Klaus Dittert¹

¹ Division of Plant Nutrition and Crop Physiology, Department of Crop Science, University of Göttingen, Germany

² Institute of Microbiology and Genetics, Department of Genomic and Applied Microbiology, University of Göttingen, Germany

³ Agroecology, Faculty for Biology, Chemistry, and Earth Sciences, University of Bayreuth, Germany

⁴ Thünen Institute of Climate-Smart Agriculture, Federal Research Institute for Rural Areas, Forestry and Fisheries, Braunschweig, Germany

* corresponding author: pauline.rummel@uni-goettingen.de; Phone: ++49 551 39 4471, Fax: ++49 551 39 25570

Published in: Biogeosciences, 17, 1181–1198, 2020; <https://doi.org/10.5194/bg-17-1181-2020>

Author contributions:

PSR, RW, and KD designed the experiment and PSR carried them out. BP and DS carried out microbial analyses and sequence processing and provided figures. JP, RW, and KD contributed to interpretation of results. PSR prepared the manuscript with contributions from all co-authors.



Maize root and shoot litter quality controls short-term CO₂ and N₂O emissions and bacterial community structure of arable soil

Pauline Sophie Rummel¹, Birgit Pfeiffer^{1,2}, Johanna Pausch³, Reinhard Well⁴, Dominik Schneider², and Klaus Dittert¹

¹Division of Plant Nutrition and Crop Physiology, Department of Crop Science, University of Göttingen, Göttingen, Germany

²Institute of Microbiology and Genetics, Department of Genomic and Applied Microbiology, University of Göttingen, Göttingen, Germany

³Agroecology, Faculty for Biology, Chemistry, and Earth Sciences, University of Bayreuth, Bayreuth, Germany

⁴Thünen Institute, Climate-Smart Agriculture, Braunschweig, Germany

Correspondence: Pauline Sophie Rummel (pauline.rummel@uni-goettingen.de)

Received: 15 August 2019 – Discussion started: 13 September 2019

Revised: 27 January 2020 – Accepted: 28 January 2020 – Published: 28 February 2020

Abstract. Chemical composition of root and shoot litter controls decomposition and, subsequently, C availability for biological nitrogen transformation processes in soils. While aboveground plant residues have been proven to increase N₂O emissions, studies on root litter effects are scarce. This study aimed (1) to evaluate how fresh maize root litter affects N₂O emissions compared to fresh maize shoot litter, (2) to assess whether N₂O emissions are related to the interaction of C and N mineralization from soil and litter, and (3) to analyze changes in soil microbial community structures related to litter input and N₂O emissions.

To obtain root and shoot litter, maize plants (*Zea mays* L.) were cultivated with two N fertilizer levels in a greenhouse and harvested. A two-factorial 22 d laboratory incubation experiment was set up with soil from both N levels (N1, N2) and three litter addition treatments (control, root, root + shoot). We measured CO₂ and N₂O fluxes, analyzed soil mineral N and water-extractable organic C (WEOC) concentrations, and determined quality parameters of maize litter. Bacterial community structures were analyzed using 16S rRNA gene sequencing.

Maize litter quality controlled NO₃[−] and WEOC availability and decomposition-related CO₂ emissions. Emissions induced by maize root litter remained low, while high bioavailability of maize shoot litter strongly increased CO₂ and N₂O emissions when both root and shoot litter were added. We

identified a strong positive correlation between cumulative CO₂ and N₂O emissions, supporting our hypothesis that litter quality affects denitrification by creating plant-litter-associated anaerobic microsites. The interdependency of C and N availability was validated by analyses of regression. Moreover, there was a strong positive interaction between soil NO₃[−] and WEOC concentration resulting in much higher N₂O emissions, when both NO₃[−] and WEOC were available. A significant correlation was observed between total CO₂ and N₂O emissions, the soil bacterial community composition, and the litter level, showing a clear separation of root + shoot samples of all remaining samples. Bacterial diversity decreased with higher N level and higher input of easily available C. Altogether, changes in bacterial community structure reflected degradability of maize litter with easily degradable C from maize shoot litter favoring fast-growing C-cycling and N-reducing bacteria of the phyla *Actinobacteria*, *Chloroflexi*, *Firmicutes*, and *Proteobacteria*. In conclusion, litter quality is a major driver of N₂O and CO₂ emissions from crop residues, especially when soil mineral N is limited.

1 Introduction

Chemical composition controls decomposition of both roots (Birouste et al., 2012; Redin et al., 2014; Silver and Miya, 2001) and plant litter (Jensen et al., 2005; Kögel-Knabner, 2002; Zhang et al., 2008) and, subsequently, C availability for biological nitrogen transformation processes in soils. When O₂ concentrations are low, denitrifying soil microorganisms may use nitrate (NO₃⁻) as an electron acceptor in the respiratory chain to break down organic compounds (Zumft, 1997). This leads to loss of plant-available N (Müller and Clough, 2014) and makes soils an important source of the greenhouse gas N₂O (Ciais et al., 2013).

Plant residues have been proven to increase N₂O emissions upon incorporation into soil. When different types of litter were compared, quality parameters of plant residues, such as C : N ratio, lignin : N ratio, and chemical composition of structural components explained a large share of variances in N₂O emissions (Baggs et al., 2000; Chen et al., 2013; Millar and Baggs, 2004). Especially in drier soils, denitrification is largely controlled by the supply of readily decomposable organic matter (Azam et al., 2002; Burford and Bremner, 1975; Loecke and Robertson, 2009). Availability of easily degradable C compounds stimulates microbial respiration, limiting O₂ at the microsite level and increasing N₂O emissions (Azam et al., 2002; Chen et al., 2013; Miller et al., 2008). Furthermore, plant litter enhances local anaerobicity by absorbing water from surrounding pores and retaining high moisture concentrations (Kravchenko et al., 2017, 2018).

While effects of aboveground plant residues on N₂O emissions have been studied extensively, studies of root residues on N₂O emissions are scarce. In a temperate forest soil, fine root litter of maize and native tree species did not cause any N₂O emissions, but a very close interrelation between C mineralization of fine root litter and N₂O emissions was found in other biomes (Hu et al., 2016). In other studies, lower cumulative N₂O emissions were reported after addition of sugar beet roots compared to leaves (Velthof et al., 2002) and rice roots compared to rice straw (Lou et al., 2007). Furthermore, decomposition dynamics of roots have been studied in great detail, revealing that chemical composition explains most of its variation (Birouste et al., 2012; Johnson et al., 2007; Machinet et al., 2011; Redin et al., 2014; Silver and Miya, 2001; Zhang and Wang, 2015). In general, decomposition rates of hemicelluloses and pectin are higher than that of cellulose, while among cell wall components lignin is most resistant against microbial decomposition (Kögel-Knabner, 2002).

Soil microorganisms are often specialized in specific substrates with fungi being regarded as the main decomposers of plant materials rich in cellulose and lignin, while hemicelluloses and pectin are decomposed by many aerobic and anaerobic bacteria and fungi (Kögel-Knabner, 2002). While the phyla *Firmicutes*, *Proteobacteria*, and *Bacteroidetes* are described as fast-growing copiotrophic bacteria that are stim-

ulated by input of easily degradable C compounds (Fierer et al., 2016; Pascault et al., 2013), abundance of *Acidobacteria* decreased following the addition of dissolved organic matter into the soil (Fierer et al., 2016). Similarly, denitrifying microorganisms are found in bacteria, fungi, and archaea depending on substrate availability and environmental conditions (Zumft, 1997). Fungi are seen as major contributors to denitrification under aerobic and weakly anaerobic conditions, while bacterial denitrification predominates under strongly anaerobic conditions (Hayatsu et al., 2008). Denitrifying bacteria can be found in most phyla (Zumft, 1997), with dominant populations in *Pseudomonas* and *Alcaligenes* (Gamble et al., 1977; Megonigal et al., 2013). The most abundant denitrifying bacteria in soil are heterotrophic and, as such, require a source of electrons or reducing equivalents contained in C compounds of organic matter or plant residues. Availability of organic C may thus affect both decomposing and denitrifying soil microorganisms.

In most reported studies on decomposition and N₂O emissions, dried and often ground plant material was used. This facilitates a homogenous distribution in soil and minimizes differences between replicates. Nevertheless, drying of fine roots prior to incubation increased their decomposition rate and led to overestimation of decomposition and nutrient cycling rates (Ludovici and Kress, 2006). Additionally, formation of plant-litter-associated anaerobic hot spots was reduced when ground plant material was homogeneously mixed with the soil, while litter aggregation significantly increased soil N₂O emissions (Loecke and Robertson, 2009). Differences in N₂O emissions between two clover species were observed only with intact (but dried) leaves, but not when ground material was used (Kravchenko et al., 2018).

The aims of this study were (1) to evaluate how fresh maize root litter affects N₂O emissions compared to fresh maize shoot litter, (2) to assess to what extent N₂O emissions are related to the interaction of C and N mineralization from soil and litter, and (3) to analyze the changes in soil microbial community structures related to litter input and N₂O emissions. We hypothesize that differences in N₂O emissions between treatments can be related to degradability of maize litter with more easily degradable shoot litter leading to higher N₂O formation. We further expect that differences in litter chemical quality are reflected in the structural composition of the soil microbial community with higher availability of N and C leading to a more specialized community.

Maize plants were grown in a greenhouse to produce root and shoot litter. As in many European countries the law prohibits addition of mineral N with incorporation of crop residues or catch crops, we applied two N fertilizer regimes (low vs. high) to realize differences in soil N_{min} concentration at harvest. We then set up a laboratory incubation experiment with fresh maize root or root and shoot litter under fully controlled conditions and determined CO₂ and N₂O fluxes for 22 d. Soil samples were taken in regular intervals and analyzed for soil mineral N and water-extractable organic C

(WEOC) concentrations. At the end of the incubation experiment, soil microbial community structures were analyzed to identify adaptations to litter input.

2 Material and methods

2.1 Preparation of plants and soils prior to incubation experiment

The soil for the experiment was collected 10 km south of Göttingen, Germany, at the experimental farm Reinshof of the University of Göttingen (51.484° N, 9.923° E). Soil was classified as gleyic Fluvisol (21 % clay, 68 % silt, 11 % sand) containing 1.5 % C and 2.81 % humus, with a pH (CaCl₂) = 7.44.

Prior to the incubation experiment, maize plants were cultivated to obtain shoot and root biomass. For maize cultivation, Mitscherlich pots were filled with 5 kg of air-dried and sieved (2 mm) soil previously mixed with fertilizers (0.2 g N kg⁻¹ as NH₄NO₃, 0.14 g P kg⁻¹ as Ca(H₂PO₄)₂, 0.2 g K kg⁻¹ as K₂SO₄ and 0.04 g Mg kg⁻¹ as MgSO₄ × 7 H₂O including 0.135 g S kg⁻¹). Soil moisture was adjusted to 25 vol. %, and volumetric water content (VWC) sensors (EC-5, Decagon Devices, Pullman, USA) were used to monitor soil water content. Six maize plants (*Zea mays* L. var. Ronaldinio) were sown per pot and cultivated in a greenhouse with 16 h light and 8 h dark cycles. Pots were randomized in regular intervals to avoid microclimatic effects in the greenhouse.

To get different soil mineral N concentrations in soil, a second N fertilizer dose (0.2 g N kg⁻¹ as Ca(NO₃)₂ × 4 H₂O) was applied to half of the pots 6 weeks after sowing. Soil with one N dose is referred to as N1 (0.2 g N kg⁻¹) and soil with two N doses is referred to as N2 (2 × 0.2 g N kg⁻¹). Plants were harvested 8 weeks after sowing: maize plants were cut above the soil surface and roots were removed from soil by sieving and handpicking. Fresh roots were shaken and slightly brushed to remove adhering soil.

A subsample of aboveground maize biomass and maize roots was dried at 60 °C to determine dry matter contents and milled to a particle size < 1 mm. To determine water-extractable C and N concentrations, subsamples were extracted with H₂O_{bidest} (maize root 1 : 1000 w/v; maize shoot 1 : 10000 w/v) for 16 h and analyzed using a multi N/C[®] analyzer (model 3100, Analytik Jena, Jena, Germany). Another subsample was analyzed for the sum of structural components following established feedstuff analysis protocols based on the method proposed by Goering and Van Soest (1970), namely ash-free neutral detergent fiber aNDFom (VDLUFA, 2012a), acid detergent fiber ADFom (VDLUFA, 2011), and acid detergent lignin ADL (VDLUFA, 2012b). According to the definitions, hemicellulose, cellulose, and lignin contents were calculated as follows: hemicellulose is equal to aNDFom minus ADFom; cellulose is

equal to ADFom minus ADL; lignin is equal to ADL. Another subsample was milled using a ball mill, and total carbon and nitrogen concentrations were analyzed using a C : N analyzer (model 1110, Carlo Erba, Milan, Italy).

2.2 Incubation experiment

The incubation experiment consisted of a two-factorial setup comprising two N levels (N1 and N2) and three litter levels (control: Cn; root: Rt; root + shoot: RS) (see Table 1 and Fig. 1 for details). To allow comparison of litter treatments over soil conditions, the same litter types for both soil N levels were used. As N2 plants had produced greater and healthier biomass during the pre-experimental growth phase, only N2 shoots were used for both soils. Roots from N1 and N2 plants were mixed to ensure sufficient amounts for all replicates. Control soils (N1-Cn and N2-Cn) did not receive plant biomass, yet they contained C input from rhizodeposition of the previous maize growth. C remaining from rhizodeposition, root hairs, and small root fragments was calculated as the difference in soil C concentration before and after maize growth. For the root treatment 100 g of fresh root biomass was added per kilogram of dry soil (N1-Rt and N2-Rt), and in the root-and-shoot treatment, 100 g of fresh root and 100 g of fresh shoot biomass were added per kilogram of dry soil (N1-RS, N2-RS). Each treatment was replicated four times.

Within each N level, soil was homogenized to ensure similar starting conditions. Subsamples of both soils were taken for analysis of mineral N, water-extractable C_{org} concentration, and total soil C. Soil mineral N concentrations were 0.93 and 1.97 µg N g⁻¹ for N1 and N2, respectively. Plant litter was cut to a size of 2 cm and homogeneously mixed with the soil, simulating residue incorporation and tillage. PVC pots with a diameter of 20 cm and a total volume of 6.8 L were filled with fresh soil equivalent to 3.5 kg dry weight previously mixed with plant litter. Soil was compacted in a step-wise mode by filling a 2 cm layer of soil in pots and compacting it with a plunger. To ensure continuity between soil layers, the surface of the compacted layer was gently scratched before adding the next soil layer. Due to high litter input, target bulk density was 1.1 g cm⁻³. Actual bulk density was determined by measuring headspace height, and these values were used for calculations.

To adjust soil moisture of all pots to 70 % water holding capacity (WHC), equivalent to 49 % WFPS, water was dripped on the soil surface through hollow needles (outer diameter 0.9 mm). Pots were covered with PVC lids to minimize evaporation from the soil and to incubate samples in the dark. The incubation experiment was carried out under controlled temperature conditions (16 h day at 25 °C, 8 h night at 19 °C) for 22 d. Volumetric water content (VWC) sensors (EC-5, Decagon Devices, Pullman, USA) were used to monitor soil water content.

Table 1. Two-factorial setup of the incubation experiment. Soil mineral N (N_{\min}) concentrations were measured directly before onset of the incubation experiment. C input in the control treatment is from rhizodeposition (RD) only, C input in the root treatment is from rhizodeposition and roots, and C input in root + shoot is from rhizodeposition, roots, and shoot biomass. N input is from root and shoot biomass, respectively (FM: fresh matter).

N level	N_{\min} ($\mu\text{g NO}_3^- \text{-N g}^{-1}$ dry soil)	Treatment	Litter input (mg FM g^{-1} dry soil)	C input (mg C g^{-1} dry soil)	N input (mg N g^{-1} dry soil)
N1	0.93	Control	RD	3.47	n.d.
		Root	RD + 100	3.47 + 4.18 = 7.65	0.25
		Root + shoot	RD + 100 + 100	3.47 + 4.18 + 6.16 = 13.80	0.25 + 0.27 = 0.52
N2	1.97	Control	RD	2.74	n.d.
		Root	RD + 100	2.74 + 4.18 = 6.92	0.25
		Root + shoot	RD + 100 + 100	2.74 + 4.18 + 6.16 = 13.07	0.25 + 0.27 = 0.52

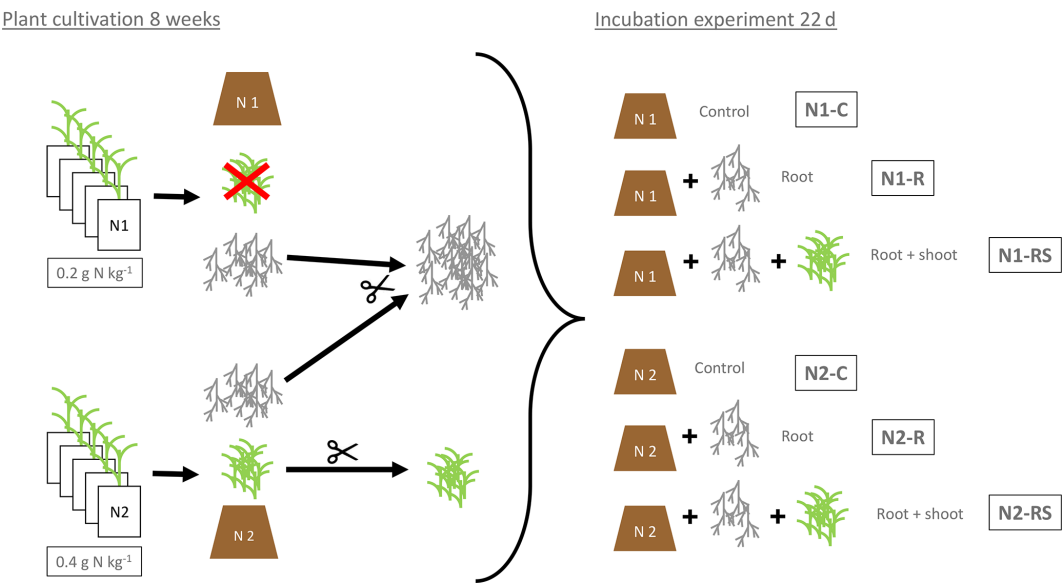


Figure 1. Preparation and experimental setup of the incubation experiment. N1 (0.2 g N kg^{-1}) and N2 ($2 \times 0.2 \text{ g N kg}^{-1}$) referring to the N levels during plant growth. Control soil (N1-C and N2-C) without addition of plant litter. Root treatment with addition of 100 g of fresh root biomass per kilogram of dry soil (N1-R and N2-R) and root + shoot treatment with addition of 100 g of root and 100 g of shoot biomass per kilogram of dry soil (N1-RS, N2-RS).

2.3 Gas sampling and analysis

Gas fluxes were measured using the closed-chamber method (Hutchinson and Mosier, 1981). Gas samples were taken every 12 h (morning and evening) for the first 15 d and every 24 h (midday) for the remaining 7 d. Due to technical issues, gas samples taken in the morning of day 10 to day 15 had to be discarded. Before gas sampling, all pots were opened for ventilation to ensure homogenous ambient air background conditions. Pots were closed with gastight PVC lids, and 30 mL gas samples were taken from each pot 0, 20, and 40 min after closure and filled into pre-evacuated 12 mL Ex-tainer glass bottles (Labco, High Wycombe, UK). Samples were analyzed on a Bruker gas chromatograph (456-GC, Bruker, Billerica, USA) deploying an electron capture de-

tector (ECD) for N₂O and a thermal conductivity detector (TCD) for CO₂. Samples were introduced using a Gilson autosampler (Gilson Inc., Middleton, WI, USA). Data processing was performed using CompassCDS software. The analytical precision was determined by repeated measurements of standard gases (2500 and 550 ppm CO₂, 307, 760, and 6110 ppb N₂O) and was consistently < 2 %.

2.4 Soil analyses

Soil samples were taken from the pots using a soil auger of 16 mm diameter on 5, 9, 14, and 22 DAO (days after onset of experiment). Holes were closed with glass tubes to avoid variation in the soil surface. Fresh subsamples were analyzed for water-extractable C_{org} concentration (WEOC), and a sub-sample was frozen at −20 °C for soil mineral N analysis. To-

tal soil carbon and nitrogen concentrations were analyzed using a C : N analyzer (model 1110, Carlo Erba, Milan, Italy). For determination of soil mineral N content, frozen samples were extracted with a 0.0125 M CaCl₂ solution (1 : 5 *w/v*) for 60 min on an overhead shaker (85 rpm). The extracts were filtered with 615 1/4 filter paper (Macherey-Nagel GmbH & Co. KG, Düren, Germany) and stored at −20 °C. The extracts were analyzed colorimetrically for the concentrations of NO₃[−] and NH₄⁺ using the San⁺⁺ continuous-flow analyzer (Skalar Analytical B.V., Breda, the Netherlands). Soil water content was determined with a parallel set of samples. Net N mineralization was calculated as the difference between the NH₄⁺ − N + NO₃[−] − N concentrations at the start and end of the incubation period plus N lost as N₂O-N (Eq. 1).

$$\text{Net mineralization} = (\text{NO}_3^- + \text{NH}_4^+)_{\text{end}} - (\text{NO}_3^- + \text{NH}_4^+)_{\text{start}} + \text{N}_2\text{O} \quad (1)$$

WEOC was determined according to Chantigny et al. (2007). Briefly, fresh soil was homogenized with deionized water (1 : 2 *w/v*), and samples were centrifuged and filtered with 0.45 µm polyether sulfone syringe filters (Labsolute, Rinnig, Germany) and stored at −20 °C. The extracts were analyzed using a multi N/C[®] analyzer (Analytik Jena, Jena, Germany).

2.5 Analysis of bacterial community structures

2.5.1 DNA isolation and 16S rRNA gene amplification

To analyze the soil-inhabiting bacterial communities, DNA was extracted from 0.5 g (fresh weight) of soil sample taken at the end of the incubation experiment (22 DAO) using the DNA extraction protocol described by Griffiths et al. (2000). Plant litter was removed from samples prior to extraction. In brief, cells were mechanically disrupted using bead beating, and nucleic acids were extracted using phenol : chloroform : isoamyl alcohol (25 : 24 : 1; Carl Roth, Karlsruhe, Germany). Nucleic acids were then precipitated using polyethylene glycol (Carl Roth, Karlsruhe, Germany) and washed with 70 % ice-cold ethanol (VWR, Radnor, Pennsylvania, USA). Subsequently, RNA was removed by RNase A digestion (Thermo Fischer Scientific, Waltham, Massachusetts, USA) as described by the manufacturer. The RNA-free DNA was used for amplification of the V3 to V4 region of the 16S rRNA gene. We used the bacterial primer pair S-D-Bact-0341-b-S-17 and S-D-Bact-0785-a-A-21 targeting the V3–V4 region of the 16S rRNA gene described by Klindworth et al. (2013) with adapters for Illumina MiSeq sequencing. The polymerase chain reaction (PCR) reaction mixture contained five-fold Phusion GC buffer, 200 µM of each of the four deoxynucleoside triphosphates, 5 % DMSO, 0.4 µM of each primer, 1 U of Phusion HF DNA polymerase (Fisher Scientific GmbH, Schwerte, Germany), and 25 ng of RNA-free DNA as template. The following cycling scheme

was used for DNA amplification: initial denaturation at 98 °C for 5 min and 25 cycles of denaturation at 98 °C for 45 s, annealing at 60 °C for 30 s, and extension at 72 °C for 30 s, followed by a final extension at 72 °C for 10 min. For each sample, PCR reactions were performed in triplicate. Resulting PCR products were pooled in equimolar amounts and purified using the QIAquick Gel Extraction kit (Qiagen, Hilden, Germany) as recommended by the manufacturer. Quantification of the PCR products was performed using the Quant-iT dsDNA HS assay kit and a Qubit fluorometer as described by the manufacturer (Invitrogen GmbH, Karlsruhe, Germany). Indexing of the PCR products was performed by the Göttingen Genomics Lab (G2L, Göttingen, Germany) using the Nextera XT Index kit as recommended by the supplier (Illumina, San Diego, CA, USA), and sequencing of 16S rRNA amplicons was performed using the dual index paired-end approach (2 × 300 bp) with v3 chemistry for the Illumina MiSeq platform.

2.5.2 Sequence processing

All bioinformatic processing of sequence data was done using Linux-based software packages. Adapter removal and quality filtering of raw paired-end sequences was done using fastp v0.19.6 (Chen et al., 2018), with base correction in overlapped regions, a qualified quality phred of 20, size exclusion of sequences shorter than 50 bp, and per read trimming by quality (phred 20). Merging of quality-filtered paired-end reads was done by PEAR v0.9.11 (64 bit) with default parameters (Zhang et al., 2014). Primer removal was conducted using cutadapt v1.18 (Martin, 2013). Subsequently, dereplication, denoising, and chimera detection and removal (denovo followed by reference based against the SILVA 132 SSU database) were performed with VSEARCH v2.13.0 (64 bit) (Rognes et al., 2016). Taxonomic classification of the amplicon sequence variants (ASVs, 100 % sequence identity) was performed with BLAST+ v2.7.1 against the SILVA 132 SSU reference database (Quast et al., 2013). Subsequently, extrinsic domain ASVs and chloroplasts were removed from the dataset. Sample comparisons were performed at the same surveying effort of 61200 sequences. Statistical analyses were done using ASVs in R version 3.5.3 (R Core Team, 2019). The R package ampvis2 v2.4.7 (Andersen et al., 2018) was used to determine species richness, alpha diversity estimates, and rarefaction curves and to prepare all graphs. To visualize the multivariate constrained dispersion, canonical correspondence analysis (CCA) was conducted with Hellinger transformed data (Legendre and Gallagher, 2001), and ASVs with a relative abundance lower than 0.1 % in any sample were removed. Correlations of environmental parameters to the bacterial communities were analyzed using the envfit function of the vegan package v2.5-4 (Oksanen et al., 2015) and projected into the ordination with arrows with a *p*-value cutoff of 0.005. For further statistical analysis of the microbial community

composition (on phyla, order, and genus levels) and diversity (Shannon, Simpson, and PD index), multivariate generalized linear models (MGLMs; with N level and litter addition as factors) as implemented in the mvabund R package v4.0.1 were employed with adjusted *p* values (Wang et al., 2019). For the generalized linear model analysis of variance (MGLM-ANOVA) tests, *p* values < 0.05 were considered to be significant. In addition, core microbiomes and respective responders were analyzed at the genus level, grouped by either the applied litter treatment or N fertilizer levels using ampvis2 v2.4.7.

For one replicate of N2-Rt, DNA concentration was very low and the 16S rRNA gene could not be amplified. Thus, we only evaluated the remaining three replicates of this treatment. In addition, we attempted to analyze the soil-inhabiting fungal community using the fungus-specific primer set ITS3_KYO2 and ITS4 (Toju et al., 2012), but we were not able to amplify them.

2.6 Calculations and statistical analyses

All statistical analyses were performed using the statistical software R version 3.5.2 (R Core Team, 2018). Arithmetic means and standard error of the four replicates were calculated for CO₂ and N₂O fluxes. Cumulative gas emissions were calculated by linear interpolation between measured fluxes. To account for different C input in treatments, cumulative CO₂ and N₂O emissions were standardized against the C input per treatment (see Table 1 for details on C input). Tukey's HSD test was used after analysis of variance to test for treatment effects (i.e., N level and litter addition) on cumulative CO₂ emissions. An interaction was identified between N level and litter addition on cumulative N₂O emissions using interaction plots from the package HH v3.1-35 (Heiberger, 2018). A linear model using generalized least squares (glS) was fitted between cumulative N₂O as a response variable and N level, litter addition, and their interaction as fixed effects. Additionally, the model was fitted to account for inhomogeneous within-class variances. Estimated marginal means were then computed to analyze treatment effects using the R package emmeans v1.3.4 (Lenth, 2018). Several regression models were tested to analyze the effect of maize litter on cumulative N₂O emissions including the factors cumulative CO₂ emissions, initial soil NO₃⁻ concentration, and net N mineralization during the incubation period. For cumulative CO₂ emissions, regression models included the factors total C input, water-extractable C input, hemicellulose fraction, cellulose fraction, and lignin fraction from all litter treatments (Cn, Rt, RS, *n* = 24).

To evaluate effects of soil environmental variables on N₂O and CO₂ fluxes, a linear mixed-effect model (lme) was fitted between N₂O fluxes (ln transformed), soil NO₃⁻-N and WEOC concentrations using the lme function from the package nlme v3.1-131 (Pinheiro et al., 2017). Pseudo-*R*² for lme was calculated using r.squaredGLMM from the package Mu-

Table 2. Chemical characteristics of maize root and shoot litter used in the incubation experiment. Hemicellulose and cellulose are expressed relative to lignin content.

	Root	Shoot
Dry matter (%)	62.9	14.7
C : N ratio	17.0	23.2
Lignin : N ratio	2.82	1.44
Water-soluble C _{org} (percent of total C)	11.6	23.4
Water-soluble N (percent of total N)	8.8	25.8
Hemicellulose (relative content)	3.36	9.08
Cellulose (relative content)	3.18	11.5
Lignin (relative content)	1	1

MIn v1.42.1 (Barton, 2018). Soil NO₃⁻-N and WEOC concentrations between sampling dates were estimated by linear interpolation. Only evening and midday gas measurements were included in model calculations. To account for repeated measurements, incubation vessel and sampling day were set as random effects. Models were compared using maximum likelihood (ML), selected using AIC (Akaike's information criterion), and fitted using restricted maximum likelihood (REML).

All plots were made using the statistical software R version 3.5.2 (R Core Team, 2018) including the packages plotrix v3.7.4 (Lemon, 2006), plot3D v1.1.1 (Soetaert, 2017), and viridisLite v0.3.0 (Garnier, 2018).

3 Results

3.1 Chemical analyses of maize litter

Maize root and shoot litter differed in their chemical compositions (Table 2). Dry matter content of maize roots was much higher compared to shoot as roots had not been washed prior to analyses, so some soil adhering to roots was included in dry matter determinations. Thus, we calculated water-extractable concentrations in relation to total C instead of dry matter. Maize shoot litter was characterized by higher concentrations of water-soluble C and N and a higher share of easily degradable compounds like hemicellulose and cellulose compared to maize roots.

3.2 CO₂ and N₂O fluxes and cumulative emissions

Addition of maize litter increased CO₂ fluxes compared to the control treatment (Fig. 2), where addition of root and shoot litter (N1-RS, N2-RS) resulted in much higher fluxes compared to roots only (N1-Rt, N2-Rt). While absolute emission rates were strongly affected by litter input, time courses were similar in all litter treatments without visible differences between N1 and N2. CO₂ fluxes stayed on a similar level for the first 10 d after onset of incubation, showing fluc-

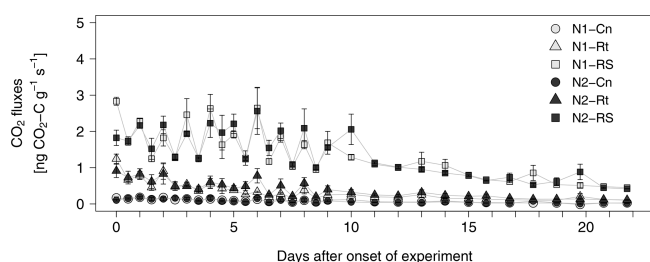


Figure 2. CO₂ fluxes from soils with two N levels (N1, N2) after incorporation of maize root litter (Rt), maize root + shoot litter (RS), and control (Cn) without litter. Error bars show the standard error of mean values ($n = 4$). When not visible, error bars are smaller than the symbols.

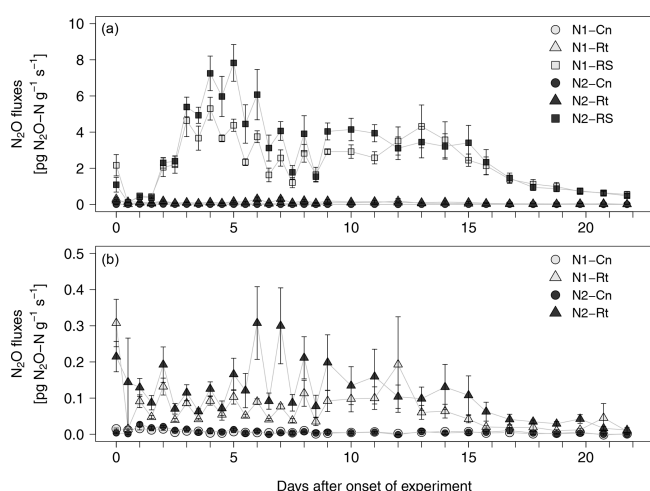


Figure 3. (a, b) N₂O fluxes from soils with two N levels (N1, N2) after incorporation of maize root litter (Rt), maize root + shoot litter (RS), and control (Cn) without litter. Error bars show the standard error of mean values ($n = 4$). When not visible, error bars are smaller than the symbols. Note: data of (b) are excerpts from (a) and are shown with a different scaling.

tuations between morning and evening sampling times, and then constantly decreased until the end of the experiment.

After a short lag phase right after the onset of experiment, N₂O emissions increased in all litter treatments compared to control treatments (Fig. 3a, b). The highest fluxes were measured in N2-RS, reaching 7.8 pg N₂O-N g⁻¹ s⁻¹ on day 5. Fluxes stayed on a similar level from day 7 to day 15 and then declined until the end of the experiment. N₂O fluxes from root (N1-Rt, N2-Rt) and control treatments (N1-Cn, N2-Cn) remained at a low level during the whole incubation period (≤ 0.59 pg and ≤ 0.04 pg N₂O-N g⁻¹ s⁻¹, for Rt and Cn, respectively). N₂O fluxes from N1 were slightly lower than from N2 in both litter treatments. Over all treatments and sampling dates, CO₂ and N₂O fluxes were positively correlated ($R^2 = 0.5993$, $p < 0.001$, data not shown).

To account for different C inputs in treatments, cumulative CO₂ and N₂O emissions were standardized against the C in-

put per treatment (Table 3). Still, cumulative CO₂ emissions were almost twice as high in Rt and about 4 times higher in RS compared to Cn ($p < 0.05$), indicating that differences between litter treatments cannot simply be explained by differences in C input. Addition of maize root and shoot litter increased cumulative N₂O emissions by roughly a factor of 100 compared to control treatments ($p < 0.05$). In contrast, root litter increased cumulative N₂O emissions only by a factor of 5.4 (N1-Rt) and 7 (N2-Rt) compared to the respective controls ($p < 0.05$).

3.3 Soil NO₃⁻, NH₄⁺, and water-extractable C_{org} concentrations

Addition of maize litter affected the time course of soil NO₃⁻, NH₄⁺, and WEOC concentrations (Fig. 4a–c). In control treatments, initial soil NO₃⁻ concentrations of 0.93 (N1-Cn) and 1.97 μg NO₃⁻-N g⁻¹ dry soil (N2-Cn) continuously increased until the end of the experiment, reaching concentrations of 8.24 μg N g⁻¹ (N1-Cn) and 11.74 μg N g⁻¹ (N2-Cn), respectively. Soil NH₄⁺ concentrations showed variations at a low level only. Soil NO₃⁻ concentrations were continuously higher in N2 than in N1 and differences in soil NH₄⁺ concentration were small. Higher fertilization in N2 during previous plant growth led to higher residual organic N and higher net N mineralization (7.61 and 10.08 μg N g⁻¹ for N1-Cn and N2-Cn, respectively, Table 4) during the incubation experiment. In treatments with litter, soil NO₃⁻ concentrations decreased after an initial increase. In root treatments, soil NO₃⁻ concentrations continuously decreased until the end of the incubation experiment to 1.9 (N1-Rt) and 2.5 μg N g⁻¹ (N2-Rt), while in root-plus-shoot treatments soil NO₃⁻ concentrations increased again until the end of the experiment, reaching concentrations of 9.46 (N1-RS) and 9.52 μg N g⁻¹ (N2-RS). During the whole incubation period, soil NO₃⁻ concentrations in RS were higher than in Rt. Soil NH₄⁺ concentrations only marginally increased for Rt. Contrary to Rt and Cn, soil NH₄⁺ concentrations increased until the end of the incubation experiment to 1.68 (N1-RS) and 1.52 μg N g⁻¹ (N2-RS) in root-and-shoot treatments. Net N mineralization was 1.44 (N1-Rt) and 1.10 μg N g⁻¹ (N2-Rt) in root treatments, and 14.32 (N1-RS) and 14.14 μg N g⁻¹ (N2-RS) in root-and-shoot treatments (Table 4). Maize root litter did not affect WEOC, as concentrations were similar to Cn throughout the incubation period. However, in RS treatments, WEOC increased after the onset of incubation, reaching the highest values (45.32 μg C g⁻¹) for N1-RS at day 9, after which it decreased until the end of the experiment.

3.4 Relations between N₂O emissions and C and N parameters of plant litter and soil

To identify the effect of N and C availability on N₂O fluxes, a linear mixed-effect model was applied. The best model included a significant interaction between soil NO₃⁻ and

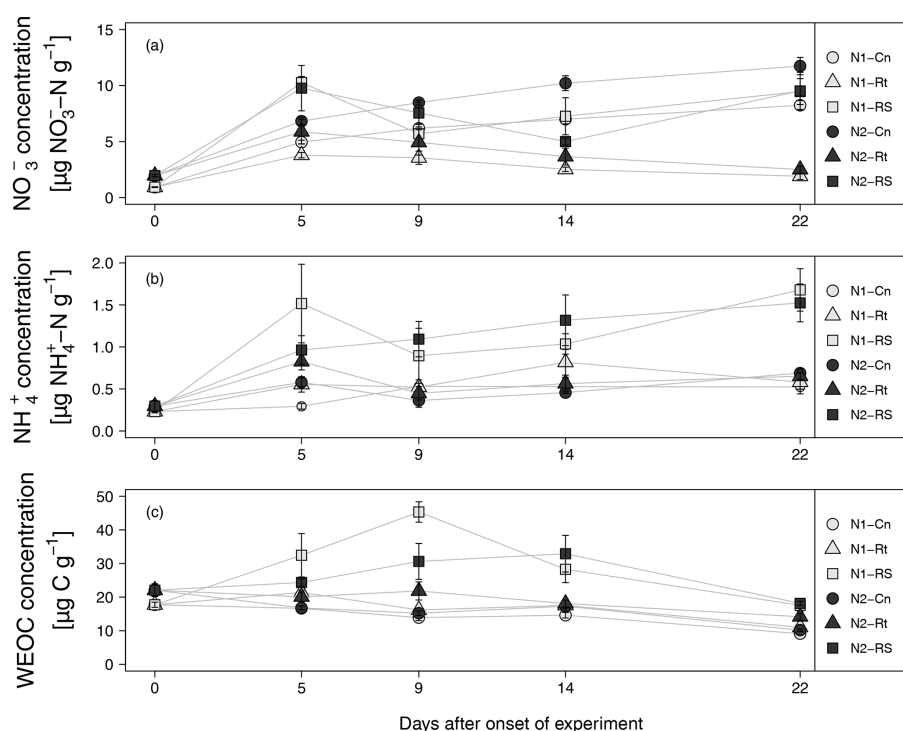


Figure 4. (a–c) NO_3^- , WEOC, and NH_4^+ concentration from soils with two N levels (N1, N2) after incorporation of maize root litter (Rt), maize root + shoot litter (RS), and control (Cn) without litter. Error bars show the standard error of mean values ($n = 4$) (day 0: $n = 3$). When not visible, error bars are smaller than the symbols.

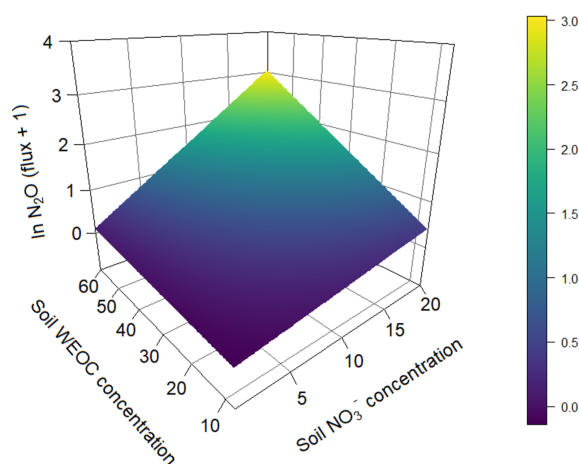


Figure 5. Prediction of N_2O fluxes ($\text{pg N}_2\text{O-N g}^{-1} \text{ s}^{-1}$) (ln transformed) based on soil NO_3^- ($\mu\text{g N g}^{-1}$) and water-extractable C_{org} ($\mu\text{g C g}^{-1}$) concentrations based on a linear mixed-effect model (pseudo- $R^2 = 0.82$).

WEOC ($p < 0.0024$, pseudo- $R^2 = 0.82$, Table 5) and incubation vessel and sampling time as random parameters. Predictions of N_2O fluxes based on this model are shown in Fig. 5.

Linear regression analyses were used to identify relations between cumulative CO_2 and N_2O emissions, litter quality, and N parameters. Either hemicellulose + cellulose frac-

tion or water-extractable C fraction of plant litter explained more than 96 % of variance of total cumulative CO_2 emissions ($p < 2.2 \times 10^{-16}$) (Table 6). Regression analyses of the relationships between total cumulative N_2O emissions and influencing factors identified a strong positive relationship between total cumulative N_2O emissions and total cumulative CO_2 emissions ($R^2 = 0.9362$, $p < 7.632 \times 10^{-15}$) (Table 7) and between cumulative N_2O emissions and mineralized N ($R^2 = 0.5791$, $p < 9.551 \times 10^{-06}$), while initial soil NO_3^- concentration did not explain any variance.

3.5 Bacterial community structure

The comparison over all maize litter treatments revealed that the bacterial diversity was slightly higher in N1 than in N2 soil as shown by a higher number of amplicon sequence variants (ASVs, $R^2 = 0.1195$, $p = 0.059$, Fig. S1 in the Supplement). In addition, the alpha diversity indices Shannon ($R^2 = 0.1844$, $p = 0.023$) and Simpson ($R^2 = 0.1131$, $p = 0.065$) as well as Faith's phylogenetic diversity (PD; $R^2 = 0.1844$, $p = 0.059$) were higher for N1 than for N2 samples (Table S4 in the Supplement).

The canonical correspondence analysis revealed a significant correlation ($p < 0.001$) of the bacterial community composition with total CO_2 ($R^2 = 0.6758$) and N_2O ($R^2 = 0.6179$) emissions and the litter level, expressed by a clear separation of the N1-RS and N2-RS samples of all other sam-

Table 3. Absolute cumulative N₂O and CO₂ emissions and relative to C input and N₂O/CO₂ ratio of 22 d incubation experiment with two pre-incubation N levels (N1, N2) and three litter addition treatments (control: no litter input; root: 100 mg root M g⁻¹ dry soil; root + shoot: 100 mg root FM + 100 mg shoot FM g⁻¹ dry soil).

N level	Treatment	N ₂ O (ng N ₂ O-N g ⁻¹ dry soil)	N ₂ O (ng N ₂ O-N mg ⁻¹ C input)	CO ₂ (μg CO ₂ -C g ⁻¹ dry soil)	CO ₂ (μg CO ₂ -C mg ⁻¹ C input)	N ₂ O/CO ₂ ratio (ng N μg ⁻¹ C)
N1	Control	10.21 ± 4.23	a	141.89 ± 29.74	a	0.07
	Root	120.91 ± 24.09	b	533.51 ± 83.19	b	0.23
	Root + shoot	4337.31 ± 424.98	c	2287.23 ± 289.48	c	1.91
N2	Control	11.35 ± 6.75	a	129.44 ± 47.47	a	0.08
	Root	201.14 ± 105.62	ab	647.48 ± 196.13	b	0.31
	Root + shoot	5357.87 ± 1193.50	c	2361.19 ± 287.20	c	2.25

Values represent means ($n = 4$) ± standard deviation. Different letters in the same column indicate a significant difference according to Tukey's HSD post hoc tests at $p \leq 0.05$.

Table 4. N mineralization during the incubation period.

N level	Treatment	N mineralized during incubation (μg N g ⁻¹ dry soil)	
N1	Control	7.61 ± 0.98	b
	Root	1.44 ± 0.72	a
	Root + shoot	14.32 ± 2.66	c
N2	Control	10.08 ± 1.76	b
	Root	1.10 ± 0.68	a
	Root + shoot	14.14 ± 4.83	c

Values represent means ($n = 4$) ± standard deviation. Different letters in the same column indicate a significant difference according to Tukey's HSD post hoc tests at $p \leq 0.05$.

Table 5. Significance of fixed effects of soil NO₃⁻-N (μg NO₃⁻-N g⁻¹), water-extractable organic C (WEOC, μg C g⁻¹), and first-order interaction on N₂O fluxes (pg N₂O-N g⁻¹ h⁻¹; ln transformed) using a linear mixed-effect model.

	Estimate	Standard error	p value
Intercept	−0.2181	0.1268	0.0860
NO ₃ ⁻ -N	−0.0043	0.0165	0.7930
WEOC	0.0094	0.0053	0.0770
NO ₃ ⁻ -N × WEOC	0.0023	0.0008	0.0024

ples (Fig. 6). With increasing C input, N2 samples cluster more closely than N1 samples. No significant correlation of litter level and microbial diversity was observed and PD index increased in N1 samples with increasing C input, while the opposite was found for N2 samples. Comparison of N1-Cn and N1-RS revealed no difference in diversity indices (Shannon and Simpson), while N1-Rt showed lower Shannon and Simpson diversity indices (Table S4). The Shannon diversity index was lowest in N2-Rt comparing all N2 treatments, while the Simpson index was lowest for N2-RS.

Overall, the soil bacterial communities were dominated by *Actinobacteria*, *Proteobacteria*, and *Chloroflexi* accounting for 151 % to 31 % (Fig. S2). The highest relative abundance of *Actinobacteria* and *Chloroflexi* was found in N2-Rt and of *Proteobacteria* in N1-R. Among these phyla, the orders *Gaiellales* (*Actinobacteria*), *Sphingomonadales* (*Proteobacteria*), and *Thermomicrobiales* (*Chloroflexi*) showed the highest relative abundance, especially in N2-Rt (9.3 %), N1-Rt (7.5 %), and N2-RS (9 %), respectively. Nevertheless, the phyla *Acidobacteria*, *Planctomycetes*, *Verrucomicrobia*, *Gemmatimonadetes*, *Firmicutes*, *Patescibacteria*, and *Bacteroidetes* were also detected (> 1 %) (Fig. 7). In detail, *Bacteroidetes* and *Gemmatimonadetes* decreased (with a negative slope, but not significant) with increasing N level, while the abundance of *Firmicutes* increased significantly ($p = 0.038$). In addition, although present only in low relative abundance, the *Cyanobacteria* decreased significantly ($p = 0.003$) with increasing N levels. At the genus level,

Table 6. Results of regression analyses of the relationship between total cumulative CO₂ emissions and C quality parameters of plant litter (AICc: Akaike's information criterion).

Regression model	Residual standard error	Degrees of freedom	Adjusted R^2	p value	AICc
CO ₂ ~ Total litter C input	274.5	22	0.9213	7.65×10^{-14}	342.73
CO ₂ ~ Water-soluble C input	181.9	22	0.9655	$< 2.2 \times 10^{-16}$	322.98
CO ₂ ~ Hemicellulose	272.4	22	0.9225	6.497×10^{-14}	342.38
CO ₂ ~ Cellulose	221.1	22	0.9489	6.478×10^{-16}	332.35
CO ₂ ~ Lignin	496.6	22	0.7425	3.873×10^{-08}	371.19
CO ₂ ~ Hemicellulose + cellulose	180.2	21	0.9661	$< 2.2 \times 10^{-16}$	324.32

Table 7. Results of regression analyses of the relationship between total cumulative N₂O emissions, total cumulative CO₂ emissions, and N parameters of plant litter and soil (AIC: Akaike's information criterion).

Regression model	Residual standard error	Degrees of freedom	Adjusted R^2	p value	AIC
N ₂ O ~ CO ₂	593.9	22	0.9366	7.073×10^{-15}	379.78
N ₂ O ~ Initial soil NO ₃ [−]	2404	22	−0.03885	0.7119	446.89
N ₂ O ~ Mineralized N	2191	22	0.5791	9.551×10^{-06}	425.21

Pseudomonas, *Altererythrobacter*, *Gaiella*, *Nocardioides*, *Agromyces*, *Bacillus*, and *Lysobacter* were most abundant, accounting for up to 5.7 % of all ASVs. Accordingly, these were also the most abundant genera attributed to the core microbiome (Tables S6 and S8). Overall, 80 genera represented the core microbiome, when grouped by N levels, while 21 genera and six genera were identified as responders to N1 and N2, respectively (Fig. S5). In detail, the classified responders to the applied N treatments were the genera *Chthonibacter*, *Luteimonas*, *Sphingobium*, *Novosphingobium*, *Adhaeribacter*, *Nitrospira*, *Gemmata*, and *Devosia* for N1 and *Conexibacter* for N2 samples (Table S8). The genera *Bacillus*, *Gaiella*, *Altererythrobacter*, *Blastococcus*, and *Pseudomonas* showed the highest abundance in N2 samples, while *Lysobacter* and *Sphingomonas* were more abundant in N1 samples (Fig. S3). When grouped by litter treatment, the core microbiome comprised 77 genera accounting for 73 % of the relative abundance, while 9, 3, and 10 genera were identified as responders to the applied litter treatments control, root, and root + shoot, respectively (Fig. S5). *Nonomuraea*, *Fluviicola*, and *Nitrospira* responded to the root + shoot treatment, while the genera *Lapillicoccus* and *Adhaeribacter* responded to the root treatment (Table S7). The genera *Litorilinea*, *Gemmata*, *Novosphingobium*, and *Opitutus* were identified as responders to the control treatment. For N levels and litter treatments, respectively, 833 and 838 genera were identified as non-core microbiomes, accounting for 20 % and 19.5 % of relative abundance (Fig. S5).

The most abundant classified species found were *Agromyces* sp., *Bacillus* sp., and *Sphingomonas* sp. Nevertheless, species such as *Pseudomonas* sp., *Nitrosospira* sp.,

Nitrosospira briensis, *Alcaligenes* sp., and *Mesorhizobium* sp. were also identified. Overall, the bacterial community composition was significantly influenced by N level ($p = 0.005$) and maize litter treatment ($p = 0.033$).

4 Discussion

4.1 Decomposability of maize litter

Maize root and shoot litter quality controlled NO₃[−] and WEOC availability and decomposition-related CO₂ emissions during the initial phase of maize litter decomposition. Harvest of plants, removal of roots, and mixing of soil fostered mineralization and nitrification, as reflected by gradually increasing soil NO₃[−] concentrations. The absence of changes in soil NH₄⁺ concentrations in control treatments without litter addition (N1-Cn, N2-Cn) indicates that all NH₄⁺ was directly nitrified. Also in controls, available C was low as indicated by low CO₂ emissions and decreasing WEOC concentrations. The potential for mineralization in soil is known to be high after tillage (Höper, 2002) and positive net mineralization has been reported in control soil without litter addition (Machinet et al., 2009; Velthof et al., 2002) and in the fallow period after rice harvest (Aulakh et al., 2001).

Maize shoot litter was characterized by a high share of easily degradable compounds. High percentages of water-soluble N and water-soluble C_{org} from maize shoot litter strongly increased soil WEOC and NO₃[−] concentrations. Availability of easily degradable compounds was also reflected by strongly increased CO₂ fluxes and cumulative

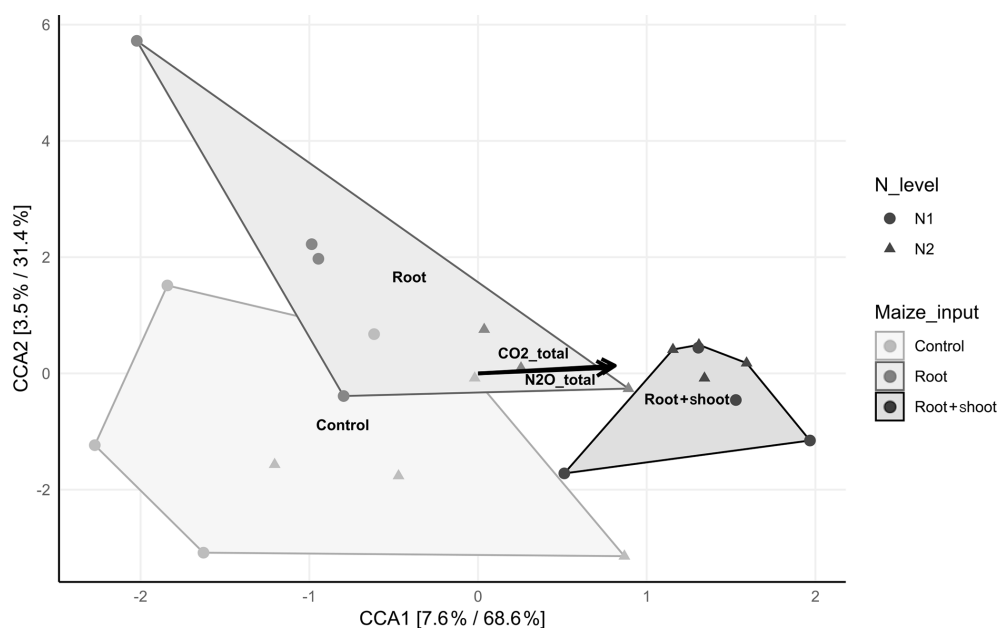


Figure 6. Canonical correspondence analysis (CCA) displaying the compositional distribution of the soil-inhabiting bacterial communities between the control (N1-C and N2-C; $n = 4$), root (N1-R and N2-R; $n = 4$ and $n = 3$), and root + shoot (N1-RS and N2-RS; $n = 4$) treatments. Significant correlations of total CO₂ and N₂O emissions are shown by black arrows ($p \leq 0.005$). The relative contribution (eigenvalue) of each axis to the total inertia in the data as well as to the constrained space only are indicated in percent in the axis titles.

emission from N1-RS and N2-RS. While net mineralization in RS was similar to Cn, it was very small in Rt, indicating that N from mineralization was immobilized by soil microorganisms to decompose root C compounds (Robertson and Groffman, 2015). Cumulative CO₂ emissions in litter treatments were clearly higher than in the control treatment, but CO₂ fluxes continuously decreased after the onset of incubation, as easily degradable C was consumed. This is in accordance with results of Hu et al. (2016), who reported that maize fine root input initially increased CO₂ fluxes, which then decreased during the first 20 d of incubation.

Mineralization of plant litter may increase soil NO₃⁻ concentrations in particular when C : N ratios are low (Li et al., 2013; Millar and Baggs, 2004). However, net N immobilization has been reported after addition of roots of maize (Machinet et al., 2009; Mary et al., 1993; Velthof et al., 2002), wheat (Jin et al., 2008; Velthof et al., 2002), barley, and sugar beet (Velthof et al., 2002), reaching a maximum around day 21 (Mary et al., 1993). Chemical composition has been proven to be the primary controller of decomposition rates of both roots (Birouste et al., 2012; Redin et al., 2014; Silver and Miya, 2001) and aboveground plant litter (Jensen et al., 2005; Zhang et al., 2008) of many different species. Slower decomposition of roots compared to leaves and stems was related to differences in chemical composition of plant organs (Jenkinson, 1965; Johnson et al., 2007). Accordingly, decomposition of roots from 16 maize genotypes was controlled by soluble residue components in the short term, whereas lignin and the interconnections be-

tween cell wall polymers were important in the long term (Machinet et al., 2011). In our study, regression analyses identified a strong positive relationship between cumulative CO₂ emissions and water-extractable C fraction of plant litter ($R^2 = 0.966$, $p < 2.2 \times 10^{-16}$) (Table 6).

4.2 N₂O emissions as affected by biodegradability of maize litter and soil N level

Denitrification in soil is largely controlled by the supply of readily decomposable organic matter (Azam et al., 2002; Burford and Bremner, 1975; Loecke and Robertson, 2009), leading to significant correlations between both N₂O and CO₂ fluxes and cumulative emissions (Azam et al., 2002; Fiedler et al., 2017; Frimpong and Baggs, 2010; Huang et al., 2004; Millar and Baggs, 2004, 2005). CO₂ fluxes increased directly with the onset of incubation and started to decline after day 10; thus mostly C compounds with a short turnover time, i.e., sugars, proteins, starch, and hemicellulose, were decomposed and contributed to CO₂ fluxes. Availability of easily degradable C compounds stimulates microbial respiration, limiting O₂ at the microsite level and thus increasing N₂O emissions from denitrification (Azam et al., 2002; Chen et al., 2013; Miller et al., 2008). Accordingly, N₂O fluxes increased after a lag phase of 2 d. The strong positive correlation ($R^2 = 0.9362$, $p \leq 7.632 \times 10^{-15}$) between cumulative CO₂ and N₂O emissions (Table 7) further supports our hypothesis that litter quality, in particular degradability of C compounds, affects N₂O fluxes from denitrification by creat-

ing plant-litter-associated microsites with low O₂ concentrations.

High mineralization in RS treatments may have especially favored coupled nitrification–denitrification where NO₂[−] and NO₃[−] are produced by nitrifiers in aerobic habitats and subsequently denitrified by denitrifiers in close-by anaerobic habitats (Butterbach-Bahl et al., 2013; Wrage et al., 2001). Here, N₂O is mainly produced in the interface of aerobic and anaerobic zones, which are typically found in plant litter associated hot spots (Kravchenko et al., 2017). In addition, N₂O can also be produced aerobically during heterotrophic and autotrophic nitrification (Anderson et al., 1993; van Groenigen et al., 2015; Wrage et al., 2001; Zhang et al., 2015). In both processes, N₂O can be formed as a byproduct from chemical hydroxylamine oxidation (Butterbach-Bahl et al., 2013; van Groenigen et al., 2015). Nitrifier denitrification as a pathway of autotrophic nitrification has been reported mostly under soil conditions differing from our study, namely high NO₂[−], NH₃, or urea concentrations and low organic C availability (Wrage-Mönnig et al., 2018; Wrage et al., 2001). In contrast, with high availability of organic C and N compounds, high N₂O emissions from heterotrophic nitrification have been reported (Anderson et al., 1993; Hu et al., 2016; Papen et al., 1989; Wrage et al., 2001). Zhang et al. (2015) reported 72 %–77 % of N₂O being produced by heterotrophic nitrification from an arable soil under incubation conditions similar to our study. However, Li et al. (2016) estimated that denitrification was the dominant source of N₂O in residue-amended soil at 40 %–60 % WFPS. High correlation of cumulative N₂O emissions and mineralized N during the incubation period ($R^2 = 0.5791$, $p < 9.551 \times 10^{-06}$) indicates that, in addition to denitrification, heterotrophic nitrification may have contributed to N₂O production in our study. However, to further differentiate between processes contributing to N₂O production, stable isotope methods need to be used (Baggs, 2008; Butterbach-Bahl et al., 2013; van Groenigen et al., 2015; Wrage-Mönnig et al., 2018).

Another aim of this study was to investigate the effect of residual mineral N on plant-litter-induced N₂O emissions. To this end, we included two N levels that were obtained by different N fertilization during the pre-experimental plant growth phase (N1: 0.2 µg N g^{−1}, N2: 2 × 0.2 µg N g^{−1}). At the onset of the incubation experiment, soil mineral N concentration was twice as high in N2 compared to N1 but generally very low (0.93 and 1.97 µg NO₃[−]-N g^{−1} dry soil for N1 and N2, respectively). Higher N fertilizer input in N2 during plant growth led to lower C input from rhizodeposition (Table 1), which is consistent with literature findings (Kuzakov and Domanski, 2000; Paterson and Sim, 1999). Cumulative N₂O emissions tended to be higher in N2 than in N1, suggesting that NO₃[−] was limited, especially in RS treatments where C availability was highest. In addition, litter chemical quality strongly affected N availability.

Under N-limiting conditions, a higher portion of N is recovered in soil microbial biomass in relation to litter N input

(Bending and Turner, 1999; Troung and Marschner, 2018). When N is abundant relative to C availability, excess N is released by soil microorganisms and can be lost as N₂O. In Rt, where N availability was low, N was immobilized by soil microorganisms and N₂O emission were low. When more easily degradable N was added with maize shoots, N released from decomposition of maize shoots presumably fostered decomposition of maize roots (Robertson and Groffman, 2015) and denitrification of excess N, leading to strongly increased CO₂ and N₂O emissions in RS. To estimate the contribution of plant litter N to mineralization, immobilization, and denitrification, ¹⁵N-labeled litter together with analysis of microbial biomass N and ¹⁵N₂O emissions could be used (e.g., Frimpong and Baggs, 2010; Ladd et al., 1981).

The interdependency of C and N availability was further validated by analyses of regression, highlighting a strong positive interaction between soil NO₃[−] and WEOC concentrations resulting in much higher N₂O emissions only when both NO₃[−] and WEOC were available. This further supports our findings that high bioavailability of maize shoot litter increased microbial respiration by heterotrophic microorganisms, resulting in plant-litter-associated hot spots with high N₂O formation.

Variation in N₂O emissions is often related to quality parameters of plant residues, mostly the C : N ratio (Baggs et al., 2000; Chen et al., 2013; Millar and Baggs, 2004; Novoa and Tejeda, 2006). Especially easily degradable fractions, such as water-soluble C (Burford and Bremner, 1975) or the holocellulose fraction (hemicelluloses + cellulose) (Jensen et al., 2005), explained a large share of variability of C mineralization and N₂O emissions, while lignin content was not relevant (Redin et al., 2014; Silver and Miya, 2001). Comparing 28 laboratory and field studies, Chen et al. (2013) reported that microbial-growth-induced microsite anaerobicity could be the major driver for the dynamic change in soil N₂O emissions following residue amendment, and Kravchenko et al. (2017) showed that water absorption by plant residues further enhances formation of plant-litter-associated anaerobic hot spots. In the initial phase of decomposition, water-soluble compounds (sugars, amino acids) are leached from litter, providing easily degradable compounds for microbial metabolism. After litter addition, CO₂ fluxes increased immediately due to increased respiration, rapidly reducing *p*O₂, and creating anaerobic microsites. We anticipate that formation of such hot spots was further enhanced by the amount of litter addition, as litter input was higher in RS than in Rt, and higher compared to other studies (Chen et al., 2013).

In addition to soil mineral N concentration and plant litter, soil type and soil moisture may have influenced our results (e.g., Aulakh et al., 1991). Increasing soil moisture leads to increasing N₂O emissions, but relative contribution of nitrification and denitrification to N₂O formation may change with increasing soil moisture (Bateman and Baggs, 2005; Baral et al., 2016; Li et al., 2016). Therefore, future experiments with

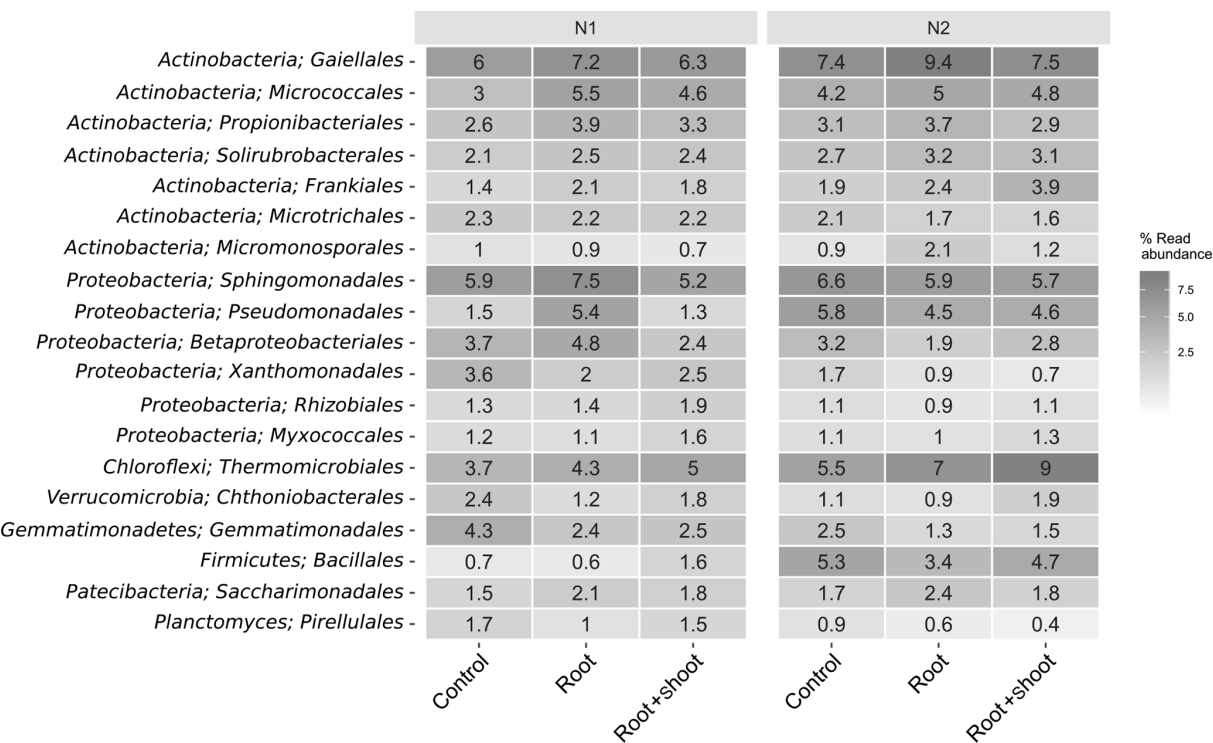


Figure 7. Heat map of the 16 most abundant bacterial orders of the soil-inhabiting bacterial community grouped by N levels and litter input ($n = 4$, except for N2 root: $n = 3$).

different soil moisture contents should include methods to differentiate between N₂O formation pathways.

4.3 Bacterial community response to maize litter input and soil N level

After litter addition, the bacterial community adapts within a few days to substrate availability (Pascualt et al., 2013). The canonical correspondence analysis (CCA) showed a clear correlation of the soil-inhabiting bacterial community, litter input, and total CO₂ and N₂O emissions. As shown by the CCA, the bacterial community structure in N1-RS and N2-RS was distinct from that in the control samples and soil with addition of root residues. Combined addition of root and shoot litter affected the soil bacterial community, leading to a less diverse and more specialized community structure, which was also shown by the alpha diversity indices (see Table S1). A significant reduction of soil bacterial diversity was induced by different N levels, as previously shown by Zeng et al. (2016). In addition, Rousk and Bååth (2007) observed a negative correlation between mineral N addition and bacterial growth, while the addition of barley straw and alfalfa correlated positively. The phylogenetic diversity (PD) supports these findings by showing a more complex picture. While PD in N1 samples increased with increasing C input, it decreased in N2 samples with increasing C input, indicating a shift of the influencing factors from the C input to the N

level. Accordingly, the increase in N₂O emissions from N2 compared to N1 was smaller in RS where C availability was the highest, indicating that N was limited here.

The most abundant phyla in our soil samples were the *Actinobacteria*, *Proteobacteria*, and *Chloroflexi*. Among these phyla, the genera *Pseudomonas* (*Proteobacteria*) and *Gaiella* (*Actinobacteria*) were also affiliated with the core microbiomes. *Thermomicrobiales* (*Chloroflexi*) showed the highest abundance in N2 samples, indicating their involvement in N cycling. *Pseudomonas* species such as *Pseudomonas aeruginosa*, *P. stutzeri*, and *P. denitrificans* are known to reduce NO₃⁻ and to contribute to N₂O and N₂ emissions (Carlson and Ingraham, 1983). *Gaiella occulta*, belonging to *Actinobacteria*, is also known for the reduction of NO₃⁻ to NO₂⁻ (Albuquerque et al., 2011). The genus *Thermomicrobiales* comprises species which can grow on nitrate, ammonia, and alanine as sole nitrogen sources and are able to hydrolyze cellulose or starch (Houghton et al., 2015). Relative abundance of *Thermomicrobiales* increased with N and C input, indicating favorable growth conditions for this genus (Fig. 7).

We further identified several genera involved in C cycling including members of *Agromyces*, *Bacillus*, and *Micromonospora*, which were also affiliated with the core microbiome. *Agromyces ulmi* was present in low abundance in our samples and it is known to contribute to C cycling in soils through xylanolytic activity (Rivas et al., 2004). Members of the genus *Bacillus* (*Firmicutes*) have been reported to play

a crucial role in carbon cycling in a wide range of environments by functions such as plant growth promotion or production of amylases and cellulases (Lyngwi and Joshi, 2014). Among the genus *Bacillus*, we found one species, *Bacillus* sp. KSM-N252, in relatively high abundance (1 %–2 %) in N2 samples. This species encodes an alkaline endoglucanase, which can hydrolyze cellulose (Endo et al., 2001). Similarly, *Micromonospora* (*Actinobacteria*) are known to produce hydrolytic enzymes showing cellulolytic and xylanolytic activity (Carro et al., 2018; de Menezes et al., 2012). Abundance of *Bacillus* sp. KSM-N252 (N2-Cn 2 %, N2-Rt 1.1 %, and N2-RS 0.8 %) and *Micromonospora* (N2-R 1.9 %, N2-RS 1 %) decreased with increasing input of water-extractable C, indicating that cellulose was only decomposed when no easily degradable C was available.

Culture-independent sequence techniques have revealed that members of the phyla *Actinobacteria*, *Chloroflexi*, *Firmicutes*, *Bacteroidetes*, and *Nitrospirae* possess *nirK* or *nirS* and can reduce nitrite to nitric oxide (Cantera and Stein, 2007; Nolan et al., 2009). In our treatments, *Actinobacteria*, *Chloroflexi*, and *Firmicutes* were more abundant in N2 samples, whereas *Bacteroidetes* and *Nitrospirae* were more abundant in N1 samples, which may indicate that the latter are more competitive under conditions of very low mineral nitrogen availability in soil. This was further validated as *Nitrospira* (*Nitrospirae*), known to oxidize nitrite (Koch et al., 2015), was identified as a responder for N1 and RS. The reduction of nitrate has been shown for *Mesorhizobium* sp. (Okada et al., 2005) and *Rhizobium* sp. (Daniel et al., 1982). Although only in low abundance, we found these species predominantly in N2 samples. Species belonging to the genus *Agromyces* (*Actinobacteria*), which was affiliated with the core microbiomes, are also known to reduce nitrate (Zgurskaya et al., 2008). In addition, species capable of denitrification under anaerobic, O₂-limited, and aerobic conditions can be found in the genera *Bacillus* and *Micromonospora*, as well as *Pseudomonas* and *Rhodococcus* (Verbaendert et al., 2011) that were affiliated with the core microbiome but were more abundant in N2 samples. The genus *Opitutus* was identified as a responder to Cn and comprises the bacterium *Opitutus terrae* that was only found in anoxic habitats in soils (Chin et al., 2001).

Altogether, the higher relative abundances of C-cycling and N-reducing bacteria in N2 samples and their affiliation with the core microbiomes reflect the tendency of increased N₂O emissions with increasing N level and further supports our hypothesis that C and N availability from plant litter were the main drivers of N₂O emissions in our study.

5 Conclusions

We examined CO₂ and N₂O emissions after simulated post-harvest incorporation of maize root or root-plus-shoot litter in a laboratory incubation study. High bioavailability

of maize shoot litter strongly increased microbial respiration in plant-litter-associated hot spots, leading to increased N₂O emissions when both C and NO₃[−] were available. Coupled nitrification–denitrification and heterotrophic nitrification presumably contributed to N₂O formation. Maize root litter was characterized by a higher share of slowly degradable C compounds and lower concentrations of water-soluble N; hence formation of anaerobic hot spots was limited and microbial N immobilization restricted N₂O emissions. Bacterial community structures reflected degradability of maize litter types. Its diversity decreased with increasing C and N availability, favoring fast-growing C-cycling and N-reducing bacteria, namely *Actinobacteria*, *Chloroflexi*, *Firmicutes*, and *Proteobacteria*.

Hence, litter quality is a major driver of N₂O and CO₂ emissions from crop residues, especially when soil mineral N is limited.

Data availability. The 16S rRNA gene sequences were deposited in the National Centre for Biotechnology Information (NCBI) Sequence Read Archive (SRA) under bioproject number PRJNA557843. Data from measurements are available upon request from the corresponding author.

Supplement. The supplement related to this article is available online at: <https://doi.org/10.5194/bg-17-1181-2020-supplement>.

Author contributions. PSR, RW, and KD designed the experiments and PSR carried them out. BP and DS carried out microbial analyses and sequence processing and provided figures. JP, RW, and KD contributed to interpretation of results. PSR prepared the manuscript with contributions from all co-authors.

Competing interests. The authors declare that they have no conflict of interest.

Acknowledgements. The authors thank Jakob Streuber, Simone Urstadt, and Finn Malinowski for gas sampling and laboratory analyses, as well as Alexander Silbersdorff (ZfS Statistical Consulting) and Oliver Caré for advice on data handling and statistical analysis.

Financial support. This research has been supported by the Deutsche Forschungsgemeinschaft through the research unit DFG-FOR 2337: Denitrification in Agricultural Soils: Integrated Control and Modelling at Various Scales (DASIM).

This open-access publication was funded by the University of Göttingen.

Review statement. This paper was edited by Michael Bahn and reviewed by two anonymous referees.

References

- Albuquerque, L., França, L., Rainey, F. A., Schumann, P., Nobre, M. F., and Da Costa, M. S.: *Gaiella occulta* gen. nov., sp. nov., a novel representative of a deep branching phylogenetic lineage within the class *Actinobacteria* and proposal of *Gaiellaceae* fam. nov. and *Gaiellales* ord. nov., *Syst. Appl. Microbiol.*, 34, 595–599, <https://doi.org/10.1016/j.syapm.2011.07.001>, 2011.
- Andersen, K. S., Kirkegaard, R. H., Karst, S. M., and Albertsen, M.: ampvis2: an R package to analyse and visualise 16S rRNA amplicon data, *bioRxiv* 299537, <https://doi.org/10.1101/299537>, 2018.
- Anderson, I. C., Poth, M., Homstead, J., and Burdige, D.: A comparison of NO and N₂O production by the autotrophic nitrifier *Nitrosomonas europaea* and the heterotrophic nitrifier *Alcaligenes faecalis*, *Appl. Environ. Microbiol.*, 59, 3525–3533, 1993.
- Aulakh, M. S., Doran, J. W., Walters, D. T., and Power, J. F.: Legume residue and soil water effects on denitrification in soils of different textures, *Soil. Biol. Biochem.*, 23, 1161–1167, [https://doi.org/10.1016/0038-0717\(91\)90029-J](https://doi.org/10.1016/0038-0717(91)90029-J), 1991.
- Aulakh, M. S., Khera, T. S., Doran, J. W., and Bronson, K. F.: Denitrification, N₂O and CO₂ fluxes in rice-wheat cropping system as affected by crop residues, fertilizer N and legume green manure, *Biol. Fert. Soils*, 34, 375–389, <https://doi.org/10.1007/s003740100420>, 2001.
- Azam, F., Müller, C., Weiske, A., Benckiser, G., and Ottow, J. C. G.: Nitrification and denitrification as sources of atmospheric nitrous oxide – Role of oxidizable carbon and applied nitrogen, *Biol. Fert. Soils*, 35, 54–61, <https://doi.org/10.1007/s00374-001-0441-5>, 2002.
- Baggs, E. M.: A review of stable isotope techniques for N₂O source partitioning in soils: Recent progress, remaining challenges and future considerations, *Rapid Commun. Mass Sp.*, 22, 1664–1672, <https://doi.org/10.1002/rcm.3456>, 2008.
- Baggs, E. M., Rees, R. M., Smith, K. A., and Vinten, A. J. A.: Nitrous oxide emission from soils after incorporating crop residues, *Soil Use Manage.*, 16, 82–87, <https://doi.org/10.1111/j.1475-2743.2000.tb00179.x>, 2000.
- Baral, K. R., Arthur, E., Olesen, J. E., and Petersen, S. P.: Predicting nitrous oxide emissions from manure properties and soil moisture: An incubation experiment, *Soil. Biol. Biochem.*, 97, 112–120, <https://doi.org/10.1016/j.soilbio.2016.03.005>, 2016.
- Barton, K.: MuMIn: Multi-Model Inference, R package version 1.43.6, available at: <https://cran.r-project.org/package=MuMIn>, 2018.
- Bateman, E. J. and Baggs, E. M.: Contributions of nitrification and denitrification to N₂O emissions from soils at different water-filled pore space, *Biol. Fert. Soils*, 41, 379–388, <https://doi.org/10.1007/s00374-005-0858-3>, 2005.
- Bending, G. D. and Turner, M. K.: Interaction of biochemical quality and particle size of crop residues and its effect on the microbial biomass and nitrogen dynamics following incorporation into soil, *Biol. Fert. Soils*, 29, 319–327, <https://doi.org/10.1007/s003740050559>, 1999.
- Birouste, M., Kazakou, E., Blanchard, A., and Roumet, C.: Plant traits and decomposition: Are the relationships for roots comparable to those for leaves?, *Ann. Bot.*, 109, 463–472, <https://doi.org/10.1093/aob/mcr297>, 2012.
- Burford, J. R. and Bremner, J. M.: Relationships between the denitrification capacities of soils and total, water-soluble and readily decomposable soil organic matter, *Soil Biol. Biochem.*, 7, 389–394, [https://doi.org/10.1016/0038-0717\(75\)90055-3](https://doi.org/10.1016/0038-0717(75)90055-3), 1975.
- Butterbach-Bahl, K., Baggs, E. M., Dannenmann, M., Kiese, R., and Zechmeister-Boltenstern, S.: Nitrous oxide emissions from soils?: how well do we understand the processes and their controls?, *Philos. T. R. Soc. B*, 368, 1–13, <https://doi.org/10.1098/rstb.2013.0122>, 2013.
- Cantera, J. J. L. and Stein, L. Y.: Molecular diversity of nitrite reductase genes (nirK) in nitrifying bacteria, *Environ. Microbiol.*, 9, 765–776, <https://doi.org/10.1111/j.1462-2920.2006.01198.x>, 2007.
- Carlson, C. A. and Ingraham, J. L.: Comparison of denitrification by *Pseudomonas stutzeri*, *Pseudomonas aeruginosa*, and *Paracoccus denitrificans*, *Appl. Environ. Microbiol.*, 45, 1247–1253, 1983.
- Carro, L., Nouioui, I., Sangal, V., Meier-Kolthoff, J. P., Trujillo, M. E., Montero-Calasanz, M. D. C., Sahin, N., Smith, D. L., Kim, K. E., Peluso, P., Deshpande, S., Woyke, T., Shapiro, N., Kyrpides, N. C., Klenk, H. P., Göker, M., and Goodfellow, M.: Genome-based classification of micromonosporae with a focus on their biotechnological and ecological potential, *Sci. Rep.*, 8, 1–23, <https://doi.org/10.1038/s41598-017-17392-0>, 2018.
- Chantigny, M. H., Angers, D. A., Kaiser, K., and Kalbitz, K.: Extraction and Characterization of Dissolved Organic Matter, in: *Soil Sampling and Methods of Analysis*, 2nd Edn., edited by: Carter, M. R. and Gregorich, E. G., Taylor & Francis Group, International Standard Book Number-13: 978-0-8493-3586-0 (Hardcover), 2007.
- Chen, H., Li, X., Hu, F., and Shi, W.: Soil nitrous oxide emissions following crop residue addition: a meta-analysis, *Glob. Change Biol.*, 19, 2956–2964, <https://doi.org/10.1111/gcb.12274>, 2013.
- Chen, S., Zhou, Y., Chen, Y., and Gu, J.: Fastp: An ultra-fast all-in-one FASTQ preprocessor, *Bioinformatics*, 34, i884–i890, <https://doi.org/10.1093/bioinformatics/bty560>, 2018.
- Chin, K.-J., Liesack, W., and Janssen, P. H.: *Opitutus terrae* gen. nov., sp. nov., to accommodate novel strains of the division “*Verucomicrobia*” isolated from rice paddy soil, *Int. J. Syst. Evol. Microbiol.*, 51, 1965–1968, <https://doi.org/10.1099/00207713-51-6-1965>, 2001.
- Ciais, P., Sabine, C., Bala, G., Bopp, L., Brovkin, V., Canadell, J., Chhabra, A., DeFries, R., Galloway, J., Heimann, M., Jones, C., Le Quéré, C., Myneni, R. B., Piao, S., and Thornton, P.: Carbon and Other Biogeochemical Cycles, in *Climate Change 2013: The Physical Science Basis. Contribution of Working Group I to the Fifth Assessment Report of the Intergovernmental Panel on Climate Change*, 465–570, 2013.
- Daniel, R. M., Limmer, A. W., Stelle, K. W., and Smith, I. M.: Anaerobic Growth, Nitrate Reduction and Denitrification in 46 Rhizobium Strains, *J. Gen. Microbiol.* 128, 1811–1815, <https://doi.org/10.1099/00221287-128-8-1811>, 1982.
- de Menezes, A. B., McDonald, J. E., Allison, H. E., and McCarthy, A. J.: Importance of *Micromonospora* spp. as colonizers of cellulose in freshwater lakes as demonstrated by quantitative reverse

- transcriptase PCR of 16s rRNA, *Appl. Environ. Microbiol.*, 78, 3495–3499, <https://doi.org/10.1128/AEM.07314-11>, 2012.
- Endo, K., Hakamada, Y., Takizawa, S., Kubota, H., Sumitomo, N., Kobayashi, T., and Ito, S.: A novel alkaline endoglucanase from an alkaliphilic *Bacillus* isolate: Enzymatic properties, and nucleotide and deduced amino acid sequences, *Appl. Microbiol. Biotechnol.*, 57, 109–116, <https://doi.org/10.1007/s002530100744>, 2001.
- Fiedler, S. R., Augustin, J., Wrage-Mönnig, N., Jurasinski, G., Gusovius, B., and Glatzel, S.: Potential short-term losses of N₂O and N₂ from high concentrations of biogas digestate in arable soils, *SOIL*, 3, 161–176, <https://doi.org/10.5194/soil-3-161-2017>, 2017.
- Fierer, N., Bradford, M. A., and Jackson, R. B.: Toward an Ecological Classification of Soil Bacteria, *Ecology*, 88, 1354–1364, <https://doi.org/10.1890/05-1839>, 2016.
- Frimpong, K. A. and Baggs, E. M.: Do combined applications of crop residues and inorganic fertilizer lower emission of N₂O from soil?, *Soil Use Manage.*, 26, 412–424, <https://doi.org/10.1111/j.1475-2743.2010.00293.x>, 2010.
- Gamble, T. N., Betlach, M. R., and Tiedje, J. M.: Numerically dominant denitrifying bacteria from world soils, *Appl. Environ. Microbiol.*, 33, 926–939, 1977.
- Garnier, S.: viridisLite: Default Color Maps from “matplotlib” (Lite Version), R package version 0.3.0, available at: <https://cran.r-project.org/package=viridisLite>, 2018.
- Goering, H. K. and Van Soest, P. J.: Forage fiber analyses, *Agric. Handb. No. 379*, 12–20, 1970.
- Griffiths, R. I., Whiteley, A. S., O'Donnell, A. G., and Bailey, M. J.: Rapid Method for Coextraction of DNA and RNA from Natural Environments for Analysis of Ribosomal DNA- and rRNA-Based Microbial Community Composition, *Appl. Environ. Microbiol.* 66, 1–5, <https://doi.org/10.1128/AEM.66.12.5488-5491.2000>, 2000.
- Hayatsu, M., Tago, K., and Saito, M.: Various players in the nitrogen cycle: Diversity and functions of the microorganisms involved in nitrification and denitrification, *Soil Sci. Plant Nutr.*, 54, 33–45, <https://doi.org/10.1111/j.1747-0765.2007.00195.x>, 2008.
- Heiberger, R. M.: HH: Statistical Analysis and Data Display: Heiberger and Holland, R package version 3.1-35, available at: <https://cran.r-project.org/package=HH>, 2018.
- Höper, H.: Carbon and nitrogen mineralisation rates of fens in Germany used for agriculture, in: *Wetlands in Central Europe*, edited by: Broll, G., Mehrbach, W., and Pfeiffer, E.-M., Springer, Berlin, Heidelberg, 149–164, 2002.
- Houghton, K. M., Morgan, X. C., Lagutin, K., Mackenzie, A. D., Vyssotskii, M., Mitchell, K. A., McDonald, I. R., Morgan, H. W., Power, J. F., Moreau, J. W., Hanssen, E., and Stott, M. B.: *Thermorudis pharmacophila* sp. Nov., a novel member of the class *Thermomicrobia* isolated from geothermal soil, and emended descriptions of *Thermomicrobium roseum*, *Thermomicrobium carboxidum*, *Thermorudis peleae* and *Sphaerobacter thermophilus*, *Int. J. Syst. Evol. Microbiol.*, 65, 4479–4487, <https://doi.org/10.1099/ijsem.0.000598>, 2015.
- Hu, X., Liu, L., Zhu, B., Du, E., Hu, X., Li, P., Zhou, Z., Ji, C., Zhu, J., Shen, H., and Fang, J.: Asynchronous responses of soil carbon dioxide, nitrous oxide emissions and net nitrogen mineralization to enhanced fine root input, *Soil Biol. Biochem.*, 92, 67–78, <https://doi.org/10.1016/j.soilbio.2015.09.019>, 2016.
- Huang, Y., Zou, J., Zheng, X., Wang, Y., and Xu, X.: Nitrous oxide emissions as influenced by amendment of plant residues with different C : N ratios, *Soil Biol. Biochem.*, 36, 973–981, <https://doi.org/10.1016/j.soilbio.2004.02.009>, 2004.
- Hutchinson, G. and Mosier, A.: Improved soil cover method for field measurement of nitrous oxide fluxes, *Soil Sci. Soc. Am. J.*, 45, 311–316, 1981.
- Jenkinson, D. S.: Studies on the Decomposition Of Plant Material in Soil. I. Losses of Carbon from ¹⁴C labelled Ryegrass incubated with soil in the field, *J. Soil Sci.*, 16, 104–115, <https://doi.org/10.1111/j.1365-2389.1965.tb01424.x>, 1965.
- Jensen, L. S., Salo, T., Palmason, F., Breland, T. A., Henriksen, T. M., Stenberg, B., Pedersen, A., Lundström, C., and Esala, M.: Influence of biochemical quality on C and N mineralisation from a broad variety of plant materials in soil, *Plant Soil*, 273, 307–326, <https://doi.org/10.1007/s11104-004-8128-y>, 2005.
- Jin, K., Sleutel, S., De Neve, S., Gabriels, D., Cai, D., Jin, J., and Hofman, G.: Nitrogen and carbon mineralization of surface-applied and incorporated winter wheat and peanut residues, *Biol. Fert. Soils*, 44, 661–665, <https://doi.org/10.1007/s00374-008-0267-5>, 2008.
- Johnson, J. M.-F., Barbour, N. W., and Weyers, S. L.: Chemical Composition of Crop Biomass Impacts Its Decomposition, *Soil Sci. Soc. Am. J.*, 71, 155–162, <https://doi.org/10.2136/sssaj2005.0419>, 2007.
- Klindworth, A., Pruesse, E., Schweer, T., Peplies, J., Quast, C., Horn, M., and Glöckner, F. O.: Evaluation of general 16S ribosomal RNA gene PCR primers for classical and next-generation sequencing-based diversity studies, *Nucleic Acids Res.*, 41, 1–11, <https://doi.org/10.1093/nar/gks808>, 2013.
- Koch, H., Lückner, S., Albertsen, M., Kitzinger, K., Herbold, C., Spieck, E., Nielsen, P. H., Wagner, M., and Daims, H.: Expanded metabolic versatility of ubiquitous nitrite-oxidizing bacteria from the genus *Nitrospira*, *PNAS*, 112, 11371–11376, <https://doi.org/10.1073/pnas.1506533112>, 2015.
- Kögel-Knabner, I.: The macromolecular organic composition of plant and microbial residues as inputs to soil organic matter, *Soil Biol. Biochem.*, 34, 139–162, [https://doi.org/10.1016/S0038-0717\(01\)00158-4](https://doi.org/10.1016/S0038-0717(01)00158-4), 2002.
- Kravchenko, A. N., Toosi, E. R., Guber, A. K., Ostrom, N. E., Yu, J., Azeem, K., Rivers, M. L., and Robertson, G. P.: Hotspots of soil N₂O emission enhanced through water absorption by plant residue, *Nat. Geosci.*, 10, 496–500, <https://doi.org/10.1038/NGEO2963>, 2017.
- Kravchenko, A. N., Fry, J. E., and Guber, A. K.: Water absorption capacity of soil-incorporated plant leaves can affect N₂O emissions and soil inorganic N concentrations, *Soil Biol. Biochem.*, 121, 113–119, <https://doi.org/10.1016/j.soilbio.2018.03.013>, 2018.
- Kuzyakov, Y. and Domanski, G.: Carbon input by plants into the soil. Review, *J. Plant Nutr. Soil Sci.*, 163, 421–431, [https://doi.org/10.1002/1522-2624\(200008\)163:4<421::AID-JPLN421>3.0.CO;2-R](https://doi.org/10.1002/1522-2624(200008)163:4<421::AID-JPLN421>3.0.CO;2-R), 2000.
- Ladd, J. N., Oades, J. M., and Amato, M.: Microbial biomass formed from ¹⁴C, ¹⁵N-labelled plant material decomposing in soils in the field, *Soil Biol. Biochem.*, 13, 119–162, [https://doi.org/10.1016/0038-0717\(81\)90007-9](https://doi.org/10.1016/0038-0717(81)90007-9), 1981.

- Legendre, P. and Gallagher, E. D.: Ecologically meaningful transformations for ordination of species data, *Oecologia*, 129, 271–280, <https://doi.org/10.1007/s004420100716>, 2001.
- Lemon, J.: Plotrix: a package in the red light district of R, *R-News*, 6, 8–12, 2006.
- Lenth, R.: Emmeans: Estimated Marginal Means, aka Least-Squares Means. R package version 1.3.4, available at: <https://cran.r-project.org/package=emmeans>, 2018.
- Li, X., Hu, F., and Shi, W.: Plant material addition affects soil nitrous oxide production differently between aerobic and oxygen-limited conditions, *Appl. Soil Ecol.*, 64, 91–98, <https://doi.org/10.1016/j.apsoil.2012.10.003>, 2013.
- Li, X., Sørensen, P., Olesen, J. E., and Petersen, S. O.: Evidence for denitrification as main source of N₂O emission from residue-amended soil, *Soil Biol. Biochem.*, 92, 153–160, <https://doi.org/10.1016/j.soilbio.2015.10.008>, 2016.
- Loecke, T. D. and Robertson, G. P.: Soil resource heterogeneity in terms of litter aggregation promotes nitrous oxide fluxes and slows decomposition, *Soil Biol. Biochem.*, 41, 228–235, <https://doi.org/10.1016/j.soilbio.2008.10.017>, 2009.
- Lou, Y., Ren, L., Li, Z., Zhang, T., and Inubushi, K.: Effect of Rice Residues on Carbon Dioxide and Nitrous Oxide Emissions from a Paddy Soil of Subtropical China, *Water, Air, Soil Pollut.*, 178, 157–168, <https://doi.org/10.1007/s11270-006-9187-x>, 2007.
- Ludovici, K. H. and Kress, L. W.: Decomposition and nutrient release from fresh and dried pine roots under two fertilizer regimes, *Can. J. Forest Res.*, 36, 105–111, <https://doi.org/10.1139/X05-227>, 2006.
- Lyngwi, N. A. and Joshi, S.: Economically important *Bacillus* and related genera: a mini review, in: *Biology of Useful Plants and Microbes*, edited by: Sen, A., Narosa Publishing House, New Delhi, India, 33–43, 2014.
- Machinet, G. E., Bertrand, I., Chabbert, B., and Recous, S.: Decomposition in soil and chemical changes of maize roots with genetic variations affecting cell wall quality, *Eur. J. Soil Sci.*, 60, 176–185, <https://doi.org/10.1111/j.1365-2389.2008.01109.x>, 2009.
- Machinet, G. E., Bertrand, I., Barrière, Y., Chabbert, B., and Recous, S.: Impact of plant cell wall network on biodegradation in soil: Role of lignin composition and phenolic acids in roots from 16 maize genotypes, *Soil Biol. Biochem.*, 43, 1544–1552, <https://doi.org/10.1016/j.soilbio.2011.04.002>, 2011.
- Martin, M.: Cutadapt removes adapter sequences from high-throughput sequencing reads, *EMBnet J.*, 17, 10–12, <https://doi.org/10.14806/ej.17.1.200>, 2013.
- Mary, B., Fresneau, C., Morel, J. L., and Mariotti, A.: C and N cycling during decomposition of root mucilage, roots and glucose in soil, *Soil Biol. Biochem.*, 25, 1005–1014, [https://doi.org/10.1016/0038-0717\(93\)90147-4](https://doi.org/10.1016/0038-0717(93)90147-4), 1993.
- Megonigal, J. P., Hines, M. E., and Visscher, P. T.: Anaerobic Metabolism: Linkages to Trace Gases and Aerobic Processes, in: *Treatise on Geochemistry*, Vol. 10, 2nd Edn., edited by: Turekian, K. and Holland, H., Volume Editors: Karl, D. M. and Schlesinger, W. H., <https://www.sciencedirect.com/referencework/9780080983004/treatise-on-geochemistry>, 10, 273–359, 2013.
- Millar, N. and Baggs, E. M.: Chemical composition, or quality, of agroforestry residues influences N₂O emissions after their addition to soil, *Soil Biol. Biochem.*, 36, 935–943, <https://doi.org/10.1016/j.soilbio.2004.02.008>, 2004.
- Millar, N. and Baggs, E. M.: Relationships between N₂O emissions and water-soluble C and N contents of agroforestry residues after their addition to soil, *Soil Biol. Biochem.*, 37, 605–608, <https://doi.org/10.1016/j.soilbio.2004.08.016>, 2005.
- Miller, M. N., Zebbarth, B. J., Dandie, C. E., Burton, D. L., Goyer, C., and Trevors, J. T.: Crop residue influence on denitrification, N₂O emissions and denitrifier community abundance in soil, *Soil Biol. Biochem.*, 40, 2553–2562, <https://doi.org/10.1016/j.soilbio.2008.06.024>, 2008.
- Müller, C. and Clough, T. J.: Advances in understanding nitrogen flows and transformations: Gaps and research pathways, *J. Agr. Sci.*, 152, S34–S44, <https://doi.org/10.1017/S0021859613000610>, 2014.
- Nolan, M., Tindall, B. J., Pomrenke, H., Lapidus, A., Copeland, A., Del Rio, T. G., Lucas, S., Chen, F., Tice, H., Chen, J.-F., Saunders, E., Han, C., Bruce, D., Goodwin, L., Chain, P., Pitluck, S., Ovchinnikova, G., Pati, A., Ivanova, N., Mavromatis, K., Chen, A., Palaniappan, K., Land, M., Hauser, L., Chang, Y.-J., Jeffries, C. D., Brettin, T., Göker, M., Bristow, J., Eisen, J. A., Markowitz, V., Hugenholtz, P., Kyrpides, N. C., Klenk, H.-P., and Detter, J. C.: Complete genome sequence of *Rhodothermus marinus*, *Stand. Genomic Sci.*, 1, 283–291, 2009.
- Novoa, R. S. A. and Tejada, H. R.: Evaluation of the N₂O emissions from N in plant residues as affected by environmental and management factors, *Nutr. Cycl. Agroecosys.*, 75, 29–46, <https://doi.org/10.1007/s10705-006-9009-y>, 2006.
- Okada, N., Nomura, N., Nakajima-Kambe, T., and Uchiyama, H.: Characterization of the Aerobic Denitrification in *Mesorhizobium* sp. Strain NH-14 in Comparison with that in Related Rhizobia, *Microbes Environ.*, 20, 208–215, <https://doi.org/10.1264/jsme2.20.208>, 2005.
- Oksanen, J., Blanchet, F. G., Friendly, M., Kindt, R., Legendre, P., McGlinn, D., Minchin, P. R., O'Hara, R. B., Simpson, G. L., Solymos, P., Henry, M., Stevens, H., Szöcs, E., and Wagner, H.: *vegan: Community Ecology Package*, R Package version 2.3-2, available at: <https://cran.r-project.org/web/packages/vegan/index.html>, 2015.
- Papen, H., von Berg, R., Hinkel, I., Thoene, B., and Rennenberg, H.: Heterotrophic Nitrification by *Alcaligenes faecalis*: NO₂⁻, NO₃⁻, N₂O, and NO Production in Exponentially Growing Cultures, *Appl. Environ. Microbiol.*, 55, 2068–2072, 1989.
- Pascault, N., Ranjard, L., Kaisermann, A., Bachar, D., Christen, R., Terrat, S., Mathieu, O., Lévêque, J., Mougél, C., Henault, C., Lemanceau, P., Péan, M., Boiry, S., Fontaine, S., and Maron, P. A.: Stimulation of Different Functional Groups of Bacteria by Various Plant Residues as a Driver of Soil Priming Effect, *Ecosystems*, 16, 810–822, <https://doi.org/10.1007/s10021-013-9650-7>, 2013.
- Paterson, E. and Sim, A.: Rhizodeposition and C-partitioning of *Lolium perenne* in axenic culture affected by nitrogen supply and defoliation, *Plant Soil*, 216, 155–164, <https://doi.org/10.1023/A:1004789407065>, 1999.
- Pinheiro, J., Bates, D., DebRoy, S., Sarkar, D., and R Core Team: *nlme: Linear and Nonlinear Mixed Effects Models*, R package version 3.1-140, available at: <https://cran.r-project.org/package=nlme>, 2017.
- Quast, C., Priesse, E., Yilmaz, P., Gerken, J., Schweer, T., Yarza, P., Peplies, J., and Glöckner, F. O.: The SILVA ribosomal RNA gene database project: Improved data process-

- ing and web-based tools, *Nucleic Acid. Res.*, 41, 590–596, <https://doi.org/10.1093/nar/gks1219>, 2013.
- R Core Team: R: A Language and Environment for Statistical Computing. R Foundation for Statistical Computing, Vienna, Austria, version 3.5.2, available at: <https://www.R-project.org/>, 2018.
- R Core Team: R: A Language and Environment for Statistical Computing. R Foundation for Statistical Computing, Vienna, Austria, version 3.5.3, available at: <https://www.R-project.org/>, 2019.
- Redin, M., Guénon, R., Recous, S., Schmatz, R., de Freitas, L. L., Aita, C., and Giacomini, S. J.: Carbon mineralization in soil of roots from twenty crop species, as affected by their chemical composition and botanical family, *Plant Soil*, 378, 205–214, <https://doi.org/10.1007/s11104-013-2021-5>, 2014.
- Rivas, R., Trujillo, M. E., Mateos, P. F., Martínez-Molina, E., and Velázquez, E.: *Agromyces ulmi* sp. nov., xylanolytic bacterium isolated from *Ulmus nigra* in Spain, *Int. J. Syst. Evol. Microbiol.*, 54, 1987–1990, <https://doi.org/10.1099/ijs.0.63058-0>, 2004.
- Robertson, G. P. and Groffman, P. M.: Nitrogen Transformations, in: *Soil microbiology, ecology and biochemistry*, edited by: Paul, E. A., Academic Press, Burlington, Massachusetts, USA, 421–446, 2015.
- Rognes, T., Flouri, T., Nichols, B., Quince, C., and Mahé, F.: VSEARCH: a versatile open source tool for metagenomics, *Peer J.*, 4, e2584, <https://doi.org/10.7717/peerj.2584>, 2016.
- Rousk, J. and Bååth, E.: Fungal and bacterial growth in soil with plant materials of different C : N ratios, *FEMS Microbiol. Ecol.*, 62, 258–267, <https://doi.org/10.1111/j.1574-6941.2007.00398.x>, 2007.
- Silver, W. L. and Miya, R. K.: Global patterns in root decomposition: Comparisons of climate and litter quality effects, *Oecologia*, 129, 407–419, <https://doi.org/10.1007/s004420100740>, 2001.
- Soetaert, K.: plot3D: Plotting Multi-Dimensional Data, R package version 1.1.1, available at: <https://cran.r-project.org/package=plot3D>, 2017.
- Toju, H., Tanabe, A. S., Yamamoto, S., and Sato, H.: High-coverage ITS primers for the DNA-based identification of Ascomycetes and Basidiomycetes in environmental samples, *PLoS One*, 7, e40863, <https://doi.org/10.1371/journal.pone.0040863>, 2012.
- Truong, T. H. H. and Marschner, P.: Respiration, available N and microbial biomass N in soil amended with mixes of organic materials differing in C : N ratio and decomposition stage, *Geoderma*, 319, 167–174, <https://doi.org/10.1016/j.geoderma.2018.01.012>, 2018.
- van Groenigen, J. W., Huygens, D., Boeckx, P., Kuyper, Th. W., Lubbers, I. M., Rütting, T., and Groffman, P. M.: The soil N cycle: new insights and key challenges, *SOIL*, 1, 235–256, <https://doi.org/10.5194/soil-1-235-2015>, 2015.
- VDLUFA (Verband Deutscher Landwirtschaftlicher Untersuchungs- und Forschungsanstalten e.V.) (Ed.): 6.5.2 Bestimmung der Säure-Detergentien-Faser (ADF), in *Methodenbuch Band III Die chemische Untersuchung von Futtermitteln*, VDLUFA-Verlag, Darmstadt, 1–4, 2011.
- VDLUFA (Ed.): 6.5.1 Bestimmung der neutral-Detergentien-Faser (NDF), in *Methodenbuch Band III Die chemische Untersuchung von Futtermitteln*, VDLUFA-Verlag, Darmstadt, 1–4, 2012a.
- VDLUFA (Ed.): 6.5.3 Bestimmung des Säure-Detergentien-Lignins (“Rohlignin”), in *Methodenbuch Band III Die chemische Untersuchung von Futtermitteln*, VDLUFA-Verlag, Darmstadt, 1–3, 2012b.
- Velthof, G. L., Kuikman, P. J., and Oenema, O.: Nitrous oxide emission from soils amended with crop residues, *Nutr. Cycl. Agroecosys.*, 62, 249–261, <https://doi.org/10.1023/A:1021259107244>, 2002.
- Verbaendert, I., De Vos, P., Boon, N., and Heylen, K.: Denitrification in Gram-positive bacteria: an underexplored trait, *Biochem. Soc. T.*, 39, 254–258, <https://doi.org/10.1042/bst0390254>, 2011.
- Wang, Y., Naumann, U., Edelbuettel, E., Wilshire, J., Warton, D., Byrnes, J., dos Santos Silva, R., Niku, J., Renner, I., and Wright, S.: mvabund: Statistical Methods for Analysing Multivariate Abundance Data, R package version 4.0.1, available at: <https://cran.r-project.org/web/packages/mvabund/index.html>, 2019.
- Wrage-Mönnig, N., Horn, M. A., Well, R., Müller, C., Velthof, G., and Oenema, O.: The role of nitrifier denitrification in the production of nitrous oxide revisited, *Soil Biol. Biochem.*, 123, A3–A16, <https://doi.org/10.1016/j.soilbio.2018.03.020>, 2018.
- Wrage, N., Velthof, G. L., van Beusichem, M. L., and Oenema, O.: The role of nitrifier denitrification in the production of nitrous oxide, *Soil Biol. Biochem.*, 33, 1723–1732, [https://doi.org/10.1016/S0038-0717\(01\)00096-7](https://doi.org/10.1016/S0038-0717(01)00096-7), 2001.
- Zeng, J., Liu, X., Song, L., Lin, X., Zhang, H., Shen, C., and Chu, H.: Nitrogen fertilization directly affects soil bacterial diversity and indirectly affects bacterial community composition, *Soil Biol. Biochem.*, 92, 41–49, <https://doi.org/10.1016/j.soilbio.2015.09.018>, 2016.
- Zgurskaya, H. I., Evtushenko, L. I., Akimov, V. N., Voyevoda, H. V., Dobrovolskaya, T. G., Lysak, L. V., and Kalakoutskaia, L. V.: Emended Description of the Genus *Agromyces* and Description of *Agromyces cerinus* subsp. *cerinus* sp. nov., subsp. nov., *Agromyces cerinus* subsp. *nitratus* sp. nov., subsp. nov., *Agromyces fucosus* subsp. *fucosus* sp. nov., subsp. nov., and *Agromyces fucosus* subsp. *hippuratus* sp. nov., subsp. nov., *Int. J. Syst. Bacteriol.*, 42, 635–641, <https://doi.org/10.1099/00207713-42-4-635>, 1992.
- Zhang, D., Hui, D., Luo, Y., and Zhou, G.: Rates of litter decomposition in terrestrial ecosystems: global patterns and controlling factors, *J. Plant Ecol.*, 1, 85–93, <https://doi.org/10.1093/jpe/rtn002>, 2008.
- Zhang, J., Kobert, K., Flouri, T., and Stamatakis, A.: PEAR: A fast and accurate Illumina Paired-End reAd mergeR, *Bioinformatics*, 30, 614–620, <https://doi.org/10.1093/bioinformatics/btt593>, 2014.
- Zhang, J., Müller, C., and Cai, Z.: Heterotrophic nitrification of organic N and its contribution to nitrous oxide emissions in soils, *Soil Biol. Biochem.*, 84, 199–209, <https://doi.org/10.1016/j.soilbio.2015.02.028>, 2015.
- Zhang, X. and Wang, W.: The decomposition of fine and coarse roots: Their global patterns and controlling factors, *Sci. Rep.*, 5, 1–10, <https://doi.org/10.1038/srep09940>, 2015.
- Zumft, W.: Cell biology and molecular basis of denitrification, *Microbiol. Molecular Biol. Rev.*, 61, 533–616, 1997.



Supplement of

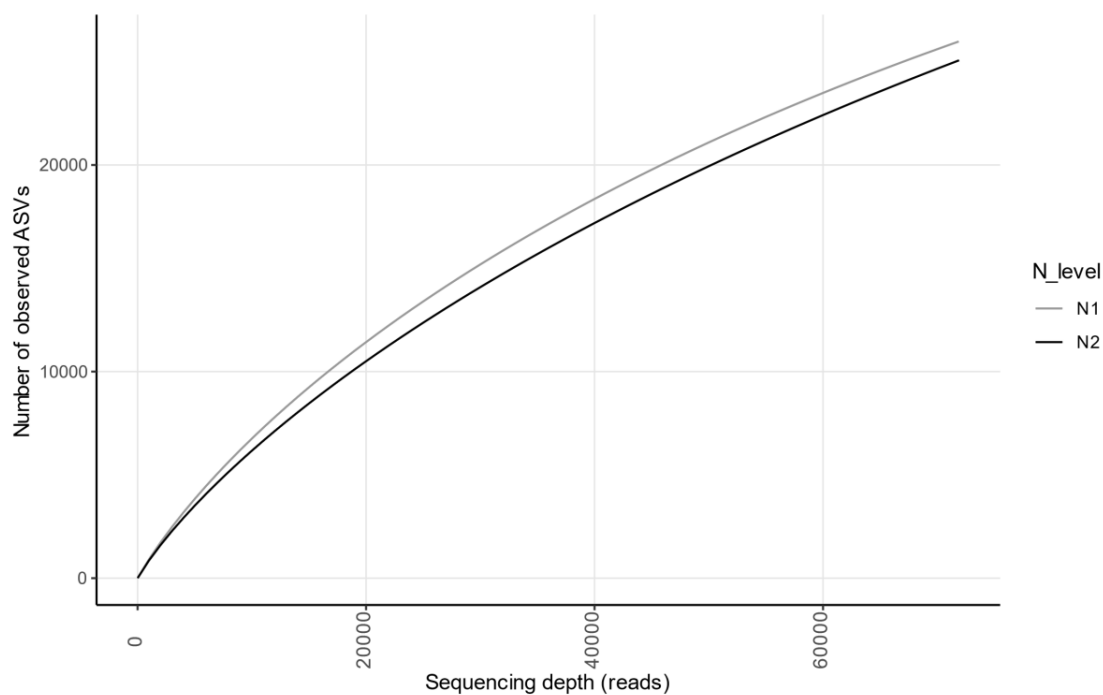
Maize root and shoot litter quality controls short-term CO₂ and N₂O emissions and bacterial community structure of arable soil

Pauline Sophie Rummel et al.

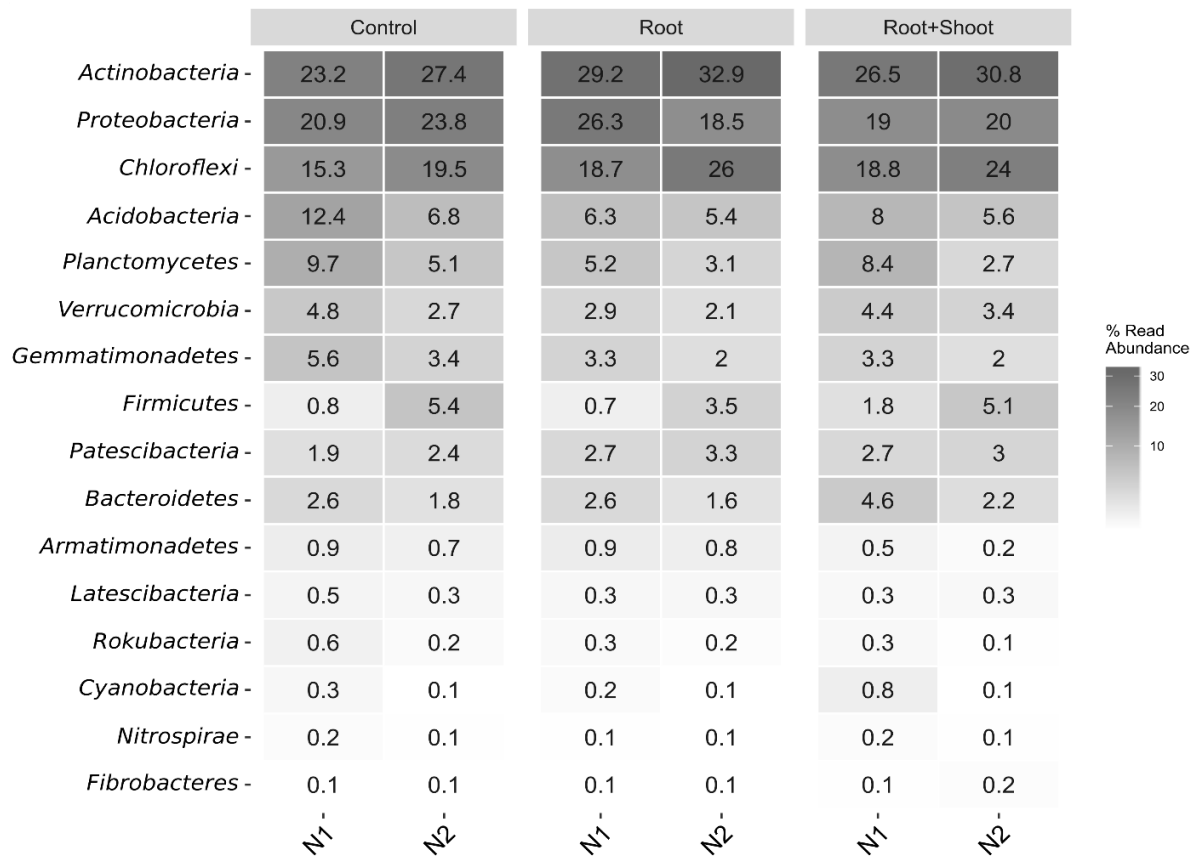
Correspondence to: Pauline Sophie Rummel (pauline.rummel@uni-goettingen.de)

The copyright of individual parts of the supplement might differ from the CC BY 4.0 License.

Supplement



5 **Figure S1: Rarefaction curve of the observed amplicon sequence variants (ASVs) of the soil inhabiting bacterial communities within the two different N-fertilizer treatments (N1 and N2). Samples of the same N treatment were aggregated and rarefied to the same number of raw reads (61206).**



10 **Figure S2: Heatmap of the 16 most abundant phyla (>0.1 %) in the analyzed soil samples grouped by N levels and litter input (n=4, except for N2 Root: n=3).**

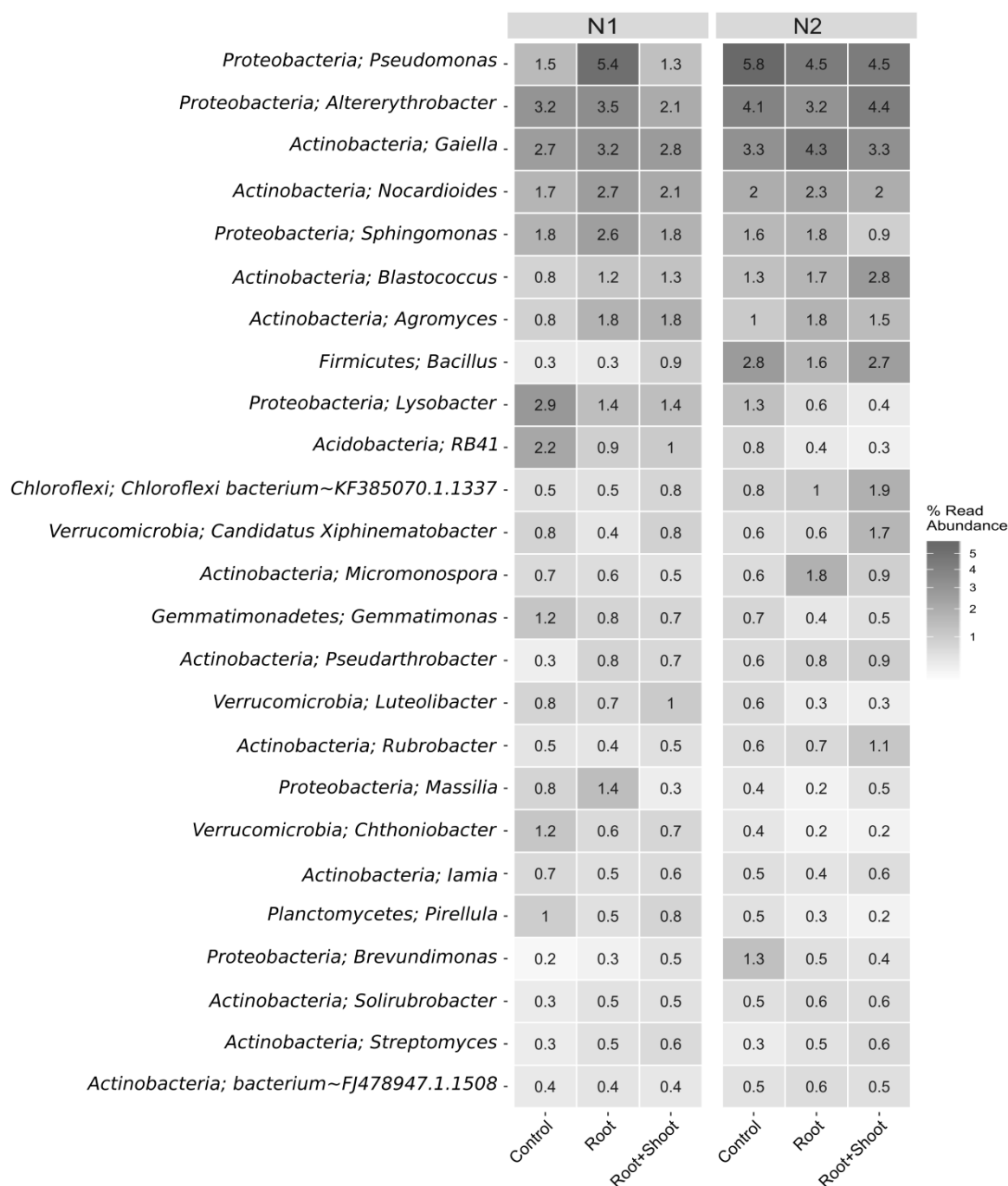


Figure S3: Heatmap of the 25 most abundant bacterial genera in the analyzed soil samples grouped by N levels and litter input (n=4, except for N2 Root: n=3).

Table S4: Sequence summary, alpha diversity indices and PD (phylogenetic diversity) for each treatment. Shown are read sums and mean values of diversity indices (ASV = amplicon sequence variant).

Sample ID	Number of Replicates	Raw Reads	Reads after Pipeline	Reads after Taxonomy filter	Subsample size	Observed ASVs	Shannon	Simpson	PD
N1_C	4	537242	443228	442610	61206	21113	9.22	0.9997	423.2
N1_R	4	590494	492088	491280	61206	21447	9.10	0.9995	431.0
N1_RS	4	557072	439132	438456	61206	21789	9.29	0.9997	436.6
N2_C	4	531926	441286	440968	61206	19142	8.79	0.9992	420.4
N2_R	3	848974	735676	735366	61206	18891	8.78	0.9991	409.2
N2_RS	4	536532	463944	463504	61206	20301	8.89	0.9990	403.3

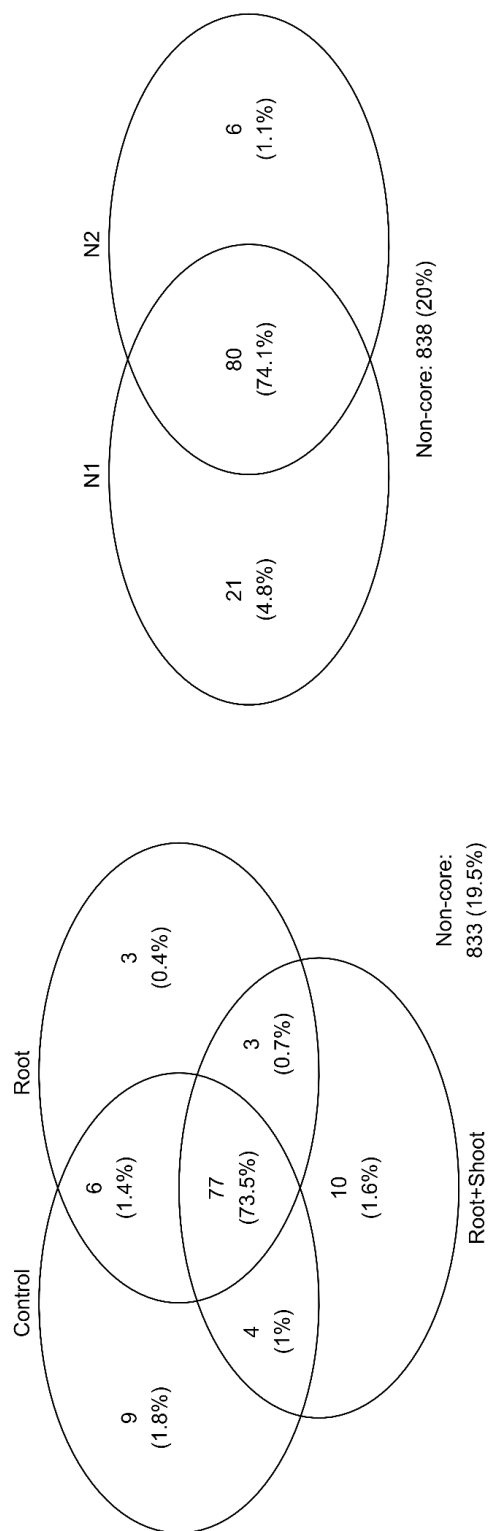


Fig. S5 a + b: Venn diagrams displaying core and non-core microbiomes of the soil inhabiting bacterial community analyzed at the end of the incubation experiment grouped by either litter input or N level (for Control and Root+Shoot n=8, for Root: n=7, for N1 n=12, for N2 n=11).

Table S6: The core microbiome of the soil inhabiting bacterial community analyzed at the end of the incubation experiment grouped by litter input (for Control and Root+Shoot n=8, for Root: n=7).

Phylum	Class	Order	Family	Genus	Relative abundance in %
<i>Acidobacteria</i>	<i>Blastocatellia</i> (Subgroup 4)	<i>Pyrinomonadales</i>	<i>Pyrinomonadaceae</i>	RB41	1.01
	<i>Holophagae</i>	Subgroup 7	uncultured bacterium		0.29
		metagenome			0.27
	<i>Subgroup 6</i>	uncultured <i>Acidobacteria</i> bacterium			2.42
		uncultured <i>Acidobacteriales</i> bacterium			0.22
<i>Actinobacteria</i>		uncultured bacterium			1.77
		<i>Actinomarinales</i>	uncultured bacterium		0.54
		IMCC26256	uncultured bacterium		0.24
	<i>Acidimicrobiia</i>	<i>Microtrichales</i>	<i>Iamiaeae</i>	<i>Iamia</i>	0.55
			<i>Ilumatobacteraceae</i>	<i>Ilumatobacter</i>	0.23
			uncultured bacterium	uncultured bacterium	0.69
			uncultured bacterium		0.23
	<i>Actinobacteria</i>	<i>Corynebacteriales</i>	<i>Mycobacteriaceae</i>	<i>Mycobacterium</i>	0.16
		<i>Frankiales</i>	<i>Geodermatophilaceae</i>	<i>Blastococcus</i>	1.54
			<i>Sporichthyaceae</i>	uncultured bacterium	0.31
		<i>Micrococcales</i>	<i>Intrasporangiaceae</i>	<i>Intrasporangium</i>	0.36
				<i>Tetrasphaera</i>	0.20
				uncultured bacterium	0.67
			<i>Microbacteriaceae</i>	<i>Agromyces</i>	1.48
			<i>Micrococcaceae</i>	<i>Pseudarthrobacter</i>	0.65
			uncultured bacterium		0.25

	<i>Micromonosporales</i>	<i>Micromonosporaceae</i>	<i>Micromonospora</i>	0.87	
		<i>Propionibacteriales</i>	<i>Aeromicrobium</i>	0.31	
			<i>Marmoricola</i>	0.35	
			<i>Nocardioides</i>	2.03	
		<i>Propionibacteriaceae</i>	uncultured bacterium	0.26	
	<i>Streptomycetales</i>	<i>Streptomycetaceae</i>	<i>Streptomyces</i>	0.56	
		uncultured bacterium		1.87	
		<i>Rubrobacteriales</i>	<i>Rubrobacteriaceae</i>	<i>Rubrobacter</i>	0.60
		<i>Gaiellales</i>	<i>Gaiellaceae</i>	<i>Gaiella</i>	3.08
		uncultured bacterium		3.67	
	<i>Solirubrobacterales</i>	67-14	uncultured bacterium	1.53	
		<i>Solirubrobacteraceae</i>	<i>Solirubrobacter</i>	0.48	
		uncultured bacterium		0.27	
		<i>Chthonomonadetes</i>	uncultured bacterium		0.66
			<i>Cytophagales</i>	<i>Microscillaceae</i>	uncultured bacterium
	<i>Caldilineales</i>		<i>Caldilineaceae</i>	uncultured bacterium	0.54
	<i>Chloroflexales</i>		<i>Herpetosiphonaceae</i>	<i>Herpetosiphon</i>	0.24
			<i>Roseiflexaceae</i>	uncultured bacterium	0.61
		<i>Chloroflexia</i>	JG30-KF-CM45	metagenome	0.30
	uncultured bacterium			2.72	
uncultured <i>Chloroflexi</i> bacterium	1.98				
<i>Dehalococcoidia</i>	S085	uncultured bacterium	0.34		
Gitt-GS-136	uncultured bacterium		3.89		
	uncultured <i>Chloroflexus</i> sp.		0.35		

	JG30-KF-CM66	uncultured bacterium		0.19
		metagenome		0.48
	KD4-96	uncultured <i>Anaerolineaceae</i> bacterium		0.55
		uncultured bacterium		3.08
		uncultured <i>Chloroflexi</i> bacterium		1.05
<i>Firmicutes</i>	<i>Ktedonobacteria</i>	C0119	uncultured bacterium	0.91
	TK10	uncultured bacterium		0.31
	<i>Bacilli</i>	<i>Bacillales</i>	<i>Bacillaceae</i>	1.38
<i>Gemmatimonadetes</i>	<i>Gemmatimonadetes</i>	<i>Gemmatimonadales</i>	<i>Gemmatimonadaceae</i>	0.71
			uncultured bacterium	1.65
	<i>Longimicrobia</i>	<i>Longimicrobiales</i>	<i>Longimicrobiaceae</i>	0.21
<i>Latescibacteria</i>	uncultured bacterium			0.20
<i>Patescibacteria</i>	<i>Saccharimonadia</i>	<i>Saccharimonadales</i>	uncultured bacterium	1.31
			uncultured soil bacterium	0.30
<i>Planctomycetes</i>	OM190	uncultured bacterium		0.35
	<i>Phycisphaerae</i>	<i>Tepidisphaerales</i>	WD2101 soil group	1.61
	<i>Planctomycetacia</i>	<i>Pirellulales</i>	<i>Pirellulaceae</i>	0.65
		<i>Caulobacteriales</i>	<i>Caulobacteraceae</i>	0.54
<i>Proteobacteria</i>	<i>Alphaproteobacteria</i>	<i>Sphingomonadales</i>	<i>Sphingomonadaceae</i>	0.61
			<i>Altererythrobacter</i>	3.75
			<i>Sphingomonas</i>	1.86
	<i>Deltaproteobacteria</i>	<i>Myxococcales</i>	<i>Haliangium</i>	0.37
		<i>Burkholderiales</i>	<i>Oxalobacteraceae</i>	0.79
	<i>Betaproteobacteria</i>		<i>Burkholderiaceae</i>	0.30
		<i>Nitrosomonadales</i>	<i>Nitrosomonadaceae</i>	MND1
				0.51

	<i>Gammaproteobacteria</i>	<i>Gammaproteobacteria</i> <i>Incertae Sedis</i>	Unknown Family	<i>Acidibacter</i>	0.18
		<i>Pseudomonadales</i>	<i>Pseudomonadaceae</i>	<i>Pseudomonas</i>	3.64
		<i>Xanthomonadales</i>	<i>Xanthomonadaceae</i>	<i>Lysobacter</i>	1.31
		<i>Chthoniobacteriales</i>	<i>Xiphinematobacteraceae</i>	<i>Candidatus</i> <i>Xiphinematobacter</i>	0.89
<i>Verrucomicrobia</i>	<i>Verrucomicrobiae</i>	<i>Pedospaerales</i>	<i>Pedospaeraceae</i>	uncultured bacterium	0.43
		<i>Verrucomicrobiales</i>	<i>Rubritaleaceae</i>	<i>Luteolibacter</i>	0.71

25 Table S7: The responders of the soil inhabiting bacterial community analyzed at the end of the incubation experiment grouped by litter input (for Control and Root+Shoot n=8, for Root: n=7).

Phylum	Class	Order	Family	Genus	Relative abundance in %
Root					
Actinobacteria	Actinobacteria	Micrococcales	Intrasporangiaceae	Lapillicoccus	0.09
	Thermoleophilia	Solirubrobacterales	67-14	Uncultured bacterium	0.13
Bacteroidetes	Bacteroidia	Cytophagales	Hymenobacteraceae	Adhaeribacter	0.17
Root+Shoot					
Actinobacteria	Actinobacteria	Streptosporangiales	Streptosporangiaceae	Nonomuraea	0.10
Bacteroidetes	Bacteroidia	Chitinophagales	Chitinophagaceae	uncultured bacterium	0.27
		Flavobacteriales	Crocinitomicaceae	Fluviicola	0.18
Chloroflexi	Anaerolineae	SBR1031	uncultured bacterium		0.13
Chloroflexi	Gitt-GS-136	uncultured Anaerolineae bacterium			0.16
Nitrospirae	Nitrospira	Nitrospirales	Nitrospiraceae	Nitrospira	0.13
Patescibacteria	Parcubacteria	Candidatus Kaiserbacteria	uncultured bacterium		0.15
		uncultured bacterium			0.22
Proteobacteria	Alphaproteobacteria	Rhizobiales	Rhizobiaceae	Allorhizobium-Neorhizobium-Pararhizobium-Rhizobium	0.21
	Gammaproteobacteria	Cellvibrionales	Cellvibrionaceae	Cellvibrio	0.10
Root & Root+Shoot					
Chloroflexi	Anaerolineae	SBR1031	A4b	uncultured bacterium	0.23
	Chloroflexia	Kallotenales	AKIW781	uncultured bacterium	0.19
Proteobacteria	Alphaproteobacteria	Sphingomonadales	Sphingomonadaceae	Sphingobium	0.31
Control & Root					

<i>Acidobacteria</i>	<i>Blastocatellia</i> (Subgroup 4)	<i>Blastocatellales</i>	<i>Blastocatellaceae</i>	<i>uncultured bacterium</i>	0.34
<i>Actinobacteria</i>	<i>Actinobacteria</i>	<i>Pseudonocardiales</i>	<i>Pseudonocardaceae</i>	<i>Pseudonocardia</i>	0.16
	<i>Thermoleophilina</i>	<i>Gaiellales</i>	uncultured <i>actinobacterium</i>		
<i>Proteobacteria</i>	<i>Alphaproteobacteria</i>	<i>Sphingomonadales</i>	<i>Sphingomonadaceae</i>	Ellin6055	0.21
				uncultured bacterium	0.22
		<i>Tistrellales</i>	<i>Geminicoccaceae</i>	<i>Candidatus Alysiosphaera</i>	0.29
Control & Root+Shoot					
<i>Gemmatimonadetes</i>	S0134 terrestrial group	uncultured bacterium			0.14
<i>Proteobacteria</i>	<i>Deltaproteobacteria</i>	NB1-j	uncultured bacterium		0.17
	<i>Gammaproteobacteria</i>	PLTA13	uncultured bacterium		0.14
<i>Verrucomicrobia</i>	<i>Verrucomicrobiae</i>	<i>Chthoniobacterales</i>	<i>Chthoniobacteraceae</i>	<i>Chthoniobacter</i>	0.56
Control					
<i>Acidobacteria</i>	<i>Thermoanaerobaculia</i>	<i>Thermoanaerobaculales</i>	<i>Thermoanaerobaculaceae</i>	Subgroup 10	0.15
<i>Chloroflexi</i>	<i>Anaerolineae</i>	<i>Caldilineales</i>	<i>Caldilineaceae</i>	<i>Litorilinea</i>	0.12
<i>Gemmatimonadetes</i>	AKAU4049	uncultured bacterium			0.23
<i>Planctomycetes</i>	<i>Planctomycetacia</i>	<i>Gemmatales</i>	<i>Gemmataceae</i>	<i>Gemmata</i>	0.20
		<i>Pirellulales</i>	<i>Pirellulaceae</i>	uncultured bacterium	0.47
<i>Proteobacteria</i>	<i>Alphaproteobacteria</i>	<i>Sphingomonadales</i>	<i>Sphingomonadaceae</i>	Pir4 lineage	0.18
		<i>Tistrellales</i>	<i>Geminicoccaceae</i>	<i>Novosphingobium</i>	0.13
<i>Verrucomicrobia</i>	<i>Verrucomicrobiae</i>			uncultured bacterium	0.15
			<i>Opitutaceae</i>	<i>Opitutus</i>	0.19

Table S8: The core microbiome and responders of the soil inhabiting bacterial community analyzed at the end of the incubation experiment grouped by soil N level (for N1 n=12, for N2 n=11).

Phylum	Class	Order	Family	Genus	Relative abundance in %
Core Microbiome					
<i>Acidobacteria</i>	<i>Blastocatellia</i> (Subgroup 4)	<i>Pyrinomonadales</i>	<i>Pyrinomonadaceae</i>	RB41	1.01
	<i>Holophagae</i>	Subgroup 7	uncultured bacterium		0.29
	Subgroup 6		metagenome		0.27
			uncultured <i>Acidobacteria</i> bacterium		2.42
			uncultured <i>Acidobacteriales</i> bacterium		0.22
<i>Actinobacteria</i>	<i>Acidimicrobiia</i>	<i>Actinomarinales</i>	uncultured bacterium		1.77
			uncultured bacterium		0.54
		IMCC26256	uncultured bacterium		0.24
		<i>Microtrichales</i>	<i>Iamiaeae</i>	<i>Iamia</i>	0.55
			<i>Illumatobacteraceae</i>	<i>Illumatobacter</i>	0.23
			<i>Illumatobacteraceae</i>	uncultured bacterium	0.69
	<i>Corynebacteriales</i>	<i>Frankiales</i>	uncultured bacterium		0.23
			<i>Mycobacteriaceae</i>	<i>Mycobacterium</i>	0.16
			<i>Geodermatophilaceae</i>	<i>Blastococcus</i>	1.54
	<i>Actinobacteria</i>		<i>Sporichthyaceae</i>	uncultured bacterium	0.31
			<i>Intrasporangiaceae</i>	<i>Intrasporangium</i>	0.36
			<i>Tetrasphaera</i>		0.20
			uncultured bacterium		0.67
			<i>Microbacteriaceae</i>	<i>Agromyces</i>	1.48
			<i>Micrococcaceae</i>	<i>Pseudarthrobacter</i>	0.65
			uncultured bacterium		0.25
		<i>Micromonosporales</i>	<i>Micromonosporaceae</i>	<i>Micromonospora</i>	0.87
			<i>Aeromicrobium</i>		0.31
	<i>Propionibacteriales</i>		<i>Nocardioidaceae</i>	<i>Marmoricola</i>	0.35
				<i>Nocardioides</i>	2.03
			<i>Propionibacteriaceae</i>	uncultured bacterium	0.26
	<i>Pseudonocardiales</i>		<i>Pseudonocardaceae</i>	<i>Pseudonocardia</i>	0.16
	<i>Streptomycetales</i>		<i>Streptomycetaceae</i>	<i>Streptomyces</i>	0.56
	MB-A2-108		uncultured bacterium		1.87
	<i>Rubrobacteria</i>	<i>Rubrobacteriales</i>	<i>Rubrobacteriaceae</i>	<i>Rubrobacter</i>	0.60
	<i>Thermoleophilii</i>	<i>Gaiellales</i>	<i>Gaiellaceae</i>	<i>Gaiella</i>	3.08
			uncultured <i>actinobacterium</i>		0.18
			uncultured bacterium		3.67

		<i>Solirubrobacterales</i>	<i>Solirubrobacteraceae</i> 67-14 uncultured bacterium	uncultured bacterium <i>Solirubrobacter</i>	1.53 0.48 0.27
<i>Armatimonadetes</i>	<i>Chthonomonadetes</i>	<i>Chthonomonadales</i>	uncultured bacterium	uncultured bacterium	0.66
<i>Bacteroidetes</i>	<i>Bacteroidia</i>	<i>Cytophagales</i>	<i>Microscillaceae</i>	uncultured bacterium	0.45
	<i>Anaerolineae</i>	<i>Caldilineales</i>	<i>Caldilineaceae</i>	uncultured bacterium	0.54
		<i>Chloroflexales</i>	<i>Herpetosiphonaceae</i>	<i>Herpetosiphon</i>	0.24
			<i>Roseiflexaceae</i>	uncultured bacterium	0.61
	<i>Chloroflexia</i>			metagenome	0.30
		<i>Thermomicrobiales</i>	JG30-KF-CM45	uncultured bacterium	2.72
				uncultured <i>Chloroflexi</i> bacterium	1.98
<i>Chloroflexi</i>	<i>Dehalococcoidia</i>	S085	uncultured bacterium	uncultured bacterium	0.34
	Gitt-GS-136		uncultured bacterium		3.89
	JG30-KF-CM66		uncultured <i>Chloroflexus</i> sp.		0.35
	KD4-96		uncultured bacterium		0.19
			metagenome		0.48
			uncultured <i>Anaerolineaceae</i> bacterium		0.55
			uncultured bacterium		3.08
			uncultured <i>Chloroflexi</i> bacterium		1.05
	<i>Kiedonobacteria</i>	C0119	uncultured bacterium	uncultured bacterium	0.91
	TK10		uncultured bacterium		0.31
<i>Firmicutes</i>	<i>Bacilli</i>	<i>Bacillales</i>	<i>Bacillaceae</i>	<i>Bacillus</i>	1.38
<i>Gemmatimonadetes</i>	<i>Gemmatimonadetes</i>	<i>Gemmatimonadales</i>	<i>Gemmatimonadaceae</i>	<i>Gemmatimonas</i>	0.71
				uncultured bacterium	1.65
<i>Latescibacteria</i>			uncultured bacterium		0.20
<i>Patescibacteria</i>	<i>Saccharimonadia</i>	<i>Saccharimonadales</i>	uncultured bacterium	uncultured bacterium	1.31
			uncultured soil bacterium		0.30
<i>Planctomycetes</i>	OM190		uncultured bacterium		0.35
	<i>Phycisphaerae</i>	<i>Tepidisphaerales</i>	WD2101 soil group	uncultured bacterium	1.61
	<i>Planctomycetacia</i>	<i>Pirellulales</i>	<i>Pirellulaceae</i>	uncultured planctomycete	0.65
		<i>Caulobacterales</i>	<i>Caulobacteraceae</i>	<i>Pirellula</i>	0.54
				<i>Brevundimonas</i>	0.61
<i>Proteobacteria</i>	<i>Alphaproteobacteria</i>	<i>Sphingomonadales</i>	<i>Sphingomonadaceae</i>	<i>Altererythrobacter</i>	3.75
		<i>Tistrellales</i>	<i>Geminicoccaceae</i>	<i>Sphingomonas</i>	1.86
		<i>Myxococcales</i>	<i>Haliangiaceae</i>	<i>Candidatus Alysiosphaera</i>	0.29
	<i>Deltaproteobacteria</i>	NB1-j	uncultured bacterium	<i>Haliangium</i>	0.37
			uncultured bacterium		0.17

	Betaproteobacteria	Burkholderiales	Oxalobacteraceae	Massilia uncultured bacterium	0.79
		Nitrosomonadales	Burkholderiaceae	uncultured bacterium	0.30
			Nitrosomonadaceae	MND1	0.51
	Gammaproteobacteria	Gammaproteobacteria Incertae Sedis	Unknown Family	Acidibacter	0.18
		Pseudomonadales	Pseudomonadaceae	Pseudomonas	3.64
		Xanthomonadales	Xanthomonadaceae	Lysobacter	1.31
				Candidatus Xiphinematobacter	0.89
	Chthoniobacteriales	Chthoniobacteriales	Xiphinematobacteraceae	uncultured bacterium	0.43
		Pedospirales	Pedospiraceae	Luteolibacter	0.71
	Verrucomicrobiales	Verrucomicrobiales	Rubritaleaceae		
Responders					
N1					
Acidobacteria	Blastocatellia (Subgroup 4)	Blastocatellales	Blastocatellaceae	uncultured bacterium	0.34
	Thermoanaerobaculia	Thermoanaerobaculales	Thermoanaerobaculaceae	Subgroup 10	0.15
Bacteroidetes	Bacteroidia	Chitinophagales	Chitinophagaceae	uncultured bacterium	0.27
		Cytophagales	Hymenobacteraceae	Adhaeribacter	0.17
	AKAU4049		uncultured bacterium		0.23
Gemmatimonadetes	Longimicrobia	Longimicrobiales	Longimicrobiaceae	uncultured bacterium	0.21
	S0134 terrestrial group		uncultured bacterium		0.14
Nitrospirae	Nitrospira	Nitrospirales	Nitrospiraceae	Nitrospira	0.13
				Gemmata	0.20
Planctomycetes	Planctomycetacia	Gemmatales	Gemmataceae	uncultured bacterium	0.47
		Caulobacteriales	Caulobacteraceae	Phenylobacterium	0.14
			Devosiaceae	Devosia	0.15
		Rhizobiales	Xanthobacteraceae	uncultured bacterium	0.13
	Alphaproteobacteria			Ellin6055	0.21
		Sphingomonadales	Sphingomonadaceae	Novosphingobium	0.13
				Sphingobium	0.31
				uncultured bacterium	0.22
		PLTA13	uncultured bacterium		0.14
	Gammaproteobacteria	Xanthomonadales	Xanthomonadaceae	Luteimonas	0.22
	NC10	Rokubacteriales	uncultured bacterium		0.27
Rokubacteria					
Verrucomicrobia	Verrucomicrobiae	Chthoniobacteriales	Chthoniobacteraceae	Chthoniobacter	0.56
N2					
Actinobacteria	Thermoleophilina	Solirubrobacteriales	67-14	uncultured Rubrobacteria bacterium	0.13
			Solirubrobacteraceae	Conexibacter	0.15

<i>Chloroflexi</i>	<i>Anaerolineae</i>	SBR1031	A4b	uncultured bacterium	0.23
	<i>Chloroflexia</i>	<i>Kallotenuales</i>	AKIW781	uncultured bacterium	0.19
	Gitt-GS-136	uncultured <i>Anaerolineae</i> bacterium			0.16
<i>Patescibacteria</i>	<i>Parcubacteria</i>	uncultured bacterium			0.22

Chapter 3

Carbon Availability and Nitrogen Mineralization Control Denitrification Rates and Product Stoichiometry during Initial Maize Litter Decomposition

Pauline Sophie Rummel^{1*}, Reinhard Well², Johanna Pausch³, Birgit Pfeiffer^{1,4},
and Klaus Dittert¹

¹ Division of Plant Nutrition and Crop Physiology, Department of Crop Science, University of Göttingen, Germany

² Thünen Institute of Climate-Smart Agriculture, Federal Research Institute for Rural Areas, Forestry and Fisheries, Braunschweig, Germany

³ Agroecology, Faculty for Biology, Chemistry, and Earth Sciences, University of Bayreuth, Germany

⁴ Institute of Microbiology and Genetics, Department of Genomic and Applied Microbiology, University of Göttingen, Germany

* corresponding author: pauline.rummel@uni-goettingen.de; Phone: ++49 551 39 4471, Fax: ++49 551 39 25570

Published in: Applied Sciences, 11, 5309, 2021; <https://doi.org/10.3390/app11115309>

Author contributions:

Conceptualization: P.S.R., R.W., J.P., and K.D.; methodology (incubation system): P.S.R., B.P., K.D.; investigation: P.S.R.; data analysis: P.S.R.; data validation: P.S.R., R.W. and J.P.; writing—original draft preparation: P.S.R.; writing—review and editing: P.S.R., R.W., J.P., B.P., and K.D.; visualization: P.S.R.; supervision: R.W., J.P. and K.D.; funding acquisition: K.D.

Article

Carbon Availability and Nitrogen Mineralization Control Denitrification Rates and Product Stoichiometry during Initial Maize Litter Decomposition

Pauline Sophie Rummel ^{1,*} , Reinhard Well ², Johanna Pausch ³, Birgit Pfeiffer ^{1,4} and Klaus Dittert ¹

¹ Section of Plant Nutrition and Crop Physiology, Department of Crop Science, University of Göttingen, 37073 Göttingen, Germany; Birgit.Pfeiffer@biologie.uni-goettingen.de (B.P.); klaus.dittert@agr.uni-goettingen.de (K.D.)

² Thünen Institute of Climate-Smart Agriculture, Federal Research Institute for Rural Areas, Forestry and Fisheries, 38116 Braunschweig, Germany; reinhard.well@thuenen.de

³ Agroecology, Faculty for Biology, Chemistry, and Earth Sciences, University of Bayreuth, 95447 Bayreuth, Germany; Johanna.Pausch@uni-bayreuth.de

⁴ Institute of Microbiology and Genetics, Department of Genomic and Applied Microbiology, University of Göttingen, 37073 Göttingen, Germany

* Correspondence: pauline.rummel@uni-goettingen.de



Citation: Rummel, P.S.; Well, R.; Pausch, J.; Pfeiffer, B.; Dittert, K. Carbon Availability and Nitrogen Mineralization Control Denitrification Rates and Product Stoichiometry during Initial Maize Litter Decomposition. *Appl. Sci.* **2021**, *11*, 5309. <https://doi.org/10.3390/app11115309>

Academic Editor: Micòl Mastrocicco

Received: 16 April 2021

Accepted: 2 June 2021

Published: 7 June 2021

Publisher's Note: MDPI stays neutral with regard to jurisdictional claims in published maps and institutional affiliations.



Copyright: © 2021 by the authors. Licensee MDPI, Basel, Switzerland. This article is an open access article distributed under the terms and conditions of the Creative Commons Attribution (CC BY) license (<https://creativecommons.org/licenses/by/4.0/>).

Abstract: Returning crop residues to agricultural fields can accelerate nutrient turnover and increase N₂O and NO emissions. Increased microbial respiration may lead to formation of local hotspots with anoxic or microoxic conditions promoting denitrification. To investigate the effect of litter quality on CO₂, NO, N₂O, and N₂ emissions, we conducted a laboratory incubation study in a controlled atmosphere (He/O₂, or pure He) with different maize litter types (*Zea mays* L., young leaves and roots, straw). We applied the N₂O isotopocule mapping approach to distinguish between N₂O emitting processes and partitioned the CO₂ efflux into litter- and soil organic matter (SOM)-derived CO₂ based on the natural ¹³C isotope abundances. Maize litter increased total and SOM derived CO₂ emissions leading to a positive priming effect. Although C turnover was high, NO and N₂O fluxes were low under oxic conditions as high O₂ diffusivity limited denitrification. In the first week, nitrification contributed to NO emissions, which increased with increasing net N mineralization. Isotopocule mapping indicated that bacterial processes dominated N₂O formation in litter-amended soil in the beginning of the incubation experiment with a subsequent shift towards fungal denitrification. With onset of anoxic incubation conditions after 47 days, N fluxes strongly increased, and heterotrophic bacterial denitrification became the main source of N₂O. The N₂O/(N₂O+N₂) ratio decreased with increasing litter C:N ratio and C_{org}:NO₃[−] ratio in soil, confirming that the ratio of available C:N is a major control of denitrification product stoichiometry.

Keywords: fungal denitrification; nitrification; isotopocules; priming effect; nitric oxide; nitrous oxide; dinitrogen; greenhouse gas; decomposition

1. Introduction

Returning of crop residues is a common agricultural management strategy to prevent nutrient losses and to increase soil fertility. However, acceleration of N and C cycling processes often lead to increased losses of climate-relevant gases.

Addition of plant litter to soils has been proven to increase CO₂ and N₂O emissions over a vast range of soil conditions and litter types [1–4]. Upon degradation, plant litter provides nutrients for decomposing and denitrifying microorganisms. Thus, variations in N₂O emissions have often been related to litter quality, especially the C:N ratio [1,2]. For litter with C:N < 25:1, mineralization increases soil NO₃[−] content leading to increased denitrification [5,6], while for C:N > 25:1, N is immobilized by soil microorganisms to decompose litter C compounds [7] and restricts N₂O emissions [8]. When litter quality

was analyzed in more detail, easily degradable fractions explained a large share of the variability of N_2O emissions [9,10], while the lignin content was not relevant [11,12]. Recent studies confirm that the quality of C compounds (especially water-soluble C) from litter is a main driver of denitrification after litter addition [13,14].

Easily degradable C compounds (e.g., sugars, proteins, amino acids, and carbohydrates) control litter decomposition dynamics in the initial phase and subsequent CO_2 efflux from soils [4,15,16]. Furthermore, the quality of organic substrates affects decomposition of soil organic matter (SOM) [17]. Readily accessible high-quality substrates increase SOM decomposition, leading to a positive priming effect in soils [18,19]. When litter and SOM turnover are increased after litter addition, microbial O_2 demand increases with increasing microbial respiration. This may lead to formation of local hotspots with anoxic or microoxic conditions providing favorable conditions for denitrifying soil microorganisms [20]. Accordingly, a recent study reported the highest denitrification-derived N_2O losses in soils with high SOM priming after addition of labile C substrates (glucose, vanillin) [21]. However, further studies with plant residues are necessary to better understand the interactions between C turnover and denitrification.

The aim of this study was to investigate the effect of litter C quality and SOM turnover on denitrification. We anticipate that increased SOM turnover after litter addition promotes the formation of anoxic hotspots for denitrification and expect higher litter and SOM turnover from litter with high degradability. Thus, we hypothesize that (i) N_2O fluxes from denitrification increase when C turnover from litter and SOM is high, leading to (ii) higher $\text{N}_2\text{O}+\text{N}_2$ losses when litter with a high share of easily degradable C is added, while (iii) the $\text{N}_2\text{O}/(\text{N}_2\text{O}+\text{N}_2)$ ratio is controlled by the availability of C_{org} in relation to NO_3^- .

Therefore, we setup a laboratory incubation experiment in an artificial N_2 -free atmosphere under fully controlled conditions. We compared different types of maize litter (fresh leaves and roots, straw) and investigated the effect of litter quality on total CO_2 , NO , N_2O , and N_2 emissions. To trace maize litter (C_4 plant) and SOM turnover, we used a grassland soil whose organic C originates solely from C_3 vegetation and partitioned the CO_2 efflux into its sources (i.e., litter- and SOM-derived CO_2) based on the natural ^{13}C isotope abundances. In addition, we analyzed the intramolecular distribution of the naturally occurring ^{15}N and ^{18}O isotopes in the linear N_2O molecule and applied the N_2O isotopocule mapping approach to estimate the contribution of denitrification to N_2O formation [22,23].

2. Materials and Methods

2.1. Preparation of Soil and Plant Material

The soil for the experiment was taken from a long-term field experiment at the grassland research station of the University of Gießen (latitude $\text{N}50^\circ 32'$, longitude $\text{E}8^\circ 41.3'$, elevation 172 m a.s.l.), sieved to 10 mm, air-dried, and stored at 4°C . The soil was classified as Fluvic Gleysol of clay loam texture (32% clay, 41% silt, and 27% sand) with a pH (CaCl_2) of 5.67. Total soil N content was 0.42%, total soil C content was 4.2%, and $\delta^{13}\text{C}$ was -28.37‰ . Prior to the incubation experiment, the soil was pre-incubated in the dark for 5 weeks at 50% water holding capacity (WHC) and 20°C .

Maize plants (*Zea mays* L. cv. Ronaldinio) were grown in nutrient solution [24] for 5 weeks. Leaves were cut from stems and left to wilt at room temperature for 4 h. Roots were rinsed with $\text{H}_2\text{O}_{\text{dest}}$ and carefully dried with paper towels. Leaves and roots were stored at 4°C and 90% relative humidity until experimental setup. Maize straw was collected from an experimental field site of the University of Göttingen after grain harvest in October 2018. Maize straw was shock frozen in liquid N_2 and stored at -20°C . Prior to setting up the experiment, maize straw was unfrozen and all maize litter was cut to a size of 2 cm. A subsample of soil and maize litter was analyzed for total N, total C, and $\delta^{13}\text{C}$ using an elemental analyzer (NA1110, CE-Instruments, Rodano, Milano, Italy) linked to a gas-isotope ratio mass spectrometer (Delta Plus, Finnigan MAT, Bremen, Germany) via a Conflo III Interface (Finnigan MAT, Bremen, Germany). Further, plant litter was

analyzed for water-extractable C and N content. Briefly, 0.2 g of finely ground plant litter were extracted in 100 mL $\text{H}_2\text{O}_{\text{bidest}}$, shaken for 1 h, filtered with 0.45 μm polyether sulfone filters (Labsolute, Renningen, Germany), and stored at -20°C . The extracts were analyzed for organic C and total N content using a multi N/C[®] Analyzer (Analytik Jena, Jena, Germany). Another subsample of finely ground plant litter was analyzed by ^{13}C solid-state cross polarization magic angle spinning nuclear magnetic resonance spectroscopy (^{13}C -CPMAS NMR) using a Bruker Avance^{III} 200 spectrometer (Bruker BioSpin GmbH, Karlsruhe, Germany). Samples were weighed into zircon oxide rotors and spun around a magic angle at a speed of 6.8 kHz. Contact time was 1 ms and the recycle delay time was set to 2 s, line broadening was set at 0. Peak integration areas were separated into -10 – 45 ppm (alkyl C), 45 – 110 ppm (O/N-alkyl C), 110 – 160 ppm (aryl C), and 160 – 220 ppm (carboxylic C).

2.2. Automatized Laboratory Incubation Experiment and Gas Analysis

The incubation experiment was carried out under fully controlled conditions using an automated soil incubation system with artificial atmosphere similar to systems described earlier [25–28]. For the incubation experiment, soil moisture was adjusted to 70% water-filled pore space (WFPS, equivalent to 67.7% WHC or 31.9% gravimetric water content) and 50 mg N kg^{-1} was added by spraying a KNO_3 solution onto the soil and thoroughly stirring it with a spoon. For treatments with litter, litter was homogenously mixed with soil (Maize leaves: 40.5 g FM kg^{-1} , maize roots: 42 g FM kg^{-1} , maize straw: 12.8 g FM kg^{-1}). The soil for each pot was prepared separately to ensure the same amount of litter was added. Then, the equivalent of 2.5 kg dry soil was filled into acrylic glass pots (inner diameter 172 mm, height 210 mm) with a porous ceramic plate at the bottom and compacted in a stepwise mode by filling a 2 cm-layer of soil in pots and compacting it with a plunger. To ensure continuity between soil layers, the surface of the compacted layer was gently scratched before adding the next soil layer. Soil height in the pots was 10 cm, and bulk density was 1.1 g cm^{-3} . Each litter treatment was replicated five times, a control treatment without litter was replicated four times, and one empty pot was included as reference to determine background gas concentrations.

Pots were tightly closed with transparent acrylic glass lids with rubber seals, and the outside of the pots was covered with dark plastic sheets to prevent algae growth. Pots were alternately evacuated using a rotary vacuum pump (Pfeiffer Vacuum GmbH, Asslar, Germany) and flushed with a gas mixture (80% He, 20% O_2) for 24 h. The gas mixture was prepared by using stainless steel capillaries of different length and inner diameter. For the first cycles, pots were evacuated from the top and the bottom and, subsequently, flushed with the He/ O_2 gas mixture. Then, pots were evacuated from the bottom and simultaneously flushed from the top to replace the atmosphere inside the soil column. For measurements, the outlet of all pots was connected to flow-through multi-position valves (16 ports, Vici Valco Instruments, Houston, TX, USA) with multi-position actuator control modules (Vici Valco Instruments, Houston, TX, USA), and controlled by Trilution Software (Gilson Inc., Middleton, WI, USA) via an interface module (506C System Interface, Gilson Inc., Middleton, WI, USA). The selected stream outlet tube of the multi-position valve was connected to a gas chromatograph (GC-450, Bruker, Billerica, USA) equipped with a thermal conductivity detector (TCD) for measurement of CO_2 and a pulsed discharge detector (PDD, Vici AG International, Schenkon, Switzerland) for N_2O and N_2 . The sample gas outlet of the GC was connected to a flow-through massflowmeter (Alicat Scientific, Tucson, AZ, USA), and a trace-level gas analyzer (CLD 88Yp, Eco Physics AG, Dürnten, Switzerland) equipped with a chemoluminescence detector (CLD) to analyze NO concentrations. To add up to the required 300-mL-flow of the NO analyzer, samples were diluted with synthetic air. Processing of GC data was done using CompassCDS software (SCION Instruments, Livingston, UK). Data from the NO analyzer and flowmeter were read out every 10 s via a serial port.

The analytical precision of the GC was determined by repeated measurements of standard gases (CO_2 , N_2O , N_2) and was consistently $< 2\%$. Detection limits were $0.08 \mu\text{g N}_2\text{O-N kg}^{-1} \text{ h}^{-1}$ and $5.5 \mu\text{g N}_2\text{-N kg}^{-1} \text{ h}^{-1}$. The non-selected outlet streams of the multi-position valves were used to sample headspace gas for analysis of isotopic compositions ($\delta^{13}\text{C}$ of CO_2 , isotopocules of N_2O). After 47 days, the pots were flushed with pure helium to establish anoxic conditions to determine potential denitrification. After 8 days of anoxic incubation (55 days in total), the pots were opened for final sampling.

2.3. $^{13}\text{CO}_2$ Sampling, Analysis, and Calculations

For determination of $\delta^{13}\text{C}$ of soil-emitted CO_2 , samples were flushed into 12 mL Exetainer[®] septum-capped vials (Labco, High Wycombe, UK). Samples were taken twice a day for the first 5 days, daily for the next 12 days, every second day for the next 14 days, and every 3 days until day 43. Samples were introduced by a Combi-Pal autosampler (CTC-Analytics, Zwingen, Switzerland) to a GC (GC-Box, Thermo Fisher Scientific, Bremen, Germany) coupled to an isotope ratio mass spectrometer (Delta plus XP, Thermo Fisher Scientific, Bremen, Germany) via a ConFlo III Interface (Thermo Fisher Scientific, Bremen, Germany). The fractions of CO_2 derived from litter (f_{litter}) and SOM (f_{SOM}) were calculated using Equations (1) and (2):

$$f_{\text{litter}} = (\delta^{13}\text{C}_{\text{treatment}} - \delta^{13}\text{C}_{\text{Control}}) / (\delta^{13}\text{C}_{\text{litter}} - \delta^{13}\text{C}_{\text{Control}}) \quad (1)$$

$$f_{\text{litter}} + f_{\text{SOM}} = 1 \quad (2)$$

where $\delta^{13}\text{C}_{\text{treatment}}$ is the measured $\delta^{13}\text{C}$ (‰) of CO_2 from litter treatment, $\delta^{13}\text{C}_{\text{Control}}$ is the measured $\delta^{13}\text{C}$ (‰) of CO_2 from control treatment without litter addition, and $\delta^{13}\text{C}_{\text{litter}}$ is the mean measured $\delta^{13}\text{C}$ (‰) of CO_2 lost from maize litter (Leaf: -7.91 ‰ , Root: -7.50 ‰ , Straw: -9.33 ‰ , see supplement for details, Figure S2). For each treatment, the priming effect (PE) was calculated as the difference between SOM-derived $\text{CO}_2\text{-C}$ (C_{SOM}) and $\text{CO}_2\text{-C}$ from control treatment without litter ($\text{C}_{\text{Control}}$) (3):

$$\text{PE} = \text{C}_{\text{SOM}} - \text{C}_{\text{Control}} \quad (3)$$

2.4. $^{15}\text{N}_2\text{O}$ Sampling, Analysis, and Isotopocule Mapping Approach

On 2, 5, 8, 15, 23, 31, 39, 48, 51, and 54 days after onset of incubation (DAO), samples for analyses of N_2O isotopomers were flushed into 100 mL crimp-top vials with butyl rubber septa. Samples were analyzed on a gas-isotope ratio mass spectrometer (Delta plus XP, Finnigan MAT, Bremen, Germany) coupled to a trace gas pre-concentration unit Precon (Thermo Electron Cooperation, Bremen, Germany) via a GC/GP Interface (Thermo Electron Cooperation, Bremen, Germany). In this setup, m/z 44, 45, and 46 of the intact N_2O^+ molecular ions and m/z 30 and 31 of the NO^+ fragment ions are measured simultaneously [29], and $\delta^{15}\text{N}^{\text{bulk}}_{\text{N}_2\text{O}}$, $\delta^{15}\text{N}^{\alpha}_{\text{N}_2\text{O}}$, and $\delta^{18}\text{O}_{\text{N}_2\text{O}}$ values were determined [30]. $\delta^{15}\text{N}^{\beta}_{\text{N}_2\text{O}}$ values were calculated based on the following Equation (4):

$$\delta^{15}\text{N}^{\text{bulk}}_{\text{N}_2\text{O}} = (\delta^{15}\text{N}^{\alpha}_{\text{N}_2\text{O}} + \delta^{15}\text{N}^{\beta}_{\text{N}_2\text{O}}) / 2 \quad (4)$$

Site preference ($\delta^{15}\text{N}^{\text{SP}}_{\text{N}_2\text{O}}$) was calculated as the difference between $\delta^{15}\text{N}^{\alpha}_{\text{N}_2\text{O}}$ and $\delta^{15}\text{N}^{\beta}_{\text{N}_2\text{O}}$. We used the scrambling factor of 0.096 determined by Buchen et al. (2018) [31] to correct measured data [32]. $\delta^{18}\text{O}$ of soil water was -6.7 ‰ .

We applied the isotopocule mapping approach by Lewicka-Szczepak et al. (2017) [22] to calculate the fraction of residual unreduced N_2O ($r_{\text{N}_2\text{O}}$) and the N_2O fraction from heterotrophic bacterial denitrification (f_{bD}) based on the sample position in the $\delta^{15}\text{N}^{\text{SP}}/\delta^{18}\text{O}$ map using a mixing equation for the bacterial fraction (6) and the Rayleigh equation for N_2O reduction (5):

$$r_{\text{N}_2\text{O}} = e^{((\delta_r - \delta_0)/\eta_{\text{red}})} \quad (5)$$

$$\delta_{0,\text{sample}} = \delta_{\text{bD}} * f_{\text{bD}} + \delta_{\text{fD/Ni}} * (1 - f_{\text{bD}}) \quad (6)$$

where δ_r is the isotopic signature of residual N_2O after partial reduction, δ_0 is the isotopic signature of initial N_2O before reduction, and η_{red} is the isotopic fractionation factor associated with N_2O reduction to N_2 . Two main scenarios were considered: (1) N_2O emitted from bacterial denitrification is first reduced to N_2 and residual N_2O is then mixed with N_2O originating from nitrification or fungal denitrification (Scenario 1, reduction-mixing). Alternatively, (2) N_2O from bacterial denitrification and nitrification or fungal denitrification is first mixed and then partially reduced to N_2 (Scenario 2, mixing-reduction). Recently, non-overlapping signatures for N_2O produced by nitrification or fungal denitrification were proposed [23], and we calculated both scenarios for mixing of bacterial denitrification with either nitrification or fungal denitrification. A detailed description of the calculations can be found in [33]. We used the isotopic fractionation factors proposed by [23] (Supplementary Table S1), which were corrected for $\delta^{18}O$ of soil water (-6.7 ‰) for mapping and calculations.

In addition, calculations can be based on minimum or maximum end-member values, fractionation factors, and reduction factors, leading to a total of 14 different scenarios [31]. In our study, we used mean values for mixing, fractionation, and reduction whenever possible. However, as during anoxic incubation, samples were distributed outside the mean mixing-reduction area, we used minimum reduction values (mean mixing, mean fractionation) for 51 and 54 DAO. When calculations yielded values < 0 or > 1 for fbD or rN $_2O$, these values were removed from the dataset before calculating means and plotting.

2.5. Soil Analyses

Samples of pre-incubated soil were taken prior to experimental setup. After opening pots at the end of the experiment, soil from each pot was homogenized and a sample was taken for analyses. Subsamples were analyzed for soil mineral N, water-extractable organic C (WEOC), and soil water content. For analysis of mineral N (NO_3^- and NH_4^+), 50 g fresh soil were weighed into plastic bottles and frozen at -20 °C until analysis. Frozen samples were extracted with 2 M KCl solution (1:5 w:v) and shaken on an overhead shaker for 60 min. Samples were filtered with 615 $\frac{1}{4}$ filter paper (Macherey–Nagel GmbH & Co. KG, Düren, Germany) and extracts were analyzed colorimetrically using the San⁺⁺Continuous-Flow Analyzer (Skalar Analytical B.V., Breda, The Netherlands). To determine isotopic signatures of nitrate, the bacterial denitrification method with *Pseudomonas aureofaciens* was applied [34,35].

WEOC was extracted by homogenizing 2 g of fresh soil with 10 mL H_2O_{bidest} . Samples were centrifuged, filtered with 0.45 μm polyether sulfone filters (Labsolute, Renningen, Germany), and stored at -20 °C . The extracts were analyzed for organic C and total N content using a multi N/C[®] Analyzer (Analytik Jena, Jena, Germany). Soil water content was determined by oven drying at 105 °C .

2.6. Calculations and Statistics

For all calculations and statistical analyses, the statistical software R version 3.6.0 [36] was used. Fluxes of CO_2 , N_2O , N_2 , and NO (F , $\mu g \text{ kg}^{-1} \text{ h}^{-1}$) were calculated using the dynamic chamber approach (7):

$$F = (C_o - C_i) * Q/m \quad (7)$$

where C_o is the concentration at the outflow and C_i is the concentration at the inflow of each vessel ($mg \text{ N m}^{-3}$, or $mg \text{ C m}^{-3}$), Q is the flow rate through the headspace ($m^3 \text{ h}^{-1}$), and m is the dry mass of soil per vessel (kg).

Net N mineralization was calculated according to Equation (8):

$$\text{Net N mineralization} = NO_3^-_{\text{end}} + NH_4^+_{\text{end}} + NO_{\text{cml}} + N_2O_{\text{cml}} + N_{2\text{cml}} - (NO_3^-_{\text{start}} + NH_4^+_{\text{start}} + NO_3^-_{\text{fertilizer}}) \quad (8)$$

Mean values and standard deviations were calculated using the *SlidingWindow* function from the package *evobiR* v.1.1 [37] or the *rollapply* function from the package *zoo* [38].

Cumulative emissions were calculated by interpolation between measured fluxes. To test for differences between treatments, a one-way ANOVA was calculated when data were normally distributed or the Kruskal–Wallis rank sum test for non-normally distributed data followed by the LSD post hoc test. A *t*-test at $p < 0.05$ was used to compare soil NO_3^- , NH_4^+ , and WEOC content before and after the incubation. To analyze the effect of litter input and litter quality on CO_2 and N emissions, simple linear regression models were tested. In all plots, color schemes from the R package viridisLite v0.3.0 [39] were used.

3. Results

3.1. Characterization of Maize Litter

Maize litter types differed in their chemical composition (Table 1). Total C content ranged between 40% in maize roots and 47% in maize leaves. Total N content ranged between 3.8% in maize leaves and 0.85% in maize straw. C:N ratio was highest in maize straw (51.4) and similar in maize leaves and roots (12.3 and 13.8, respectively). Water-soluble C contents were similar in all maize litter types (8–8.5%). Water-soluble N content was highest in maize roots (1.22%) and lowest in maize straw (0.39%). Thus, water-soluble C:N was highest in maize straw and lowest in maize roots. ^{13}C -CPMAS NMR spectroscopy of maize litter revealed that maize straw and maize leaves were closer in their chemical composition than maize roots (Table 1, spectra in Supplementary Figure S1). Maize roots were characterized by the lowest shares of alkyl C and carboxyl C and the highest share of O/N-alkyl C, while maize leaves had highest shares of carboxyl C and alkyl C.

3.2. Soil N and C Content

Soil NO_3^- content increased in Control, Leaf, and Root treatments during the incubation experiment due to a net mineralization of N (Table 2). In contrast, addition of maize straw significantly decreased soil NO_3^- content and immobilized N. Soil NH_4^+ content strongly decreased in all treatments during the incubation period and was significantly higher in all maize litter treatments than in Control, but differences between treatments were small. WEOC content increased in all maize litter treatments, but did not change in Control. No differences were found in soil WEOC content between different litter treatments at the end of the experiment.

$\delta^{15}\text{N}_{\text{NO}_3}$ and $\delta^{18}\text{O}_{\text{NO}_3}$ of added KNO_3 were higher compared to initial soil NO_3^- at onset of incubation (Table 2). At the end of the incubation experiment, $\delta^{15}\text{N}_{\text{NO}_3}$ and $\delta^{18}\text{O}_{\text{NO}_3}$ of soil NO_3^- differed between litter treatments. The lowest $\delta^{15}\text{N}_{\text{NO}_3}$ was measured in Root, and the lowest $\delta^{18}\text{O}_{\text{NO}_3}$ in Control and Leaf. The highest $\delta^{15}\text{N}_{\text{NO}_3}$ and $\delta^{18}\text{O}_{\text{NO}_3}$ were measured in Straw. $\delta^{15}\text{N}_{\text{NO}_3}$ increased with decreasing net N mineralization (adj. $R^2 = 0.73$, $p < 0.001$, Table 3).

Table 1. Characteristics of maize litter used in the incubation experiment: total and water-soluble C and N content, C:N ratios, $\delta^{13}\text{C}$, and distribution of C species in different plant litter types (values represent the percentage contribution of the different integrated chemical shift regions determined by ^{13}C -CPMAS NMR spectroscopy).

	Dry Matter (%)	C (%)	$\delta^{13}\text{C}$ (‰)	N (%)	C:N	Water Soluble C (%)	Water Soluble N (%)	Water Soluble C:N	Alkyl C (%)	O/N-Alkyl C (%)	Aryl C (%)	Carboxyl C (%)
Maize leaves	27.9	46.58	-14.70	3.80	12.27	8.03	0.69	11.6	16.05	63.67	10.96	9.31
Maize roots	7.8	40.12	-12.97	2.90	13.82	8.53	1.22	7.0	8.08	80.65	10.19	1.10
Maize straw	31.4	43.84	-14.11	0.85	51.36	8.25	0.39	21.4	11.48	69.93	11.23	7.23

Table 2. Soil mineral N and water-extractable organic C (WEOC) before setup (initial) and at the end of the incubation experiment. Net N mineralization over the whole incubation period of 55 days.

	NO_3^- (mg N kg $^{-1}$ dry soil)		NH_4^+ (mg N kg $^{-1}$ dry soil)		WEOC (mg C kg $^{-1}$ dry soil)	Net N Mineralization (mg N kg $^{-1}$ dry soil)	$\delta^{15}\text{N}_{\text{NO}_3}$ of Soil NO_3^- (‰)	$\delta^{18}\text{O}_{\text{NO}_3}$ of Soil NO_3^- (‰)
Initial	102.9 ± 4.59		34.7 ± 3.16		51.4 ± 6.49	-	-5.74 ± 0.19/2.44 ± 0.22 ¹	1.84 ± 0.29/22.95 ± 0.40 ¹
Control	142.1 ± 7.8	b ***	4.12 ± 0.27	c ***	56.3 ± 8.0	26.4 ± 5.5	7.80 ± 0.58	9.21 ± 1.05
Maize Leaves	169.6 ± 4.4	a ***	5.84 ± 0.28	a ***	76.4 ± 3.1	75.5 ± 15.1	8.58 ± 0.24	9.27 ± 0.31
Maize Roots	176.1 ± 6.9	a ***	4.85 ± 0.39	b ***	72.0 ± 5.7	69.3 ± 5.4	6.64 ± 0.62	11.49 ± 0.52
Maize Straw	70.6 ± 5.6	c ***	6.00 ± 0.60	a ***	71.9 ± 5.3	-26.8 ± 5.7	16.40 ± 1.63	14.53 ± 0.34

Values represent means ± standard deviation (n = 5, Control and Initial n = 4). Different letters in the same column indicate a significant difference according to the LSD post hoc test at $p \leq 0.05$. *** indicates a significant difference to Initial content according to t -test at $p \leq 0.05$. ¹ initial soil NO_3^- after pre-incubation/added KNO_3 (means ± standard deviation, n = 4).

Table 3. Coefficients of determination and *p*-values for simple linear regressions.

	Adjusted R ²	<i>p</i> -Value	n
<i>Oxic incubation period</i>			
Cumulative NO+N ₂ O emissions ~ water-soluble litter C input	0.4401	0.001172	19
Cumulative N ₂ O emissions ~ litter C:N ratio	0.247	0.03428	15
Cumulative NO emissions ~ water-soluble litter C:N ratio	0.8703	2.427×10^{-7}	15
Cumulative NO emission ~ net N mineralization	0.5671	0.0001197	19
NO+N ₂ O flux ~ CO ₂ flux	0.08023	$<2.2 \times 10^{-16}$	1715
<i>Anoxic incubation period</i>			
Cumulative N ₂ emissions ~ water-soluble litter C:N ratio	0.2553	0.03158	15
Cumulative NO+N ₂ O+N ₂ emissions ~ total litter C input	0.5087	0.0003655	19
N ₂ O/(N ₂ O+N ₂) ratio ~ water-soluble litter C:N ratio	0.5061	1.886×10^{-6}	19
N ₂ O/(N ₂ O+N ₂) ratio ~ WEOC: NO ₃ [−] ratio	0.4127	0.0018	19
NO+N ₂ O+N ₂ flux ~ CO ₂ flux	0.864	$<2.2 \times 10^{-16}$	176
<i>Total incubation period</i>			
Cumulative CO ₂ emissions ~ total litter C input	0.8974	4.84×10^{-10}	19
Cumulative CO ₂ emissions ~ water-soluble litter C input	0.798	1.606×10^{-7}	19
Litter-derived CO ₂ flux ~ SOM-derived CO ₂ flux	0.8838	$<2.2 \times 10^{-16}$	495
δ ¹⁵ N _{NO3} of soil NO ₃ [−] ~ net N mineralization (52 DAO)	0.729	$<2.024 \times 10^{-6}$	19

3.3. CO₂ and ¹³CO₂ Fluxes and Cumulative Emissions

CO₂ fluxes from all litter treatments increased after onset of incubation compared to Control (Figure 1a,b, Supplementary Figure S3). Total CO₂ fluxes were highest in Leaf reaching 5.1 mg C kg^{−1} h^{−1} on 2 DAO. In Root, CO₂ flux peaked on 2 DAO (2.57 mg C kg^{−1} h^{−1}) and then decreased throughout the incubation period. In Straw, the highest CO₂ fluxes were measured directly after onset of incubation (2.8 mg C kg^{−1} h^{−1}), and continuously decreased afterwards. Litter-derived and SOM-derived CO₂ followed a similar pattern as total CO₂ fluxes and were highly correlated (adj. R² = 0.88, *p* < 0.001, Table 3). Highest litter-derived CO₂ fluxes were measured in Leaf on 3 DAO (3.0 mg C kg^{−1} h^{−1}), in Straw on 1 DAO (1.2 mg C kg^{−1} h^{−1}), and in Root on 2 DAO (1.7 mg C kg^{−1} h^{−1}) (Figure 1a). SOM-derived CO₂ was highest in Leaf and higher in all litter treatments compared to Control for the first week after onset of incubation (Figure 1b). Accordingly, the cumulative priming effect increased most strongly in all litter treatments during the first days of incubation (Figure 1c) with highest values in Leaf.

Cumulative CO₂ emissions from all litter treatments were significantly higher than from Control without litter (*p* < 0.05, Table 4). The highest cumulative and litter-derived CO₂ emissions were measured after addition of maize leaves, followed by maize straw and maize roots; however, cumulative SOM-derived CO₂ emissions were higher than litter-derived CO₂ emissions in all treatments (Table 4). Total cumulative CO₂ emissions were significantly positively correlated with total C and water-soluble C input from maize litter (adj. R² = 0.80 and adj. R² = 0.90, respectively, *p* < 0.001, Table 3). When total cumulative CO₂ emissions were standardized against C input from litter, no differences were found (Supplementary Table S2).

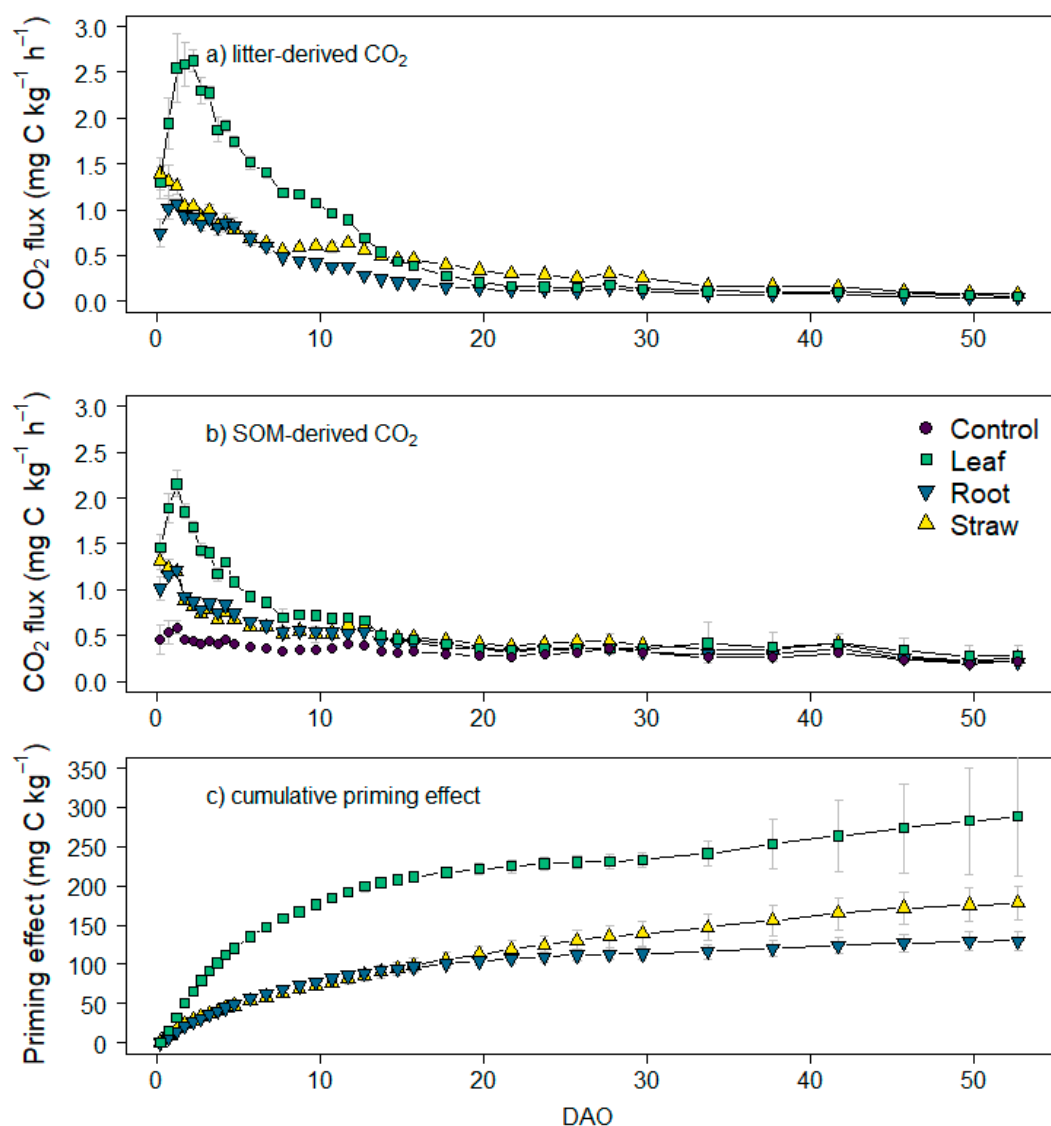


Figure 1. (a) Litter-derived CO₂ fluxes, (b) SOM-derived CO₂ fluxes, and (c) cumulative priming effect (means and standard deviation for n = 5, n = 4 for Control, when not visible, error bars are smaller than the symbols).

Table 4. Cumulative SOM and litter-derived CO₂ emissions, and priming effect.

	Total CO ₂ (mg C kg ⁻¹ dry soil)		SOM-Derived CO ₂ (mg C kg ⁻¹ dry soil)		Litter-Derived CO ₂ (mg C kg ⁻¹ dry soil)		Priming Effect (mg C kg ⁻¹ dry soil)	
Control	359.5 ± 13.2	d	359.5 ± 13.2	c	-	-	-	-
Maize Leaves	1266.0 ± 118.8	a	654.8 ± 83.5	a	597.5 ± 33.9	a	288.2 ± 76.2	a
Maize Roots	749.8 ± 68.1	c	504.9 ± 10.7	b	281.6 ± 17.6	c	130.0 ± 12.0	b
Maize Straw	970.8 ± 34.3	b	561.9 ± 26.9	b	449.7 ± 21.1	b	178.4 ± 21.5	b

Values represent means (n = 5, for Control n = 4) ± standard deviation. Different letters in the same column indicate a significant difference.

3.4. N Fluxes and Cumulative Emissions

During the oxic incubation phase, only N₂O and NO fluxes were measured as N₂ fluxes were below the detection limit (Figure 2a,b). N₂O fluxes from litter treatments were higher than 3.7 µg N kg⁻¹ h⁻¹ for the first measurements on 1 DAO and declined to <1 µg N kg⁻¹ h⁻¹ until 5 DAO. N₂O fluxes from litter-amended soils were in tendency higher than N₂O fluxes from Control. Initial NO fluxes were ~0.08 µg N kg⁻¹ h⁻¹ in Control and Root, and ~0.06 µg N kg⁻¹ h⁻¹ in leaves and straw. In Leaf, a second NO

peak was detected on 5 DAO. NO fluxes in Control were in tendency higher than in all litter treatments until 14 DAO, while NO flux declined fastest in Straw, where fluxes were smaller than in all other treatments after 3 DAO. The ratio of NO/N₂O was highest in Control directly after onset of incubation with maximum values of 0.47 (Supplementary Figure S5). In Root and Leaf, it reached maximum values of 0.2 and 0.1 on 5 and 6 DAO. In Straw, highest measured values were 0.1 on 2 DAO. With onset of the anoxic phase, NO/N₂O decreased to 0.015 in all treatments.

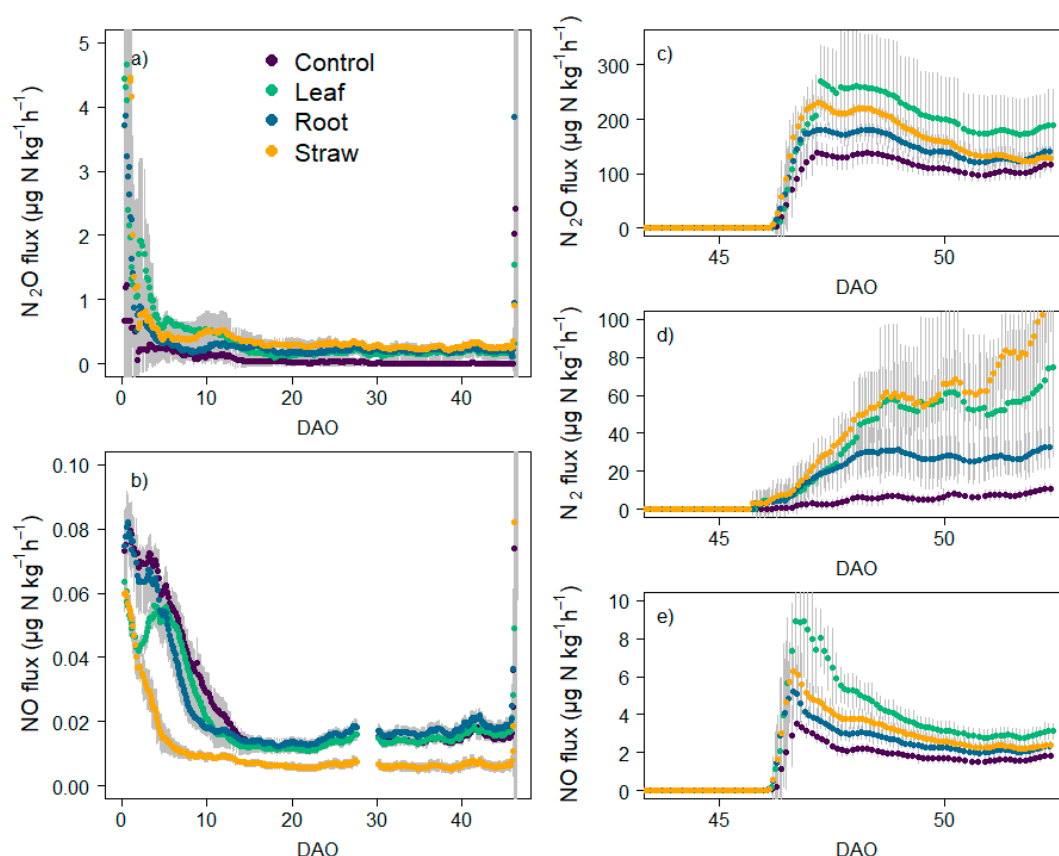


Figure 2. (a,b) N₂O, and NO fluxes during oxic incubation period (0–47 DAO). (c–e) N₂O, N₂, and NO fluxes during anoxic incubation (47–55 DAO) of maize litter on grassland soil (means and standard deviation for n = 5, n = 4 for Control, when not visible, error bars are smaller than the symbols).

During the oxic phase, cumulative N₂O emissions from litter-amended soil were higher than from Control ($p < 0.05$, Table 5). Cumulative emissions in Straw were higher than in Root and similar to Leaf. Cumulative NO emissions were highest in Control and lowest in Straw, and NO/N₂O ratio was significantly higher in Control than in litter-amended treatments. NO emissions strongly decreased with decreasing litter C:N ratio (adj. $R^2 = 0.86$, $p < 0.001$) and increased with increasing N mineralization (adj. $R^2 = 0.57$, $p < 0.001$) confirming that litter quality affected nitrification-derived NO emissions during the oxic incubation phase.

Table 5. Cumulative NO, N₂O, and N₂ emissions and ratios of gaseous products during oxic and anoxic incubation.

	Oxic Incubation Phase (0–46 DAO)			Anoxic Incubation Phase (47–55 DAO)			
	Cumulative NO ($\mu\text{g N kg}^{-1}$ dry soil)	Cumulative N ₂ O ($\mu\text{g N kg}^{-1}$ dry soil)	NO/N ₂ O	Cumulative NO (mg N kg^{-1} dry soil)	Cumulative N ₂ O (mg N kg^{-1} dry soil)	Cumulative N ₂ (mg N kg^{-1} dry soil)	N ₂ O/(N ₂ O+N ₂)
Control	24.1 \pm 2.5	78.3 \pm 97.2	0.37 \pm 0.19	0.29 \pm 0.04	16.6 \pm 2.5	0.88 \pm 0.33	0.95 \pm 0.03
Maize Leaves	20.8 \pm 1.4	387.2 \pm 94.4	0.05 \pm 0.02	0.64 \pm 0.10	29.8 \pm 9.0	6.75 \pm 4.28	0.83 \pm 0.04
Maize Roots	22.9 \pm 2.8	319.0 \pm 81.0	0.07 \pm 0.01	0.41 \pm 0.06	21.5 \pm 1.5	3.70 \pm 1.58	0.85 \pm 0.05
Maize Straw	10.0 \pm 1.7	552.2 \pm 260.7	0.02 \pm 0.01	0.48 \pm 0.06	24.8 \pm 1.0	8.36 \pm 2.06	0.75 \pm 0.05

Values represent means (n = 5, for Control n = 4) \pm standard deviation. Different letters in the same column indicate a significant difference according to the LSD post hoc test at $p \leq 0.05$. N.b. different units for gas emissions during oxic and anoxic incubation phases.

After 47 days, anoxic incubation conditions were induced by flushing the headspace with pure helium gas. N_2O , NO , and N_2 fluxes strongly increased with onset of anoxic incubation conditions (Figure 2c–e). N_2O and NO fluxes peaked on 48 DAO and then decreased until the end of the experiment. N_2 fluxes increased after onset of anoxic conditions until the end of the experiment. During the anoxic phase, cumulative N_2O , NO , and N_2 emissions were higher in litter treatments than in Control, although the effect was not always statistically significant for maize roots (Table 5). The highest cumulative emissions were measured for NO ($0.64 \text{ mg N kg}^{-1}$) and N_2O in Leaf ($29.8 \text{ mg N kg}^{-1}$), and for N_2 in Straw (8.4 mg N kg^{-1}). The ratio of the gaseous end products $\text{N}_2\text{O}/(\text{N}_2\text{O}+\text{N}_2)$ was highest in Control (0.95) and lowest in Straw (0.75).

3.5. N_2O Isotopocule Mapping Approach, fbD and rN_2O Values

The $\delta^{15}\text{N}^{\text{SP}}/\delta^{18}\text{O}_{\text{N}_2\text{O}}$ isotopocule map showed a strong influence of the incubation day on the isotopic signature of soil-emitted N_2O (Figure 3). Most data points were distributed between the mixing line of bacterial and fungal denitrification and the N_2O reduction line during the oxic incubation phase (0–47 DAO). With onset of anoxic incubation conditions, bacterial denitrification became the dominant process as samples measured on 48 DAO cluster tightly above the reported ranges for heterotrophic bacterial denitrification. With ongoing anoxic incubation, the samples cluster along the reduction line indicating increasing N_2O reduction with ongoing anoxic incubation conditions (51 and 54 DAO).

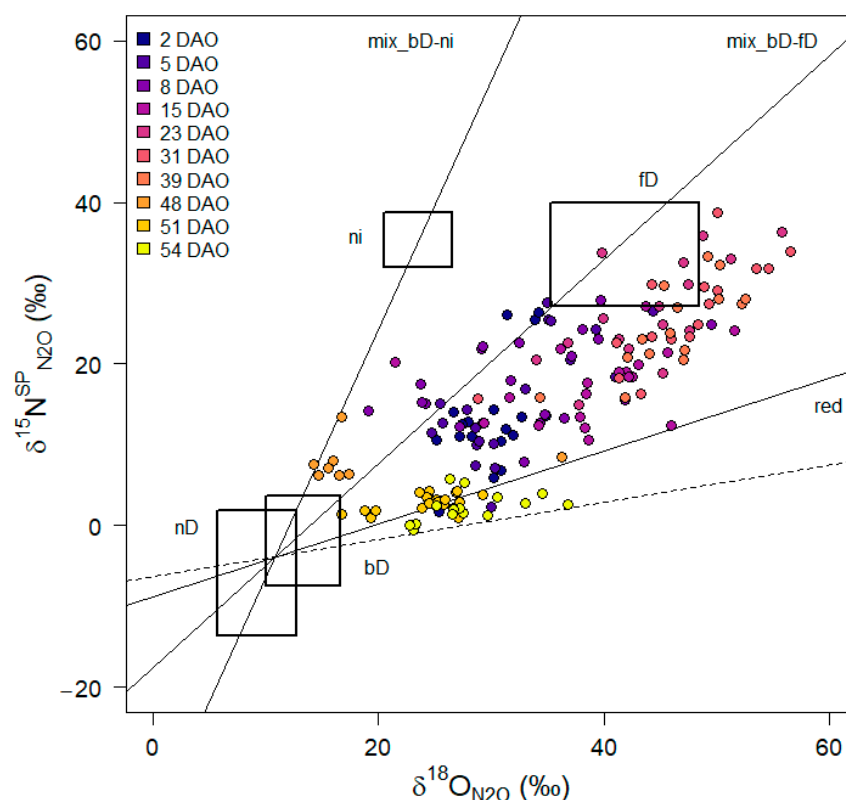


Figure 3. Isotopocule values of soil-emitted N_2O per day plotted in the isotopocule map based on Lewicka-Szczebak et al. (2017) [22] and Yu et al. (2020) [23]. Boxes indicate the mean ranges for end-member values of $\delta^{15}\text{N}^{\text{SP}}_{\text{N}_2\text{O}}$ and $\delta^{18}\text{O}_{\text{N}_2\text{O}}$ (corrected for $\delta^{18}\text{O}_{\text{H}_2\text{O}}$) for heterotrophic bacterial denitrification (bD), nitrifier denitrification (nD), nitrification (ni), and fungal denitrification (fD) (view Table S1 for details). The mixing line connects the mean values of bD and fD (mix_bD-fD) or bD and ni (mix_bD-ni), respectively. The slope of the reduction lines (red) is based on the isotopic fractionation factor associated with N_2O reduction to N_2 . Dashed line represents the minimum reduction line ($n = 178$, oxic incubation conditions from 0 DAO to 46 DAO, anoxic incubation conditions from 47 DAO to 55 DAO).

$\delta^{15}\text{N}_{\text{bulk}}$ and $\delta^{18}\text{O}_{\text{N}_2\text{O}}$ of soil-emitted N_2O followed a similar pattern. Both values increased slightly during anoxic incubation (Figures 4 and S6). With onset of anoxic conditions, both $\delta^{15}\text{N}_{\text{bulk}}$ and $\delta^{18}\text{O}_{\text{N}_2\text{O}}$ decreased strongly and increased again until the end of the experiment.

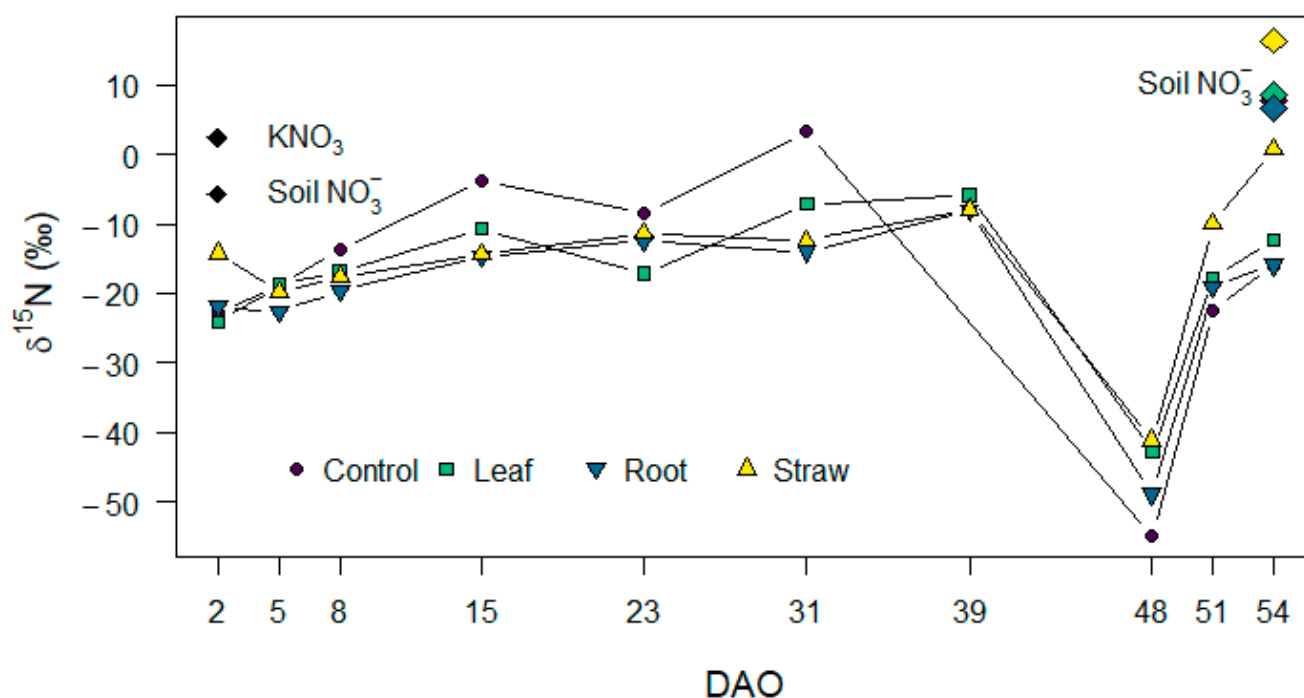


Figure 4. $\delta^{15}\text{N}_{\text{bulk}}$ of N_2O (colored symbols and lines), added KNO_3 and soil NO_3^- at first day of incubation (black symbols) and soil NO_3^- at last day of incubation (colored symbols with black borders) (means for $n = 5$, $n = 4$ for Control).

fbD and rN_2O values exhibited similar patterns for mixing between heterotrophic bacterial denitrification/nitrifier denitrification and nitrification or fungal denitrification (Figure 5a,b, Supplementary Figure S6). After onset of incubation, the fraction of soil-emitted N_2O from heterotrophic bacterial denitrification/nitrifier denitrification (fbD, Figure 5a) was in tendency higher in maize litter treatments compared to Control. While fbD decreased in maize litter treatments during the oxic incubation period, it increased in Control without litter addition. With onset of anoxic incubation conditions, fbD increased strongly in all treatments, reaching values > 0.9 , indicating that bacterial denitrification became the dominant process under anoxic incubation conditions. The residual, unreduced N_2O fraction (rN_2O , Figure 5b) was mostly < 0.5 and decreased during the oxic incubation phase, highlighting the significance of N_2O reduction. On 51 DAO, rN_2O was highest and decreased until 54 DAO.

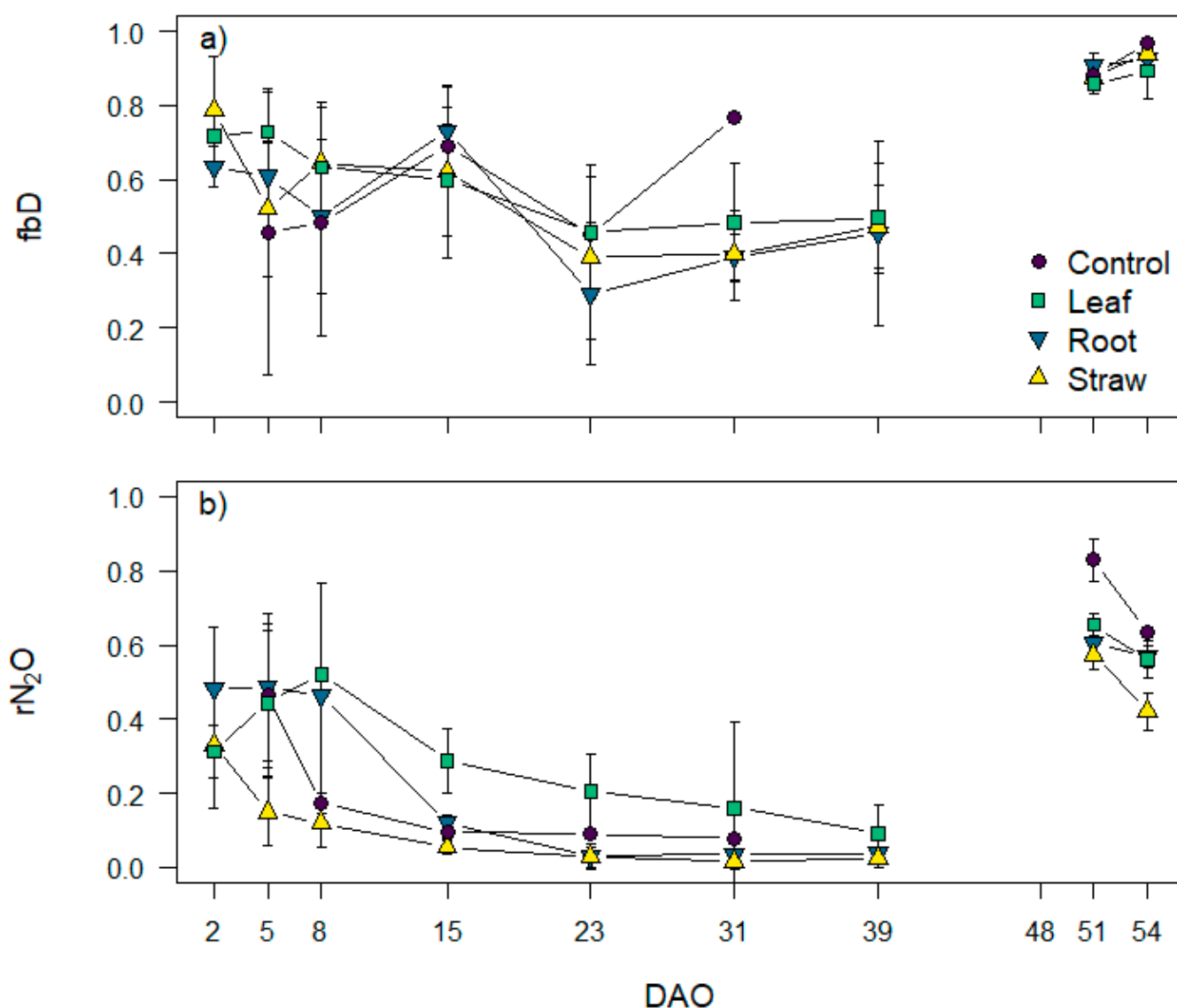


Figure 5. (a) Fraction of N_2O originating from heterotrophic bacterial denitrification/nitrifier denitrification (fbD) and (b) fraction of residual unreduced N_2O (rN₂O). Values were calculated based on the isotopocule mapping approach by Lewicka-Szczepak et al. (2017) [22] and represent results for scenario 1 (reduction-mixing) of bacterial denitrification with fungal denitrification (mean and standard deviation for $n = 5$, $n = 4$ for Control, data points missing for samples with an isotopic signature outside the reduction-mixing area, no N_2O emitted from Control on 39 DAO).

3.6. Interactions between C and N Availability and N Fluxes

To test the effect of C availability and SOM turnover on N fluxes and cumulative emissions, simple linear regression models were tested (Table 3).

The relationship between hourly $NO+N_2O$ and CO_2 fluxes was very weak during the oxic incubation phase (adj. $R^2 = 0.08$, $p < 0.001$, Table 3). In contrast, $NO+N_2O+N_2$ fluxes were highly positively correlated with CO_2 fluxes during the anoxic incubation period (adj. $R^2 = 0.86$, $p < 0.001$, Table 3). Similarly, fbD and rN₂O were positively correlated with total CO_2 flux from soil, but the relationship was weak (adj. $R^2 = 0.23$ and 0.31 , respectively, $p < 0.001$, Table 3).

Cumulative anoxic N emissions ($NO+N_2O+N_2$) were significantly positively correlated with total litter C input (adj. $R^2 = 0.51$, $p < 0.001$, Table 3). Furthermore, we found a significant negative correlation between the ratio of cumulative $N_2O/(N_2O+N_2)$ emissions during anoxic incubation and the ratio of water-soluble C:N of maize litter types (adj.

$R^2 = 0.51$, $p < 0.001$, Table 3) and also with the soil NO_3^- :WEOC ratio at the end of the experiment (adj. $R^2 = 0.41$, $p < 0.01$, Table 3). When standardized against C input from litter, total cumulative N emissions did not differ between litter treatments (Supplementary Table S2).

4. Discussion

4.1. Maize Litter Quality Controls N Mineralization

Soil mineral N content, mineralization, and immobilization strongly depended on maize litter quality. In Control without litter addition, soil NH_4^+ content decreased, but soil NO_3^- content strongly increased due to mineralization and nitrification of soil organic N. Tillage often leads to increased soil mineral N content [40,41], and net N mineralization from control soils without litter addition has been reported [8,13,42]. In Leaf and Root, mineralization was higher than in Control as additional organic N from litter was mineralized. In contrast, addition of maize straw immobilized N, which coincides with the higher C:N ratio in Straw compared to Leaf and Root. In general, immobilization of N follows the addition of litter with C:N ratios $> 25:1$ [7]. Net N mineralization after addition of maize roots is in contrast to most other studies reporting net N immobilization after addition of maize roots [8,13,42,43]. However, we used maize roots grown in a nutrient solution, which had higher total and water-soluble N content than those reported in other studies [13,44].

4.2. Effect of Maize Litter Quality on CO_2 Emissions and Priming Effect

After onset of incubation, both litter and SOM-derived CO_2 fluxes strongly increased in litter treatments, while CO_2 efflux in Control was stable. Total cumulative CO_2 emissions increased with increasing input of total and water-soluble C, indicating that decomposition dynamics were controlled by the amount and quality of added plant material. The chemical composition of plant litter is known to be a primary controller of decomposition rates of both roots [11,12,15] and aboveground plant litter [4,10].

Especially during the first week after litter addition, SOM turnover was increased in all litter treatments, leading to a positive priming effect. The highest increase in SOM turnover was observed after addition of maize leaves which were characterized by high amounts of easily degradable compounds as indicated by high shares of carboxyl C (i.e., organic acids, amino acids) and alkyl C (i.e., fatty acids, amino acids, paraffines) [45]. Litter and SOM-derived CO_2 fluxes followed the same pattern and were highly positively correlated confirming that litter and SOM turnover are interrelated. Thus, our results are in accordance with the concept that litter with high degradability increases SOM turnover leading to a positive priming effect [17–19].

4.3. Effect of Litter Quality and N Mineralization on N Emissions and Production Pathways under Oxidic Atmosphere

Directly after onset of oxic incubation, NO fluxes were highest in Control and Root while N_2O fluxes were higher in litter amended treatments than in Control. The ratio of $\text{NO}/\text{N}_2\text{O}$ can be used as an indicator whether NO is produced from nitrification or denitrification [46,47]. While the $\text{NO}/\text{N}_2\text{O}$ emission ratio of bacterial denitrification is mostly around 0.01, the emission ratios of $\text{NO}/\text{N}_2\text{O}$ from nitrification are often higher than 1 [47]. In our study, the emission ratio of $\text{NO}/\text{N}_2\text{O}$ was highest during the first 10 days after onset of incubation, with maximum values of 0.47 in Control indicating a high contribution of nitrification to NO formation. Analysis of soil samples taken prior to the onset of incubation revealed high NH_4^+ content of soil, which further supports that nitrification contributed to NO emissions during the initial incubation phase. In Straw, where N was immobilized to decompose C compounds, NO fluxes decreased faster and were lower than in all other treatments. Furthermore, oxic cumulative NO emissions strongly decreased with increasing litter C:N ratio (adj. $R^2 = 0.86$, $p < 0.001$) and increased with increasing N mineralization (adj. $R^2 = 0.57$, $p < 0.001$) confirming that litter quality affected nitrification-derived NO emissions in the beginning of the oxic incubation phase.

Addition of maize litter increased N_2O fluxes compared to non-amended Control. As first, the headspace atmosphere had to be replaced by the mixture of He/O_2 , measurements started approximately one day after onset of incubation conditions. At this time, decreasing N_2O fluxes indicated that N_2O fluxes had peaked within 24 h after water and NO_3^- addition. After this initial increase, N_2O fluxes decreased rapidly and then stayed on a similar level throughout the oxic phase. Immediately after onset of the incubation, bacterial denitrification (i.e., heterotrophic bacterial denitrification and nitrifier denitrification) was the dominant N_2O emitting process in litter-amended treatments as indicated by the fraction of bacterial denitrification (fbD) > 0.6 . Gradually decreasing fbD values then indicate a shift towards nitrification or fungal denitrification. Litter addition [27,48] and soil moisture of 70% WFPS may have promoted fungi, which often contribute to denitrification under weakly anoxic conditions [49,50]. Several studies have described a shift from bacterial to fungal dominance with ongoing incubations [27,51–53]. However, nitrification may have contributed to N_2O formation in Root and Leaf as indicated by high mineralization and $\text{NO}/\text{N}_2\text{O}$ ratio. In Control, nitrification presumably contributed to N_2O formation, especially during the first days of the experiment, when fbD was < 0.3 and the $\text{NO}/\text{N}_2\text{O}$ ratio was high.

$r\text{N}_2\text{O}$ values were mostly < 0.5 , highlighting the significance of N_2O reduction, also during the oxic incubation period. Thus, although N_2 fluxes were lower than the detection limit of our incubation system ($5.5 \mu\text{g N}_2\text{-N kg}^{-1} \text{ h}^{-1}$), they significantly contributed to gaseous N losses. N_2O reduction to N_2 is the last step of denitrification [54] and it usually takes place when availability of NO_x is limited [55]. Furthermore, pore size and distribution, and soil moisture may affect N_2O reduction to N_2 , as they control diffusion of O_2 and N_2O in soil [20,56]. Accordingly, for interpretation of the isotopocule mapping approach in our experiment, we think that the reduction-mixing scenario is more plausible: N_2O was produced by denitrifying bacteria and partly reduced to N_2 in anoxic microsites, and then N_2O diffusing out of these hotspots was mixed with N_2O from nitrification and fungal denitrification [57]. We anticipate that nitrification contributed to N_2O formation when mineralization was high, while fungal denitrification became more important in litter-amended treatments with ongoing incubation.

4.4. Effect of Maize Litter Quality and Mineralization on Potential Denitrification

With onset of anoxic incubation conditions on 47 DAO, total NO and N_2O fluxes increased rapidly, while N_2 fluxes increased more slowly. $\delta^{18}\text{O}_{\text{N}_2\text{O}}$ of N_2O emitted on 48 DAO falls in the range of heterotrophic bacterial denitrification reported in earlier studies [23], indicating that heterotrophic bacterial denitrification was the main N_2O -emitting process with low reduction to N_2 . Interestingly, the $\delta^{15}\text{N}^{\text{bulk}}$ values on 48 DAO strongly deviated from measured $\delta^{15}\text{N}^{\text{bulk}}$ values on all other sampling days and were slightly outside the reported endmember values of heterotrophic bacterial denitrification. Under oxic conditions, denitrification mostly took place in anoxic hotspots where ongoing reduction led to a fractionation in the NO_3^- pool undergoing denitrification, which is reflected in gradually increasing $\delta^{15}\text{N}^{\text{bulk}}$ values. With onset of anoxic conditions, previously unreduced NO_3^- contributed to N_2O formation leading to a shift towards more negative $\delta^{15}\text{N}^{\text{bulk}}$ values [29,58]. When the contribution of pools with different N dynamics changes, shifts in the isotopic signature have been reported [59–61]. For our study, low $\delta^{15}\text{N}^{\text{bulk}}$ values on 48 DAO are consistent with very high N_2O fluxes and the low measured $\text{N}_2\text{O}/(\text{N}_2\text{O} + \text{N}_2)$ ratio on 48 DAO leading to strong fractionation effects.

Analysis of $\delta^{15}\text{N}$ and $\delta^{18}\text{O}$ in soil NO_3^- may improve accuracy of the N_2O mapping approach and estimation of N_2O formation processes [23]. $\delta^{15}\text{N}_{\text{NO}_3}$ was higher at the end of the experiment compared to initial soil NO_3^- and added KNO_3 , confirming the ongoing fractionation during the reduction of the soil NO_3^- pool. Furthermore, $\delta^{15}\text{N}_{\text{NO}_3}$ increased with decreasing mineralization, indicating a higher share of added KNO_3 to residual NO_3^- at the end of the incubation experiment. Higher $\delta^{18}\text{O}$ in Straw and Root may point towards a higher contribution of fungal denitrification, which is consistent with

the higher contribution of fungi to decomposition of plant materials rich in celluloses and lignin [16,27]. Overall, it needs to be taken into account, that estimating N_2O formation processes based on N_2O isotopomers is subject to large uncertainties. Endmember values, reduction and fractionation factors have been obtained under differing incubation and environmental conditions, and may thus lead to over or underestimation of contributing processes [57,61,62].

4.5. Interaction between C Turnover and Denitrification

In agricultural soils, denitrification is often controlled by the availability of readily decomposable organic matter with increasing C availability leading to increased N losses [6,13,14,63,64]. In contrast, we measured low denitrification derived N fluxes under oxic conditions, and the correlation between oxic N and CO_2 fluxes was very weak indicating that denitrification was not directly affected by litter decomposition in our study. Although soil NO_3^- content was high and high litter and SOM turnover confirmed high C_{org} availability, N_2O fluxes were very low, indicating that conditions for denitrifying microorganisms were not optimal. Rohe et al. (2021) [65] reported very low $\text{N}_2\text{O} + \text{N}_2$ fluxes from an incubation study with the same soil at 60% WFPS and higher fluxes compared to our study for 75 and 85% WFPS. Thus, our incubation conditions with a soil moisture of 70% WFPS may have been too low to promote denitrifying soil microorganisms. With onset of anoxic conditions, N fluxes increased immediately, confirming that high pO_2 was restricting denitrification during the oxic incubation phase. In contrast to our expectations, the microbial respiration of litter and SOM did not promote the formation of litter associated anoxic hotspots for denitrification as high O_2 diffusivity limited denitrification [65,66].

In contrast, N and CO_2 fluxes were highly positively correlated (adj. $R^2 = 0.86$, $p < 0.001$) under anoxic conditions, and cumulative N emissions increased with increasing litter C input (adj. $R^2 = 0.51$, $p < 0.001$) confirming our hypothesis that higher C availability leads to increased gaseous N losses. However, this effect was based on the role of C as energy source for denitrifiers, as the potential O_2 consumption by C decomposition was not relevant under anoxic conditions.

The ratio of denitrification end products $\text{N}_2\text{O}/(\text{N}_2\text{O} + \text{N}_2)$ decreased with increasing water-extractable C:N ratio of litter (adj. $R^2 = 0.73$, $p < 0.001$) and increasing soil WEOC: NO_3^- ratio at the end of the experiment (adj. $R^2 = 0.41$, $p < 0.01$) confirming that the ratio of available C to oxidized N is a major control of denitrification product stoichiometry [67]. Immobilization of N after addition of maize straw with high C:N ratio restricted N availability leading to higher N_2O reduction to N_2 . However, as soil NO_3^- content was still very high ($> 70 \text{ mg NO}_3^- \text{-N kg}^{-1}$ in all treatments at the end of the incubation experiment), N_2O was the dominant end product, as NO_3^- is preferentially used as electron acceptor and high soil NO_3^- content can inhibit the reduction of N_2O to N_2 [27,67].

5. Conclusions

We investigated the effect of different maize litter types (young leaves and roots, straw) on CO_2 , NO, N_2O , and N_2 emissions under oxic and anoxic conditions in a laboratory incubation study. Addition of maize litter increased litter and SOM derived CO_2 emissions, leading to a positive priming effect. SOM priming was highest after addition of maize leaves with a high share of easily degradable C compounds during the first week after onset of incubation. Although litter and SOM turnover were high, NO and N_2O fluxes were low under oxic conditions as high O_2 diffusivity limited denitrification.

The NO/ N_2O ratio indicated that nitrification contributed to NO and N_2O formation during the first two weeks of incubation, especially in Control without litter addition. In the litter-amended treatments, isotopocule mapping revealed that bacterial denitrification dominated N_2O formation in the beginning of the incubation experiment with a subsequent shift towards fungal denitrification. With onset of anoxic incubation conditions after 47 days, N fluxes strongly increased and heterotrophic bacterial denitrification became the dominating source of N_2O . The $\text{N}_2\text{O}/(\text{N}_2\text{O} + \text{N}_2)$ ratio decreased with increasing litter

C:N ratio and $C_{org}:NO_3^-$ ratio in soil confirming that the ratio of available C:N is a major control of denitrification product stoichiometry.

Supplementary Materials: The following are available online at <https://www.mdpi.com/article/10.3390/app11115309/s1>, Figure S1a–c: Solid state ^{13}C -CPMAS NMR spectra of maize litter used in the incubation experiment, Figure S2: $\delta^{13}C$ of CO_2 derived from maize litter, Figure S3: Total CO_2 efflux from soil during oxic and anoxic incubation, Figure S4a: $\delta^{13}C$ of CO_2 evolving from soil and b: fraction of litter-derived CO_2 , Figure S5: NO/N_2O ratio during oxic and anoxic incubation, Figure S6: $\delta^{18}O$ of N_2O , added KNO_3 , and soil NO_3^- at first and last day of incubation, Figure S7a: Fraction of N_2O originating from heterotrophic bacterial denitrification/nitrifier denitrification and b+c: fraction of residual unreduced N_2O , Table S1: $\delta^{15}N^{SP}_{N_2O}$, $\delta^{18}O_{N_2O/H_2O}$, and $\delta^{15}N^{bulk}_{N_2O}$ endmember values from literature used for isotopocule mapping, Table S2: Cumulative CO_2 , NO , N_2O , and N_2 emissions and denitrification product ratio standardized against litter C input.

Author Contributions: Conceptualization: P.S.R., R.W., J.P., and K.D.; methodology (incubation system): P.S.R., B.P., K.D.; investigation: P.S.R.; data analysis: P.S.R.; data validation: P.S.R., R.W. and J.P.; writing—original draft preparation: P.S.R.; writing—review and editing: P.S.R., R.W., J.P., B.P., and K.D.; visualization: P.S.R.; supervision: R.W., J.P. and K.D.; funding acquisition: K.D. All authors have read and agreed to the published version of the manuscript.

Funding: This research work was supported by the Deutsche Forschungsgemeinschaft through the research unit DFG-FOR 2337: Denitrification in Agricultural Soils: Integrated Control and Modelling at Various Scales (DASIM, grant number DI 546/4-1). The APC was funded by the University of Göttingen.

Institutional Review Board Statement: Not applicable.

Informed Consent Statement: Not applicable.

Data Availability Statement: The datasets from this study can be found at <https://doi.org/10.25625/FKSRMX>.

Acknowledgments: We thank Simone Urstadt and Justus Detring for experimental and laboratory assistance and Jürgen Böttcher for soil classification. We acknowledge the Centre for Stable Isotope Research and Analysis of the University of Göttingen for all isotopic analyses, Jan Reent Köster for help with NO analysis, and Carsten W. Mueller for ^{13}C -CPMAS NMR analyses. Further, we thank Ronny Surey for discussions about plant litter effects under anoxic conditions.

Conflicts of Interest: The authors declare no conflict of interest. The funders had no role in the design of the study; in the collection, analyses, or interpretation of data; in the writing of the manuscript, or in the decision to publish the results.

References

1. Baggs, E.M.; Rees, R.M.; Smith, K.A.; Vinten, A.J.A. Nitrous oxide emission from soils after incorporating crop residues. *Soil Use Manag.* **2000**, *16*, 82–87. [CrossRef]
2. Chen, H.; Li, X.; Hu, F.; Shi, W. Soil nitrous oxide emissions following crop residue addition: A meta-analysis. *Glob. Chang. Biol.* **2013**, *19*, 2956–2964. [CrossRef]
3. Johnson, J.M.-F.; Barbour, N.W.; Weyers, S.L. Chemical Composition of Crop Biomass Impacts Its Decomposition. *Soil Sci. Soc. Am. J.* **2007**, *71*, 155–162. [CrossRef]
4. Zhang, D.; Hui, D.; Luo, Y.; Zhou, G. Rates of litter decomposition in terrestrial ecosystems: Global patterns and controlling factors. *J. Plant Ecol.* **2008**, *1*, 85–93. [CrossRef]
5. Li, X.; Hu, F.; Shi, W. Plant material addition affects soil nitrous oxide production differently between aerobic and oxygen-limited conditions. *Appl. Soil Ecol.* **2013**, *64*, 91–98. [CrossRef]
6. Millar, N.; Baggs, E.M. Chemical composition, or quality, of agroforestry residues influences N_2O emissions after their addition to soil. *Soil Biol. Biochem.* **2004**, *36*, 935–943. [CrossRef]
7. Robertson, G.P.; Groffman, P.M. Nitrogen Transformations. In *Soil Microbiology, Ecology and Biochemistry*; Paul, E.A., Ed.; Academic Press: Burlington, MA, USA, 2015; pp. 421–446. ISBN 9780128132692.
8. Velthof, G.L.; Kuikman, P.J.; Oenema, O. Nitrous oxide emission from soils amended with crop residues. *Nutr. Cycl. Agroecosyst.* **2002**, *62*, 249–261. [CrossRef]
9. Burford, J.R.; Bremner, J.M. Relationships between the denitrification capacities of soils and total, water-soluble and readily decomposable soil organic matter. *Soil Biol. Biochem.* **1975**, *7*, 389–394. [CrossRef]

10. Jensen, L.S.; Salo, T.; Palmason, F.; Breland, T.A.; Henriksen, T.M.; Stenberg, B.; Pedersen, A.; Lundström, C.; Esala, M. Influence of biochemical quality on C and N mineralisation from a broad variety of plant materials in soil. *Plant Soil* **2005**, *273*, 307–326. [\[CrossRef\]](#)
11. Redin, M.; Guénon, R.; Recous, S.; Schmatz, R.; de Freitas, L.L.; Aita, C.; Giacomini, S.J. Carbon mineralization in soil of roots from twenty crop species, as affected by their chemical composition and botanical family. *Plant Soil* **2014**, *378*, 205–214. [\[CrossRef\]](#)
12. Silver, W.L.; Miya, R.K. Global patterns in root decomposition: Comparisons of climate and litter quality effects. *Oecologia* **2001**, *129*, 407–419. [\[CrossRef\]](#) [\[PubMed\]](#)
13. Rummel, P.S.; Pfeiffer, B.; Pausch, J.; Well, R.; Schneider, D.; Dittert, K. Maize root and shoot litter quality controls short-term CO₂ and N₂O emissions and bacterial community structure of arable soil. *Biogeosciences* **2020**, *17*, 1181–1198. [\[CrossRef\]](#)
14. Surey, R.; Schimpf, C.M.; Sauheitl, L.; Mueller, C.W.; Rummel, P.S.; Dittert, K.; Kaiser, K.; Böttcher, J.; Mikutta, R. Potential denitrification stimulated by water-soluble organic carbon from plant residues during initial decomposition. *Soil Biol. Biochem.* **2020**. [\[CrossRef\]](#)
15. Birouste, M.; Kazakou, E.; Blanchard, A.; Roumet, C. Plant traits and decomposition: Are the relationships for roots comparable to those for leaves? *Ann. Bot.* **2012**, *109*, 463–472. [\[CrossRef\]](#) [\[PubMed\]](#)
16. Kögel-Knabner, I. The macromolecular organic composition of plant and microbial residues as inputs to soil organic matter. *Soil Biol. Biochem.* **2002**, *34*, 139–162. [\[CrossRef\]](#)
17. Six, J.; Jastrow, J.D. Organic Matter Turnover. In *Encyclopedia of Soil Science*; Lal, R., Ed.; Dekker: New York, NY, USA, 2002.
18. Kuzakov, Y.; Bol, R. Sources and mechanisms of priming effect induced in two grassland soils amended with slurry and sugar. *Soil Biol. Biochem.* **2006**, *38*, 747–758. [\[CrossRef\]](#)
19. Rinkes, Z.L.; DeForest, J.L.; Grandy, A.S.; Moorhead, D.L.; Weintraub, M.N. Interactions between leaf litter quality, particle size, and microbial community during the earliest stage of decay. *Biogeochemistry* **2014**, *117*, 153–168. [\[CrossRef\]](#)
20. Kravchenko, A.N.; Toosi, E.R.; Guber, A.K.; Ostrom, N.E.; Yu, J.; Azeem, K.; Rivers, M.L.; Robertson, G.P. Hotspots of soil N₂O emission enhanced through water absorption by plant residue. *Nat. Geosci.* **2017**, *10*, 496–500. [\[CrossRef\]](#)
21. Arcand, M.M.; Congreves, K.A. Elucidating microbial carbon utilization and nitrous oxide dynamics with ¹³C-substrates and N₂O isotopomers in contrasting horticultural soils. *Appl. Soil Ecol.* **2020**, *147*, 103401. [\[CrossRef\]](#)
22. Lewicka-Szczebak, D.; Augustin, J.; Giesemann, A.; Well, R. Quantifying N₂O reduction to N₂ based on N₂O isotopocules-validation with independent methods (helium incubation and ¹⁵N gas flux method). *Biogeosciences* **2017**, *14*, 711–732. [\[CrossRef\]](#)
23. Yu, L.; Harris, E.; Lewicka-Szczebak, D.; Barthel, M.; Blomberg, M.R.A.; Harris, S.J.; Johnson, M.S.; Lehmann, M.F.; Liisberg, J.; Müller, C.; et al. What can we learn from N₂O isotope data?—Analytics, processes and modelling. *Rapid Commun. Mass Spectrom.* **2020**, *34*, 1–14. [\[CrossRef\]](#) [\[PubMed\]](#)
24. Mengutay, M.; Ceylan, Y.; Kutman, U.B.; Cakmak, I. Adequate magnesium nutrition mitigates adverse effects of heat stress on maize and wheat. *Plant Soil* **2013**, *368*, 57–72. [\[CrossRef\]](#)
25. Köster, J.R.; Well, R.; Dittert, K.; Giesemann, A.; Lewicka-Szczebak, D.; Mühling, K.H.; Herrmann, A.; Lammel, J.; Senbayram, M. Soil denitrification potential and its influence on N₂O reduction and N₂O isotopomer ratios. *Rapid Commun. Mass Spectrom.* **2013**, *27*, 2363–2373. [\[CrossRef\]](#)
26. Scholefield, D.; Hawkins, J.M.B.B.; Jackson, S.M. Development of a helium atmosphere soil incubation technique for direct measurement of nitrous oxide and dinitrogen fluxes during denitrification. *Soil Biol. Biochem.* **1997**, *29*, 1345–1352. [\[CrossRef\]](#)
27. Senbayram, M.; Well, R.; Bol, R.; Chadwick, D.R.; Jones, D.L.; Wu, D. Interaction of straw amendment and soil NO₃[−] content controls fungal denitrification and denitrification product stoichiometry in a sandy soil. *Soil Biol. Biochem.* **2018**, *126*, 204–212. [\[CrossRef\]](#)
28. Wang, R.; Willibald, G.; Feng, Q.; Zheng, X.; Liao, T.; Brüggemann, N.; Butterbach-Bahl, K. Measurement of N₂, N₂O, NO, and CO₂ emissions from soil with the gas-flow-soil-core technique. *Environ. Sci. Technol.* **2011**, *45*, 6066–6072. [\[CrossRef\]](#) [\[PubMed\]](#)
29. Lewicka-Szczebak, D.; Well, R.; Köster, J.R.; Fuß, R.; Senbayram, M.; Dittert, K.; Flessa, H. Experimental determinations of isotopic fractionation factors associated with N₂O production and reduction during denitrification in soils. *Geochim. Cosmochim. Acta* **2014**, *134*, 55–73. [\[CrossRef\]](#)
30. Toyoda, S.; Yoshida, N. Determination of Nitrogen Isotopomers of Nitrous. *Anal. Chem.* **1999**, *71*, 4711–4718. [\[CrossRef\]](#)
31. Buchen, C.; Lewicka-Szczebak, D.; Flessa, H.; Well, R. Estimating N₂O processes during grassland renewal and grassland conversion to maize cropping using N₂O isotopocules. *Rapid Commun. Mass Spectrom.* **2018**, *32*, 1053–1067. [\[CrossRef\]](#) [\[PubMed\]](#)
32. Röckmann, T.; Kaiser, J.; Brenninkmeijer, C.A.M.; Brand, W.A. Gas chromatography/isotope-ratio mass spectrometry method for high-precision position-dependent ¹⁵N and ¹⁸O measurements of atmospheric nitrous oxide. *Rapid Commun. Mass Spectrom.* **2003**, *17*, 1897–1908. [\[CrossRef\]](#) [\[PubMed\]](#)
33. Lewicka-Szczebak, D. Mapping approach model after Lewicka-Szczebak et al. (2017)-detailed description of calculation procedures. *RG* **2018**. [\[CrossRef\]](#)
34. Casciotti, K.L.; Sigman, D.M.; Hastings, M.G.; Böhlke, J.K.; Hilkert, A. Measurement of the oxygen isotopic composition of nitrate in seawater and freshwater using the denitrifier method. *Anal. Chem.* **2002**, *74*, 4905–4912. [\[CrossRef\]](#)
35. Sigman, D.M.; Casciotti, K.L.; Andreani, M.; Barford, C.; Galanter, M.; Böhlke, J.K. A bacterial method for the nitrogen isotopic analysis of nitrate in seawater and freshwater. *Anal. Chem.* **2001**, *73*, 4145–4153. [\[CrossRef\]](#)
36. R Core Team R: A Language and Environment for Statistical Computing 2019. R version 3.6.0 – “Planting of a Tree”; R Foundation for Statistical Computing: Vienna, Austria, 2019.

37. Blackmon, H.; Adams, R.H. *evobiR: Comparative and Population Genetic Analyses 2015. R Package Version 1.1*; R Foundation for Statistical Computing: Vienna, Austria, 2015.
38. Zeileis, A.; Grothendieck, G. zoo: S3 Infrastructure for Regular and Irregular Time Series. *J. Stat. Softw.* **2005**, *14*, 1–27. [[CrossRef](#)]
39. Garnier, S. *viridisLite: Default Color Maps from “matplotlib” (Lite Version) 2018. R Package Version 0.3.0*; R Foundation for Statistical Computing: Vienna, Austria, 2018.
40. Höper, H. Carbon and nitrogen mineralisation rates of fens in Germany used for agriculture. In *Wetlands in Central Europe*; Broll, G., Merbach, W., Pfeiffer, E.M., Eds.; Springer: Berlin/Heidelberg, Germany, 2002; pp. 149–164. ISBN 978-3-662-05054-5.
41. Kristensen, H.L.; Debosz, K.; McCarty, G.W. Short-term effects of tillage on mineralization of nitrogen and carbon in soil. *Soil Biol. Biochem.* **2003**, *35*, 979–986. [[CrossRef](#)]
42. Machinet, G.E.; Bertrand, I.; Chabbert, B.; Recous, S. Decomposition in soil and chemical changes of maize roots with genetic variations affecting cell wall quality. *Eur. J. Soil Sci.* **2009**, *60*, 176–185. [[CrossRef](#)]
43. Mary, B.; Fresneau, C.; Morel, J.L.; Mariotti, A. C and N cycling during decomposition of root mucilage, roots and glucose in soil. *Soil Biol. Biochem.* **1993**, *25*, 1005–1014. [[CrossRef](#)]
44. Machinet, G.E.; Bertrand, I.; Barrière, Y.; Chabbert, B.; Recous, S. Impact of plant cell wall network on biodegradation in soil: Role of lignin composition and phenolic acids in roots from 16 maize genotypes. *Soil Biol. Biochem.* **2011**, *43*, 1544–1552. [[CrossRef](#)]
45. Knicker, H. Solid state CPMAS ¹³C and ¹⁵N NMR spectroscopy in organic geochemistry and how spin dynamics can either aggravate or improve spectra interpretation. *Org. Geochem.* **2011**, *42*, 867–890. [[CrossRef](#)]
46. Cheng, W.; Tsuruta, H.; Chen, G.; Yagi, K. N₂O and NO production in various Chinese agricultural soils by nitrification. *Soil Biol. Biochem.* **2004**, *36*, 953–963. [[CrossRef](#)]
47. Skiba, U.; Fowler, D.; Smith, K.A. Nitric oxide emissions from agricultural soils in temperate and tropical climates: Sources, controls and mitigation options. *Nutr. Cycl. Agroecosyst.* **1997**, *48*, 139–153. [[CrossRef](#)]
48. Chen, H.; Mothapo, N.V.; Shi, W. Fungal and bacterial N₂O production regulated by soil amendments of simple and complex substrates. *Soil Biol. Biochem.* **2015**, *84*, 116–126. [[CrossRef](#)]
49. Hayatsu, M.; Tago, K.; Saito, M. Various players in the nitrogen cycle: Diversity and functions of the microorganisms involved in nitrification and denitrification. *Soil Sci. Plant Nutr.* **2008**, *54*, 33–45. [[CrossRef](#)]
50. Lavrent'ev, R.B.; Zaitsev, S.A.; Sudnitsyn, I.I.; Kurakov, A.V. Nitrous oxide production by fungi in soils under different moisture levels. *Moscow Univ. Soil Sci. Bull.* **2008**, *63*, 178–183. [[CrossRef](#)]
51. Laughlin, R.J.; Stevens, R.J. Evidence for Fungal Dominance of Denitrification and Codenitrification in a Grassland Soil. *Soil Sci. Soc. Am. J.* **2002**, *66*, 1540–1548. [[CrossRef](#)]
52. Wu, D.; Senbayram, M.; Well, R.; Brüggemann, N.; Pfeiffer, B.; Loick, N.; Stempfhuber, B.; Dittert, K.; Bol, R. Nitrification inhibitors mitigate N₂O emissions more effectively under straw-induced conditions favoring denitrification. *Soil Biol. Biochem.* **2017**, *104*, 197–207. [[CrossRef](#)]
53. Zhong, L.; Bowatte, S.; Newton, P.C.D.; Hoogendoorn, C.J.; Luo, D. An increased ratio of fungi to bacteria indicates greater potential for N₂O production in a grazed grassland exposed to elevated CO₂. *Agric. Ecosyst. Environ.* **2018**, *254*, 111–116. [[CrossRef](#)]
54. Zumft, W.G. Cell biology and molecular basis of denitrification. *Microbiol. Mol. Biol. Rev.* **1997**, *61*, 533–616. [[CrossRef](#)] [[PubMed](#)]
55. Firestone, M.K.; Smith, M.S.; Firestone, R.B.; Tiedje, J.M. The Influence of Nitrate, Nitrite, and Oxygen on the Composition of the Gaseous Products of Denitrification in Soil. *Soil Sci. Soc. Am. J.* **1979**, *43*, 1140–1144. [[CrossRef](#)]
56. Schlüter, S.; Henjes, S.; Zawallich, J.; Bergaust, L.; Horn, M.; Ippisch, O.; Vogel, H.-J.; Dörsch, P. Denitrification in Soil Aggregate Analogues-Effect of Aggregate Size and Oxygen Diffusion. *Front. Environ. Sci.* **2018**, *6*, 1–10. [[CrossRef](#)]
57. Wu, D.; Well, R.; Cárdenas, L.M.; Fuß, R.; Lewicka-Szczebak, D.; Köster, J.R.; Brüggemann, N.; Bol, R. Quantifying N₂O reduction to N₂ during denitrification in soils via isotopic mapping approach: Model evaluation and uncertainty analysis. *Environ. Res.* **2019**, *179*, 1–6. [[CrossRef](#)]
58. Ostrom, N.E.; Piit, A.; Sutka, R.; Ostrom, P.H.; Grandy, A.S.; Huizinga, K.M.; Robertson, G.P. Isotopologue effects during N₂O reduction in soils and in pure cultures of denitrifiers. *J. Geophys. Res. Biogeosci.* **2007**, *112*, 1–12. [[CrossRef](#)]
59. Bergstermann, A.; Cárdenas, L.; Bol, R.; Gilliam, L.; Goulding, K.; Meijide, A.; Scholefield, D.; Vallejo, A.; Well, R. Effect of antecedent soil moisture conditions on emissions and isotopologue distribution of N₂O during denitrification. *Soil Biol. Biochem.* **2011**, *43*, 240–250. [[CrossRef](#)]
60. Cardenas, L.M.; Bol, R.; Lewicka-Szczebak, D.; Gregory, A.S.; Matthews, G.P.; Whalley, W.R.; Misselbrook, T.H.; Scholefield, D.; Well, R. Effect of soil saturation on denitrification in a grassland soil. *Biogeosciences* **2017**, *14*, 4691–4710. [[CrossRef](#)]
61. Lewicka-Szczebak, D.; Well, R.; Bol, R.; Gregory, A.S.; Matthews, G.P.; Misselbrook, T.; Whalley, W.R.; Cardenas, L.M. Isotope fractionation factors controlling isotopocule signatures of soil-emitted N₂O produced by denitrification processes of various rates. *Rapid Commun. Mass Spectrom.* **2015**, *29*, 269–282. [[CrossRef](#)]
62. Lewicka-Szczebak, D.; Piotr Lewicki, M.; Well, R. N₂O isotope approaches for source partitioning of N₂O production and estimation of N₂O reduction-validation with the ¹⁵N gas-flux method in laboratory and field studies. *Biogeosciences* **2020**, *17*, 5513–5537. [[CrossRef](#)]
63. Azam, F.; Müller, C.; Weiske, A.; Benckiser, G.; Ottow, J.C.G. Nitrification and denitrification as sources of atmospheric nitrous oxide-Role of oxidizable carbon and applied nitrogen. *Biol. Fertil. Soils* **2002**, *35*, 54–61. [[CrossRef](#)]

64. Millar, N.; Baggs, E.M. Relationships between N₂O emissions and water-soluble C and N contents of agroforestry residues after their addition to soil. *Soil Biol. Biochem.* **2005**, *37*, 605–608. [[CrossRef](#)]
65. Rohe, L.; Apelt, B.; Vogel, H.-J.; Well, R.; Wu, G.-M.; Schlüter, S. Denitrification in soil as a function of oxygen supply and demand at the microscale. *Biogeosciences* **2021**, 1–32.
66. Schlüter, S.; Zawallich, J.; Vogel, H.J.; Dörsch, P. Physical constraints for respiration in microbial hotspots in soil and their importance for denitrification. *Biogeosciences* **2019**, *16*, 3665–3675. [[CrossRef](#)]
67. Firestone, M.K. Biological denitrification. In *Nitrogen in Agricultural Soils, Agronomy Monograph*; American Society of Agronomy, Inc.: Madison, WI, USA; Crop Science Society of America, Inc.: Madison, WI, USA; Soil Science Society of America, Inc.: Madison, WI, USA, 1982; Volume 22, pp. 289–326. [[CrossRef](#)]

Supplementary: Carbon Availability and Nitrogen Mineralization Control Denitrification Rates and Product Stoichiometry During Initial Maize Litter Decomposition

Pauline Sophie Rummel ^{1,*}, Reinhard Well ², Johanna Pausch ³, Birgit Pfeiffer ^{1,4} and Klaus Dittert ¹

¹ Section of Plant Nutrition and Crop Physiology, Department of Crop Science, University of Göttingen, 37073 Göttingen, Germany; Birgit.Pfeiffer@biologie.uni-goettingen.de (B.P.); klaus.dittert@agr.uni-goettingen.de (K.D.)

² Thünen Institute of Climate-Smart Agriculture, Federal Research Institute for Rural Areas, Forestry and Fisheries, 38116 Braunschweig, Germany; reinhard.well@thuenen.de

³ Agroecology, Faculty for Biology, Chemistry, and Earth Sciences, University of Bayreuth, 95447 Bayreuth, Germany; Johanna.Pausch@uni-bayreuth.de

⁴ Institute of Microbiology and Genetics, Department of Genomic and Applied Microbiology, University of Göttingen, 37073 Göttingen, Germany

* Correspondence: pauline.rummel@uni-goettingen.de

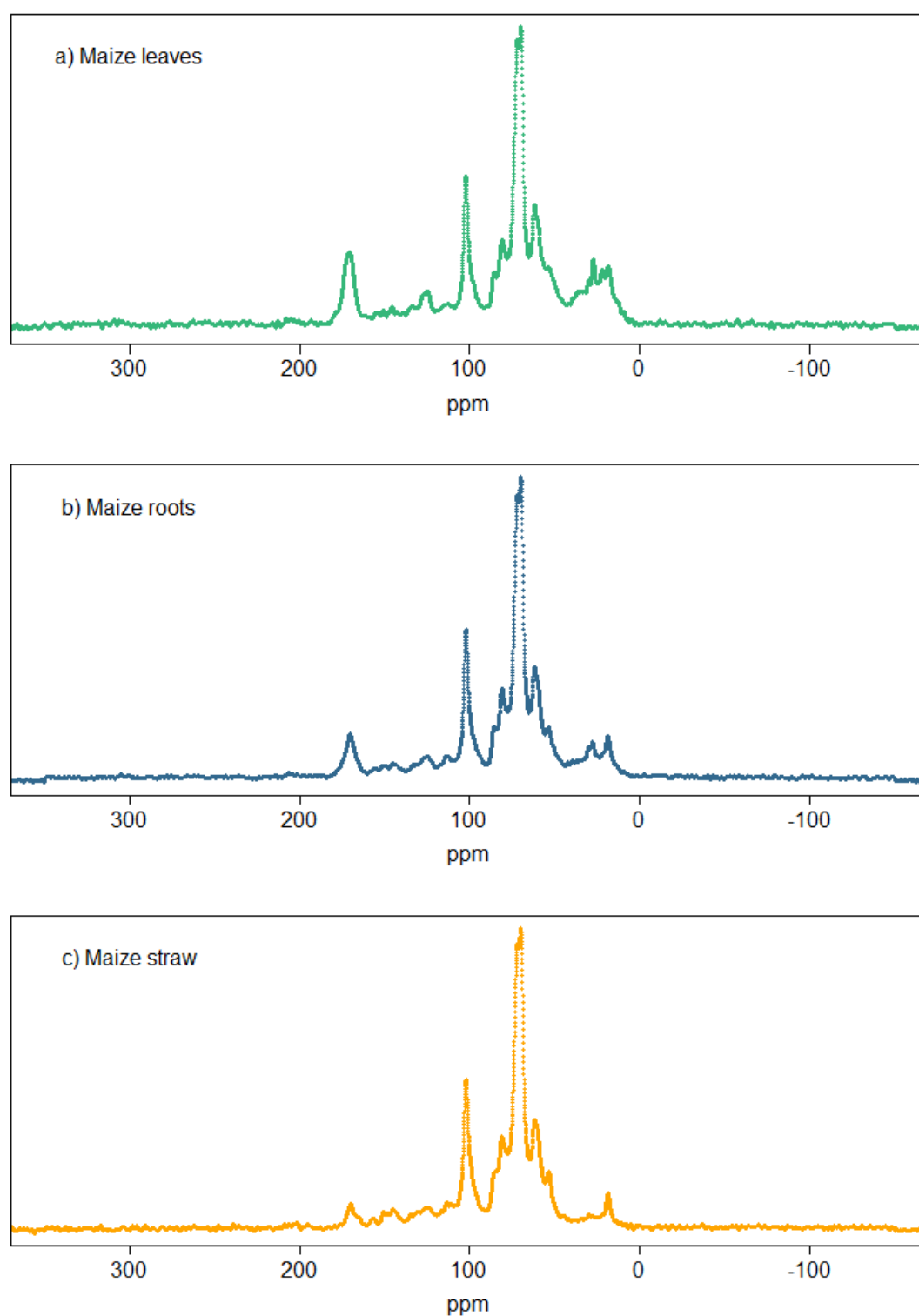


Figure S1. a–c: Solid state ^{13}C -CPMAS NMR spectra of maize litter used in the incubation experiment.

Determination of $\delta^{13}\text{C}$ of CO_2 respired from maize litter

To determine the $\delta^{13}\text{C}$ of CO_2 released from maize litter decomposition, dried maize litter was incubated without soil. Then, 20 g of washed quartz sand were filled into 100 ml glass bottles. Dried and ground maize litter was mixed with sand in amounts equaling 2 mg C g^{-1} . To provide incubation conditions similar to the main experiment, 70 g of pre-incubated soil was homogenized with 140 ml of $\text{H}_2\text{O}_{\text{bidest}}$ and stirred for 45 min. The soil suspension was filtered through paper filters and centrifuged at 5000 rpm for 30 min. The supernatant was discarded, and the pellet was resuspended in KNO_3 solution. Two milliliters of the soil-microorganisms- KNO_3 solution were added to the sand-litter-mixture providing $50 \mu\text{g N g}^{-1}$.

Gas samples were taken from the gas bottles 1, 5, 9, 14, 19, 26, and 33 days after mixing. Before sampling, bottles were flushed for 30 min with HeO_2 (80:20) at a flowrate of 50 ml min^{-1} to remove any CO_2 from the bottles. Then, soil gases were accumulated in the bottles for 60 min and 25 ml of gas samples were filled in evacuated 12 ml Exetainer® septum-capped vials (Labco, High Wycombe, UK). Samples were introduced by a Combi-Pal autosampler (CTC-Analytics, Zwingen, Switzerland) to a GC (GC-Box, Thermo Fisher Scientific, Bremen, Germany) coupled to an isotope mass spectrometer (Delta plus XP, Thermo Fisher Scientific, Bremen, Germany) via a ConFlo III Interface (Thermo Fisher Scientific, Bremen, Germany).

$\delta^{13}\text{C}$ values of CO_2 derived from litter are shown in Figure S2. On the first sampling day, values were similar to the Control without litter (-13.75‰). Thus, the mean of 5 to 33 DAO was taken as the average $\delta^{13}\text{C}$ of CO_2 derived from maize litter (Leaf = -7.910‰ , Root = -7.497‰ , Straw = -9.327‰).

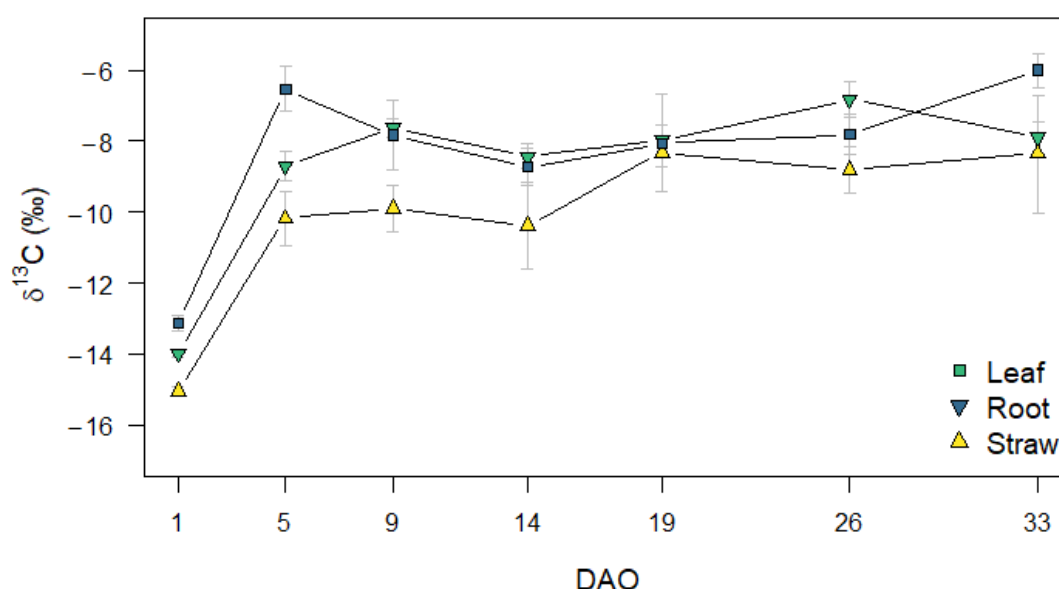


Figure S2. $\delta^{13}\text{C}$ of CO_2 derived from maize litter.

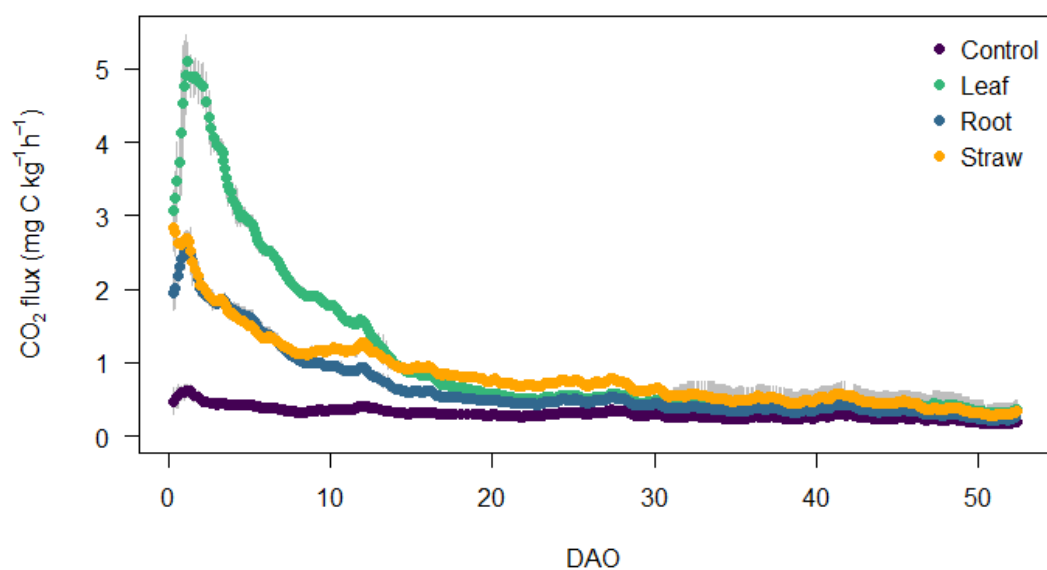


Figure S3. Total CO₂ efflux from soil during oxic incubation from Day 0 to Day 46 and during an-oxic incubation from Day 47 to Day 55 (means and standard deviation for n = 5, n = 4 for Control, when not visible, error bars are smaller than the symbols).

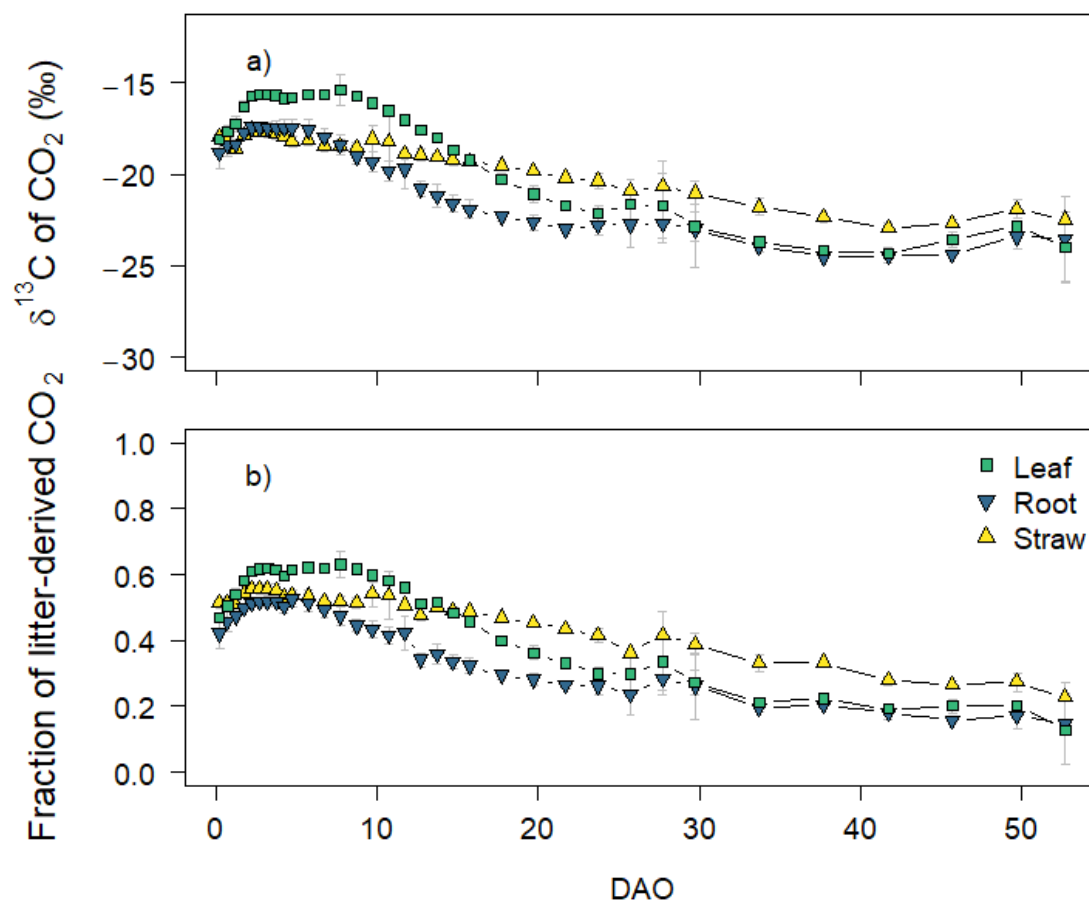


Figure S4. a: $\delta^{13}\text{C}$ of CO_2 evolving from soil and b: fraction of litter-derived CO_2 (means and standard deviation for $n = 5$, $n = 4$ for Control, when not visible, error bars are smaller than the symbols).

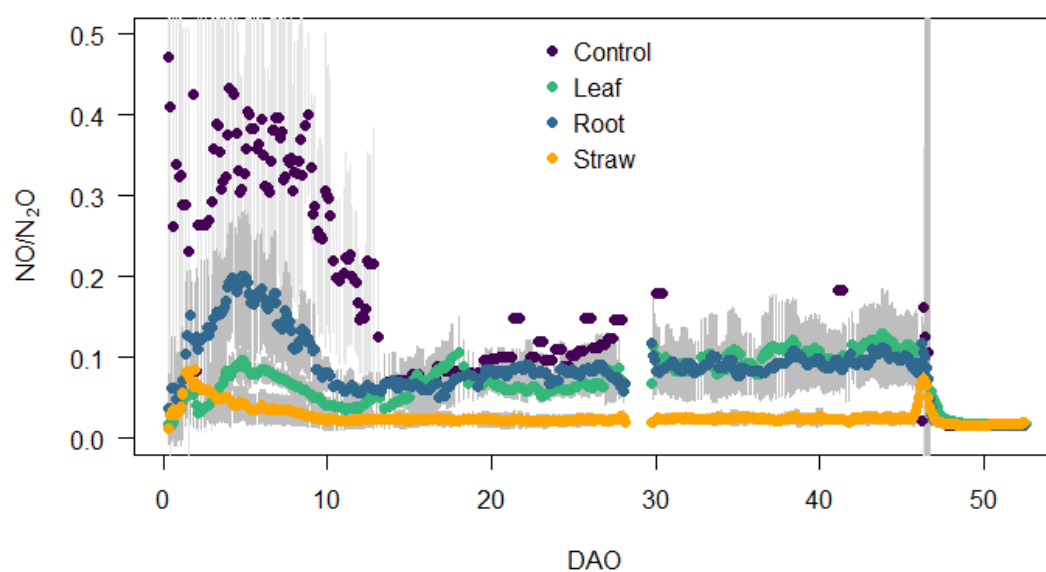


Figure S5. NO/N₂O ratio during oxenic incubation from Day 0 to Day 46 and during anoxic incubation from Day 47 to Day 55 (means and standard deviation for n = 5, n = 4 for Control, when not visible, error bars are smaller than the symbols).

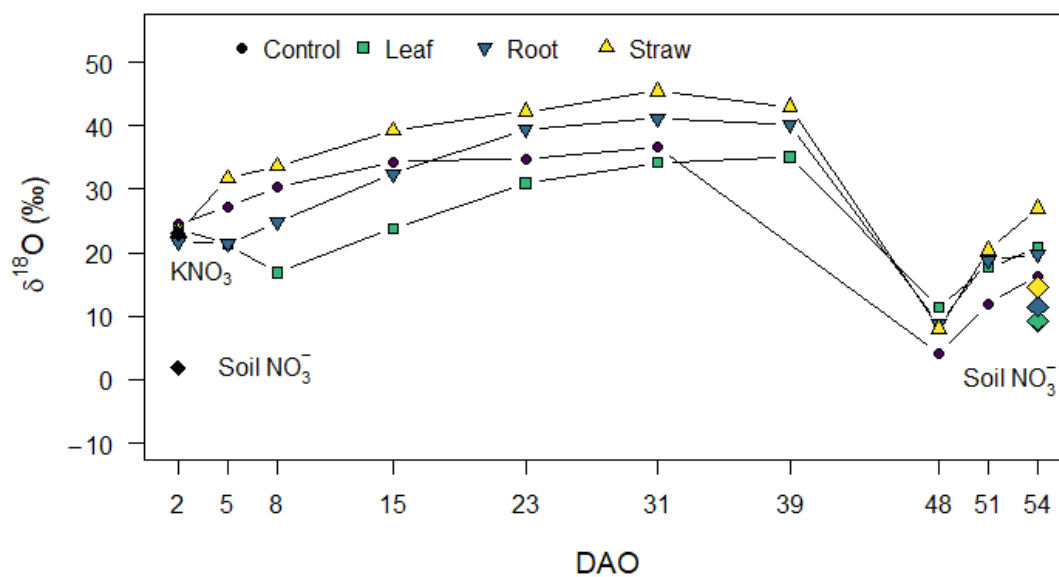


Figure S6. $\delta^{18}\text{O}$ of N_2O (colored symbols and lines), added KNO_3 , and soil NO_3^- at first and last day of incubation. $\delta^{18}\text{O}$ of N_2O was corrected for $\delta^{18}\text{O}$ of soil water (-6.7 ‰) (means for $n = 5$, $n = 4$ for Control).

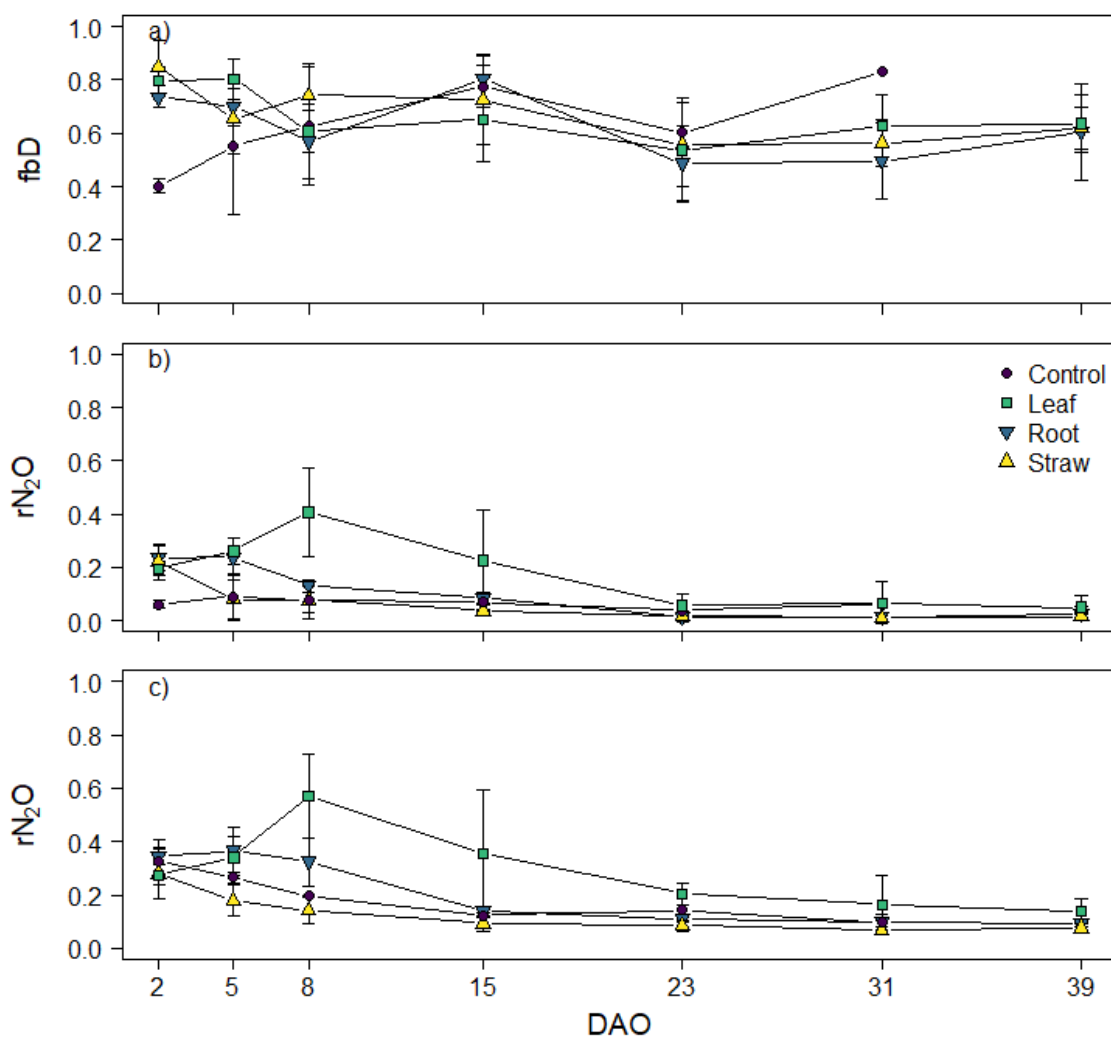


Figure S7. a: Fraction of N₂O originating from heterotrophic bacterial denitrification/nitrifier denitrification (fbD) and b+c: fraction of residual unreduced N₂O (rN₂O). Values were calculated based on the isotopocule mapping approach by Lewicka-Szczebak et al. (2017) [1] and represent results for scenario 1 (b, reduction-mixing) and scenario 2 (c, mixing-reduction) of bacterial denitrification with nitrification (mean and standard deviation for n = 5, data points missing for samples with an isotopic signature outside the reduction-mixing area, no N₂O emitted from Control on 39 DAO).

Table S1. $\delta^{15}\text{N}^{\text{SP}}_{\text{N}_2\text{O}}$, $\delta^{18}\text{O}_{\text{N}_2\text{O}/\text{H}_2\text{O}}$, and $\delta^{15}\text{N}^{\text{bulk}}_{\text{N}_2\text{O}}$ endmember values from literature used for isotopocouple mapping.

Process	$\delta^{15}\text{N}^{\text{SP}}_{\text{N}_2\text{O}}$			$\delta^{18}\text{O}_{\text{N}_2\text{O}/\text{H}_2\text{O}}$			$\delta^{15}\text{N}^{\text{bulk}}_{\text{N}_2\text{O}}$			References
	Min	Max	Mean	Min	Max	Mean	Min	Max	Mean	
Heterotrophic bacterial denitrification	-7.5	3.7	-1.9	16.7	23.3	19.2	-52.8	2.3	-25.9	[2–5]
Nitrifier denitrification	-13.6	1.9	-5.9	12.4	19.4	15.9	-60.7	-53.1	-56.9	[3,6]
Fungal denitrification	27.2	39.9	33.5	42.0	55.1	47.2	-46.0	-31.0	-38.0	[7–10]
Nitrification	32.0	38.7	35.0	20.5	26.5	23.5	-64.0	-47.0	-57.0	[3,6]

Table S2: Cumulative CO₂, NO, N₂O, and N₂ emissions and denitrification product ratio standardized against litter C input.

	Total CO ₂		Total N ₂ O		Total N ₂		Total NO		N ₂ O/(N ₂ O+N ₂)	
	(mg C g ⁻¹ C input)		(mg N g ⁻¹ C input)		(mg N g ⁻¹ C input)		(mg N g ⁻¹ C input)			
Maize Leaves	240.2 ± 22.5	n.s.	5.73 ± 1.72	n.s.	1.30 ± 0.84	n.s.	0.13 ± 0.02	n.s.	0.83 ± 0.04	a
Maize Roots	227.9 ± 20.7	n.s.	6.62 ± 0.46	n.s.	1.15 ± 0.48	n.s.	0.13 ± 0.02	n.s.	0.85 ± 0.05	a
Maize Straw	220.1 ± 7.8	n.s.	5.74 ± 0.20	n.s.	1.90 ± 0.48	n.s.	0.11 ± 0.01	n.s.	0.75 ± 0.05	b

Values represent means (n = 5) ± standard deviation. Different letters in the same column indicate a significant difference according to the LSD post hoc tests at p ≤ 0.05. n.s. indicates no significant difference.

References

1. Lewicka-Szczebak, D.; Augustin, J.; Giesemann, A.; Well, R. Quantifying N₂O reduction to N₂ based on N₂O isotopocules-validation with independent methods (helium incubation and ¹⁵N gas flux method). *Biogeosciences* **2017**, *14*, 711–732, doi:10.5194/bg-14-711-2017.
2. Toyoda, S.; Muto, H.; Yamagishi, H.; Yoshida, N.; Tanji, Y. Fractionation of N₂O isotopomers during production by denitrifier. *Soil Biol. Biochem.* **2005**, *37*, 1535–1545, doi:10.1016/j.soilbio.2005.01.009.
3. Sutka, R.L.; Ostrom, N.E.; Ostrom, P.H.; Breznak, J.A.; Gandhi, H.; Pitt, A.J.; Li, F. Distinguishing Nitrous Oxide Production from Nitrification and Denitrification on the Basis of Isotopomer Abundances. *Appl. Environ. Microbiol.* **2006**, *72*, 638–644, doi:10.1128/AEM.72.1.638–644.2006.
4. Kool, D.M.; Wragg, N.; Oenema, O.; Van Kessel, C.; Van Groenigen, J.W. Oxygen exchange with water alters the oxygen isotopic signature of nitrate in soil ecosystems. *Soil Biol. Biochem.* **2011**, *43*, 1180–1185, doi:10.1016/j.soilbio.2011.02.006.
5. Snider, D.M.; Venkiteswaran, J.J.; Schiff, S.L.; Spoelstra, J. A new mechanistic model of $\delta^{18}\text{O}$ -N₂O formation by denitrification. *Geochim. Cosmochim. Acta* **2013**, *112*, 102–115, doi:10.1016/j.gca.2013.03.003.
6. Frame, C.H.; Casciotti, K.L. Biogeochemical controls and isotopic signatures of nitrous oxide production by a marine ammonia-oxidizing bacterium. *Biogeosciences* **2010**, *7*, 2695–2709, doi:10.5194/bg-7-2695-2010.
7. Rohe, L.; Well, R.; Lewicka-Szczebak, D. Use of oxygen isotopes to differentiate between nitrous oxide produced by fungi or bacteria during denitrification. *Rapid Commun. Mass Spectrom.* **2017**, *31*, 1297–1312, doi:10.1002/rcm.7909.
8. Rohe, L.; Anderson, T.H.; Braker, G.; Flessa, H.; Giesemann, A.; Lewicka-Szczebak, D.; Wragg-Mönnig, N.; Well, R. Dual isotope and isotopomer signatures of nitrous oxide from fungal denitrification - A pure culture study. *Rapid Commun. Mass Spectrom.* **2014**, *28*, 1893–1903, doi:10.1002/rcm.6975.
9. Maeda, K.; Spor, A.; Edel-Hermann, V.; Heraud, C.; Breuil, M.C.; Bizouard, F.; Toyoda, S.; Yoshida, N.; Steinberg, C.; Philippot, L. N₂O production, a widespread trait in fungi. *Sci. Rep.* **2015**, *5*, 1–7, doi:10.1038/srep09697.
10. Sutka, R.L.; Adams, G.C.; Ostrom, N.E.; Ostrom, P.H. Isotopologue fractionation during N₂O production by fungal denitrification. *Rapid Commun. Mass Spectrom.* **2008**, *22*, 3989, doi:10.1002/rcm.3820.

DISCUSSION

Plants control C_{org} and NO_3^- availability for denitrification

The presence of plants or plant litter increased C_{org} availability in all studies presented in this thesis. Together with NO_3^- availability from fertilization and mineralization, it largely controlled N_2O+N_2 emissions and the $N_2O/(N_2O+N_2)$ product ratio.

Growing plants contribute to C input into the soil through rhizodeposition, dying roots and root hairs. Accordingly, ^{13}C recovery in soil increased with root dry mass in the first chapter. Plant NO_3^- uptake after labeling also increased with root dry mass. In treatments that had received N fertilizer before labeling, mineralization further increased N availability. However, low soil mineral N content at the end of the experiment indicated that most mineralized N was also taken up by plants. In these treatments with rapid NO_3^- uptake, N_2O+N_2 fluxes remained low during the whole experiment, while reduced NO_3^- uptake resulted in substantial N_2O+N_2 emissions from denitrification. Although C exudation was higher in plants with larger root dry mass, it did not increase N_2O+N_2 emissions as NO_3^- was limiting denitrification.

Other studies have reported a strong increase of N_2O and N_2 emissions with root growth during the first 20-30 days after emergence (Klemedtsson et al., 1987; Senbayram et al., 2020; Stefanson, 1972). However, with increasing plant growth, soil NO_3^- content and N_2O emissions decreased (Haider et al., 1985). Similar to our study, von Rheinbaben and Trolldenier (1984) reported reduced denitrification with optimal plant growth whereas high N_2O production was observed only when reduced crop growth restricted water and NO_3^- uptake. Potentially, C_{org} availability from rhizodeposition stimulates denitrification only in the early stages of plant growth when plant N uptake is low and NO_3^- is abundant in soil. With increasing plant and root growth, N uptake increases and lower NO_3^- availability restricts denitrification although C_{org} is readily available.

In both litter experiments, the addition of litter increased CO₂ emissions compared to control treatments indicating higher C availability and higher microbial activity (chapter 2 and 3). Furthermore, litter chemical quality affected CO₂ emissions: total CO₂ emissions increased with input of water-soluble C (Chapter 2) and litter with a high share of easily degradable C compounds led to increased microbial C use from litter (Chapter 3).

Tillage often increases soil mineral N content (Höper, 2002; Kristensen et al., 2003). Similarly, mixing of soil after plant growth or pre-incubation enhanced mineralization of organic N (Chapters 2 and 3). When easily degradable litter was added, N mineralization was higher than in control treatments without litter addition. In contrast, addition of litter with high C:N ratio or low share of easily available N led to an immobilization of N. When soil NO₃⁻ content was low, immobilization restricted gaseous N losses while mineralization strongly increased N₂O emissions (Chapter 2). When NO₃⁻ was abundant in soil, immobilization of N led to a lower N₂O/(N₂O+N₂) ratio, but total gaseous N loss per unit C input were comparable (Chapter 3).

Interestingly, the effect of maize roots on N emissions was different in both studies presented. While addition of maize roots immobilized N and limited N₂O emissions in chapter 2, it mineralized N in chapter 3. However, quality of maize roots from both studies was not comparable. While maize plants had been grown in soil in chapter 2, for chapter 3, maize plants had been cultivated in nutrient solution. Although the C:N ratio was in a similar range, the amount of water-soluble C and N was much lower in the soil-grown roots compared to the solution-grown roots. Potentially, root morphology was affected by growth medium and soil-grown roots may be harder to decompose than solution-grown roots. Accordingly, the results from chapter 3 give insights about litter quality effects but should not be extrapolated to soil-grown roots.

In contrast to other studies (Baggs et al., 2000; Chen et al., 2013), N₂O emissions could not be estimated by litter C:N ratio. In chapter 2, C:N ratio of residues was similar but variance in N₂O emissions could best be explained by water-soluble C content of

litter. In chapter 3, cumulative N emissions increased with total C input irrespective of litter C:N ratio. However, litter C:N ratio (especially water-soluble C:N ratio) correlated with NO emissions from nitrification during the oxic incubation phase and the $\text{N}_2\text{O}/(\text{N}_2\text{O}+\text{N}_2)$ ratio of denitrification during the anoxic phase. Litter quality, especially litter C:N ratio, governs whether N is mineralized or immobilized during decomposition. In the initial stage, water-soluble and easily degradable C and N compounds are decomposed (Kögel-Knabner, 2002). Accordingly, litter quality controls C and N availability in soil which, in turn, regulates nitrification, denitrification, and gaseous N losses. This was confirmed by the study presented in chapter 2 where N_2O emissions were highest, when both NO_3^- and WEOC were high after addition of easily degradable litter. Furthermore, the ratio of available C to NO_3^- controls the ratio of the gaseous end products of denitrification $\text{N}_2\text{O}/(\text{N}_2\text{O}+\text{N}_2)$ (Firestone, 1982; Morley et al., 2014; Qin et al., 2017). When NO_3^- availability was limiting denitrification in chapter 1, N_2 was the dominant end product of denitrification. In contrast, N_2O was the main end product of denitrification during anoxic incubation conditions, as high NO_3^- availability restricted N_2O reduction to N_2 in chapter 3. The $\text{N}_2\text{O}/(\text{N}_2\text{O}+\text{N}_2)$ ratio from anoxic incubation was positively correlated with the ratio of soil WEOC: NO_3^- at the end of the experiment confirming that the ratio of available C to N is a major control of denitrification product stoichiometry.

Effect of plants and O_2 availability on the contribution of different processes to N_2O formation

N_2O is an end or by-product of several N cycling processes (Baggs, 2011; Butterbach-Bahl et al., 2013; van Groenigen et al., 2015; Wrage-Mönnig et al., 2018) with denitrification and nitrification being the most important ones in terms of amounts of N_2O lost to the atmosphere (Reay et al., 2012). In soils, both processes contribute to N_2O formation in varying fractions depending largely on oxygen partial pressure ($p\text{O}_2$). Nitrification is an obligate aerobic process (Stein and Klotz, 2016), while fungal

denitrification often takes place under microaerobic conditions (Lavrent'ev et al., 2008), and bacterial denitrification dominates under strongly anoxic conditions (Hayatsu et al., 2008). Accordingly, bacterial denitrification became the dominating source of N_2O under anoxic incubation conditions in chapter 3. Under natural conditions, soil moisture is an important controller of O_2 availability as it restricts diffusion of gases in soil (Schlüter et al., 2018). Thus, nitrification is considered the main N_2O source in dry soils, while denitrification mostly accounts for N_2O formation in soils over 60% WFPS (Davidson, 1991; Linn and Doran, 1984). Accordingly, the ^{15}N enrichment of soil-emitted N_2O showed that most N_2O derived from denitrification in the Maize S treatment where soil moisture was highest (Chapter 1). In the other treatments, unlabeled organic N was mineralized and diluted the labeled NO_3^- pool indicating that nitrification, nitrifier denitrification, and coupled nitrification-denitrification may have contributed to N_2O formation (van Groenigen et al., 2015; Wrage-Mönnig et al., 2018; Wrage et al., 2001), while denitrification mostly took place in anoxic microsites where labeled NO_3^- was not diluted by nitrification.

Similarly, in chapter 3, most denitrification occurred in anoxic hotspots where O_2 and NO_3^- diffusivity were limited. Analysis of N_2O isotopomers and $\text{NO}/\text{N}_2\text{O}$ ratio showed that nitrification, bacterial and fungal denitrification contributed to N_2O formation during the oxic incubation phase. While nitrification largely contributed to NO and N_2O formation in Control, in litter-amended treatments most N_2O originated from bacterial denitrification, which further supports the concept of plant litter associated anoxic hotspots for denitrification.

Soil moisture was lower (~49 % WFPS) in the incubation study in chapter 2 compared to chapter 3 (~70 % WFPS). Nevertheless, addition of easily degradable litter strongly increased N_2O emissions. In this study, increased N_2O emissions were mainly associated to the formation of anoxic hotspots due to increased O_2 consumption after crop residue addition (Chen et al., 2013; Kravchenko et al., 2017). However, high mineralization rates after addition of easily degradable litter indicate that nitrification-

derived N_2O emissions (including nitrifier denitrification) contributed substantially to N_2O emissions (Anderson et al., 1993; Hu et al., 2016; Papen et al., 1989; Wrage et al., 2001; Zhang et al., 2015). Furthermore, addition of plant litter may have promoted fungi which often contribute to N_2O formation after litter addition (Chen et al., 2015; Senbayram et al., 2018) and under slightly anoxic conditions (Laughlin and Stevens, 2002; Lavrent'ev et al., 2008). Analysis of the soil-inhabiting microbial community revealed that easily degradable litter promoted fast-growing C-cycling and N-reducing bacteria (Chapter 2). However, in studies with high NO_3^- and C_{org} availability, high fungal contribution was reported (Laughlin and Stevens, 2002; Senbayram et al., 2018). Altogether, this thesis showed that pO_2 , NO_3^- and C_{org} availability affect the share of nitrification, fungal and bacterial denitrification, but all processes may contribute simultaneously to N_2O emissions occurring in adjacent hotspots.

Conclusions and Outlook

The studies presented in thesis show that plants and plant litter have the potential to increase N_2O emissions from nitrification and denitrification. While healthy growing plants decreased soil moisture and NO_3^- content restricting N_2O emissions, high denitrification-derived $\text{N}_2\text{O}+\text{N}_2$ emissions were measured from poorly growing plants with lower water and NO_3^- uptake. As NO_3^- was the limiting substrate for denitrifiers, C_{org} availability did not affect $\text{N}_2\text{O}+\text{N}_2$ emissions. To better understand the interactions between water and N uptake and C deposition on denitrification and other N cycling processes, further studies with in-situ measurements of soil gases (CO_2 , NO , N_2O , N_2) and soil conditions (WFPS, mineral N, C_{org} , WEOC) are needed. Next, mitigation strategies can be developed focusing on fertilizer formulation and application, crop management strategies, and plant breeding.

Addition of plant litter increased N_2O losses compared to unamended control in both studies. When NO_3^- was limiting, mineralization of easily degradable litter strongly increased microbial respiration leading to the formation of anoxic hotspots, although

the soil was relatively dry. Hence, denitrification, nitrification and coupled processes contributed to N_2O formation. Similarly, in the second litter study, most denitrification occurred in anoxic hotspots where N_2O was directly reduced to N_2 . Nitrification contributed to NO and N_2O formation in the beginning of the incubation with a subsequent shift towards fungal denitrification. The quality of maize litter, especially the share of directly available C and N, controlled $\text{N}_2\text{O}+\text{N}_2$ formation and the $\text{N}_2\text{O}/(\text{N}_2\text{O}+\text{N}_2)$ ratio, although NO_3^- was not limited.

Bacterial denitrification mostly occurred in anoxic microsites while nitrification and fungal denitrification contributed to N_2O formation in the surrounding soil unless conditions were fully anoxic. Understanding N cycling processes in soil is a crucial step to minimize N_2O emissions from agricultural soils and restrict climate change. Accordingly, more studies measuring N_2 emissions and product ratios ($\text{N}_2\text{O}/(\text{N}_2\text{O}+\text{N}_2)$, $\text{NO}/\text{N}_2\text{O}$) are needed to determine full N budgets and denitrification-derived N losses. Future studies should thus focus on identifying N_2O -emitting processes and include measurements of all gaseous N losses (NO , N_2O , N_2).

SUMMARY

Agricultural soils are the largest anthropogenic source of nitrous oxide (N_2O) – a potent greenhouse gas that is primarily originating from the microbial processes denitrification and nitrification. While denitrification mainly occurs when O_2 partial pressure ($p\text{O}_2$) is low, nitrification is a strictly aerobic process. The presence of plants strongly alters both N cycling processes in soils by affecting C and N availability for microorganisms.

Growing plants take up N from the soil competing with microorganisms for available N. At the same time, plant roots exude organic C compounds increasing C_{org} availability in rooted soils, thus controlling the main substrates for denitrification. The first chapter of this thesis investigated the effect of NO_3^- uptake and C_{org} exudation on total and denitrification-derived N_2O emissions. Healthy growing plants decreased soil moisture and NO_3^- content which restricted N_2O emissions. In contrast, high denitrification-derived $\text{N}_2\text{O}+\text{N}_2$ emissions were measured from poorly growing plants with lower water and NO_3^- uptake. As NO_3^- was the limiting substrate for denitrifiers, C_{org} availability did not affect $\text{N}_2\text{O}+\text{N}_2$ emissions.

After harvest, plant litter is incorporated into the soil increasing C availability for microorganisms. Depending on its chemical quality (C:N ratio, C compounds), litter may lead to increased NO_3^- availability from mineralization or to immobilization of N to decompose C compounds. In both studies presented, addition of plant litter increased N_2O losses compared to the unamended control. In chapter 2, water-soluble C from litter together with NO_3^- from mineralization controlled both CO_2 and N_2O emissions. Increased microbial respiration reduced $p\text{O}_2$ leading to the formation of plant litter associated hotspots for denitrification when both C_{org} and NO_3^- were available. In chapter 3, $\text{N}_2\text{O}+\text{N}_2$ emissions increased linearly with litter C input. Litter C:N ratio controlled mineralization and immobilization and the $\text{N}_2\text{O}/(\text{N}_2\text{O}+\text{N}_2)$ ratio although NO_3^- was not limited. During the oxic incubation phase, most denitrification took place in anoxic hotspots where N_2O was directly reduced to N_2 . When N was mineralized, nitrification

contributed to NO and N₂O formation with a subsequent shift towards fungal denitrification in litter-amended soil.

Altogether, these studies showed that the presence of plants increased C availability for soil microorganisms, while N availability depended on plant N uptake and mineralization. However, only when both NO₃⁻ and C_{org} availability were high, high denitrification-derived N₂O emissions were detected. Furthermore, the ratio of available C to available NO₃⁻ controlled the product ratio of denitrification N₂O/(N₂O+N₂), and together with pO₂ affected the share of nitrification, bacterial and fungal denitrification to N₂O formation.

ZUSAMMENFASSUNG

Landwirtschaftliche Böden sind die größte anthropogene Lachgasquelle (N_2O). N_2O ist ein starkes Treibhausgas, dass größtenteils in den mikrobiellen Prozessen Nitrifikation und Denitrifikation entsteht. Während Denitrifikation hauptsächlich stattfindet, wenn Sauerstoff (O_2) knapp ist, ist die Nitrifikation ein strikt aerober Prozess. Pflanzen beeinflussen beide N-Umsetzungsprozesse indem sie die Verfügbarkeit von C und N für Mikroorganismen verändern.

Wachsende Pflanzen nehmen N aus dem Boden auf und konkurrieren dabei mit Mikroorganismen um verfügbaren N. Gleichzeitig scheiden Pflanzenwurzeln C-haltige Verbindungen aus und erhöhen die C-Verfügbarkeit im Boden. Dadurch beeinflussen Pflanzen die beiden wichtigsten Substrate für die Denitrifikation. Im ersten Kapitel dieser Dissertation wurde der Einfluss von NO_3^- -Aufnahme und C_{org} -Exudation auf die gesamten und aus Denitrifikation stammenden N_2O Emissionen untersucht. Gesunde, wachsende Pflanzen verringerten die Bodenfeuchte und den NO_3^- -Gehalt, sodass nur geringe N_2O Emissionen gemessen wurden. Im Gegensatz dazu wurden hohe $\text{N}_2\text{O}+\text{N}_2$ Emissionen aus Denitrifikation gemessen, wenn die Pflanzen schlecht wuchsen und ihre Wasser- und NO_3^- -Aufnahme geringer war. Da NO_3^- das limitierende Substrat für die Denitrifikation war, hatte die C_{org} -Verfügbarkeit keinen Einfluss auf die $\text{N}_2\text{O}+\text{N}_2$ Emissionen.

Nach der Ernte werden Pflanzenrückstände in den Boden eingearbeitet und erhöhen die C-Verfügbarkeit für Mikroorganismen. Abhängig ihrer chemischen Qualität (C:N Verhältnis, C-Verbindungen) können diese Erntereste sowohl zu erhöhter NO_3^- -Verfügbarkeit durch Mineralisierung organischer Verbindungen führen als auch zu Immobilisierung von N um C-Verbindungen abzubauen. In den beiden vorgestellten Studien wurden höhere N_2O Emissionen mit Ernteresten gemessen als in der Kontrolle. Im 2. Kapitel wurden die N_2O und CO_2 Emissionen hauptsächlich durch den Anteil an wasserlöslichem C aus den Ernteresten und durch NO_3^- -Verfügbarkeit aus

Mineralisierung beeinflusst. Ein Anstieg der mikrobiellen Atmung führte zur Bildung von Hotspots für die Denitrifikation, wenn sowohl NO_3^- als auch C_{org} verfügbar waren. Im 3. Kapitel stiegen die $\text{N}_2\text{O} + \text{N}_2$ Emissionen mit steigendem C-Input aus Ernteresten linear an. Das C:N Verhältnis der Streu beeinflusste die Mineralisierung bzw. Immobilisierung und das $\text{N}_2\text{O}/(\text{N}_2\text{O} + \text{N}_2)$ Verhältnis, obwohl NO_3^- nicht limitierend war. Während der oxischen Inkubationsphase fand die meiste Denitrifikation in anoxische Hotspots statt wo N_2O direkt zu N_2 reduziert wurde. Wenn N mineralisiert wurde, trug Nitrifikation zur Bildung von NO und N_2O bei, während pilzliche Denitrifikation mit fortlaufender Inkubationszeit zunahm.

Insgesamt zeigen diese Studien, dass Pflanzen die C-Verfügbarkeit für Bodenmikroorganismen erhöhen, während die N-Verfügbarkeit von der N-Aufnahme der Pflanzen und der N-Mineralisierung im Boden abhängt. Nur wenn sowohl NO_3^- als auch C_{org} verfügbar waren, wurden hohe N_2O Emissionen aus Denitrifikation gemessen. Außerdem war beeinflusst das Verhältnis an verfügbarem C zu NO_3^- abhängig das Produktratio der Denitrifikation $\text{N}_2\text{O}/(\text{N}_2\text{O} + \text{N}_2)$ und zusammen mit der O_2 -Verfügbarkeit die Anteile von Nitrifikation, bakterieller und pilzlicher Denitrifikation an der Lachgasbildung.

REFERENCES

- Anderson, I.C., Poth, M., Homstead, J., Burdige, D., 1993. A comparison of NO and N₂O production by the autotrophic nitrifier *Nitrosomonas europaea* and the heterotrophic nitrifier *Alcaligenes faecalis*. *Applied and Environmental Microbiology* 59, 3525–3533.
- Baggs, E.M., 2011. Soil microbial sources of nitrous oxide: Recent advances in knowledge, emerging challenges and future direction. *Current Opinion in Environmental Sustainability* 3, 321–327. doi:10.1016/j.cosust.2011.08.011
- Baggs, E.M., Rees, R.M., Smith, K.A., Vinten, A.J.A., 2000. Nitrous oxide emission from soils after incorporating crop residues. *Soil Use and Management* 16, 82–87. doi:10.1111/j.1475-2743.2000.tb00179.x
- Brenninkmeijer, C.A.M., Röckmann, T., 1999. Mass spectrometry of the intramolecular nitrogen isotope distribution of environmental nitrous oxide using fragment-ion analysis. *Rapid Communications in Mass Spectrometry* 13, 2028–2033. doi:10.1002/(SICI)1097-0231(19991030)13:20<2028::AID-RCM751>3.0.CO;2-J
- Butterbach-Bahl, K., Baggs, E.M., Dannenmann, M., Kiese, R., Zechmeister-boltenstern, S., 2013. Nitrous oxide emissions from soils : how well do we understand the processes and their controls ? *Philosophical Transactions of the Royal Society B* 368, 1–13. doi:10.1098/rstb.2013.0122
- Cabello, P., Roldán, M.D., Moreno-Vivián, C., 2004. Nitrate reduction and the nitrogen cycle in archaea. *Microbiology* 150, 3527–3546. doi:10.1099/mic.0.27303-0
- Chen, H., Li, X., Hu, F., Shi, W., 2013. Soil nitrous oxide emissions following crop residue addition: a meta-analysis. *Global Change Biology* 19, 2956–2964. doi:10.1111/gcb.12274
- Chen, H., Mothapo, N. V., Shi, W., 2015. Fungal and bacterial N₂O production regulated by soil amendments of simple and complex substrates. *Soil Biology and Biochemistry* 84, 116–126. doi:10.1016/j.soilbio.2015.02.018
- Ciais, P., Sabine, C., Bala, G., Bopp, L., Brovkin, V., Canadell, J., Chhabra, A., DeFries, R., Galloway, J., Heimann, M., Jones, C., Le Quéré, C., Myneni, R.B., Piao, S., Thornton, P., 2013. Carbon and Other Biogeochemical Cycles, in: *Climate Change 2013: The Physical Science Basis. Contribution of Working Group I to the Fifth Assessment Report of the Intergovernmental Panel on Climate Change*. pp. 465–570.
- Davidson, E.A., 1991. Fluxes of nitrous oxide and nitric oxide from terrestrial ecosystems, in: Rogers, J.E., Whitman, W.B. (Eds.), *Microbial Production and Consumption of Greenhouse Gases: Methane, Nitrogen Oxides and Halomethanes*. American Society for Microbiology, Washington (DC), pp. 219–235.
- Firestone, M.K., 1982. Biological denitrification, in: *Nitrogen in Agricultural Soils*, Agronomy Monograph. pp. 289–326. doi:10.1007/978-94-017-1662-8_2
- Focht, D.D., Verstrate, W., 1977. Denitrification Biochemical Ecology of Nitrification and, in: Alexander, M. (Ed.), *Advances in Microbial Ecology*. Plenum Press, New York and London, pp. 135–214.
- Haider, K., Mosier, A., Heinemeyer, O., 1985. Phytotron Experiments to Evaluate the Effect of Growing Plants on Denitrification. *Soil Science Society of America Journal* 49, 636–641.
- Hauck, R.D., Melsted, S.W., 1956. Some Aspects of the Problem of Evaluating Denitrification in Soils. *Soil Science Society of America Journal* 20, 361–364. doi:10.2136/sssaj1956.03615995002000030017x
- Hayatsu, M., Tago, K., Saito, M., 2008. Various players in the nitrogen cycle: Diversity and functions of the microorganisms involved in nitrification and denitrification. *Soil Science and Plant Nutrition* 54, 33–45. doi:10.1111/j.1747-0765.2007.00195.x
- Hooper, A.B., Terry, K.R., 1979. Hydroxylamine oxidoreductase of *Nitrosomonas*. Production of nitric oxide from hydroxylamine. *BBA - Enzymology* 571, 12–20. doi:10.1016/0005-2744(79)90220-1
- Höper, H., 2002. Carbon and nitrogen mineralisation rates of fens in Germany used for

- agriculture, in: Broll G., W., M., EM., P. (Eds.), *Wetlands in Central Europe*. Springer, Berlin, Heidelberg, pp. 149–164. doi:https://doi.org/10.1007/978-3-662-05054-5_8
- Hu, Xiaokang, Liu, L., Zhu, B., Du, E., Hu, Xueyang, Li, P., Zhou, Z., Ji, C., Zhu, J., Shen, H., Fang, J., 2016. Asynchronous responses of soil carbon dioxide, nitrous oxide emissions and net nitrogen mineralization to enhanced fine root input. *Soil Biology and Biochemistry* 92, 67–78. doi:10.1016/j.soilbio.2015.09.019
- Ji, B., Yang, K., Zhu, L., Jiang, Y., Wang, H., Zhou, J., Zhang, H., 2015. Aerobic denitrification: A review of important advances of the last 30 years. *Biotechnology and Bioprocess Engineering* 20, 643–651. doi:10.1007/s12257-015-0009-0
- Klemetsson, L., Svensson, B.H., Rosswall, T., 1987. Dinitrogen and nitrous oxide produced by denitrification and nitrification in soil with and without barley plants. *Plant and Soil* 99, 303–319. doi:10.1007/BF02370877
- Knops, J., Bradley, K.L., Wedin, D., 2002. Mechanisms of plant species impact on ecosystem nitrogen cycling. *Ecology Letters* 5, 454–466.
- Knowles, R., 1982. Denitrification. *Microbiological Reviews* 46, 43–70.
- Kögel-Knabner, I., 2002. The macromolecular organic composition of plant and microbial residues as inputs to soil organic matter. *Soil Biology and Biochemistry* 34, 139–162. doi:10.1016/S0038-0717(01)00158-4
- Köster, J.R., Well, R., Dittert, K., Giesemann, A., Lewicka-Szczebak, D., Mühling, K.H., Herrmann, A., Lammel, J., Senbayram, M., 2013. Soil denitrification potential and its influence on N₂O reduction and N₂O isotopomer ratios. *Rapid Communications in Mass Spectrometry* 27, 2363–2373. doi:10.1002/rcm.6699
- Kravchenko, A.N., Toosi, E.R., Guber, A.K., Ostrom, N.E., Yu, J., Azeem, K., Rivers, M.L., Robertson, G.P., 2017. Hotspots of soil N₂O emission enhanced through water absorption by plant residue. *Nature Geosciences* 10, 496–500. doi:10.1038/NGEO2963
- Kristensen, H.L., Debosz, K., McCarty, G.W., 2003. Short-term effects of tillage on mineralization of nitrogen and carbon in soil. *Soil Biology and Biochemistry* 35, 979–986. doi:10.1016/S0038-0717(03)00159-7
- Kuzyakov, Y., Xu, X., 2013. Competition between roots and microorganisms for nitrogen: Mechanisms and ecological relevance. *New Phytologist* 198, 656–669. doi:10.1111/nph.12235
- Laughlin, R.J., Stevens, R.J., 2002. Evidence for Fungal Dominance of Denitrification and Codenitrification in a Grassland Soil. *Soil Science Society of America Journal* 66, 1540–1548. doi:10.2136/sssaj2002.1540
- Lavrent'ev, R.B., Zaitsev, S.A., Sudnitsyn, I.I., Kurakov, A. V., 2008. Nitrous oxide production by fungi in soils under different moisture levels. *Moscow University Soil Science Bulletin* 63, 178–183. doi:10.3103/s0147687408040054
- Lewicka-Szczebak, D., Augustin, J., Giesemann, A., Well, R., 2017. Quantifying N₂O reduction to N₂ based on N₂O isotopocules-validation with independent methods (helium incubation and 15N gas flux method). *Biogeosciences* 14, 711–732. doi:10.5194/bg-14-711-2017
- Lewicka-Szczebak, D., Well, R., Giesemann, A., Rohe, L., Wolf, U., 2013. An enhanced technique for automated determination of ¹⁵N signatures of N₂, (N₂+N₂O) and N₂O in gas samples. *Rapid Communications in Mass Spectrometry* 27, 1548–1558. doi:10.1002/rcm.6605
- Linn, D.M., Doran, J.W., 1984. Effect of Water-Filled Pore Space on Carbon Dioxide and Nitrous Oxide Production in Tilled and Nontilled Soils. *Soil Science Society of America Journal* 48, 1267–1272. doi:10.2136/sssaj1984.03615995004800060013x
- Maeda, K., Spor, A., Edel-Hermann, V., Heraud, C., Breuil, M.C., Bizouard, F., Toyoda, S., Yoshida, N., Steinberg, C., Philippot, L., 2015. N₂O production, a widespread trait in fungi. *Scientific Reports* 5, 1–7. doi:10.1038/srep09697
- Millar, N., Baggs, E.M., 2004. Chemical composition, or quality, of agroforestry residues influences N₂O emissions after their addition to soil. *Soil Biology and Biochemistry* 36, 935–943. doi:10.1016/j.soilbio.2004.02.008

- Miller, M.N., Zebarth, B.J., Dandie, C.E., Burton, D.L., Goyer, C., Trevors, J.T., 2008. Crop residue influence on denitrification, N₂O emissions and denitrifier community abundance in soil. *Soil Biology and Biochemistry* 40, 2553–2562. doi:10.1016/j.soilbio.2008.06.024
- Moreau, D., Bardgett, R.D., Finlay, R.D., Jones, D.L., Philippot, L., 2019. A plant perspective on nitrogen cycling in the rhizosphere. *Functional Ecology* 33, 540–552. doi:10.1111/1365-2435.13303
- Morley, N.J., Richardson, D.J., Baggs, E.M., 2014. Substrate induced denitrification over or under estimates shifts in soil N₂/N₂O ratios. *PLoS ONE* 9, 1–6. doi:10.1371/journal.pone.0108144
- Müller, C., Laughlin, R.J., Spott, O., Rütting, T., 2014. Quantification of N₂O emission pathways via a ¹⁵N tracing model. *Soil Biology and Biochemistry* 72, 44–54. doi:10.1016/j.soilbio.2011.03.028
- Nguyen, C., 2003. Rhizodeposition of organic C by plants: mechanisms and controls. *Agronomie* 23, 375–396. doi:10.1051/agro:2003011
- Novoa, R.S.A., Tejeda, H.R., 2006. Evaluation of the N₂O emissions from N in plant residues as affected by environmental and management factors. *Nutrient Cycling in Agroecosystems* 75, 29–46. doi:10.1007/s10705-006-9009-y
- Papen, H., von Berg, R., Hinkel, I., Thoene, B., Rennenberg, H., 1989. Heterotrophic Nitrification by *Alcaligenes faecalis*: NO₂⁻, NO₃⁻, N₂O, and NO Production in Exponentially Growing Cultures. *Applied and Environmental Microbiology* 55, 2068–2072.
- Payne, W.J., Grant, M.A., 1981. Overview of Denitrification, in: Lyons J.M., et al. (Eds.), *Genetic Engineering of Symbiotic Nitrogen Fixation and Conservation of Fixed Nitrogen*. Springer, Boston, pp. 411–427. doi:https://doi.org/10.1007/978-1-4684-3953-3_33
- Philippot, L., 2002. Denitrifying genes in bacterial and Archaeal genomes. *Biochim. Biophys. Acta* 1577, 355–376.
- Qin, S., Hu, C., Clough, T.J., Luo, J., Oenema, O., Zhou, S., 2017. Irrigation of DOC-rich liquid promotes potential denitrification rate and decreases N₂O/(N₂O+N₂) product ratio in a 0–2 m soil profile. *Soil Biology and Biochemistry* 106, 1–8. doi:10.1016/j.soilbio.2016.12.001
- Ravishankara, A.R., Daniel, J.S., Portmann, R.W., 2009. Nitrous oxide (N₂O): the dominant ozone-depleting substance emitted in the 21st century. *Science* 326, 123–125. doi:10.1126/science.1176985
- Reay, D.S., Davidson, E.A., Smith, K.A., Smith, P., Melillo, J.M., Dentener, F., Crutzen, P.J., 2012. Global agriculture and nitrous oxide emissions. *Nature Climate Change* 2, 410–416. doi:10.1038/nclimate1458
- Rohe, L., Anderson, T.H., Braker, G., Flessa, H., Giesemann, A., Lewicka-Szczebak, D., Wrage-Mönnig, N., Well, R., 2014. Dual isotope and isotopomer signatures of nitrous oxide from fungal denitrification - A pure culture study. *Rapid Communications in Mass Spectrometry* 28, 1893–1903. doi:10.1002/rcm.6975
- Rudolph-Mohr, N., Tötze, C., Kardjilov, N., Oswald, S.E., 2017. Mapping water, oxygen, and pH dynamics in the rhizosphere of young maize roots. *Journal of Plant Nutrition and Soil Science* 180, 336–346. doi:10.1002/jpln.201600120
- Schlüter, S., Henjes, S., Zawallich, J., Bergaust, L., Horn, M., Ippisch, O., Vogel, H.-J., Dörsch, P., 2018. Denitrification in Soil Aggregate Analogues-Effect of Aggregate Size and Oxygen Diffusion. *Frontiers in Environmental Science* 6, 1–10. doi:10.3389/fenvs.2018.00017
- Scholefield, D., Hawkins, J.M.B.B., Jackson, S.M., 1997. Development of a helium atmosphere soil incubation technique for direct measurement of nitrous oxide and dinitrogen fluxes during denitrification. *Soil Biology and Biochemistry* 29, 1345–1352. doi:10.1016/S0038-0717(97)00021-7
- Senbayram, M., Well, R., Bol, R., Chadwick, D.R., Jones, D.L., Wu, D., 2018. Interaction of straw amendment and soil NO₃⁻ content controls fungal denitrification and denitrification product stoichiometry in a sandy soil. *Soil Biology and Biochemistry* 126, 204–212. doi:10.1016/j.soilbio.2018.09.005
- Senbayram, M., Well, R., Shan, J., Bol, R., Burkart, S., Jones, D.L., 2020. Rhizosphere

- processes in nitrate-rich barley soil tripled both N_2O and N_2 losses due to enhanced bacterial and fungal denitrification. *Plant and Soil*. doi:10.1007/s11104-020-04457-9
- Siegel, R.S., Hauck, R.D., Kurtz, L.T., 1982. Determination of $^{30}\text{N}_2$ and Application to Measurement of N_2 Evolution During Denitrification. *Soil Science Society of America Journal* 46, 68. doi:10.2136/sssaj1982.03615995004600010013x
- Stefanson, R.C., 1972. Soil denitrification in sealed soil-plant systems I. Effect of plants, soil water content and soil organic matter content. *Plant and Soil* 127, 113–127.
- Stefanson, R.C., 1970. Sealed growth chambers for studies of the effects of plants on the soil atmosphere. *Journal of Agricultural Engineering Research* 15, 295–301. doi:10.1016/0021-8634(70)90126-5
- Stein, L.Y., Klotz, M.G., 2016. The nitrogen cycle. *Current Biology* 26, R94–R98. doi:10.1016/j.cub.2015.12.021
- Sutka, R.L., Adams, G.C., Ostrom, N.E., Ostrom, P.H., 2008. Isotopologue fractionation during N_2O production by fungal denitrification. *Rapid Communications in Mass Spectrometry* 22, 3989. doi:10.1002/rcm.3820
- Sutka, R.L., Ostrom, N.E., Ostrom, P.H., Breznak, J.A., Gandhi, H., Pitt, A.J., Li, F., 2006. Distinguishing Nitrous Oxide Production from Nitrification and Denitrification on the Basis of Isotopomer Abundances. *Applied and Environmental Microbiology* 72, 638–644. doi:10.1128/AEM.72.1.638–644.2006
- Takaya, N., 2009. Response to hypoxia, reduction of electron acceptors, and subsequent survival by filamentous fungi. *Bioscience, Biotechnology and Biochemistry* 73, 1–8. doi:10.1271/bbb.80487
- Takaya, N., Catalan-Sakairi, M.A.B., Sakaguchi, Y., Kato, I., Zhou, Z., Shoun, H., 2003. Aerobic Denitrifying Bacteria That Produce Low Levels of Nitrous Oxide. *Applied and Environmental Microbiology* 69, 3152–3157. doi:10.1128/AEM.69.6.3152
- Toyoda, S., Mutoke, H., Yamagishi, H., Yoshida, N., Tanji, Y., 2005. Fractionation of N_2O isotopomers during production by denitrifier. *Soil Biology and Biochemistry* 37, 1535–1545. doi:10.1016/j.soilbio.2005.01.009
- Toyoda, S., Yoshida, N., 1999. Determination of Nitrogen Isotopomers of Nitrous. *Anal. Chem.* 71, 4711–4718.
- van Groenigen, J.W., Huygens, D., Boeckx, P., Kuyper, T.W., Lubbers, I.M., Rütting, T., Groffman, P.M., 2015. The soil N cycle: New insights and key challenges. *Soil* 1, 235–256. doi:10.5194/soil-1-235-2015
- von Rheinbaben, W., Trollenier, G., 1984. Influence of plant growth on denitrification in relation to soil moisture and potassium nutrition. *Zeitschrift Für Pflanzenernährung Und Bodenkunde* 147, 730–738. doi:10.1002/jpln.19841470610
- Wang, R., Willibald, G., Feng, Q., Zheng, X., Liao, T., Brüggemann, N., Butterbach-Bahl, K., 2011. Measurement of N_2 , N_2O , NO , and CO_2 emissions from soil with the gas-flow-soil-core technique. *Environmental Science and Technology* 45, 6066–6072. doi:10.1021/es1036578
- Wrage-Mönnig, N., Horn, M.A., Well, R., Müller, C., Velthof, G.L., Oenema, O., 2018. The role of nitrifier denitrification in the production of nitrous oxide revisited. *Soil Biology and Biochemistry* 123, A3–A16. doi:10.1016/j.soilbio.2018.03.020
- Wrage, N., Velthof, G.L., van Beusichem, M.L., Oenema, O., 2001. The role of nitrifier denitrification in the production of nitrous oxide. *Soil Biology and Biochemistry* 33, 1723–1732. doi:10.1016/S0038-0717(01)00096-7
- Wunderlin, P., Mohn, J., Joss, A., Emmenegger, L., Siegrist, H., 2012. Mechanisms of N_2O production in biological wastewater treatment under nitrifying and denitrifying conditions. *Water Research* 46, 1027–1037. doi:10.1016/j.watres.2011.11.080
- Yu, L., Harris, E., Lewicka-Szczepak, D., Barthel, M., Blomberg, M.R.A., Harris, S.J., Johnson, M.S., Lehmann, M.F., Liisberg, J., Müller, C., Ostrom, N.E., Six, J., Toyoda, S., Yoshinari, T., Mohn, J., 2020. What can we learn from N_2O isotope data? - Analytics, processes and modelling. *Rapid Communications in Mass Spectrometry* (in review)

- Zhang, J., Müller, C., Cai, Z., 2015. Heterotrophic nitrification of organic N and its contribution to nitrous oxide emissions in soils. *Soil Biology and Biochemistry* 84, 199–209. doi:10.1016/j.soilbio.2015.02.028
- Zumft, W.G., 1997. Cell biology and molecular basis of denitrification. *Microbiology and Molecular Biology Reviews* 61, 533–616.

ACKNOWLEDGEMENTS

I would like to thank my first supervisor Prof. Dr. Klaus Dittert for the opportunity to pursue these studies and to learn how to organize a research project. I want to thank Prof. Dr. Johanna Pausch for adding the perspective of C cycling to my research, for her support, and all the enthusiasm for my work. I am grateful to PD Dr. Reinhard Well for sharing his vast knowledge on denitrification and other N₂O production pathways with me and answering numerous questions about processes, methods, and calculations. I want to thank Dr. Birgit Pfeiffer for teaching me about soil microorganisms and molecular lab techniques, and for advice of any kind.

I am thankful to all colleagues from the division of Plant Nutrition and the Institute of Applied Plant Nutrition, especially the laboratory and technical staff Simone Urstädt, Susanne Koch, Jürgen Kobbe, Ulrike Kierbaum, Reinhard Hilmer, Marlies Niebuhr, and Kirsten Fladung. Thank you for help with my experiments, analyzing samples, and preparing equipment. This work would not have been possible without you! Thanks to Christiane Lüers for all the (digital) paperwork and keeping track of my project's finances. Thanks to all my fellow PhD students from the division of Plant Nutrition, Quality of Plant Products, and IAPN for good conversations, coffee breaks, and barbecues, especially Dr. Frederike Sonntag, Annika Lingner, Larissa Kanski, Victoria Nasser, and Setareh Jamali. I also want to thank the division of Quality of Plant Products for borrowing things we were short of and help when needed. I am grateful to all my students Tim Schaare, Jakob Streuber, Gwynlyn Buchanan, Tomor Krasniqi, Bridith Angulo Schipper, Sebastian Floßmann, Finn Malinowski, and Justus Detring for help with experiments, analyses and lots of annoying work.

I want to thank all my colleagues from the DASIM research unit for discussions, scientific input, and encouragements. Especially Ronny Surey, François Malique, and Jan Zawallich for long conversations about scientific and less scientific topics; Dr. Jan Reent Köster for discussions about tubings, fittings, and valves, and for setting up our NO_x analyzer; and Dr. Kristina Kleineidam for support with everything related to the project. I would like to thank Dr. Inga Mölder from the Graduate School of Forest and Agricultural Sciences for advice on everything related to my PhD studies and some other aspects.

I want to acknowledge Delta Notch for his remixes 'Trance to study by' which helped me through long hours of writing.

Last, but not least, I want to thank my family and friends, especially Dr. Esther Grüner and Dr. Katharina Meyer. And Dr. Oliver Caré for giving me a reason to come home each and every day!

Curriculum Vitae

Pauline Sophie Rummel

Research Experience

06.2016 – present **Research Associate** in DFG Research unit Denitrification in Agricultural Soils: Integrated Control and Modelling at Various Scales (DASIM), Sub project: Crop plant root effects on the soil environment for denitrification in agricultural soils

Education

06.2016 – 07.2020 **Dr. rer. nat.**
Georg-August-Universität Göttingen, Graduate School of Forest and Agricultural Sciences

2013 – 2016 **Master of Science in Agricultural Science**
Georg-August-Universität Göttingen
Specialization on plant nutrition and nutrient dynamics in soils
Master's Thesis: "Plant availability of fertilizers from phosphorus recycling in a pot experiment with high soil pH"

2009 – 2012 **Bachelor of Science in Agricultural and Horticultural Sciences**
Technische Universität München
Bachelor's Thesis: "Effect of biogas residues as P fertilizers in a pot experiment with maize in an acid soil"

Publications

Rummel, P. S., Pfeiffer, B., Pausch, J., Well, R., Schneider, D., and Dittert, K. (2020). Maize root and shoot litter quality controls short-term CO₂ and N₂O emissions and bacterial community structure of arable soil. *Biogeosciences* 17, 1181–1198. doi:10.5194/bg-17-1181-2020.

Rummel, P. S., Well, R., Pausch, J., Pfeiffer, B., and Dittert, K. (2021a). Carbon Availability and Nitrogen Mineralization Control Denitrification Rates and Product Stoichiometry during Initial Maize Litter Decomposition. *Applied Sciences* 11, 5309. doi:10.3390/app11115309.

Rummel, P. S., Well, R., Pfeiffer, B., Dittert, K., Floßmann, S., and Pausch, J. (2021b). Nitrate uptake and carbon exudation – do plant roots stimulate or inhibit denitrification? *Plant and Soil* 459, 217–233. doi:10.1007/s11104-020-04750-7.

Surey, R., Schimpf, C. M., Sauheith, L., Mueller, C. W., Rummel, P. S., Dittert, K., Kaiser, K., Böttcher, J., and Mikutta, R. (2020). Potential denitrification stimulated by water-soluble organic carbon from plant residues during initial decomposition. *Soil Biology and Biochemistry*. 147, 107841. doi:10.1016/j.soilbio.2020.107841.

Conferences and talks

April 2021	Nitrate and water uptake, rather than rhizodeposition, control denitrification in the presence of growing plants, EGU General Assembly, Sharing Geoscience Online
May 2020	NO ₃ ⁻ uptake and C exudation – do plant roots stimulate or inhibit denitrification? EGU General Assembly, Sharing Geoscience Online
Sep 2019	Quality of Carbon compounds of Maize root and shoot litter controls short-term CO ₂ and N ₂ O emissions and bacterial communities, Annual Meeting of the German Society of Plant Nutrition, Berlin, Germany
July 2019	Combined effects of plant water uptake, N availability and rhizodeposition on denitrification, Rhizosphere 5, Saskatoon, Canada
Mar 2019	Effect of crop N uptake and rhizodeposition on denitrification, DASIM Conference “Tracing Denitrification” Gießen, Germany
Jun 2018	Quality of Carbon compounds of maize root and shoot litter controls short-term CO ₂ and N ₂ O emissions from agricultural soils, Nitrogen Workshop, Rennes, France
Apr 2018	Plant litter quality controls short-time CO ₂ and N ₂ O emissions of root and shoot residues in agricultural soils, EGU General Assembly, Vienna, Austria
Nov 2017	N ₂ O emissions from soil after incorporation of maize root and shoot biomass, Agroecology seminar, University of Bayreuth, Germany
Aug 2017	N ₂ O emissions of soils after incorporation of maize root and shoot residues, International Plant Nutrition Colloquium, Copenhagen, Denmark